UNIVERSITAT DE BARCELONA

P-Stereogenic Intermediates and MaxPHOX ligands

Iridium Catalyzed Asymmetric Hydrogenations

Ernest Salomó i Prat

P-Stereogenic Intermediates and MaxPHOX Ligands. Iridium Catalyzed Asymmetric Hydrogenations.

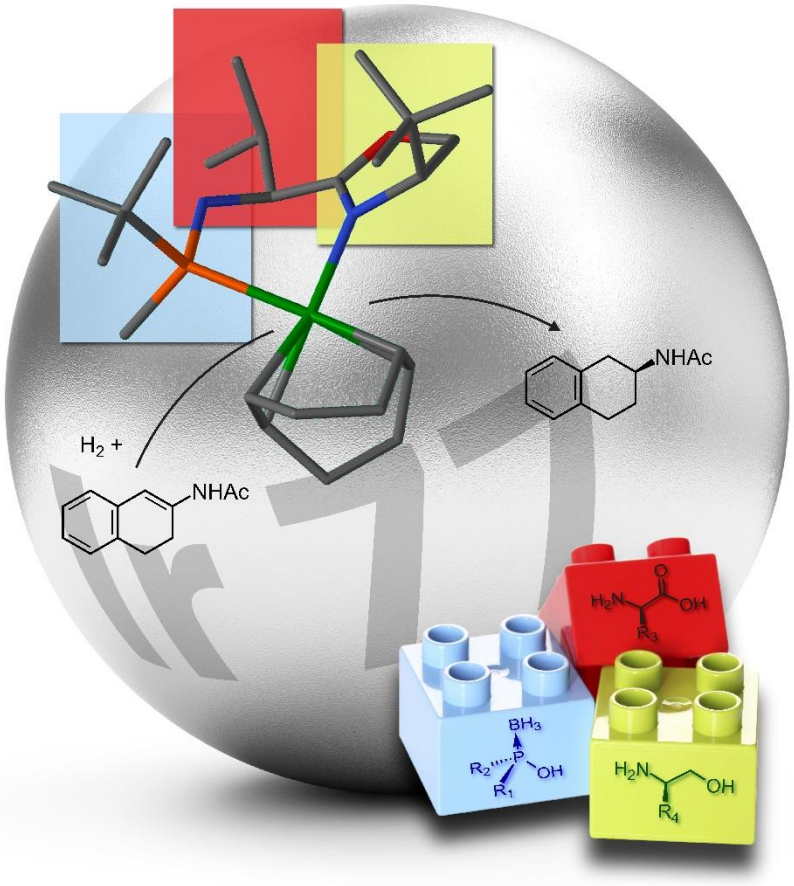

Ernest Salomó i Prat

UNIVERSITAT DE BARCELONA

Barcelona 2018

Programa de doctorat de Química Orgànica

P-Stereogenic Intermediates and MaxPHOX ligands.

Iridium Catalyzed Asymmetric Hydrogenations.

Ernest Salomó i Prat

Director de tesi: Prof. Xavier Verdaguer Espaulella

Prof. Antoni Riera Escalé

Departament de Química Orgànica i Inorgànica

Universitat de Barcelona

UNIVERSITAT DE BARCELONA

IRB BARCELONA

INSTITUTE FOR RESEARCH IN BIOMEDICINE

Memòria presentada per **Ernest Salomó i Prat** per a optar al grau de

Doctor en Química per la Universitat de Barcelona

Ernest Salomó i Prat

Revisada per:

Prof. Xavier Verdaguer Espaulella

Prof. Antoni Riera Escalé

Barcelona, Juny 2018

Aquest treball s'ha realitzat des del setembre del 2014 fins al juny del 2018 amb el suport del MINECO (beca FPI) i de l'IRB Barcelona amb una beca pont pel curs 2014-2015. La investigació s'ha finançat amb els projectes de recerca del MINECO (CTQ2014-56361-P i CTQ2017-87840-P)

El treball experimental s'ha dut a terme en el laboratori de la Unitat de Recerca en Síntesi Asimètrica (URSA) de l'Institut de Recerca Biomèdica (IRB Barcelona) de Barcelona, ubicat al Parc Científic de Barcelona (PCB).

Agraïments

Voldria començar agraint els meus dos directors de tesi. Gràcies al Prof. Xavier Verdaguer que ha estat sempre treballant amb mi en aquest projecte i ha aportat la part d'atreviment i originalitat que sovint em faltava. Fèiem un bon equip! També vull agrair-li que hagi fet d'artista pels dos amb la portada que hem reaprofitat per aquesta tesi! En segon lloc, però no menys important, gràcies al Prof. Antoni Riera per haver confiat en mi i haver-me donat la oportunitat de ser doctor (en Toni és probablement el PI amb més sentit de l'humor de tot l'IRB!!) Els dos heu tingut sempre la porta oberta i heu set sempre molt pròxims. Gràcies per transformar el doctorat en una experiència molt agradable!

Seguidament anirem agraït als del lab. Primer a l'Anna Escolà (safety manager conjuntament amb mi perquè la deixo) per poder sempre somriure tot i ser una inorgànica que treballa amb pèptids. A en Dan Byron (Pagès!!); al principi em va costar entendre't i ara que t'entenc, me'n penedeixo... A veure qui serà doctor primer!! A l'Amparo, per ajudar-me amb el meu castellà i a fer les coses delicades delicadament. A en Joan Matarín (pin, pin...) que fa els millors pastissos del món (em sap greu haver-me assegut a sobre del Cheese Cake). A l'Albert, capaç de coordinar 10 projectes i seguir el Nàstic per la radio a la vegada. A la Marta Frigolé per parlar amb el seu accent agironat (es troba a faltar a Bcn). A la Caro per tenir paciència i no començar a fer servir el seu karate. A en Craig per escoltar-me, fer-me riure, aguantar-me els moments d'estrès i sobretot per portar-me menjar de tant en tant (ets un gran amic). Per últim, al seguit de màsters i TFGs que m'han ajudat (minions): Iris, María, Marta, Pol, Pep i ara, Rúben. Tot i que avui en dia en Pep ja és doctorant (Hola Olga...T'he portat un rosa...)!

I continuem fora del lab, però dins del IRB. Vull donar les gràcies a l'Alejandro; he conegut poca gent més bona persona, però ningú més puntual! Se't troba a faltar! A en Jurgen (encara no estic segur de com va el teu nom) per fer-nos guanyar la lliga i la copa (IRBastards!!!) i sobretot ser un gran amic. Parlant del futbol, donaré les gràcies a en Juan, la meva parella en la defensa (Piqué i Ramos). Com pots ser tant culte i "gañán" a la vegada no ho sé. Seguim pel nostre president i capità: en Jordi Badia. Seràs un gran PI (gran ja ho ets de fet...). Després la Gemma, veïna i una gran acròbata que em fa sempre patir que es faci mal. A la Laura, per ser natural i espontània (festival de curts!!). Seguir per la Sara, t'escric en català perquè ja tens el C1!! Gràcies per escoltar-me sempre, "doctora amor". I per últim a l'Enric i l'Ádrian, que tots tres junts formem els tres reis gormitis! (Melchor, Gaspar y Vaarebentar). És sempre increïblement fàcil i agradable anar a menjar amb vosaltres.

I ara fora del IRB. Primer als meus companys de pis. María, gràcies per cuidar-nos a tots aquests anys. En realitat no anava tant enfeinat com per no netejar. A la Sil (my sister from another mister); mira que portem anys vivint junts i no me'n canso. Espero que en siguin uns quants més. I al quart company, l'Stuart. Merci per cuinar i fer-me menjar les coses més gordes i bones (my brother from a different mother!). Seguidament agrair als companys fora de Bcn. Gràcies a tota la gent de la colla de Vic. Sempre se'm posava bé tornar a casa. I també a l'Ori, que tot i que s'avorria segur, sempre em preguntava per la tesi.

Finalment vull agrair als meus pares: la Conxita i l'Ato. Sempre m'heu donat suport i heu estat més orgullosos de mi que jo mateix. Sense vosaltres no hauria tingut la oportunitat de fer tot això. Aquesta tesi és més vostra que meva.

Diuen que som una combinació de més o menys les 5 persones més pròximes a nosaltres. No sé quantes heu sigut exactament, però gràcies a vosaltres m'he fet una millor persona durant aquests anys.

Per tot això i molt més, merci a tots!! (I fins aviat!)

“Lisa, haz el favor...
En esta casa obedecemos las
leyes de la termodinámica!!”

Homer J. Simpson

Los Simpsons

Temporada 6, Capítol 21

Publications and patents during the present PhD thesis

- **Salomó, E**.; Orgué, S.; Riera, A.; Verdaguer, X. Transition metal phosphino-oxazoline catalysts, processes for their production, and uses thereof in the hydrogenation of cyclic enamides imines, **2016,** WO-2016203005-A1
- **Salomó, E**.; Orgué, S.; Riera, A.; Verdaguer, X. Efficient Preparation of (*S*)- and (*R*)-*Tert*-Butylmethylphosphine–Borane: A Novel Entry to Important P-Stereogenic Ligands. *Synthesis*. **2016**, 1–5.
- **Salomó, E.**; Orgué, S.; Riera, A.; Verdaguer, X. Highly Enantioselective Iridium-Catalyzed Hydrogenation of Cyclic Enamides. *Angew. Chemie Int. Ed.* **2016**, *55* (28), 7988–7992.
- **Salomó, E.**; Prades, A.; Riera, A.; Verdaguer, X. Dialkylammonium *Tert*-Butylmethylphosphinites: Stable Intermediates for the Synthesis of P-Stereogenic Ligands. *J. Org. Chem.* **2017**, *82* (13), 7065–7069.
- **Salomó, E.;** Rojo, P.; Hernández-Lladó, P.; Riera, A.; Verdaguer, X. P-Stereogenic and Non-P-Stereogenic Ir–MaxPHOX in the Asymmetric Hydrogenation of *N*-Aryl Imines. Isolation and X-Ray Analysis of Imine Iridacycles. *J. Org. Chem.* **2018**, *83* (8), 4618–4627.
- **Salomó, E.;** Gallen, A.; Grabulosa, A.; Riera, A.; Verdaguer, X. Direct Asymmetric Hydrogenation of *N*-Methyl and *N*-Alkyl Imines with an Ir(III)H Catalyst *(submitted).*

Table of Contents

Abbreviations

(*R*)	Rectus
(*S*)	Sinister
ACN	Acetonitrile
Alk	Alkyl
***o*-An**	*o*-methoxyphenyl
Ar	Aryl
Aux.	Auxiliary
BAr_F	Tetrakis[3,5-bis (trifluoromethyl)phenyl] borate
Bn	Benzyl
Calc.	Calculated
Cat.	Catalyst
GC	Gas Chromatography
COD	1,5-Cyclooctadiene
Conv.	Conversion
Crystal.	Crystallization
Cy	Cyclohexyl
DABCO	1,4-diazabicyclo [2.2.2]octane
DFT	Density Functional Theory
DIBAL-H	Diisobutylaluminium hydride
DME	Dimethoxyethane
DMSO	Dimethyl sulfoxide
dr	Diastereomeric Ratio
EDTE	*N*,*N*,*N*',*N*'-tetrakis(2-hydroxyethyl) ethylenediamine
ee	Enantiomeric excess
ent-	Enantiomer
eq	Equivalent
er	Enantiomeric ratio
Fc	Ferrocenyl
HPLC	High Performance Liquid Chromatography
HRMS	High Resolution Mass Spectroscopy
Inv.	Inversion
IR	Infrared Spectroscopy
L*	Chiral Ligand
LDA	Lithium diisopropylamide
L-DOPA	L-3,4-dihydroxy phenylalanine
MI	Migratory Insertion

Mp	Melting point
Ms	Methanesulfonyl
Naph	Naphtalene
nbd	Norbonadiene
Nu	Nucleophile
o.n.	Overnight
P*	Chiral phosphorous
Quant.	Quantitative
r.t.	Room temperature
rac	Racemic
SIP	Secondary Iminophosphorane
S_N2	Bimolecular nucleophilic substitution
S_N2@P	Bimolecular nucleophilic substitution on the P atom
TEA	Triethylamine
Temp.	Temperature
TLC	Thin Layer Chromatography
TMEDA	Tetramethylethylenediamine
Tol	Tolyl

Introduction and Objectives

Asymmetric hydrogenation of alkenes by means of organometallic catalysis is a powerful tool for organic synthesis; it is an efficient and simple method to produce valued chiral compounds. Among the many different existing ligands, phosphorous ones have proven very useful for these procedures.[1] The ligand plays a vital role in the catalysis, as the ligand's chirality can be transferred to the product. There is a wide range of P-based chiral ligands and can be classified in 3 groups depending on where the chirality lies; on the P atom, on the backbone or on both the P atom and the backbone.

The synthesis of P-stereogenic ligands was paused for many years as the P ligands with a chiral backbone proved effective too and were easier to synthesize. Nevertheless, in the last 15 years the methodologies for the synthesis of P-stereogenic compounds have advanced a lot.[2] Among the different P-stereogenic ligands, the ones with bulky substituents at the P atom have proved to be very effective. However, to synthesize such ligands is still a challenge.

For the past 8 years our research group has focused on developing new methodologies for the synthesis of P-stereogenic ligands. From all the different achievements, the two most relevant advances were the syntheses of chiral phosphorous synthons **4** and **5**. They managed to design a completely enantioselective synthesis for both of them. Reaction between *cis*-1-amino-2-indanol **1** and *tert*-butyldichlorophosphine in the presence of diethyl amine afforded the heterocycle **2** after protection of the free phosphine with borane. Then, reaction with different Grignard reagents, such as MeMgBr or PhMgBr is possible. Compound **3** is a key molecule because from it we can access both chiral synthons (*R*)-**4** and (*S*)-**5**. On one hand, chiral aminophosphine (*S*)-**5** can be accessed by cleaving the benzylic C—N bond with a Li/NH_3 reduction (reported in T. León's PhD thesis).[3] On the other hand, chiral phosphinous acid (*R*)-**4** is afforded through hydrolysis of compound **3** (reported in S. Orgué's PhD thesis).[4] Moreover, **4** and **5** can be transformed to each other by direct reaction. They complement each other as **5** can react as a nucleophile, while **4** reacts as an electrophile.

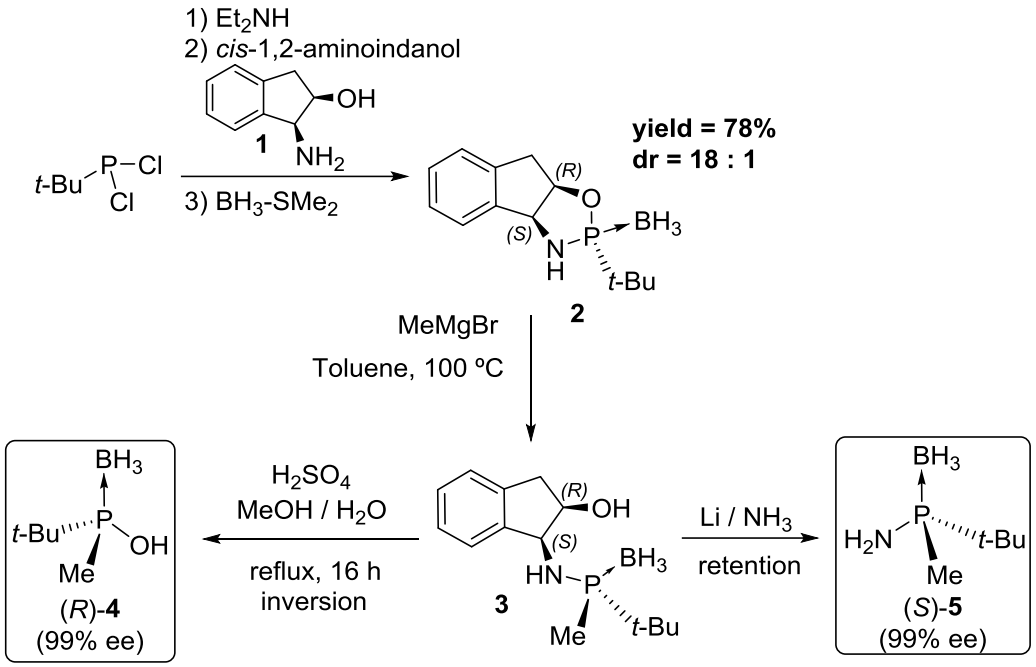

Figure 1. *Stereoselective synthesis of synthons* ***4*** *and* ***5****.*

Compound **5** afforded different ligands by nucleophilic reaction by the amine moiety, such as the MaxPHOS ligand or the SIP ligands.[5] The first one has been applied in the Rh-catalyzed asymmetric hydrogenation of α-amino acid precursors and the second one to [2+2+2] Rh-catalyzed cycloadditions of endiynes.[6]

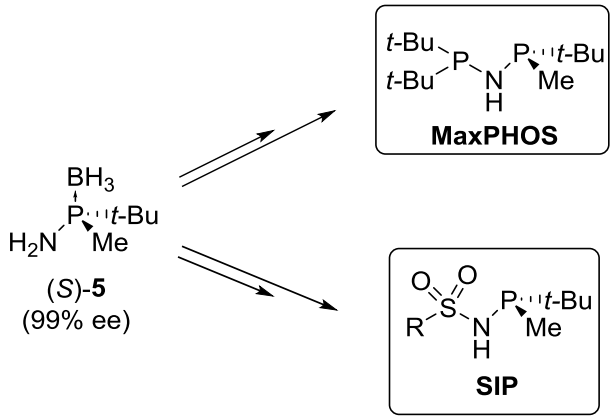

Figure 2. *Synthesis of MaxPHOS and the SIP ligands with chiral synthon* ***5*** *reacting as nucleophile.*

On the other hand, S.Orgué in her PhD thesis showed that synthon **4** after activation as mesylate can react with nucleophiles (particularly well with amines) in a completely stereospecific S_N2@P reaction. This opened the door to many different P-stereogenic compounds.

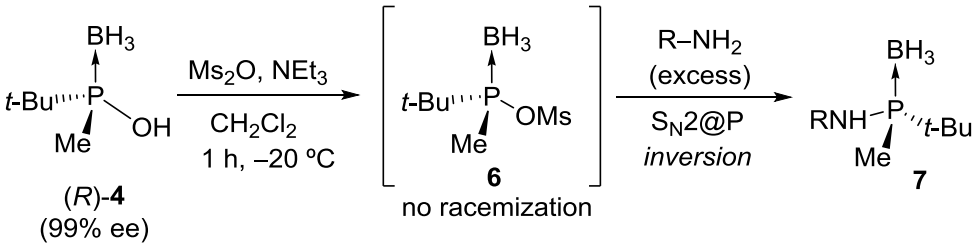

Figure 3. *Compound **4** reacts as electrophile in the S_N2@P type reaction with nucleophiles. No ee loss was observed.*

Synthon **4** is an invaluable compound for ligand synthesis, but it does have some drawbacks that hamper its extensive use. It is a difficult-to-handle gummy solid with a low melting point (54 – 56 ºC). Nevertheless, the main drawback of **4** probably is its limited stability. Upon storage, it decomposes to yield the corresponding secondary phosphine oxide and borane byproducts. We find it necessary to find a way to circumvent these issues, while preserving all of **4**'s reactivity.

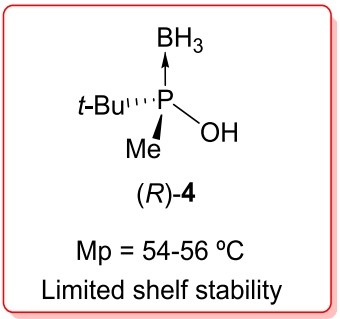

Figure 4. *Compound **4** is a low melting point gummy solid with limited shelf stability.*

P-stereogenic compound **8** was developed by Imamoto and co-workers and, although it is not a ligand itself, it is a very important P* building block.[7,8] Several noteworthy ligands such as Quinox-P*,[9] Benz-P*[10] or Pincer-P[11] are synthesized using **8**. Nonetheless, Imamoto's synthesis for **8** is not straightforward and has some weaknesses. S. Orgué in her PhD thesis studied the S_N2@P reaction of **4** with different hydride donors in order to afford **8** in a direct and simple manner. Although she managed

to produce **8**, the yields and selectivities were underwhelming. We believe that S. Orgué's synthetic approach has potential and we will attempt to improve the reaction's yield and selectivity to a satisfactory level.

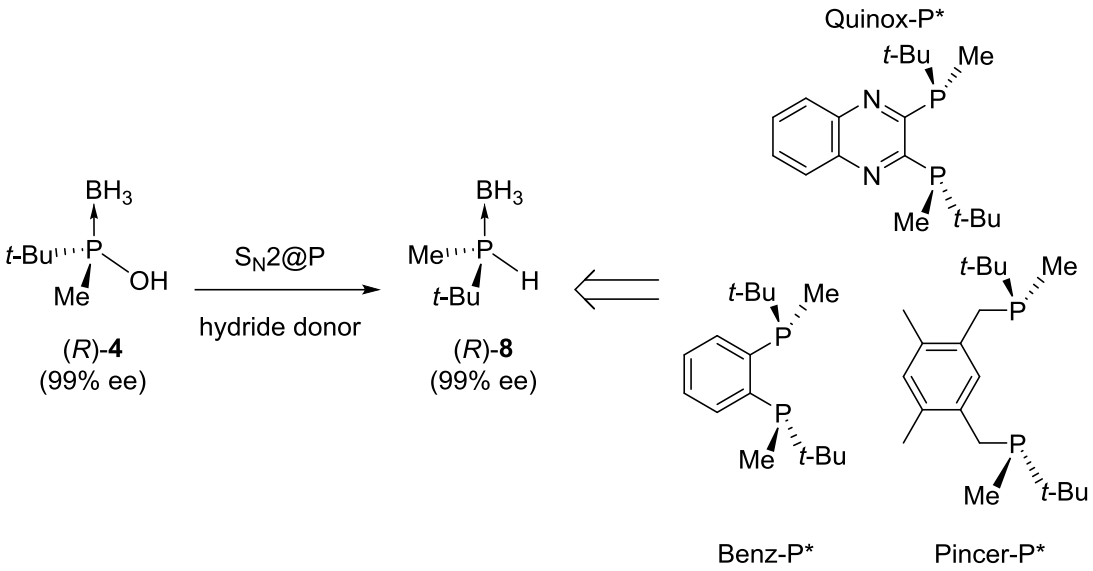

Figure 5. *Some relevant Imamoto's P-stereogenic ligands synthesized using **8**. Synthon **8** synthesis was attempted via S_N2@P reaction with **4**.*

The MaxPHOX ligand **10** was developed by S. Orgué in her PhD thesis.[4] First the oxazoline **9** was synthesized and then it was used in the S_N2@P with (S)-**4** to afford the MaxPHOX ligand **10**. This ligand coordinated to Ir and the resulting complex catalyzed different asymmetric reactions. The synthesis developed for ligand **10** was not robust and failed for other ligands with different substituents and configurations. We believe that the MaxPHOX ligands have a huge potential. However, it is mandatory to design a reliable and versatile synthesis that allows us to create a small ligand family.

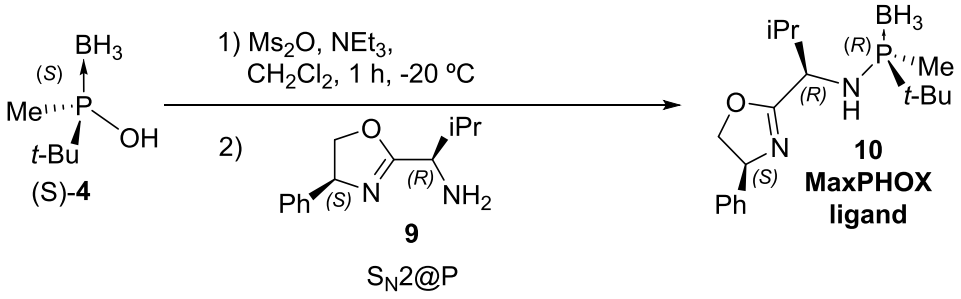

Figure 6. *S. Orgué's synthesis for the first MaxPHOX ligand.*

Once we have in our hands a small MaxPHOX family we intend to test them on the asymmetric hydrogenation of challenging substrates. Ir-P,N catalysts, such as the Ir-MaxPHOX, are often employed in the hydrogenation of imines. The asymmetric hydrogenation of imines such as **11** is very attractive as it can afford the corresponding chiral amine in a direct manner.[12–14] The resulting stereogenic amines are useful for the pharmaceutical and agrochemical industries. We will test the Ir-MaxPHOX complexes in the hydrogenation of these imines.

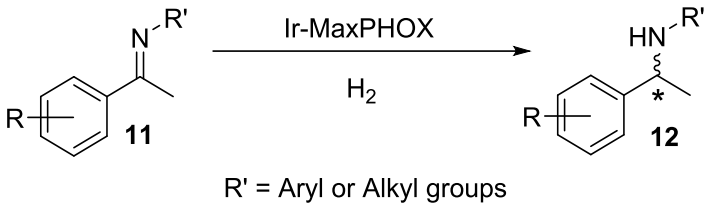

Figure 7. *Asymmetric hydrogenation of imines with Ir-MaxPHOX catalysts.*

We will attempt the hydrogenation of cyclic α- or β-enamides with the Ir-MaxPHOX catalysts.[15–21] Because these substrates possess an amide chelating moiety, they are usually hydrogenated with Rh or Ru catalysts. However, the hydrogenation with these complexes have never attained complete control over the selectivity for both α- or β-enamides. We believe that a different and novel approach like the one we propose might succeed.

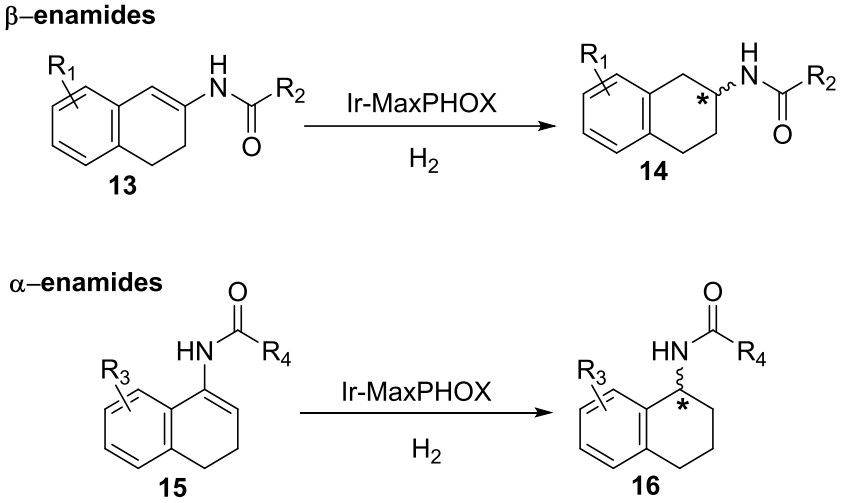

Figure 8. *Asymmetric hydrogenation of cyclic α- or β-enamides with Ir-MaxPHOX catalysts.*

- **Objective nº 1;** Overcome the drawbacks that synthon **4** presents while preserving its full reactivity range (this will be addressed in Chapter 3).

- **Objective nº 2;** Optimize an enantioselective and straightforward synthesis for Imamoto's synthon **8** using phosphinous acid **4** as precursor (this will be addressed in Chapter 2).

- **Objective nº 3;** Design and optimize a robust and reliable synthesis for the MaxPHOX ligands that allows us to create a small ligand family (this will be addressed in Chapter 5).

- **Objective nº 4;** Asymmetric hydrogenation of imines with the Ir-MaxPHOX catalysts (this will be addressed in Chapters 6 & 7).

- **Objective nº 5;** Asymmetric hydrogenation of cyclic α- or β-enamides with the Ir-MaxPHOX catalysts (this will be addressed in Chapter 8).

References

[1] A. Börner, *Phosphorus Ligands in Asymmetric Catalysis*, Wiley, **2008**.

[2] A. Grabulosa, J. Granell, G. Muller, *Coord. Chem. Rev.* **2007**, *251*, 25–90.

[3] T. León, A. Riera, X. Verdaguer, *J. Am. Chem. Soc.* **2011**, *133*, 5740–5743.

[4] S. Orgué, A. Flores-Gaspar, M. Biosca, O. Pàmies, M. Diéguez, A. Riera, X. Verdaguer, *Chem. Commun.* **2015**, *51*, 17548–17551.

[5] T. León, M. Parera, A. Roglans, A. Riera, X. Verdaguer, *Angew. Chem. Int. Ed.* **2012**, *51*, 6951–6955.

[6] E. Cristóbal-Lecina, P. Etayo, S. Doran, M. Revés, P. Martín-Gago, A. Grabulosa, A. R. Costantino, A. Vidal-Ferran, A. Riera, X. Verdaguer, *Adv. Synth. Catal.* **2014**, *356*, 795–804.

[7] K. Nagata, S. Matsukawa, T. Imamoto, *J. Org. Chem.* **2000**, *65*, 4185–4188.

[8] T. Miura, H. Yamada, S. Kikuchi, T. Imamoto, *J. Org. Chem.* **2000**, *65*, 1877–1880.

[9] T. Imamoto, K. Sugita, K. Yoshida, *J. Am. Chem. Soc.* **2005**, *127*, 11934–11935.

[10] K. Tamura, M. Sugiya, K. Yoshida, A. Yanagisawa, T. Imamoto, *Org. Lett.* **2010**, *12*, 4400–4403.

[11] B. Ding, Z. Zhang, Y. Liu, M. Sugiya, T. Imamoto, W. Zhang, *Org. Lett.* **2013**, *15*, 3690–3693.

[12] J. H. Xie, S. F. Zhu, Q. L. Zhou, *Chem. Rev.* **2011**, *111*, 1713–1760.

[13] N. Fleury-Brégeot, V. de la Fuente, S. Castillón, C. Claver, *ChemCatChem* **2010**, *2*, 1346–1371.

[14] K. H. Hopmann, A. Bayer, *Coord. Chem. Rev.* **2014**, *268*, 59–82.

[15] J. L. Renaud, P. Dupau, A.-E. Hay, M. Guingouain, P. H. Dixneuf, C. Bruneau, *Adv. Synth. Catal.* **2003**, *345*, 230–238.

[16] C. Pautigny, C. Debouit, P. Vayron, T. Ayad, V. Ratovelomanana-Vidal, *Tetrahedron: Asymmetry* **2010**, *21*, 1382–1388.

[17] X. Bin Jiang, L. Lefort, P. E. Goudriaan, A. H. M. De Vries, P. W. N. M. Van Leeuwen, J. G. De Vries, J. N. H. Reek, *Angew. Chem. Int. Ed.* **2006**, *45*, 1223–1227.

[18] I. Arribas, M. Rubio, P. Kleman, A. Pizzano, *J. Org. Chem.* **2013**, *78*, 3997–4005.

[19] G. Liu, X. Liu, Z. Cai, G. Jiao, G. Xu, W. Tang, *Angew. Chem. Int. Ed.* **2013**, *52*, 4235–4238.

[20] H. Bernsmann, M. Van Den Berg, R. Hoen, A. J. Minnaard, G. Mehler, M. T. Reetz, J. G. De Vries, B. L. Feringa, *J. Org. Chem.* **2005**, *70*, 943–951.

[21] Q. Z. Jiang, D. M. Xiao, Z. G. Zhang, P. Cao, X. M. Zhang, *Angew. Chem. Int. Ed.* **1999**, *38*, 516–518.

Chapter 1

P-Stereogenic Ligands

-Background-

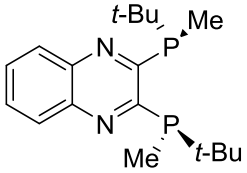

QuinoxP*
Imamoto - 2005

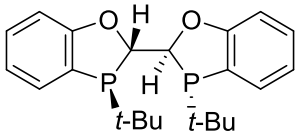

BIBOPs
Senanayake - 2010

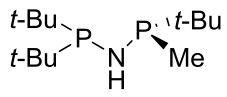

MaxPHOS
Verdaguer - 2010

1.1 P-Stereogenic and non P-Stereogenic Chiral Ligands: An historical overview

Over 150 years ago, in 1848, the French chemist and microbiologist, Louis Pasteur, discovered molecular chirality.[1] It was not until 1889 when the German Emil Fischer published the first asymmetric transformation as a result of his work with sugars.[2,3] Some twenty-two years later, in 1911, Meisenheimer and Lichtenstadt identified the first chiral phosphine oxide.[4] This chiral phosphine oxide was synthesized in a laboratory, as chiral phosphines do not spontaneously occur in nature. Fifty years from then, in 1961, Horner described the first chiral trivalent phosphine.[5] Surprisingly, unlike amines, this compounds did not racemize at room temperature. Taking this into account and also considering the fact that free phosphines coordinate remarkably well with metals useful in catalysis, such as Ru, Rh, Pd or Ir, it is not a surprise that chiral phosphines play a major role in many asymmetric catalytic procedures. [6]

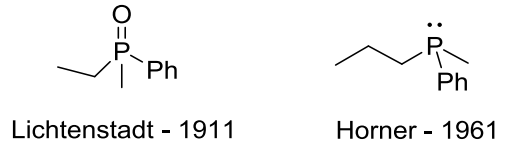

Figure 1. *Lichtenstadt discovered the first chiral tetravalent phosphine oxide. Horner isolated the first chiral trivalent phosphine.*

Wilkinson was the first to use a phosphine (triphenylphosphine) in a catalytic hydrogenation, albeit a non-asymmetric one.[7] Following Wilkinson's lead, Knowles and Horner published respectively in 1968 the first asymmetric and catalytic hydrogenations of olefins by using (*S*)-methylphenylpropyl phosphane / Rh.[8,9]

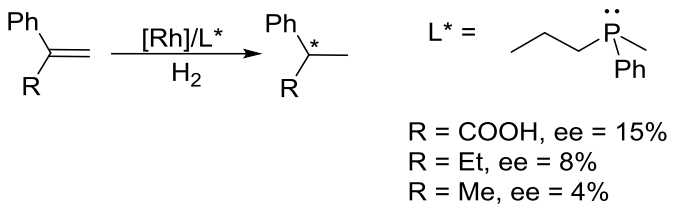

Figure 2. *First asymmetric catalytic hydrogenations.*

In the early 60's, L-DOPA (L-3,4-dihydroxyphenylalanine) was discovered as an useful drug for the treatment of Parkinson's disease. This lead to a spike in the demand for this natural occurring, non-standard amino acid. There was not an industrially

effective enantioselective synthesis for the drug at the time and the continuous necessity for more L-DOPA became the driving force behind the research for new catalysts for enantioselective hydrogenations.

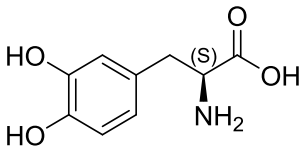

Figure 3. *Parkinson's disease drug L-DOPA.*

Knowles again was quick to react and presented the CAMP ligand.[10,11] This chiral monophosphine ligand, combined with Rh, produced L-DOPA in 85% ee through asymmetric hydrogenation. It was such a success at the time that the Montsanto Company scaled up the procedure to an industrial level.

However, Knowles did not settle for that result and focused his attention on bidentate phosphine ligands. He rationalized that by limiting the degrees of freedom at the catalyst center, the selectivity could be increased. Thus the DIPAMP ligand was developed.[12] This ligand, synthesized by dimerizing the monophosphine PAMP,[13] succeeded in hydrogenating various α-acetamidoacrylic acids with enantiomeric excesses up to 96%.

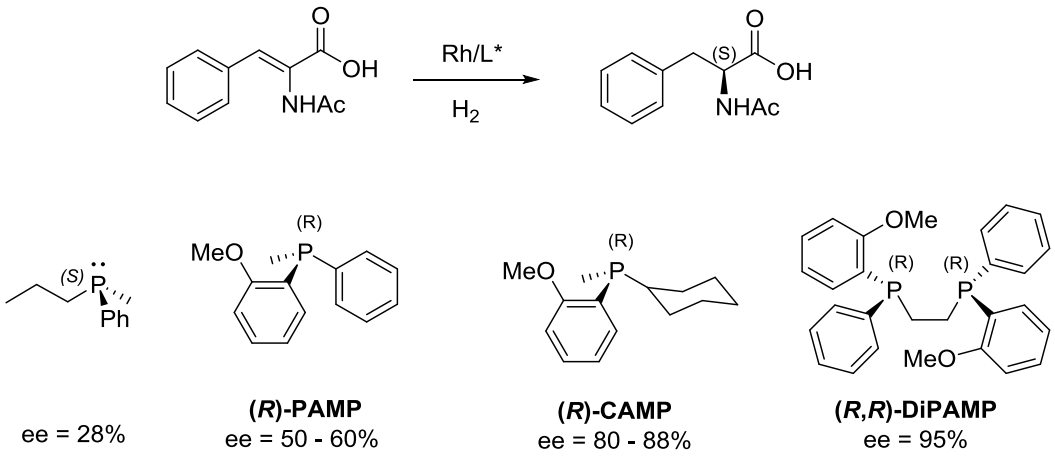

Figure 4*. Asymmetric catalytic reduction of an α-acetamidoacrylic acid.*

Concurrently, Dang and Kagan were developing the DIOP ligand.[14] This ligand, with the chirality contained not in the phosphorous atoms, but in the C-backbone, afforded ee's up to 80% on the asymmetric hydrogenation of α-amino acids;[15] similar results to the ones obtained with CAMP, and thus proving that the chirality does not have to be specifically in the P atoms to be properly transmitted into the substrate. Following this lead, other ligands like ChiraPHOS,[16] BPPFA[17] or BINAP[18,19] appeared. This last compound possesses axial chirality and is one of the most noteworthy ligands in asymmetric catalysis. About ten years later, Burk and co-workers introduced the DuPHOS ligand.[20,21] To the date, DuPHOS complexes still have one of the largest scopes of substrates. At that time, ruthenium complexes also started showing some use in catalysis and the substrate scopes expanded even further.

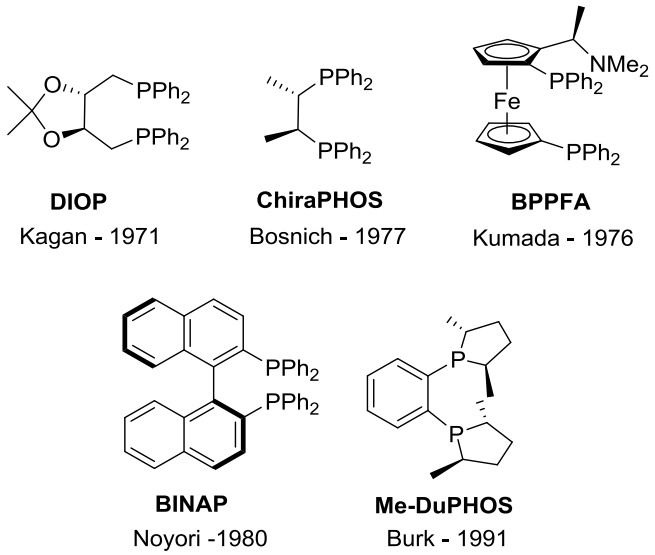

Figure 5. *Catalysts with non-stereogenic phosphorous.*

With all this success with non P-sterogenic ligands and the lack of efficient methods to obtain P-stereogenic compounds, the development of new P-stereogenic ligands was slow until the 90's, when Evans[22] and Jugé[23] reported new methodologies for the synthesis of those. As a consequence, ligands like QuinoxP*,[24] TangPHOS,[25] TCFP[26] or BIBOPs[27] showed up and excellent results came along with them.

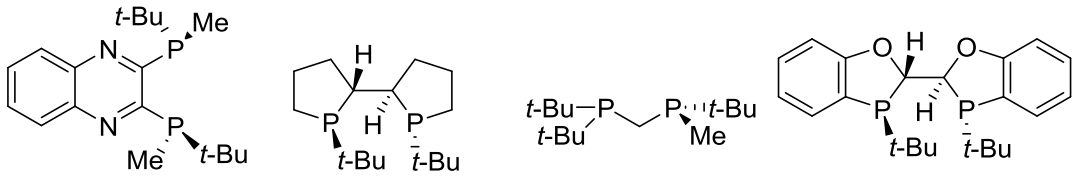

Figure 6. *Catalysts with stereogenic phosphorous.*

To the date, research groups struggle to produce new and better ligands and catalysts to broaden the scope and increase even more the conversions and ee's. This competition's finishing line is set on perfection and is still far away from where we stand.

1.2. Synthesis of P-stereogenic compounds

Chiral phosphorous does not occur naturally and it has to be obtained in a laboratory. There is more than one method for that.

a) Racemic mixtures resolution: One of the principal problems with this procedure is the inherent issue of having the yield cut down to at least 50%. Separation of enantiomers from a racemic mixture can be achieved by chiral HPLC or through crystallizations. Purification by HPLC has several disadvantages,[28] not least among them the cost of it. Purification through crystallization also has its flaws, like the difficulty of crystallizing only one of the two salt diastereoisomers, which can take several repetitions and only works for some cases. The yields obtained are usually low, plus one of the enantiomers is often harder to obtain than the other.

One example of this is Stankevic's and Pietrusiewicz's methodology for obtaining *tert*-butylphenylphosphinous acid borane **1.1**.[29] Using ephedrine and cinchonine in two consecutive crystallizations both enantiomers of 1 can be obtained with 31 and 34% yield, respectively.

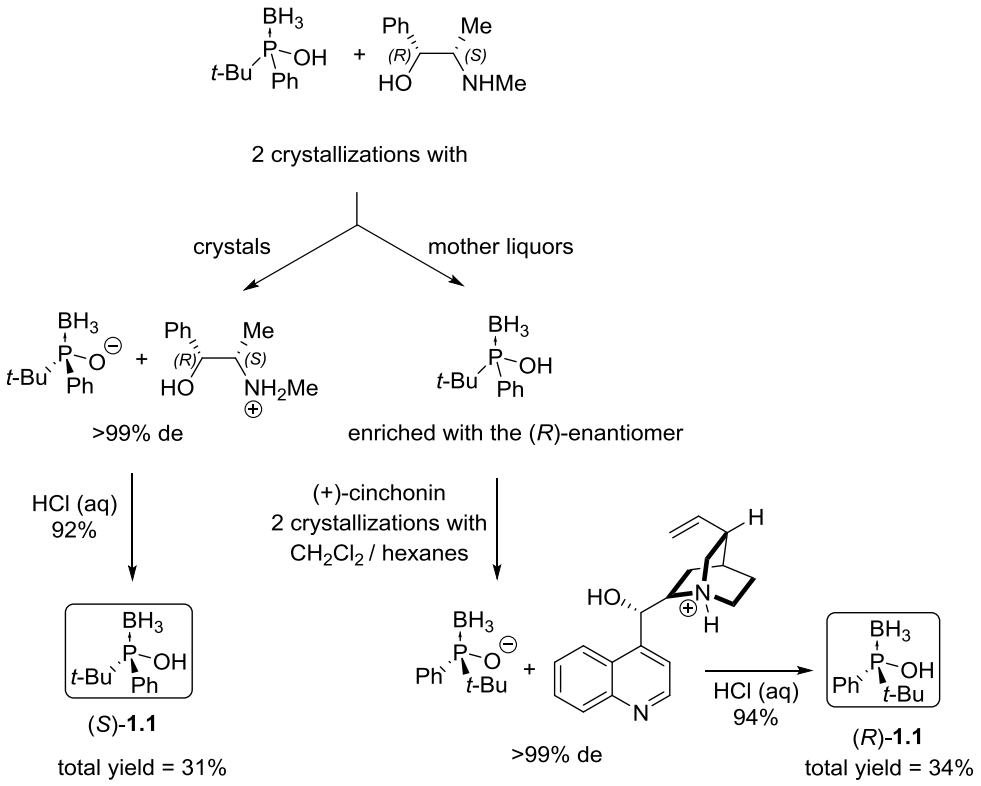

Figure 7. *Stankevic's and Pietrusiewicz's synthesis of (S) and (R)-**1.1**.*

b) Stereoselective synthesis: These methodologies rely on inducing chirality into the phosphorous compounds through stereoselective reactions. By using a chiral auxiliary, like alcohols or amines, one of the two enantiomers is favored. Ideally, this methodology could allow to obtain P-stereogenic compounds with full yields, unlike when using chiral resolution that the yields can never top 50%.

1.2.1. Menthol as chiral auxiliary

By the end of the 60's, Cram[30] and Mislow[31,32] reported the synthesis of menthyl phosphinates by reacting methylphenylphosphinic chloride and menthol under the presence of a base (Figure 8). These can be then transformed with Grignard reagents, which react in a complete S_N2@P manner. The tertiary phosphine oxides obtained can be reduced to the tertiary phosphines with $HSiCl_3$ (Figure 9a).

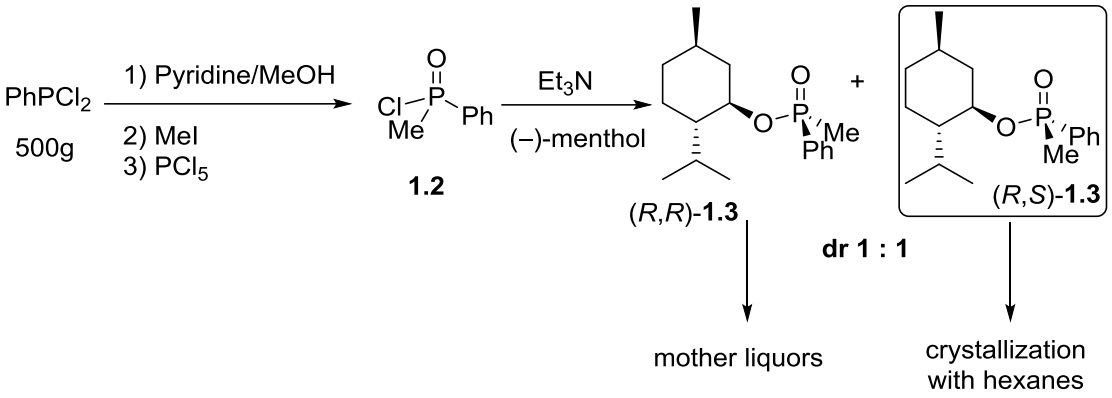

Figure 8. *Synthesis of stereogenic phosphines by using chiral auxiliaries.*

Imamoto reported a variation of the methodology that uses borane protected chlorophosphines (Figure 9b).[33] Once substituted with the menthol, these borane phosphinites can also react with Grignard reagents or the menthol can be cleaved with a Li-NH_3 reduction and then reacted with electrophiles, either way affording phosphine borane compounds. The borane is easily removed using Et_2NH.

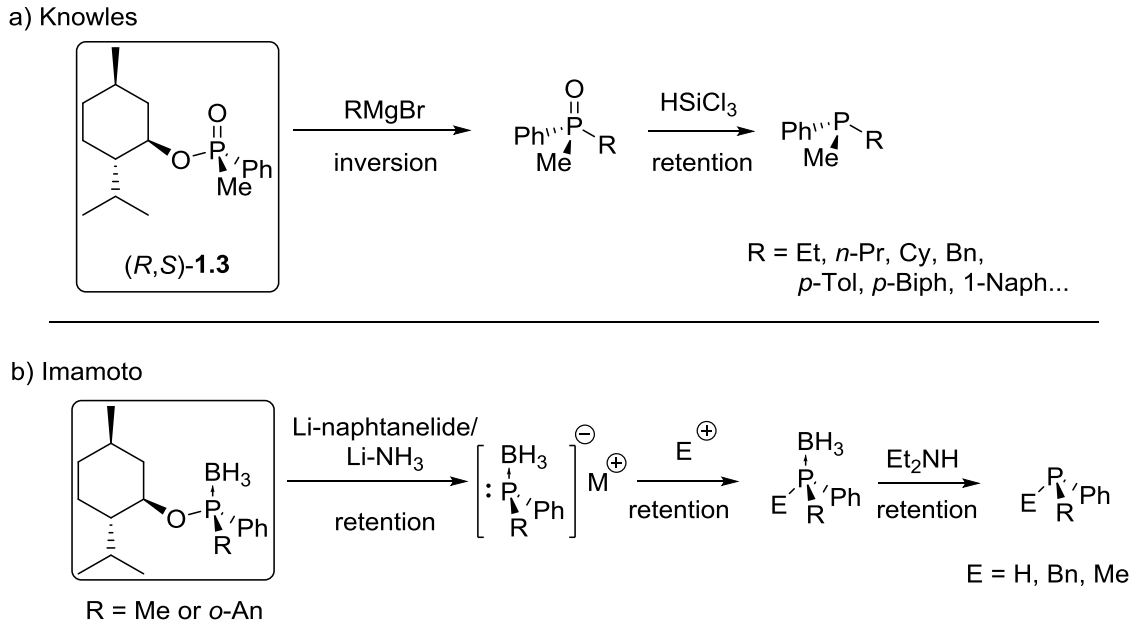

Figure 9. *a) Knowles synthesis with Gringnard reagents. b) Imamoto's synthesis using the phosphine as a nucleophile.*

Both Knowles[34] and Imamoto[35] used the "menthol methodology" to synthesize DiPAMP; the first employed the original method, using the menthyl phosphinate and Imamoto took advantage of the borane protected phosphinite. (Figure 10**)**

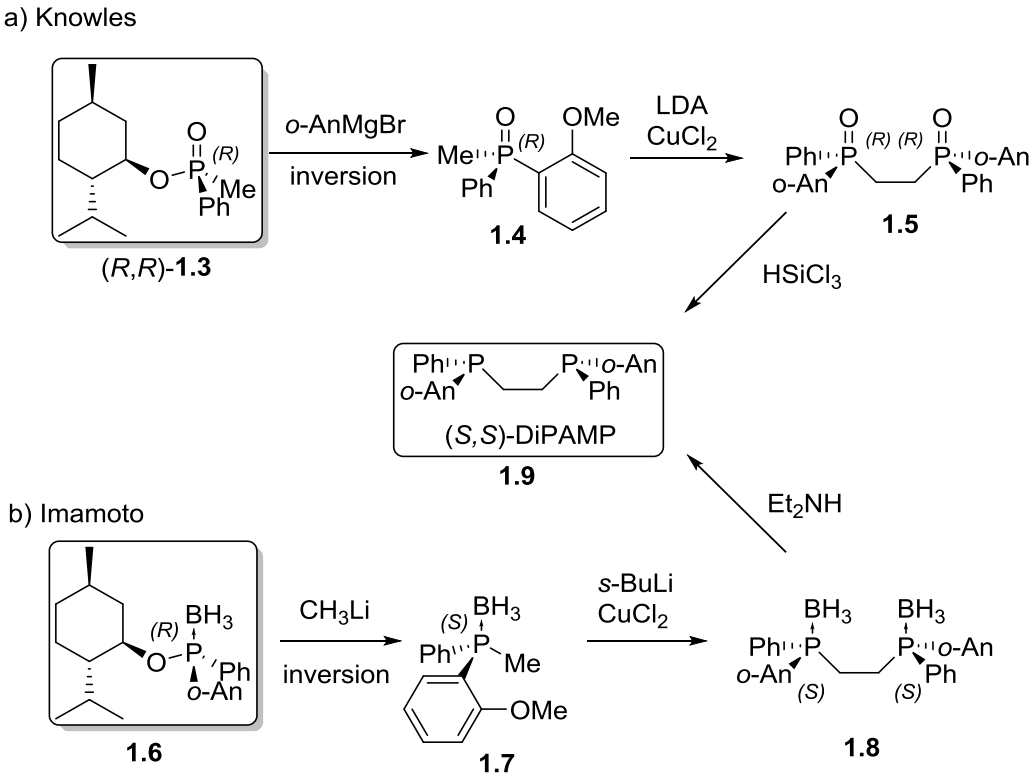

Figure 10. *Knowles' and Imamoto's routes towards the DiPAMP ligand.*

Buono[36] and Han[37] also used menthol to report the synthesis of optically pure SPO's, thus showing again the usefulness of the method.

There is a serious drawback for the menthol methodology: the formation of the methyl phosphinate affords a 1:1 diastereomeric mixture that has to be separated, cutting the yield down at least to 50%. As an alternative, there are reactions with chiral alcohols or amines that under certain conditions can afford non-equal diastereomeric mixtures due to dynamic kinetic resolution.[38–40] Next, we will provide some insights on them.

1.2.2. Amines as chiral auxiliaries

The first reaction between a phosphine chloride (III) and a chiral amine was reported in 2003 by Kolodiazhnyi.[41] With the presence of a tertiary base and optimized conditions (solvent and temperature), the reaction occurs with a certain amount of estereoselectivity due to dynamic kinetic resolution. Then, protection of the free amino phospine with borane allows for the crystallization of one of the diastereoisomers. Afterwards, the borane group can be removed to afford again the free optically pure phosphine.

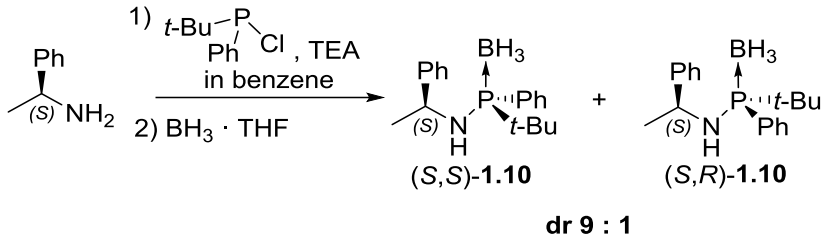

Figure 11. *Kolodiazhnyi's use of chiral amines as auxiliaries and DKR.*

Our group further developed the scope of this methodology.[42] We studied the reaction of chiral amines with (*rac*)-*t*-BuMePCl. The final reaction conditions are depicted in Figure 12. Although higher dr's were obtained with other amines, phenylglycinamide provided a mixture of diastereoisomers that were easily separated by crystallization. The procedure can be scaled up to multigram scale.

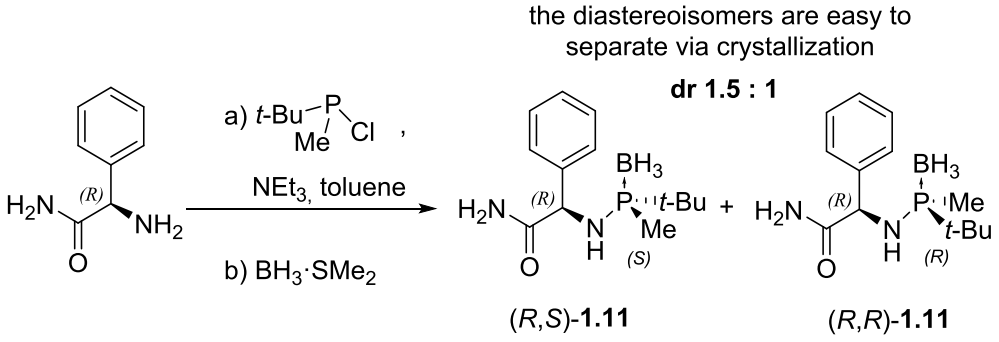

Figure 12. *Our group's methodology for the synthesis of stereogenic phosphines with chiral auxiliaries.*

Our group also studied the reductive cleavage of the benzylic bond with Li/NH_3, which afforded compound **1.12**. This synthon is key for the synthesis of phosphorous bidentate ligands such as **MaxPHOS**,[43] useful for many asymmetric hydrogenations, or the **SIP**[44] family of ligands (phosphinosulphinamides), efficient on the intramolecular cycloaddition of terminal enediynes.

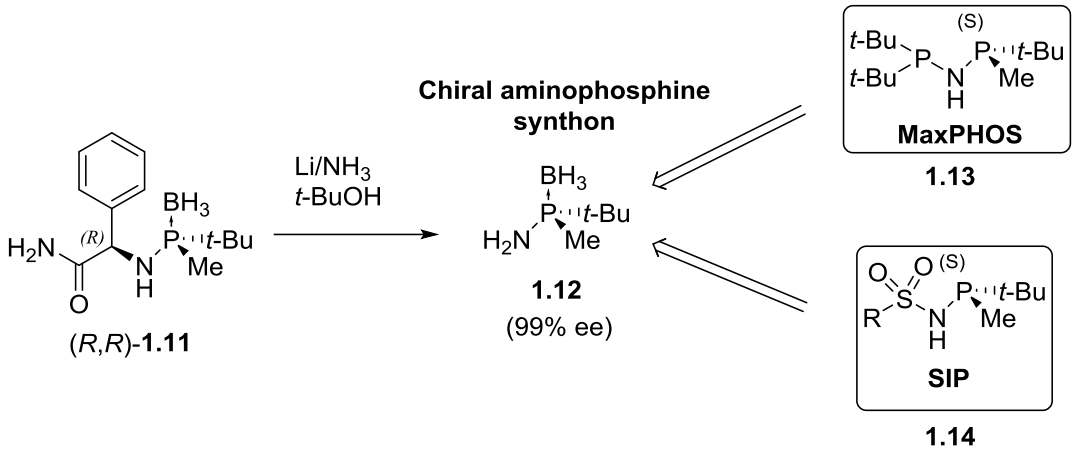

Figure 13. *Benzylic bond cleavage with Li/NH_3. Aminophosphine **2** is a key synthon for the synthesis of P* ligands.*

1.2.3. Bifunctional heterocycles as chiral auxiliaries; Juge's method

As mentioned before, Grignard and organolithium reagents perform nucleophilic substitutions on P(III) and (V) atoms. Taking advantage of this well stablished methodology, Jugé[23] and Corey[45] developed a new procedure to obtain chiral phosphines.

Figure 14 depicts the idea's core concept. An intermediate such as **III** is necessary. **A** and **B** are leaving groups tethered by a chiral backbone. First, the P—A bond is cleaved by addition of a new group (R_2). Then it is P—B that is cleaved and a second group gets in (R_3). The chiral auxiliary can be recycled.

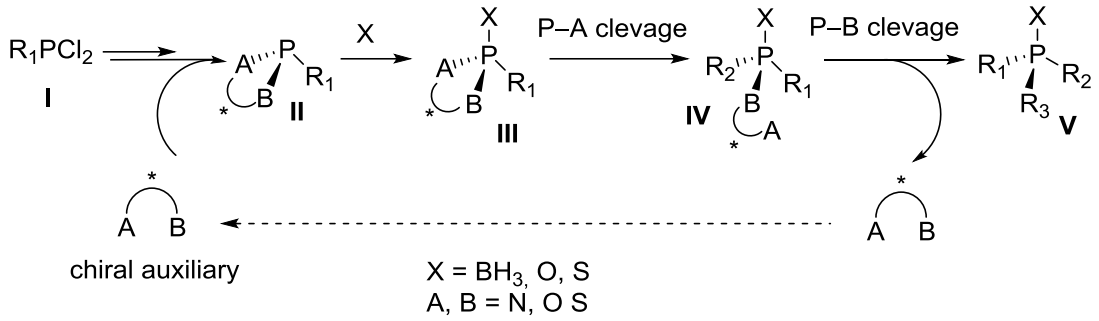

Figure 14. *Bifunctional heterocycles as chiral auxiliaries.*

Jugé and Stephan's synthesis consists of 5 steps. Ephedrine acts as the chiral auxiliary. R_1 was originally a Ph group. However, several different groups have proven to be suitable despite of a few exceptions.

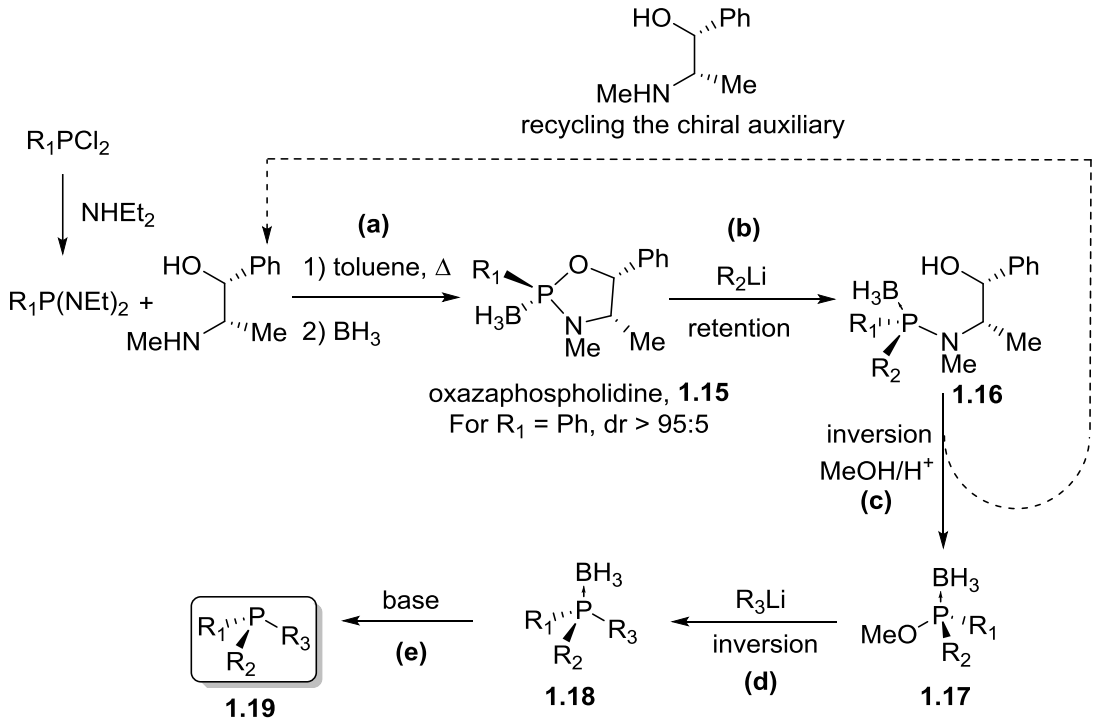

Figure 15. *Jugé and Stephan's method to synthesize chiral phosphines.*

a) It begins with the formation of the heterocycle by reacting a dichlorophosphine with $NHEt_2$ and then with ephedrine. The diastereoisomer **3** (R_1 = Ph) is formed with a dr over 95%. After crystallization, **3** can be obtained as a pure diastereroisomer with 80% yield.

b) An organolithium reagent is added. This procedure, while selectively breaking the P—O bond, adds the R_2 group to the phosphorous atom. Different alkyl and aryllithium reagents were tested on **3** (R_1 = Ph) and for most cases good yields and dr's over 98 : 2 were achieved. Nevertheless, Mezzetti and co-workers studied this reaction and reported very low yields or even no reaction for very hindered organolithium compounds such as 2,4,6-trimethoxyphenyl)lithium.[46]

c) The next step in the synthesis is the methanolysis of the P—N bond using MeOH and sulphuric acid in anhydrous conditions. The chiral auxiliary ephedrine can be recovered and reused. Steric hindrance is again an issue; the reaction does not perform well or at all with highly hindered compounds such as *tert*-butyl or ferrocenyl aminophosphines.

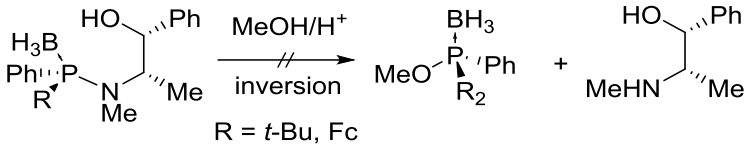

Figure 16. *Methanolysis does not work with bulky R groups on the P.*

d) By addition of an alkyl or aryllithium over the methyl phosphinite we obtain the phosphines **1.18** with good yields and ee. However, once more it does not work properly or at all for hindered organolithium compounds such as *t*-BuLi or MesLi.

e) The last step consist of the deprotection of the phosphine by removing the borane group with a base like $HNEt_2$.

Summarizing, Jugé's method is remarkably good for synthesizing new tertiary phoshpines at multigram scale. Nevertheless, it has a main drawback: the impossibility to synthesize highly hindered phosphines (e.g., *t*-Bu/Ph or *t*-Bu/Me substituted phosphines). The P—N bond in **1.16** is not exceptionally reactive with organolithium compounds, hence, Jugé uses a methanolysis on the compound to create the reactive enough P—O bond. However, very hindered phosphines cannot undergo this transformation either.

Hindered phosphines are rather interesting as they have showed great effectiveness in asymmetric procedures like hydrogenations[43,47–51], hydroborations,[52] aldol reactions[53] or hydroacylations[54] among others. That is why several groups, ours

among them, have been working on developing new methodologies for the synthesis of these compounds. Next we will report two of such methods: Verdaguer's and Senenayake's.

1.2.3.1. *cis*-1-amino-2-indanol as chiral auxiliary; Verdaguer's method

Our group used *cis*-1-amino-2-indanol in the synthesis of highly hindered P-stereogenic compounds. *cis*-1-amino-2-indanol had been previously reported as a chiral auxiliary for the preparation of enantiopure sulfoxides.[55,56]

In Figure 17 we depict the synthesis for phosphine synthons (*R*)-**1.22** and **1.12**, substituted with a *t*-Bu/Me combination.[44,57,58] Although other combinations, like *t*-Bu/Ph, are also possible, in the next few pages the focus will be on the *t*-Bu/Me combination due to its great effectivity in asymmetric catalysis (big/small group).

The synthetic route starts with the formation of the oxazaphospholidine compound. Reaction between *cis*-1-amino-2-indanol and *tert*-butyldichlorophosphine in the presence of diethyl amine affords the heterocycle **1.20** after protection of the free phosphine with borane. Then, reaction with different Grignard reagents is possible, such as MeMgBr or PhMgBr. Compound **1.21** is a key molecule because from it we can access both chiral synthons (*R*)-**1.22** and **1.12**.

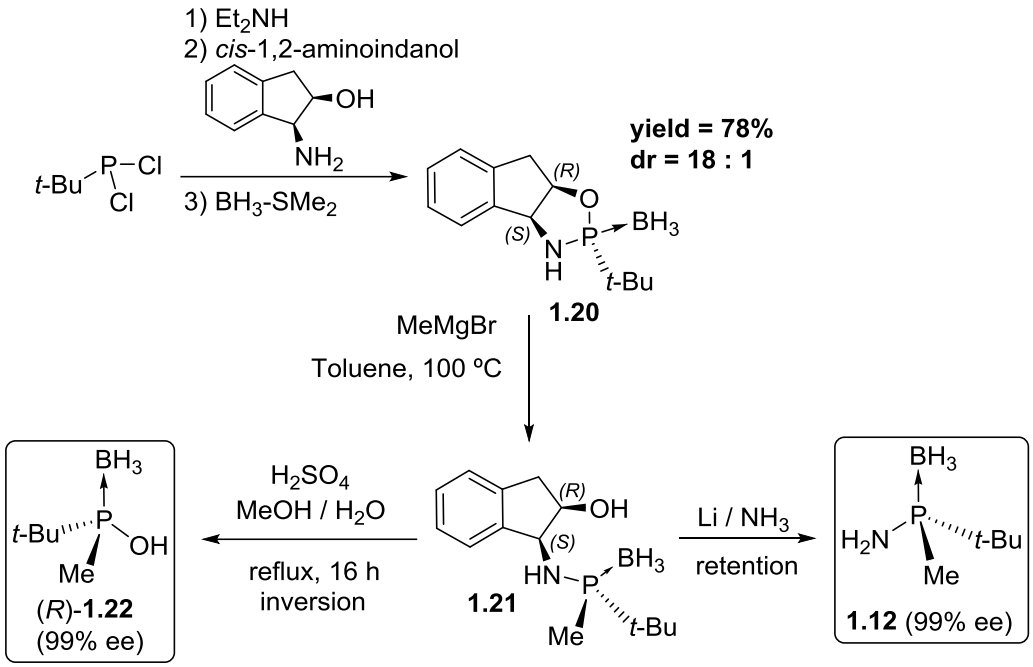

Figure 17. *Synthesis of chiral synthons aminophoshpine* ***1.12*** *and phosphinous acid (R)-****1.22****.*

On one hand, chiral aminophosphine **1.12** can be accessed by cleaving the benzylic C—N bond with a Li/NH_3 reduction. No ee is lost during the transformation. Aminophosphine **1.12**, as reported previously, is a precursor for many interesting ligands such as MaxPHOS or the SIP family. To synthesize these ligands, synthon **1.12** acts as a nucleophile. The amino group can be deprotonated with a strong, non-nucleophilic base such as NaH.

On the other hand, chiral phosphinous acid (*R*)-**1.22** is afforded through methanolysis of compound **1.21**. Contrary to the formation of aminophosphine **1.12**, this reaction occurs with inversion of configuration. Once more, the ee is preserved. Phosphinous acid (*R*)-**1.22** plays a crucial role on the synthesis of new P-stereogenic ligands in our group and complements aminophosphine **1.12** reactivity: while aminophosphine **1.12** is used as a nucleophile, (*R*)-**1.22** phosphinous acid can be used as an electrophile.

To understand how (*R*)-**1.22** can be used as an electrophile we first have to take a look at the research performed by Pietrusiewicz[29] and Buono[59] respectively. The first reported the activation of phosphinous acid (*S*)-**1.1** with MsCl, followed by the

nucleophilic reduction with $NaBH_4$ to the phosphine borane, without any ee loss (S_N2@P). Buono expanded the methodology to other aryl groups (Figure 18) by lightly modifying the reaction conditions during the phosphinous acid activation. The reduction to the phosphine borane required no modification. Buono's activation method, like Pietrusiewicz's, proceeded without any chirality loss.

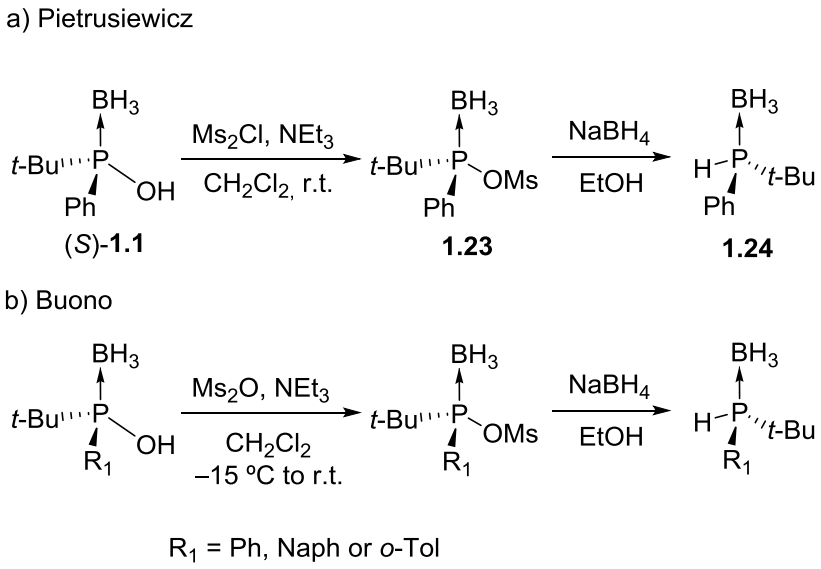

***Figure 18**. Pietrusiewicz and Buono's reduction of phosphinous acids to phosphine boranes.*

However, neither of them had a procedure to obtain the phosphinous acid (*R*)-**1.22** (combination '*t*-Bu/Me') and consequently they could not study the activation/reduction reactivity on this synthon. Our group, possessing an easy way to obtain synthon (*R*)-**1.22**, decided to investigate this reactivity on it. We soon noticed that **1.25** was less stable, once activated, than the *t*-Bu/aryl combinations. After many studies we found a set of strict conditions and managed to stabilize the phosphinyl-mesyl anhydride without any racemization. We then tested different nucleophiles on it. Unfortunately, the reduction with $NaBH_4$, analogous to Pietrusiewicz's and Buono's, does not proceed at the low temperatures required for stabilizing the intermediate. Although the S_N2@P reaction does not occur with $NaBH_4$, it does work with many other nucleophiles, for example primary and some secondary amines. As showed in Table 1, we can access many aminophosphines using the methodology described below.

Table 1. Activation of (*R*)-**1.22** and S_N2@P with amines as nucleophiles

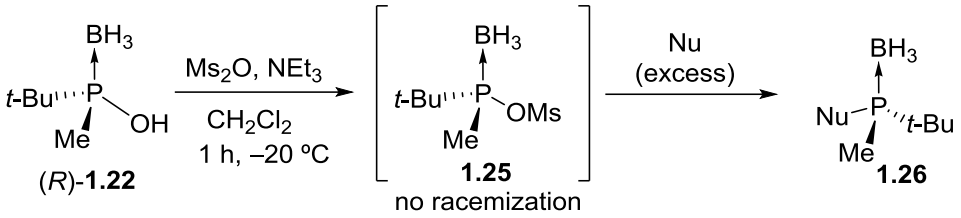

Entry	Nucleophile	Yield (%)[a]	ee/de[b]
1	NH_3	**99**	**96% ee**
2	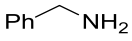	**60**	**98% ee**
3	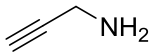	**64**	**>95% ee**
4	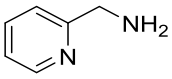	**87**	**99% ee**
5	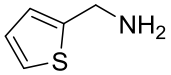	**73**	**96% ee**
6	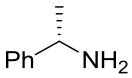	**76**	**98% de**
7	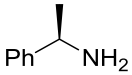	**71**	**95% de**
8	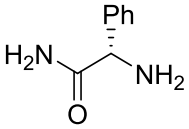	**63**	**97% de**
9		**65**	**98% ee**
10	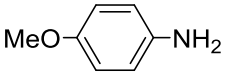	**42**	**91% ee**
11	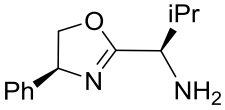	**43**	**>97% de**

a) Isolated yield after flash column chromatography. b) Enantiomeric excess was determined by either chiral GC or HPLC analysis. Diastereomeric excess determined by ^1H NMR of the crude reaction. c) Optical purity of Entry 3 was assigned tentatively by analogy with similar primary amines tested.

Two relevant cases reported in Table 1 are further discussed next;

a) Entry 1 / Reaction with NH_3 (g): The S_N2@P with ammonia gas is extremely fast (less than 5') and more importantly, it affords also the key synthon, aminophosphine **1.12**. The aminophosphine can also be transformed back to the phosphinous acid through a hydrolytic cleavage. Both reactions are completely enantioselective, thus allowing the easy transformation from one to another.

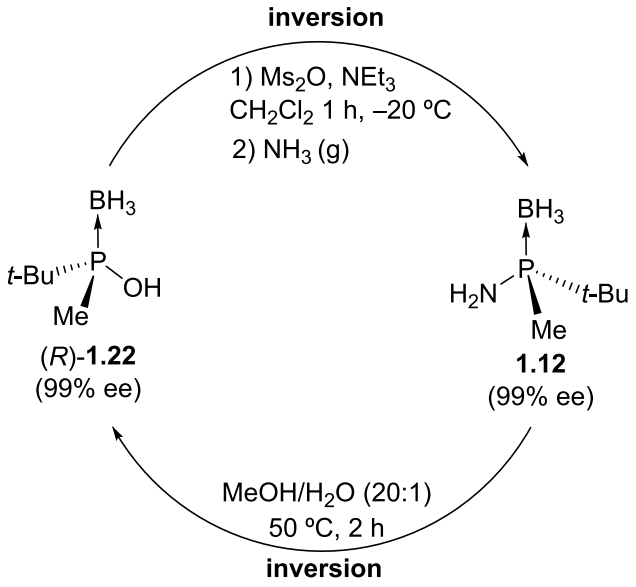

***Figure 19. 1.22** and **1.12** can afford each other without any ee loss.*

b) Entry 11 / The MaxPHOX ligands: Reaction of **1.25** with a chiral amino oxazoline in Entry 11 is most-valuable as it allows for the selective synthesis of the MaxPHOX ligands. These ligands have been crucial for the present PhD thesis. They will be more thoroughly discussed next.

1.2.3.1.1. The MaxPHOX ligands

The first MaxPHOX ligand (**1.30**) was synthesized using the methodology shown in Figure 20. As we studied different ligand configurations and substituents, we soon realized that this initial route had several shortcomings and was not able to afford MaxPHOX ligands other than **1.30**. Hence, a new synthesis was required. This issue has been addressed during the present PhD thesis and will be further discussed in Chapter 5.

The original route first synthesizes the amino oxazoline **1.29**. This amine is then utilized in the S_N2@P reaction with chiral phosphinous acid (*S*)-**1.22**.

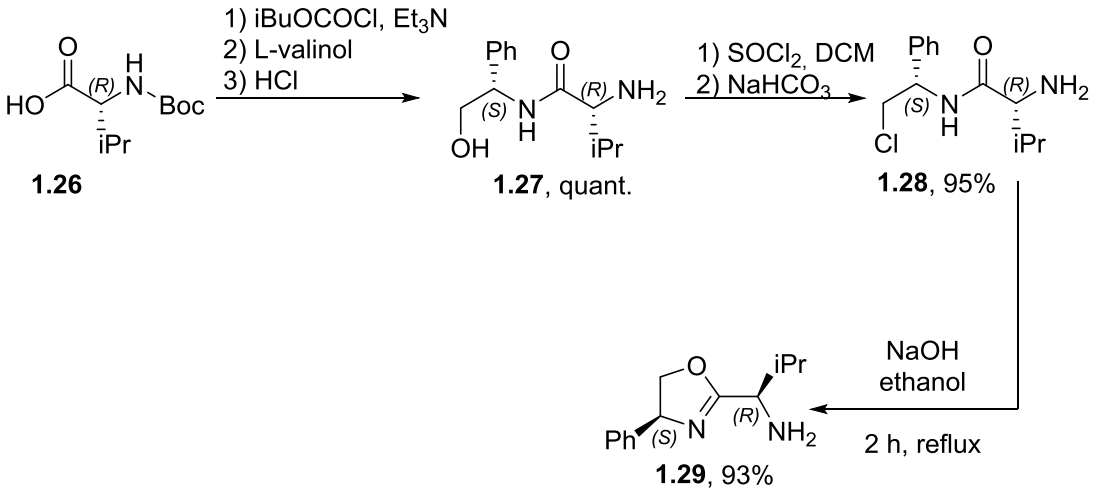

Figure 20. *Synthesis of amino oxazoline* ***1.29****.*

The route for the amino oxazoline **1.29** synthesis begins with the coupling of the Boc-protected aminoacid **1.26** with L-valinol. Then the Boc protecting group is removed under acidic conditions. This is followed by the transformation of the alcohol moiety to a chlorine. Finally, under strong basic conditions the compound undergoes a cyclization to form the oxazoline ring. Once the amino oxazoline **1.29** is obtained, it can be used on the S_N2@P reaction (Figure 21).

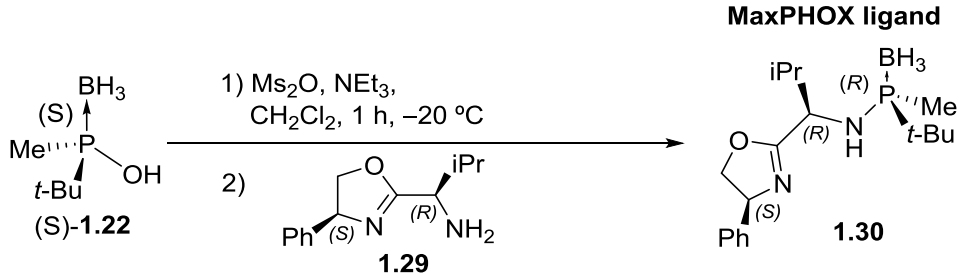

Figure 21. *S_N2@P with chiral amino oxazoline* ***1.29*** *to afford a MaxPHOX ligand.*

The MaxPHOX ligands, with three independent chiral centers that can be modulated at will, hold an enormous potential for asymmetric catalysis.

1.2.3.2. *N*-tosyl-2-(1-aminoethyl)-4-chlorophenol as chiral auxiliary; Senanayake's method

The first step in this route is the diastereoselective formation of oxazaphosphinane **1.32**. Compound **1.32** can be reacted with organometallic compounds; procedure that cleaves the P—N bond over the P—O one. Finally, by an addition of a second organometallic reagent, the P—O bond is cleaved, affording the corresponding tertiary phosphine oxide **1.34**. It is noteworthy that the chiral auxiliary contains specifically selected electrowithdrawing groups like the tosyl or the chloride in order to respectively activate the P—N and the P—O bonds, thus allowing for the sequential substitutions.

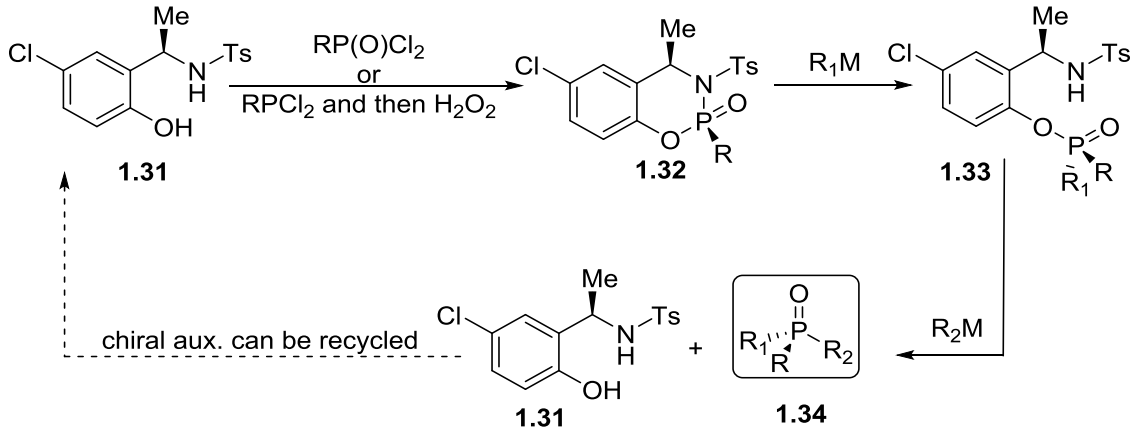

Figure 22. *Senanayake's methodology for the synthesis of chiral phosphine oxides*.

With this methodology Senanayake has developed many relevant ligands such as the BI-DIME,[60] the MeO-POP,[61] the MeO-BiPOP[27] or the BoQPHOS[62] ligands that are suitable for many asymmetric catalyses.

1.2.4. Enantiotopic methyl selective deprotonation

In 1995 Evans reported a methodology to synthetize P-stereogenic compounds by enantioselectively deprotonating proquiral phosphorous compounds using the chiral amine sparteine.[22] As depicted in Figure 23, borane protected dimethylphenylphosphine is treated with *s*-BuLi and sparteine. The resulting chiral salt can be reacted with electrophiles (E^+) or even Cu salts to form C_2 diphosphines with excellent ee's.

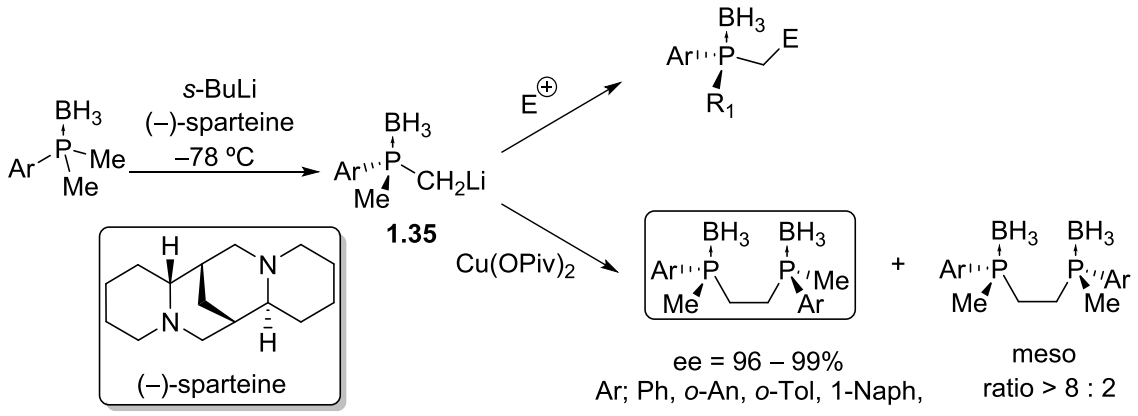

Figure 23. *Evan's synthesis of chiral phosphines by enantiotopic methyl selective deprotonation.*

Imamoto soon realized the huge potential of this methodology and expanded its scope to trialkyl phosphines (at the time the reaction had only been applied to aryldialkylphosphines). In Figure 24 we present a general and schematic overview of Imamoto's contributions on the subject.

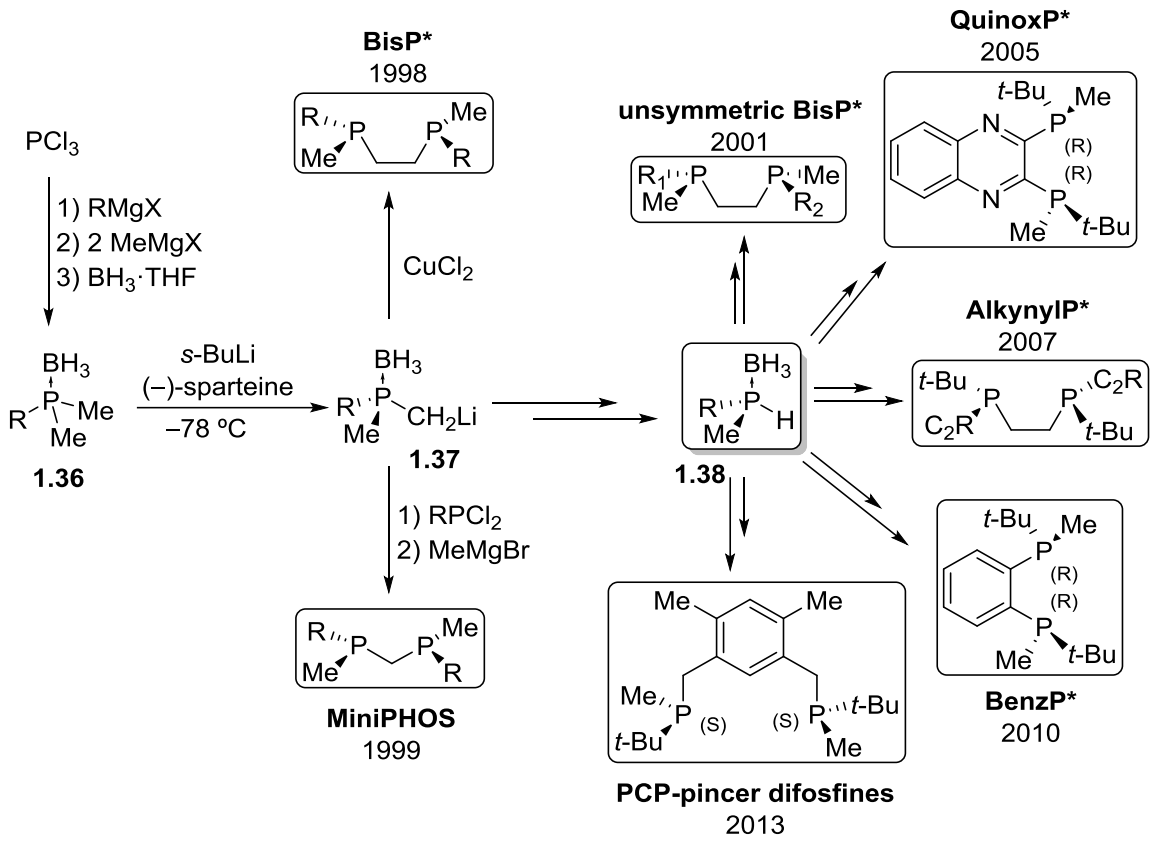

Figure 24. *Ligands developed in Imamoto's group by enantiotopic methyl selective deprotonation.*

Compound **1.37** can be synthesized with a procedure analogous to Evan's. Using this chiral lithium salt, Imamoto created three new catalyst: BisP*,[63] FerroncenylP*[64] and MiniPHOS.[65] More importantly, from compound **1.37** phosphine **1.38** can be obtained. This is a key synthon that allowed Imamoto to synthesize many remarkable ligands such as unsymmetric BisP*,[66,67] QuinoxP* (possibly Imamoto's most notorious ligand),[24] BenzP*,[68] alkynylP*[69] and PCP ligands.[70]

The relevance of synthon **1.38** is obvious. Consequently, an easy and effective synthesis for **1.38** is desirable. However, as we well explain later on, the synthetic route to the synthon is not straightforward and has some flaws. The methodology consists on the stereoselective deprotonation of phosphine borane **1.36** with the sparteine / *s*-BuLi, followed by oxidation of the corresponding phosphide with O_2 to yield the corresponding hydroxymethylphosphine **1.39** (Figure 25).[71] Further oxidation of **1.39** with $RuCl_3$ /

$K_2S_2O_8$ leads to the phosphinecarboxylic acid, which spontaneously decarboxylates to yield **1.38**.

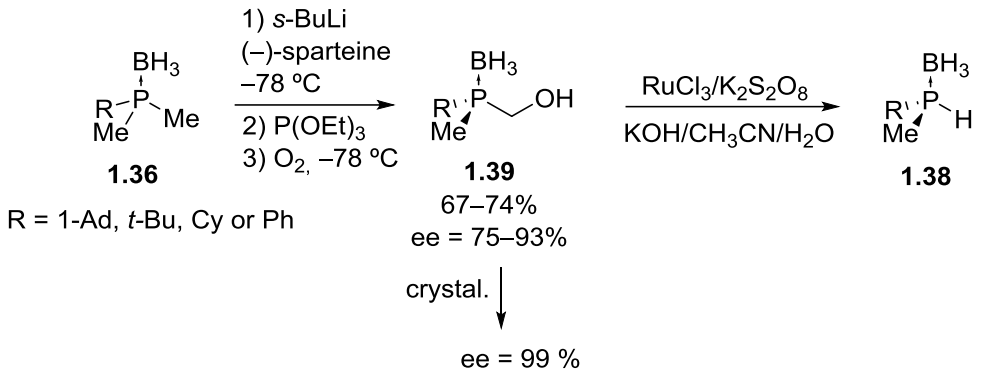

Figure 25. *Imamoto's synthesis of chiral synthon* ***1.38****.*

As previously mentioned, this procedure presents several shortcomings such as the use of sparteine, a diamine for which the non-natural enantiomer is very expensive, the need for optical enrichment of intermediate **1.39** by crystallization in order to obtain a chiral pure phosphine or the issue of using a heavy metal like Ru for the oxidation on the last step of the synthesis.

1.3. References

[1] L. Pasteur, *C. R. Seances Acad. Sci.* **1848**, *26*, 538–538.

[2] F. Fischer, E.;Passmore, *Ber. Dtsch. Chem. Ges.* **1889**, *22*, 2728–2736.

[3] E. Fischer, *Ber. Dtsch. Chem. Ges.* **1890**, *23*, 2611–2624.

[4] L. Meisenheimer, J.; Lichtenstadt, *Ber. Dtsch. Chem. Ges.* **1911**, *44*, 356–356.

[5] P. B. L. Horner, H. Winkler, A. Rapp, A. Mentrup, H. Hoffmann, *Tetrahedron Lett.* **1961**, 161–166.

[6] A. Börner, *Phosphorus Ligands in Asymmetric Catalysis*, Wiley, **2008**.

[7] J. A. Osborn, F. H. Jardine, J. F. Young, G. Wilkinson, *J. Chem. Soc. A Inorganic, Phys. Theor.* **1966**, 1711.

[8] W. S. Knowles, M. J. Sabacky, *Chem. Commun.* **1968**, 1445.

[9] L. Horner, H. Siegel, H. Büthe, *Angew. Chem. Int. Ed. Eng* **1968**, *7*, 942–942.

[10] W. S. Knowles, M. J. Sabacky, B. D. Vineyard, *J. Chem. Soc. Chem. Commun.* **1972**, 10.

[11] W. S. Knowles, *Adv. Synth. Catal. (Novel Lect. 2001)* **2003**, *345*, 1–2.

[12] B. D. Vineyard, W. S. Knowles, M. J. Sabacky, G. L. Bachman, D. J. Weinkauff, *J. Am. Chem. Soc.* **1977**, *99*, 5946–5952.

[13] W. S. Knowles, M. J. Sabacky, B. D. Vineyard, D. J. Weinkauff, *J. Am. Chem. Soc.* **1975**, *97*, 2567–2568.

[14] T. P. Dang, H. B. Kagan, *J. Chem. Soc. D* **1971**, 481.

[15] H. B. Kagan, Dang-Tuan-Phat, *J. Am. Chem. Soc.* **1972**, *94*, 6429–6433.

[16] M. D. Fryzuk, B. Bosnich, *J. Am. Chem. Soc.* **1977**, *99*, 6262–6267.

[17] M. K. T. Hayashi, T. Mise, S. Mitachi, K. Yamamoto, *Tetrahedron Lett.* **1976**, 1133–1134.

[18] A. Miyashita, A. Yasuda, H. Takaya, K. Toriumi, T. Ito, T. Souchi, R. Noyori, *J. Am. Chem. Soc.* **1980**, *102*, 7932–7934.

[19] R. Noyori, *Adv. Synth. Catal.* **2003**, *345*, 15–32.

[20] M. J. Burk, *J. Am. Chem. Soc.* **1991**, *113*, 8519–8521.

[21] M. J. Burk, J. E. Feaster, W. A. Nugent, R. L. Harlow, *J. Am. Chem. Soc.* **1993**, *115*, 10125–10138.

[22] A. R. Muci, K. R. Campos, D. A. Evans, *J. Am. Chem. Soc.* **1995**, *117*, 9075–9076.

[23] J. P. G. S. Jugé, M. Stephan, J. A. Laffitte, *Tetrahedron Lett.* **1990**, *31*, 6357–6360.

[24] T. Imamoto, K. Sugita, K. Yoshida, *J. Am. Chem. Soc.* **2005**, *127*, 11934–11935.

[25] W. Tang, X. Zhang, *Angew. Chem. Int. Ed.* **2002**, *41*, 1612–1614.

[26] G. Hoge, H.-P. Wu, W. S. Kissel, D. A. Pflum, D. J. Greene, J. Bao, *J. Am. Chem. Soc.* **2004**, *126*, 5966–5967.

[27] W. Tang, B. Qu, A. G. Capacci, S. Rodriguez, X. Wei, N. Haddad, B. Narayanan, S. Ma, N. Grinberg, N. K. Yee, et al., *Org. Lett.* **2010**, *12*, 176–179.

[28] K. M. Pietrusiewicz, M. Zablocka, *Chem. Rev.* **1994**, *94*, 1375–1411.

[29] M. Stankevič, K. M. Pietrusiewicz, *J. Org. Chem.* **2007**, *72*, 816–822.

[30] D. J. C. A. Nudelman, *J. Am. Chem. Soc.* **1967**, *269*, 3869–3870.

[31] O. Korpiun, K. Mislow, *J. Am. Chem. Soc.* **1967**, *89*, 4784–4786.

[32] O. Korpiun, R. A. Lewis, J. Chickos, K. Mislow, *J. Am. Chem. Soc.* **1968**, *90*, 4842–4846.

[33] T. Oshiki, T. Hikosaka, T. Imamoto, *Tetrahedron Lett.* **1991**, *32*, 3371–3374.

[34] B. D. Vineyard, W. S. Knowles, M. J. Sabacky, G. L. Bachman, D. J. Weinkauff, *J. Am. Chem. Soc.* **1977**, *99*, 5946–5952.

[35] T. Imamoto, T. Oshiki, T. Onozawa, T. Kusumoto, K. Sato, *J. Am. Chem. Soc.* **1990**, *112*, 5244–5252.

[36] A. Leyris, J. Bigeault, D. Nuel, L. Giordano, G. Buono, *Tetrahedron Lett.* **2007**, *48*, 5247–5250.

[37] Q. Xu, C.-Q. Zhao, L.-B. Han, *J. Am. Chem. Soc.* **2008**, *130*, 12648–12655.

[38] O. I. Kolodiazhnyi, *Tetrahedron: Asymmetry* **2012**, *23*, 1–46.

[39] J.-F. Cavalier, F. Fotiadu, R. Verger, G. Buono, *Synlett* **1998**, *1998*, 73–75.

[40] I. Fernández, N. Khiar, A. Roca, A. Benabra, A. Alcudia, J. Espartero, F. Alcudia, *Tetrahedron Lett.* **1999**, *40*, 2029–2032.

[41] O. I. Kolodiazhnyi, E. V. Gryshkun, N. V. Andrushko, M. Freytag, P. G. Jones, R. Schmutzler, *Tetrahedron: Asymmetry* **2003**, *14*, 181–183.

[42] M. Revés, C. Ferrer, T. León, S. Doran, P. Etayo, A. Vidal-Ferran, A. Riera, X. Verdaguer, *Angew. Chem. Int. Ed.* **2010**, *49*, 9452–9455.

[43] E. Cristóbal-Lecina, P. Etayo, S. Doran, M. Revés, P. Martín-Gago, A. Grabulosa, A. R. Costantino, A. Vidal-Ferran, A. Riera, X. Verdaguer, *Adv. Synth. Catal.* **2014**, *356*, 795–804.

[44] T. León, M. Parera, A. Roglans, A. Riera, X. Verdaguer, *Angew. Chem. Int. Ed.* **2012**, *51*, 6951–6955.

[45] E. J. Corey, Z. Chen, G. J. Tanoury, *J. Am. Chem. Soc.* **1993**, *115*, 11000–11001.

[46] F. Maienza, F. Spindler, M. Thommen, B. Pugin, C. Malan, A. Mezzetti, *J. Org. Chem.* **2002**, *67*, 5239–5249.

[47] C. Benhaim, L. Bouchard, G. Pelletier, J. Sellstedt, L. Kristofova, S. Daigneault, *Org. Lett.* **2010**, *12*, 2008–2011.

[48] T. Imamoto, K. Tamura, Z. Zhang, Y. Horiuchi, M. Sugiya, K. Yoshida, A. Yanagisawa, I. D. Gridnev, *J. Am. Chem. Soc.* **2012**, *134*, 1754–1769.

[49] Z. S. Han, N. Goyal, M. A. Herbage, J. D. Sieber, B. Qu, Y. Xu, Z. Li, J. T.

Reeves, J.-N. Desrosiers, S. Ma, et al., *J. Am. Chem. Soc.* **2013**, *135*, 2474–2477.

[50] H. Geng, W. Zhang, J. Chen, G. Hou, L. Zhou, Y. Zou, W. Wu, X. Zhang, *Angew. Chem.* **2009**, *121*, 6168–6170.

[51] A. Ohashi, S. Kikuchi, M. Yasutake, T. Imamoto, *European J. Org. Chem.* **2002**, *2002*, 2535.

[52] D. Noh, H. Chea, J. Ju, J. Yun, *Angew. Chem. Int. Ed.* **2009**, *48*, 6062–6064.

[53] A. Yanagisawa, S. Takeshita, Y. Izumi, K. Yoshida, *J. Am. Chem. Soc.* **2010**, *132*, 5328–5329.

[54] Y. Shibata, K. Tanaka, *J. Am. Chem. Soc.* **2009**, *131*, 12552–12553.

[55] Z. Han, D. Krishnamurthy, P. Grover, Q. K. Fang, C. H. Senanayake, *J. Am. Chem. Soc.* **2002**, *124*, 7880–7881.

[56] Z. Han, D. Krishnamurthy, P. Grover, H. S. Wilkinson, Q. K. Fang, X. Su, Z.-H. Lu, D. Magiera, C. H. Senanayake, *Angew. Chem. Int. Ed.* **2003**, *42*, 2032–2035.

[57] S. Orgué, A. Flores-Gaspar, M. Biosca, O. Pàmies, M. Diéguez, A. Riera, X. Verdaguer, *Chem. Commun.* **2015**, *51*, 17548–17551.

[58] H. Zijlstra, T. León, A. de Cózar, C. F. Guerra, D. Byrom, A. Riera, X. Verdaguer, F. M. Bickelhaupt, *J. Am. Chem. Soc.* **2013**, *135*, 4483–4491.

[59] D. Gatineau, L. Giordano, G. Buono, *J. Am. Chem. Soc.* **2011**, *133*, 10728–10731.

[60] W. Tang, A. G. Capacci, X. Wei, W. Li, A. White, N. D. Patel, J. Savoie, J. J. Gao, S. Rodriguez, B. Qu, et al., *Angew. Chem. Int. Ed.* **2010**, *49*, 5879–5883.

[61] W. Tang, A. G. Capacci, A. White, S. Ma, S. Rodriguez, B. Qu, J. Savoie, N. D. Patel, X. Wei, N. Haddad, et al., *Org. Lett.* **2010**, *12*, 1104–1107.

[62] B. Qu, L. P. Samankumara, J. Savoie, D. R. Fandrick, N. Haddad, X. Wei, S. Ma, H. Lee, S. Rodriguez, C. A. Busacca, et al., *J. Org. Chem.* **2014**, *79*, 993–1000.

[63] T. Imamoto, J. Watanabe, Y. Wada, H. Masuda, H. Yamada, H. Tsuruta, S.

Matsukawa, K. Yamaguchi, *J. Am. Chem. Soc.* **1998**, *120*, 1635–1636.

[64] N. Oohara, K. Katagiri, T. Imamoto, *Tetrahedron: Asymmetry* **2003**, *14*, 2171–2175.

[65] Y. Yamanoi, T. Imamoto, *J. Org. Chem.* **1999**, *64*, 2988–2989.

[66] A. Ohashi, T. Imamoto, *Tetrahedron Lett.* **2001**, *42*, 1099–1101.

[67] A. Ohashi, T. Imamoto, *Org. Lett.* **2001**, *3*, 373–375.

[68] K. Tamura, M. Sugiya, K. Yoshida, A. Yanagisawa, T. Imamoto, *Org. Lett.* **2010**, *12*, 4400–4403.

[69] T. Imamoto, Y. Saitoh, A. Koide, T. Ogura, K. Yoshida, *Angew. Chem. Int. Ed. Eng.* **2007**, *46*, 8636–9.

[70] B. Ding, Z. Zhang, Y. Liu, M. Sugiya, T. Imamoto, W. Zhang, *Org. Lett.* **2013**, *15*, 3690–3693.

[71] K. Nagata, S. Matsukawa, T. Imamoto, *J. Org. Chem.* **2000**, *65*, 4185–4188.

Chapter 2

Efficient Preparation of (*S*)- and (*R*)-*tert*-Butylmethylphosphine Borane: A Novel Entry to Important P-Stereogenic Ligands

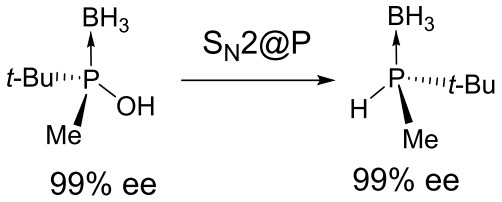

E. Salomó, S. Orgué, A. Riera, X. Verdaguer, *Synthesis.* **2016**, *48*, 2659–2663.

2.1. Introduction: Ligands derived from *tert*-butylmethylphosphine borane

Within phosphine based ligands, the subclass of P-stereogenic phosphines play a major role on asymmetric catalysis and other important industrial processes.[1–4] A very important P-stereogenic building-block, developed by Imamoto, is the *tert*-butylmethylphosphine borane **2.1**.[5–9] This molecule can be used to synthesize many noteworthy C_2 symmetric P-stereogenic ligands such as Quinox-P*, Benz-P* and Pincer-P*. These ligands have demonstrated to perform very well in numerous catalytic processes.[10–16]

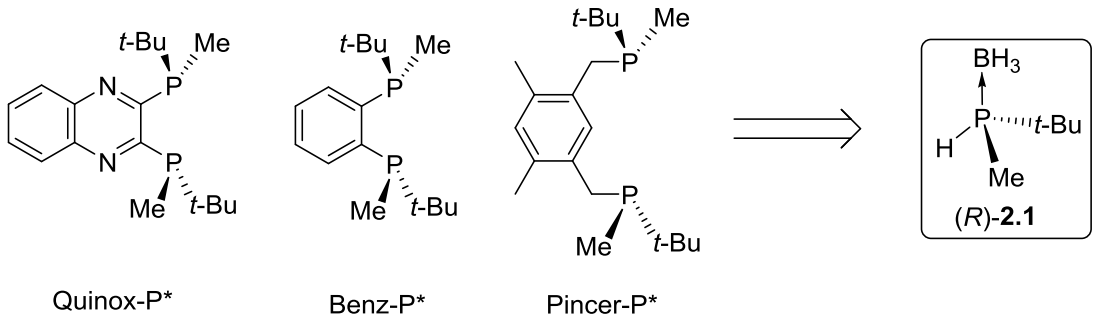

Figure 1. *Some relevant Imamoto's P-stereogenic ligands.*

When treated with a strong base such as *n*-BuLi, phosphine **2.1** is deprotonated and it can react with different electrophiles. For instance, benzyl bromide reacts in a quantitative manner with the phosphine and the product's optic purity can be determined by chiral HPLC, unlike *tert*-butylmethylphosphine borane.[9] Reaction with electrophiles like aryl halydes is also possible, but only when it is very electron poor. This S_NAr reactivity opens a door to many novel and interesting ligands.

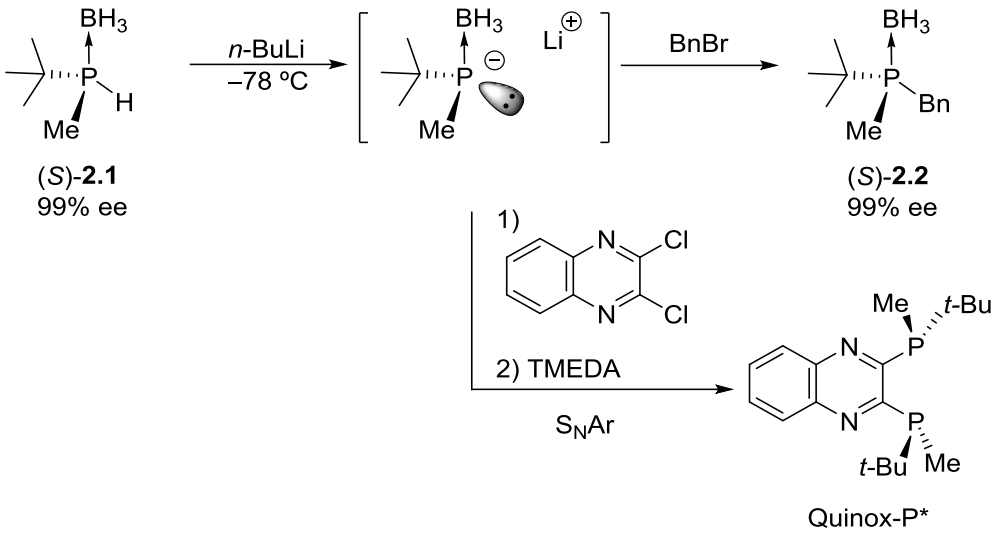

Figure 2. *S_N2 reaction of* ***2.1*** *with different nucleophiles. Synthesis of Quinox-P*.*

2.2. Synthesis of *tert*-butylmethylphosphine borane

As explained in the previous Chapter 1, the synthesis for *tert*-butylmethylphosphine borane reported by Imamoto has room for improvement; using sparteine, the non-natural enantiomer of which is expensive, or employing a transition metal like Ru are two noteworthy shortcomings.[5]

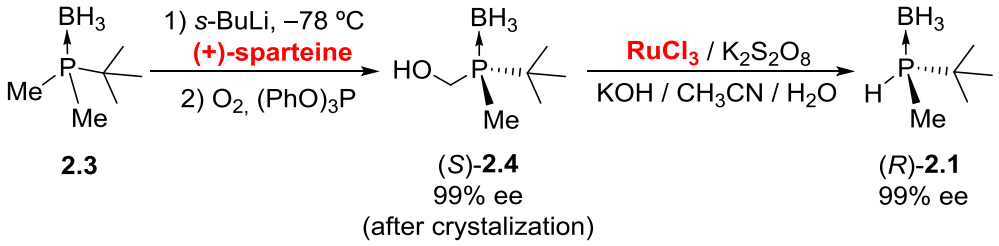

Figure 3. *Imamoto's synthesis for* ***2.1*** *employs sparteine and $RuCl_3$.*

Our group developed a methodology to synthesize **2.8** in multigram scale. Taking advantage of this, we envisioned a synthesis for compound **2.1** analogous to the ones reported by Pietrusiewicz and Buono.[17–19] These consist in the activation of optically pure *tert*-butylarylphosphinous acid borane **2.5** with MsCl or Ms_2O and then reduction to the corresponding secondary phosphine **2.7** via S_N2@P with $NaBH_4$.

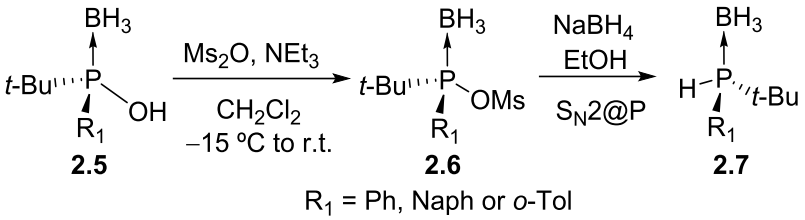

Figure 4. *Buono's methodology for the reduction of phosphinous acids via S_N2@P reaction with $NaBH_4$.*

2.3. Study of the stability of the phosphinyl-mesyl anhydride 2.9

During her PhD thesis, S. Orgué studied the configurational stability of phosphinites **2.9** with two alkyl groups (Me and *t*-Bu), when activated with MsO_2 or MsCl. She observed that their configurational stability is far inferior to Buono's or Pietrusiewicz's phosphinites **2.6**. She used the S_N2@P reaction with ammonia to study the racemization of compound **2.9**[20] This reaction was chosen as a model reaction due to the strong nucleophilic character of ammonia gas, that ensures maximum reactivity, and because the product obtained was synthon (*S*)-**2.10**, whose optical purity could be easily determined by chiral GC.

Table 1. Solvent and temperature effect on the stereochemical integrity of the phosphinyl-mesyl anhydride **2.9**.

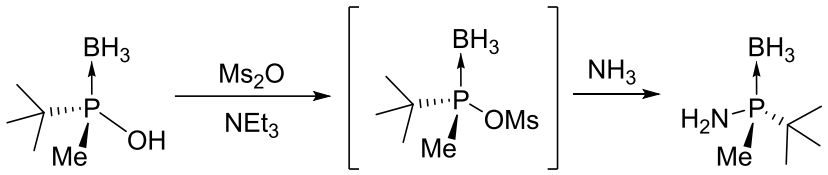

(*R*)-**2.8**, (99% ee) (*R*)-**2.9** (*S*)-**2.10**

Entry	Solvent[a]	Temp (ºC)[a]/time[b]	ee of 2.10 (%)[c]
1	Toluene	0 ºC / 1 h	29 ee
2	THF	0 ºC / 1 h	22 ee
3	Et_2O	0 ºC / 1 h	42 ee
4	DME	0 ºC / 1 h	46 ee
5	ACN	0 ºC / 1 h	80 ee
6	DCM	0 ºC / 1 h	91 ee
7	DCM	–10 ºC / 1 h	98 ee
8	DCM	–20 ºC / 1 h	99 ee
9	DCM	r.t. / 3 h	29 ee

a) Solvent and temperature employed in the formation of the mixed anhydride. b) Time left before bubbling ammonia gas into the reaction mixture. c) Enantiomeric excess of the amino phosphine product was directly determined by chiral GC.

Optically pure phosphinous acid (*R*)-**2.8**, was treated with mesyl anhydride and NEt_3 to yield the mixed anhydride (*R*)-**2.9,** which was left stirring for a period of time before bubbling an excess of $NH_{3\,(g)}$ into the reaction mixture. Initially, the formation of (*R*)-**2.9** was carried out at 0 °C and the solution was left 1 h at the temperature before bubbling ammonia (Table 1, entries 1-6). The use of toluene, THF, Et_2O and DME afforded the final substitution product **2.10** with a high degree of racemization (22 – 46% ee). On the other hand, acetonitrile and dichloromethane produced less racemization affording the final product with 80 and 91% ee respectively. At this stage we studied the effect of the temperature. Using the best solvent in the series (CH_2Cl_2) and lowering the temperature to –10 °C, the enantiomeric excess increased to 97% ee (Table 1, entry 7).

When running the reaction at –20 °C in CH_2Cl_2, the racemization was completely suppressed and the product was isolated in 99% ee (Table 1, entry 8). To show the importance of temperature, an almost complete racemization took place when a CH_2Cl_2 solution of (*R*)-**2.9** was stirred 3 h at room temperature (Table 1, entry 9).

2.4. Reduction of 2.8 to 2.1

2.4.1. Reducing agent screening

From the previous study, we concluded that intermediate **2.9** was stable to racemization at –20 °C in CH_2Cl_2. Thus, the reduction of phosphinous acid **2.8** had to be ideally performed at the same conditions of solvent and temperature. With this constraints in mind we began to search for a reagent that could fulfill such requirements (Table 2).

Table 2. Reduction trials to *tert*-butylmethylphosphine Borane

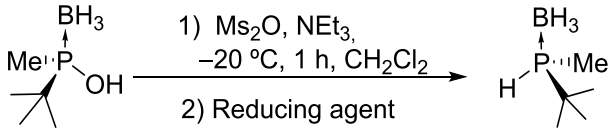

(*S*)-**2.8** (99% ee) → (*S*)-**2.1**

Entry	Reagent	Reduction Cond.	Yield (%)	ee (%)[b]
1[a]	$NaBH_4$	–20 °C, 16 h	0	-
2[a]	$BH_3{\cdot}SMe_2$	–20 °C, 16 h	0	-
3[a]	$NaBH(OAc)_3$	–20 °C, 16 h	0	-
4[a]	DIBAL–H[c]	–20 °C, 16 h	13	-
5[a]	DIBAL–H[c]	0 °C, 2 h	34	82 (*S*)
6[a]	AlH_3[d]	–20 °C, 4 h	80	97 (*S*)
7	$[NBu_4][BH_4]$[e]	–20 °C, 4 h	86	99 (*S*)
8	$[NBu_4][BH_4]$[e]	–20 °C, 4 h	88	99 (*R*)

a) Results from S. Orgué's PhD thesis. b) Enantiomeric excess was determined by chiral HPLC of the corresponding benzyl derivative of tert-butylmethylphosphine borane.[9] *c) The commercial 1 M solution in hexanes was used. d) A 1.5 M suspension of alane in Et_2O was used. The reagent suspension was prepared from $LiAlH_4$ and $AlCl_3$. e) For work-up and isolation reasons, N-methylmorpholine was used as a base instead of triethylamine.*

Sodium borohydride, which was used successfully in the reduction of **2.5** compounds by Buono, did not produce any reduction product (Table 2, entry 1). We attributed this lack of reactivity to the poor solubility of $NaBH_4$ in CH_2Cl_2 at –20 ºC. Reduction with $BH_3{\cdot}SMe_2$ or $NaBH(OAc)_3$ were also unproductive (Table 2, entries 2-3). Diisobutylaluminium hydride (DIBAl-H) at –20 °C produced a low yield (13%) for the desired secondary phosphine (Table 2, entry 2). Increasing the reaction temperature to 0 °C and shortening the reaction time to 2 h improved the yield to 34%, but with a concomitant loss of optical purity (Table 2, entry 3). We reasoned that the sluggish reactivity observed for the DIBAL-H reagent was due to the steric hindrance created by the isobutyl groups of the reagent. Hence, we next tried the smaller alane (AlH_3), generated from $LiAlH_4$ and $AlCl_3$. Addition of alane over the mixed anhydride **8** in CH_2Cl_2 at –20 °C afforded this time the secondary phosphine **3** with 80% yield and 97% enantiomeric excess (Table 2, entry 6).

Despite the good result obtained, alane is not an easy reagent to handle. We desired for a commercial reducing agent that could be easily and safely used and stored and could perform in a mild way. We then turned our attention to tetrabutylammonium borohydride ($[NBu_4][BH_4]$). The high solubility of this reagent in CH_2Cl_2 allows for reductions to be carried out in the absence of protic solvents.[7] The use of $[NBu_4][BH_4]$ provided an efficient reduction of the intermediate **8** producing the secondary phosphine **3** with inversion of configuration with complete conversion and 99% enantiomeric excess (Table 2, entry 7).[21] Using the opposite enantiomer of the phosphinous acid, the enantiomer of **3** was obtained also in 99% ee (Table 2, entry 8), thus demonstrating that the reduction process is completely stereospecific.

Although in terms of reactivity and selectivity $[NBu_4][BH_4]$ is an excellent reagent, it is not flawless. We detected and impurity that was impossible to separate by silica column caused by the use of this borohydride.

2.4.2. Base screening

The use of $[NBu_4][BH_4]$ as reducing agent produced an impurity that we determined was triethylamine borane. It was formed by the reaction of the triethylamine

in the media plus the BH_3 (g) produced by the oxidation of the borohydride. The issue with this byproduct is that coelutes with the product **2.1** in the purification with silica column, making the separation impossible. Instead of trying to avoid this subreaction, we concluded that the easiest solution would be to use another base, so the boronated amine produced would not coelute with **2.1** in a silica column.

We tried out a battery of different amines such as DIPEA, *N*-methylmorpholine, pyridine or TMEDA, among others. We easily boronated the amines using $SMe_2 \cdot BH_3$ and compared them on TLC against product **2.1**. From this scope we finally chose *N*-methylmorpholine and pyridine as possible candidates. We tested this two bases in the model S_N2@P reaction with NH_3. Although satisfyingly both cases went to full conversion with no ee loss, the reaction was cleaner with *N*-methylmorpholine.

So, when conducting the reaction under the conditions in Figure 5, the purification became simple. The yield obtained was up to 88% and there was no loss of optical purity.

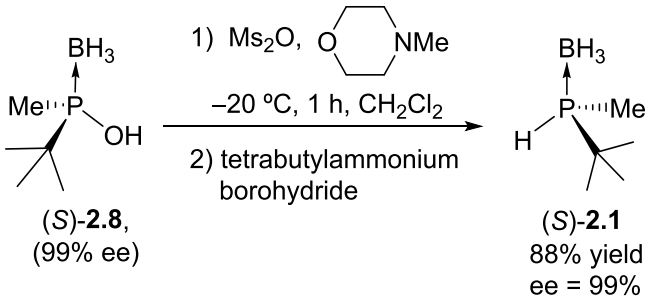

Figure 5. *Optimized conditions for the reduction of phosphinous acid* ***2.8*** *by* S_N2*@P.*

2.5. Synthesis of Quinox-P*

To demonstrate the usefulness of this novel reduction methodology, optically pure *tert*-butylmethylphosphine borane prepared by us was employed in the preparation of Quinox-P* ligand following Imamoto's procedure (Figure 6).

Deprotonation of (*R*)-**2.1** with *n*-BuLi at –78 °C provided the corresponding lithium phosphide, which was reacted in situ at low temperature with dichloroquinoxaline. Removal of the borane protecting groups provided, in a single-pot

procedure, Quinox-P* with 70% yield and 99% optical purity as determined by optical rotation.[8]

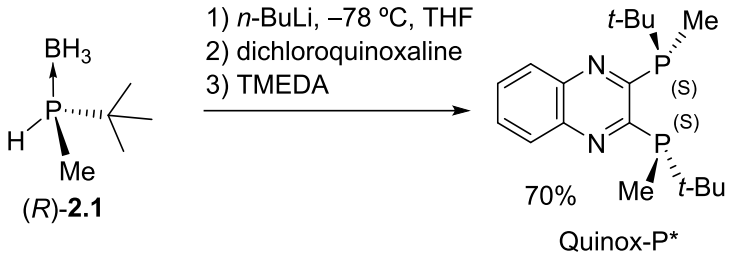

Figure 6. *Imamoto's synthesis for Quinox-P*.*

2.6. Conclusions

In summary, we have devised a new reductive methodology for the synthesis of optically pure *tert*-butylmethylphosphine borane, which is a strategic P-stereogenic intermediate for the synthesis of important chiral phosphine ligands. This novel preparation uses as starting material *tert*-butylmethylphosphinous acid borane, which is available in both enantiomeric forms thanks to the methodology developed in our group. The process is based on the reduction of the mixed mesyl anhydride derivative **2.9,** which was found to be configurationally stable in CH_2Cl_2 at –20 °C. Tetrabutylammonium borohydride was the reducing agent of choice, allowing for the development of a practical one-pot process. The usefulness of the new reductive methodology was demonstrated with the preparation of Quinox-P*, following Imamoto's original procedure. We believe that this preparation will improve the availability of **2.1** and thus foster its incorporation into novel ligand structures.

2.7. References

[1] Armi, *Phosphorous Ligands in Asymmetric Catalysis*, Wiley-WCH, Weinheim, **2008**.

[2] A. Grabulosa, *P-Stereogenic Ligands in Asymmetric Catalysis*, RSC Publishing, Cambridge, **2011**.

[3] A. Grabulosa, J. Granell, G. Muller, *Coord. Chem. Rev.* **2007**, *251*, 25–90.

[4] O. I. Kolodiazhnyi, *Top. Curr. Chem.* **2015**, *360*, 161–236.

[5] K. Nagata, S. Matsukawa, T. Imamoto, *J. Org. Chem.* **2000**, *65*, 4185–4188.

[6] T. Imamoto, K. Sugita, K. Yoshida, *J. Am. Chem. Soc.* **2005**, *127*, 11934–11935.

[7] K. Tamura, M. Sugiya, K. Yoshida, A. Yanagisawa, T. Imamoto, *Org. Lett.* **2010**, *12*, 4400–4403.

[8] B. Ding, Z. Zhang, Y. Xu, Y. Liu, M. Sugiya, T. Imamoto, W. Zhang, *Org. Lett.* **2013**, *15*, 5476–9.

[9] T. Miura, H. Yamada, S. Kikuchi, T. Imamoto, *J. Org. Chem.* **2000**, *65*, 1877–1880.

[10] T. Imamoto, K. Tamura, Z. Zhang, Y. Horiuchi, M. Sugiya, K. Yoshida, A. Yanagisawa, I. D. Gridnev, *J. Am. Chem. Soc.* **2012**, *134*, 1754–1769.

[11] I.-H. Chen, L. Yin, W. Itano, M. Kanai, M. Shibasaki, *J. Am. Chem. Soc.* **2009**, *131*, 11664–11665.

[12] H. Ito, T. Okura, K. Matsuura, M. Sawamura, *Angew. Chem. Int. Ed.* **2010**, *49*, 560–563.

[13] X. Wang, S. L. Buchwald, *J. Am. Chem. Soc.* **2011**, *133*, 19080–19083.

[14] Q. Hu, Z. Zhang, Y. Liu, T. Imamoto, W. Zhang, *Angew. Chem. Int. Ed.* **2015**, *54*, 2260–2264.

[15] Y. Shibata, K. Tanaka, *J. Am. Chem. Soc.* **2009**, *131*, 12552–3.

[16] A. Yanagisawa, S. Takeshita, Y. Izumi, K. Yoshida, *J. Am. Chem. Soc.* **2010**, *132*, 5328–9.

[17] M. Stankevic, K. M. Pietrusiewicz, *J. Org. Chem.* **2007**, *72*, 816–822.

[18] D. Moraleda, D. Gatineau, D. Martin, L. Giordano, G. Buono, *Chem. Commun.* **2008**, 3031–3033.

[19] D. Gatineau, L. Giordano, G. Buono, *J. Am. Chem. Soc.* **2011**, *133*, 10728–10731.

[20] S. Orgué, A. Flores-Gaspar, M. Biosca, O. Pàmies, M. Diéguez, A. Riera, X. Verdaguer, *Chem. Commun.* **2015**, *51*, 17548–17551.

[21] D. J. Raber, W. C. Guida, *J. Org. Chem.* **1976**, *41*, 690–696.

Chapter 3

Dialkylammonium *tert*-Butylmethylphosphinites: Stable Intermediates for the Synthesis of P-Stereogenic Ligands

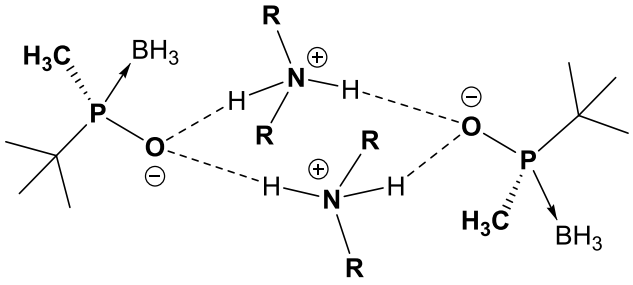

E. Salomó, A. Prades, A. Riera, X. Verdaguer, *J. Org. Chem.* **2017**, *82*, 7065–7069.

3.1. Introduction: Pros and Cons of *tert*-butylmethylphosphinous acid borane (3.1)

Despite many advances, to assemble stereogenic phosphorus centers in optically pure fashion continues to be a hurdle. In this respect, the development of efficient key intermediates, or synthons, that facilitate the synthesis of P-stereogenic compounds is essential.

In her PhD thesis, S. Orgué reported the synthesis of *tert*-butylmethylphosphinous acid borane **3.1**. This compound is a very valuable molecule that can react with different nucleophiles in a S_N2@P type reaction, giving access to many different P* compounds.[1,2]

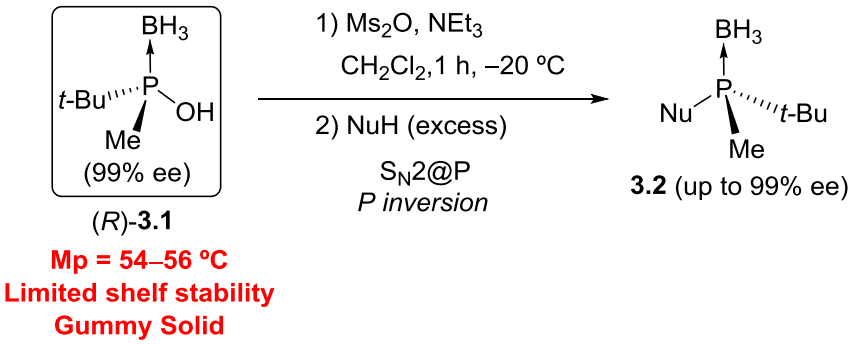

Figure 1. *Synthon **3.1** can react with nucleophiles in a S_N2@P reaction.*

3.1 is an invaluable compound for ligand synthesis, but it does have some drawbacks that hamper its extensive use. It is a difficult to handle gummy solid with a low melting point (54 – 56 ºC). On account of the compound's nature, the synthesis "work-up" step is somewhat intricate; if not executed carefully, the yield could be jeopardized. Nevertheless, the main drawback of compound **3.1** probably is its limited stability. Upon storage, phosphinous acid **3.1** decompose to yield the corresponding secondary phosphine oxide and borane byproducts. To delay this decomposition process, synthon **3.1** shall be stored very pure. To purify **3.1** a SiO_2 flash chromatography is required and, due to the nature of the molecule (small and mildly acidic), the yield drops drastically.

We theorized that acidic impurities might be involved in the transformation of **3.1** to the corresponding secondary phosphine oxide **3.4**. S. Orgué studied the transformation

of (*S*)-**3.3** to (*R*)-**3.1** while trying to avoid the formation of (*R*)-**3.4**. Without acid (H_2SO_4) the reaction does not procced at all (Entry 1). Within two hours and with 4 equivalents of H_2SO_4, the transformation to (*R*)-**3.1** is complete and no ee is lost in the process (Entry 2). However, for longer reaction times we detected increasing quantities of (*R*)-**3.4** with lower ee's (Entry 3). For a 16 h reaction, (*R*)-**3.4** is the only product obtained with an ee of 53% (Entry 4). These experiments give us base to believe that acid is involved in the deprotection of **3.1** and the transformation to **3.4**, which also implies an ee decrease for the secondary phosphine oxide product.

Table 1. Acid hydrolysis of aminophosphine (*S*)-**3.3**. (S. Orgué's PhD thesis)

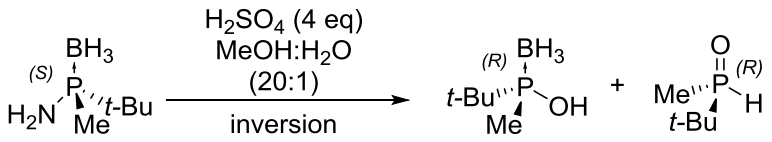

(*S*)-**3.3** (*R*)-**3.1** (*R*)-**3.4**

Entry	H_2SO_4 (eq)	Conditions	Ratio (3.1 : 3.4)	Yield and ee	
				3.1	**3.4**
1	0	16 h, reflux	–	–	–
2	4	2 h, 50 ºC	20:1	97% >99% ee[a]	–
3	4	3 h, 50 ºC	7.7:1	76% >99% ee[a]	10% 84% ee[b]
4	4	16 h, 40 ºC	0:1	–	83% 53% ee[b]

a) Enantiomeric excess determined by chiral GC or HPLC analysis of the corresponding methylated derivative. b) Enantiomeric excess determined by optical rotation

We performed a simple stability test by storing a sample of **3.1** in an uncapped vial at room temperature for a week. ^{1}H-NMR analysis revealed 35-40% of decomposition. This limited stability forced us to use **3.1** immediately after its preparation. This clearly hampers a large-scale application of **3.1**.

With this scenario in mind, we intended to find a derivative of **3.1** that could circumvent its stability issues. Also, we aimed for an easy to handle solid, crystalline and that it could be obtained pure by precipitation from the crude (very desirable in a big scale procedure).

3.2. Dialkylammonium phosphonites as analogs to 3.1

Salts of acidic compounds with small counteranions are usually crystalline and rather stable. We realized that we could use this in our favor by synthesizing a salt of phosphinous acid **3.1**. We hypothesized that the proper salt would be crystalline and polar enough to be afforded directly via crystallization/precipitation from the reaction mixture. The stability should also increase and being a crystalline solid the compound would be easier to handle. However, reactivity must be preserved. With all this considerations in mind, we studied the acidity of our chiral synthon and the nature of different salt versions of it.

3.2.1. Acidity of phosphinous acid 3.1

The acidity of the phosphinous acid boranes is usually influenced by electronic and steric factors; with pKa values ranging from 5.8 for $Cy_2P(BH_3)OH$ to 3.9 for $Ph_2P(BH_3)OH$.[3] We carefully prepared a highly pure sample of synthon **3.1** to determine its pKa by potentiometric titration. From 5 to 10 mg of **3.1** were dissolved in H_2O to afford concentrations of 1 mg / mL. The mixtures were titrated with 0.01 M NaOH and a Titrando-888 (Metrohm®) with pH-microelectrode. The pHs of the mixtures were monitorized and the ending points and pKas values were determined using Tiamo ® software. The ending points (EP1) were defined as the inflexion points of the titration curves. The pKas were determined as the pH of the samples when half the volume added at the ending point is added.

Table 2. Potentiometric titration of **3.1** in H_2O with NaOH 0.01 M

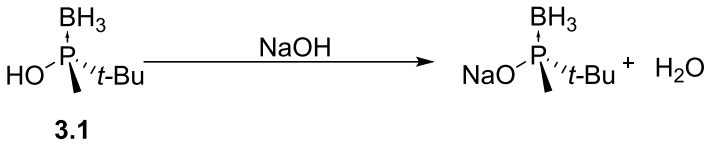

3.1

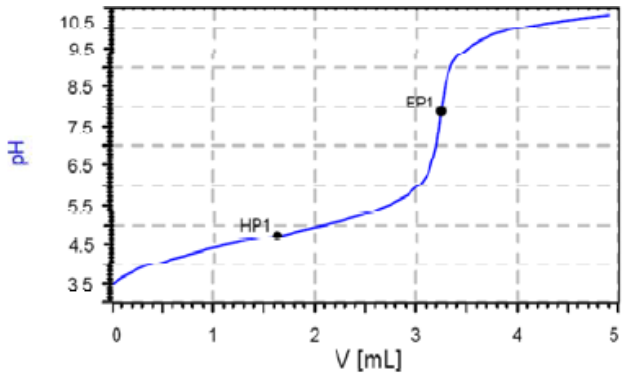

Entry	pKa	Average pKa	RSD (%)
1	4.745	4.76	0.60
2	4.739		
3	4.791		

HP1 (Half Point): *Point in which the concentration of added base/acid is equal to half of the original concentration of acid/base. Expresses the pKa of the compound*

EP1 (End Point): *Point in which the original base/acid is completely titrated. Expresses the end of the titration of the compound*

Potentiometric titration revealed that **3.1** has a pKa of 4.8 and thus should readily form salts with moderately strong inorganic and organic bases. We then performed a screening to select a base that formed a salt that suited our requirements.

3.2.2. Base screening

We placed 20 mg of pure phosphinous acid **3.1** in several vials. Then we added 0.5 mL of CH_2Cl_2. In each vial, we added 1 equivalent of one of the selected bases. After a few minutes we checked for precipitation/crystallization. We then added hexanes to

each vial and checked again for precipitation/crystallization. Finally, we left the vials uncapped overnight so the solvents would slowly evaporate. The next day we checked once more for precipitation/crystallization.

Initial tests showed that small metallic counteranions, such as Na^+ and K^+, did not fulfill our requirements. The obtained surrogates (**3.5**) of **3.1** were hygroscopic and not crystalline, therefore not adequate. We then turned our attention to organic bases. We studied various trialkyl and dialkyl amines, along with DMAP and DBU. While trialkylic amines like triethylamine provided oily salts (**3.6**), dialkyl amines like diethylamine (**3.7**), diisopropylamine (**3.8**) or dicyclohexylamine (**3.9**) afforded crystalline solids with melting points around 140 ºC. Other bases afforded acceptable salts, but at the end these three dialkylamonium salts were selected because of their high crystallinity, the yields obtained and their solubility in CH_2Cl_2. A high solubility in CH_2Cl_2 is mandatory as the S_N2@P with nucleophiles must be carried out in this solvent (check Section 2.3)

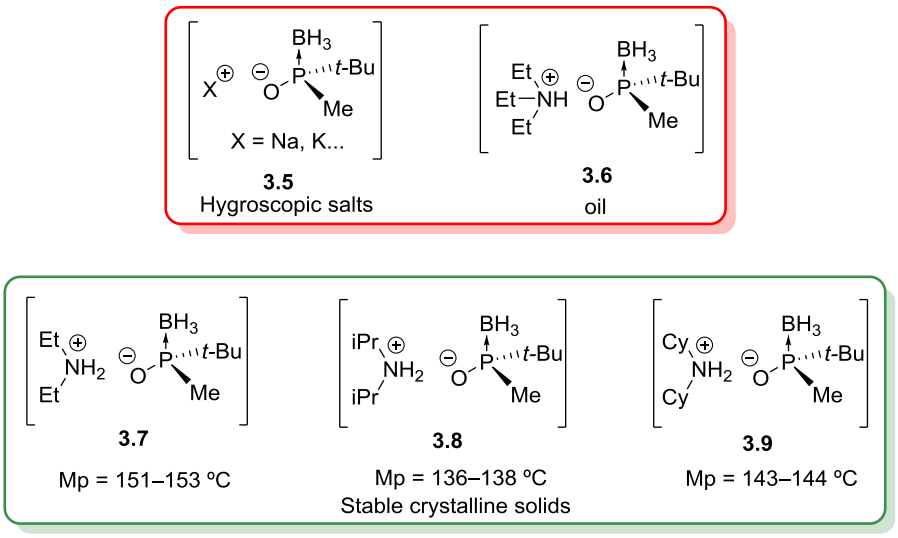

Figure 2. *Different salts of* ***3.1****.*

The next question we asked ourselves was how stable these compounds were. Pure samples of the three substrates were stored for weeks inside uncapped vials inside the fume hood. Analysis by ^{1}H-NMR revealed no degradation. We concluded that all three salts were shelf-stable and could be stored indefinitely at room temperature.

Taking into account and comparing the data obtained (stability, crystallinity, yield, solubility, etc), out of the three candidates we finally chose **3.8** as the best candidate.

3.2.3. X-Ray structure

To gain further insight on compound **3.8**, an X-ray analysis was pursued. With this aim, single crystals were grown by evaporation of a solution of **3.8** in CH_2Cl_2. The resulting solid state structure of **3.8** is depicted in Figure 3. The resolved structure is pseudo-symmetric and holds a C_2 axis of symmetry. The most characteristic feature is the cyclic hydrogen bond network connecting two *t*-BuMeP(BH_3)O^- and two $iPr_2NH_2^+$ units together in a tetrameric assembly. This cyclic H-bond network is completely planar. The two nitrogen and oxygen atoms conform a regular flat square of 2.77 Å sides. This strong hydrogen bond system probably accounts for the observed increased melting point (aprox. +100 ºC) and the enhanced stability of **3.8** with respect the free phosphinous acid **3.1**.

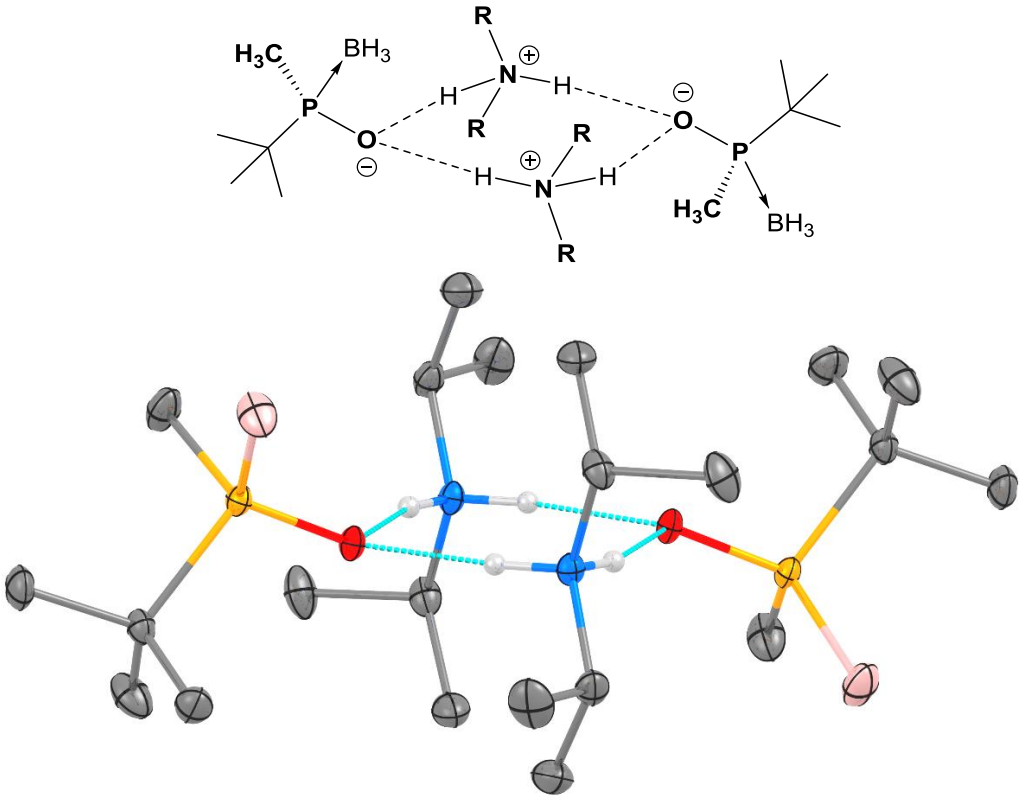

***Figure 3**: X-ray structure of **3.8**. Ortep diagram displays ellipsoids at 50% probability. Only hydrogen atoms involved in the H-bond network are depicted.*

3.2.4. Scaling up the synthesis of 3.8

As we previously mentioned, one shortcoming in the preparation of phosphinous acid **3.1** was the problematical "work-up" step. With the new salt **3.8** in our hands, we considered the possibility to crystallize it directly from the reaction crude, avoiding the "work-up" step. Such a method would allow us to scale up the production of **3.8**, thus boosting its commercial value.

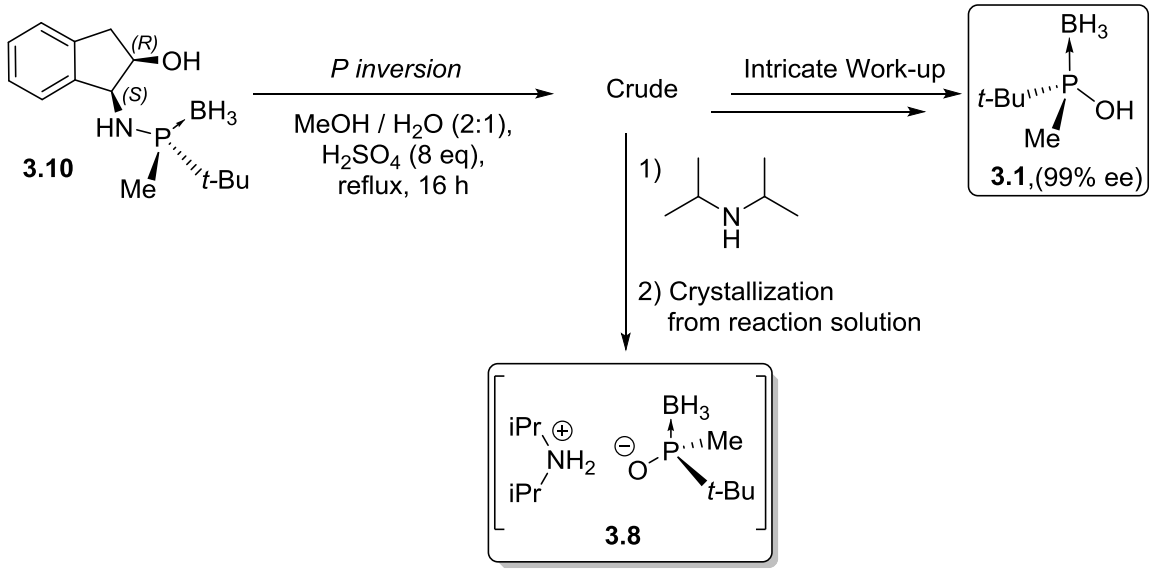

Figure 4. *Divergent synthesis for phosphinous acid **3.1** and salt **3.8**.*

We hydrolyzed compound **3.10** with the usual conditions reported in Figure 4. After 16 h, once all the starting material was consumed, we added extra H_2O and removed the MeOH under vacuum. We extracted with TBME and then by adding diisoprylamine to the solution, a white solid precipitated. We filtered the solid to obtain the salt **3.8** pure and with yields over 80%. With this methodology we were able to scale up the synthesis to multigram scale without problems.

3.2.5. The S_N2@P reaction of 3.8 with nucleophiles

The importance of phosphinous acid **3.1** resides in its potential to be used as a versatile electrophilic synthon to synthesize many P-stereogenic ligands. The salt **3.8**

would not be useful surrogate unless its reactivity was at least the same as **3.1**'s. Therefore, we proceeded to study **3.8** reactivity in the S_N2@P reactions.

We employed chiral 1-phenylethan-1-amine (either *R* or *S* enantiomer) to study the S_N2@P reaction with the salt **3.8** because is a cheap, chiral amine that should selectively afford one diastereoisomer that can be analyzed by ^{1}H-NMR to straightforwardly determine if any optical purity was lost on the P center during the reaction. S. Orgué studied the reaction of both enantiomers of 1-phenylethan-1-amine with chiral phosphinous acid **3.1** in her PhD thesis (Figure 5). Consequently, we knew beforehand the yield and d.r. we should be expecting.

Original Reaction with 3.1

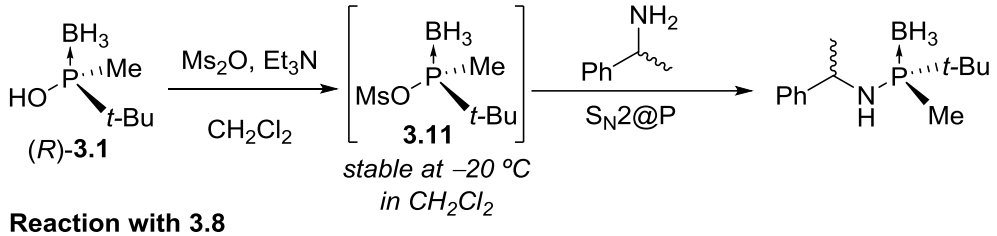

Novel Reaction with 3.8

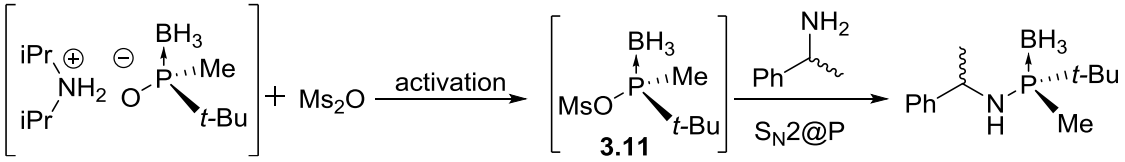

Figure 5. *Novel analogous S_N2@P reaction with salt **3.8**. Reaction conditions optimization.*

We first performed the reaction without Et_3N. Although we obtained some product, the conversion was not complete. We assumed that the salt **3.8** can react with Ms_2O (methanesulfonic anhydride) to form the phosphinyl-mesyl anhydride **3.11** without any extra base, but it does so slowly. By adding 2 equivalents of Et_3N the formation of the mixed anhydride happens in less than 1 h and the S_N2@P with amine 1-phenylethan-1-amine was complete.

We also discovered that by slowly adding the dissolved salt **3.8** over a solution of Ms_2O in CH_2Cl_2 at –20 ºC the reaction produced less byproducts than by performing the addition the other way around (adding the Ms_2O over the salt).

Taking these and some other minor facts into account, we defined a set of optimized conditions for the reaction of compound **3.8** with amines and other nucleophiles. We then studied the scope of the reaction (Table 3).

Table 3. Reaction of **3.8** with different amine nucleophiles.

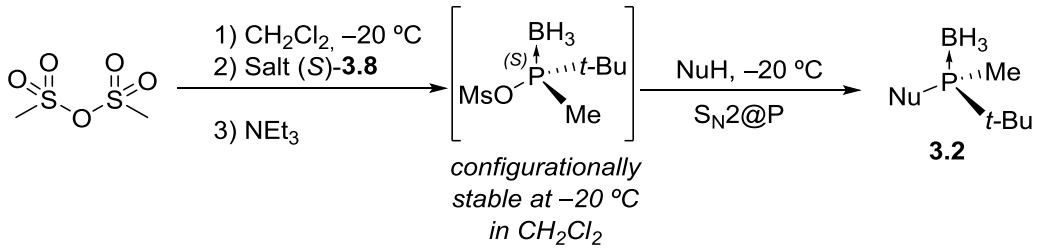

Entry	NuH	Product	Yield (%) ee[b]/de[d] for 3.8[a]	Yield (%) ee[b]/de[d] for 3.1
1	NH_3	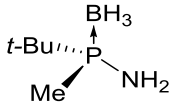 (*R*)-**3.3**	99 98% ee	99 96% ee
2	$Bu_4N{\cdot}BH_4$	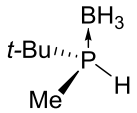 **3.12**	80 99% ee	88 99% ee[c]
3	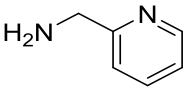	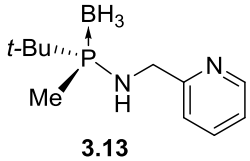 **3.13**	84 99% ee	87 99% ee
4	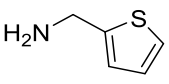	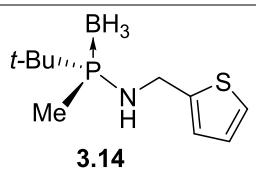 **3.14**	85 99% ee	73 99% ee

5	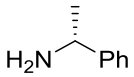	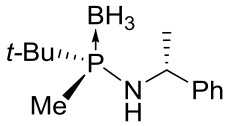 **3.15**	88 98% de	76 98% de
6	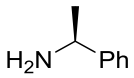	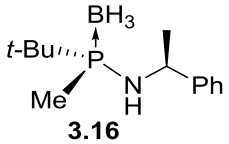 **3.16**	83 98% de	71 95% de
7	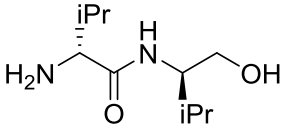	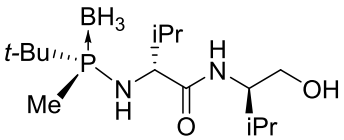 **3.17**	93 >95% de	82 >95% de
8	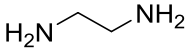	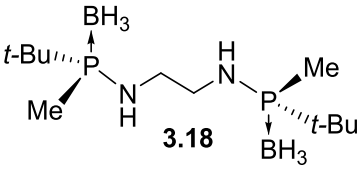 **3.18**	66 >95% de	–
9	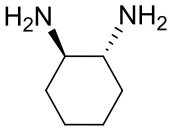	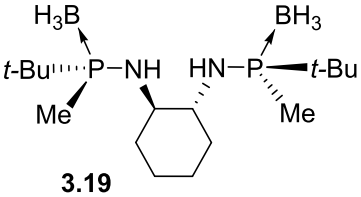 **3.19**	77 >95% de	–
10	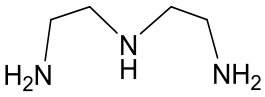	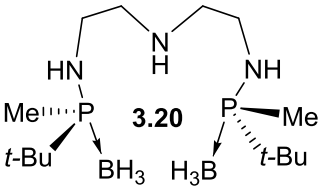 **3.20**	84 >95% de	–

a) Yield corresponds to isolated product purified by flash chromatography. b) Enantiomeric excess determined by chiral GC or HPLC analysis. c) Enantiomeric excess determined by chiral HPLC of the corresponding benzyl derivative. d) As determined by ^{1}H NMR analysis.

The reaction with ammonia afforded the resulting primary aminophosphine (*R*)-**3.3** in 98% ee (Table 3, entry 1). As previously mentioned, compound **3.3** is an important P-stereogenic synthon, useful for the synthesis of many different relevant ligands (such as MaxPHOS).[4,5] Reduction of the mixed anhydride with Bu_4NBH_4 (reaction developed

on previous Chapter 2) provided the secondary phosphine borane **3.12** in optically pure form and excellent yield (Table 3, entry 2). Compound **3.12** is also a noteworthy P-stereogenic synthon.[6–8] Reaction with primary amines provided the resulting S_N2@P products with excellent yields and stereospecificity (Table 3, entries 3-6). For both enantiomers of the α-branched chiral amine 1-phenylethan-1-amine, the resulting substitution products **3.15** and **3.16** were obtained with almost perfect inversion of configuration at phosphorus (Table 3, entries 5 and 6). Reaction with a highly functionalized amino alcohol produced solely the substitution product at the amine to yield **3.17** in excellent yield as a single diastereomer as determined by ^{1}H NMR analysis (Table 3, entry 7). Compound **3.17** is a precursor of P-stereogenic phosphino-oxazoline ligand MaxPHOX (see Chapter 5). All these results were compared to the ones obtained previously with **3.1** as starting material. We were pleased to see that most of the yields obtained with the new methodology are higher than the previous ones. The ee's and dr's are maintained and even increased in some cases. We decided to further study **3.8**'s potential and attempted the synthesis of bis-aminophosphines by using diamines as nucleophiles. Indeed, reaction of **3.8** with ethylenediamine produced in a single step the compound **3.18** in >95% diastereomeric excess and 66% yield (Table 3, entry 8). Using (*R,R*)-cyclohexane-1,2-diamine as nucleophile the corresponding disubstitution product **3.19** could be isolated readily in good yield and excellent optical and diastereomeric purity (Table 3, entry 9). Finally, **3.8** was reacted with diethylenetriamine which bears one secondary and two primary amines (Table 3, entry 10). The S_N2@P reaction showed to be highly specific for the primary positions leading to compound **3.20** which holds great potential as a wide bite-angle pincer ligand.

3.3. Conclusions

In summary, we disclosed that diisopropylammonium *tert*-butylmethylphosphonite borane **3.8** is a convenient, highly crystalline, stable, user friendly surrogate of the corresponding phosphinous acid that can be easily prepared in multigram scale.

X-ray analysis showed that the increased stability of **3.8** in solid state arises from a tetrameric assembly with a cyclic H-bond network.

Moreover, we have demonstrated that **3.8** can be directly utilized in S_N2@P reactions for the synthesis of valuable P-stereogenic intermediates and ligands. The results matched, and for some cases even surpassed, the ones obtained with phosphinous acid **3.1**. We also broadened the scope of this reaction by studying the reactivity of salt **3.8** with diamines.

We hope that dialkylammonium phosphinites boranes like **3.8** will foster the large scale preparation and the use of optically pure phosphinous acid boranes in the synthesis of diverse and valuable P-stereogenic compounds.

3.4. References

[1] S. Orgué, A. Flores-Gaspar, M. Biosca, O. Pàmies, M. Diéguez, A. Riera, X. Verdaguer, *Chem. Commun.* **2015**, *51*, 17548–17551.

[2] T. León, A. Riera, X. Verdaguer, *J. Am. Chem. Soc.* **2011**, *133*, 5740–5743.

[3] M. Stankevič, G. Andrijewski, K. M. Pietrusiewicz, *Synlett* **2004**, *2004*, 0311–0315.

[4] M. Revés, C. Ferrer, T. León, S. Doran, P. Etayo, A. Vidal-Ferran, A. Riera, X. Verdaguer, *Angew. Chem. Int. Ed.* **2010**, *49*, 9452–9455.

[5] T. León, M. Parera, A. Roglans, A. Riera, X. Verdaguer, *Angew. Chem. Int. Ed.* **2012**, *51*, 6951–6955.

[6] T. Imamoto, K. Sugita, K. Yoshida, *J. Am. Chem. Soc.* **2005**, *127*, 11934–11935.

[7] K. Tamura, M. Sugiya, K. Yoshida, A. Yanagisawa, T. Imamoto, *Org. Lett.* **2010**, *12*, 4400–4403.

[8] T. Imamoto, K. Tamura, Z. Zhang, Y. Horiuchi, M. Sugiya, K. Yoshida, A. Yanagisawa, I. D. Gridnev, *J. Am. Chem. Soc.* **2012**, *134*, 1754–1769.

Chapter 4

Catalytic Asymmetric Hydrogenation

-Background-

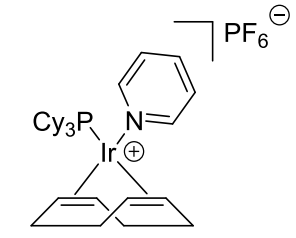

Crabtree's Catalyst

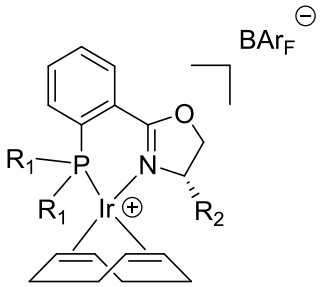

Ir-PHOX

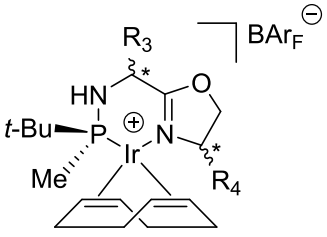

Ir-MaxPHOX

4.1. Catalysts for asymmetric hydrogenation

Asymmetric hydrogenation of double bonds is nowadays a vital tool for organic chemists whether they are in the academia or in the industry.[1,2] Chiral catalysts, whether the chirality lies on the phosphorous atoms or on the backbone, are required for such reactions.[3,4] Among the P-based catalysts we could, generalizing, differentiate two large main groups: the P,P and the P,N catalysts.[5,6]

The P,P based catalysts are obviously build around two phosphorous atoms that coordinate to the metal. With metals such as Rh or Ru, these catalysts are often proficient in the hydrogenation of functionalized olefins (amides or carboxylic acids work well as chelating groups for example). However, when it comes to selectively hydrogenating minimally or even non-functionalized double bonds, the P,N based catalysts, coordinated to Ir, usually perform better. Frequently for these procedures the solvent is chosen accordingly; for P,P catalysts coordinating solvents like alcohols are normally employed, while for the P,N type non-coordinating solvents like dichloromethane are used.

Again, this is a classification that cannot be taken very strictly. There is a broad spectrum of compounds that lay in-between the functionalized and the completely non-functionalized substrate distribution. So it is important to understand this approach as a rough arrangement, used for the sake of the discussion and to give a general overview on the topic.

In Figure 1 we depict some of the most noteworthy P,P ligands. We do not specify the coordination metal for each ligands as several of them can be coordinated to more than one.[7–16]

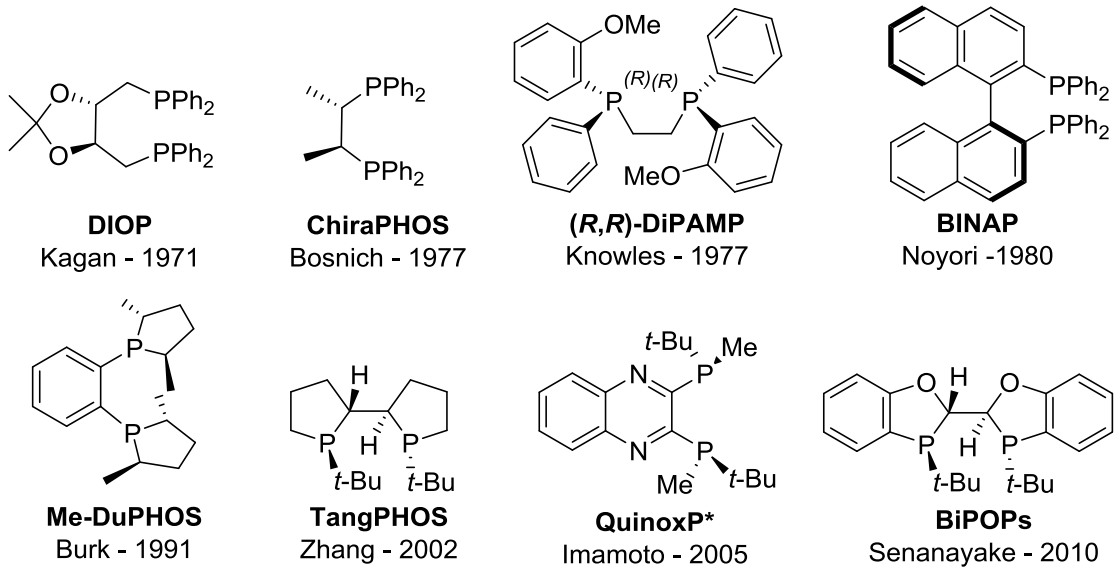

Figure 1. *Some of the most relevant P,P ligands.*

In this thesis we have worked mostly with one family of catalysts; the Ir-MaxPHOX family. The MaxPHOX are P*,N ligands developed in our group. We are next discussing different P,N based complexes in more detail.[17,18]

4.1.1. P,N iridium catalysts

4.1.1.1. The Crabtree's catalyst

During the 70's, Crabtree's group studied Schrock and Osborn type catalysts; $[M(cod)L_2][X]$.[19,20] They saw that Ir catalysts of this type where less active than their Rh counterparts when hydrogenating alkenes. They correctly concluded that coordinating solvents, during the catalysis, interacted with the metal forming too stable intermediates of the type $[Ir(H)_2(S)_2L_2][X]$. They observed an increment in the conversions, particularly for Ir complexes, when exchanging the solvent for a less coordinating one, like CH_2Cl_2.

Crabtree then designed the first P,N-Ir catalyst. This compound was both faster and more effective than its diphosphine analogs in the hydrogenation of non-functinolized tri- and tetrasubstituted alkenes.[21,22] This higher activity was attributed to the possible presence of a *cis* conformation between the pyridine and the PCy_3

(tricyclohexylphosphine) ligands. Also this catalyst, previous to H_2 activation, is air stable. However, it did have a shortcoming; when the coordination with the alkene is weak, the active catalyst dimerizes and trimerizes, ending up forming inactive clusters.[23] Consequently, high loadings were often required for full conversions.

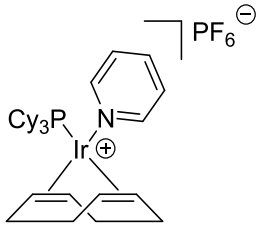

Crabtree's Catalyst

Figure 2. *The Crabtree's catalyst; the first P,N-Ir catalyst.*

4.1.1.2. The Pfaltz's catalysts

In 1997 Pfaltz and co-workers developed a chiral version of the Crabtree's catalyst, the Ir-PHOX.[24] Unlike Crabtree's, Pfaltz's catalyst has a phosphinooxazoline molecule as ligand. Consequently, the P and the N metal-chelating units are tethered together by a chiral C-backbone. This complex performs particularly well on the asymmetric hydrogenation of N-arylimines[24] and non-functionalized tri- and tetrasubstituted alkenes[25]. However, it also exhibited the issue of deactivation by aggregation into inactive clusters when the coordination with the substrate is feeble.[26] Up to 3 mol% loading of the catalyst was often required. Pfaltz overcame this shortcoming by exchanging the counteranion for BAr_F^-, a big, weakly coordinating counteranion.[27] While a more coordinating counteranion like PF_6^- might interfere with the alkene coordination to the metal, the BAr_F^- counteranion does not hamper the coordination at all. Therefore, the catalyst is "virtually saturated with alkene" and the hydrogenation pathway clearly predominates over the deactivation by formation of inactive hydride-bridged trinuclear complexes.

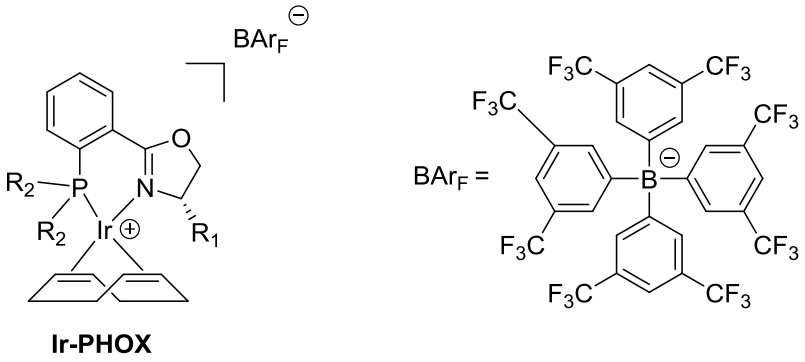

Ir-PHOX

Figure 3. *The Ir-PHOX catalyst; chiral P,N-Ir catalyst with BAr_F^- as counteranion.*

Despite the breakthrough that the Ir-PHOX meant, there was still room and also necessity for new catalysts. Pfaltz reported in 2001 a new class of Ir complexes with phosphooxazoline ligands, the SerPHOX and the ThrePHOX. [28] In comparison to the Ir-PHOX, the phosphorous unit on these catalysts is attached next to the stereogenic center coming from the oxazoline moiety.

Another quite interesting catalysts that Pfaltz developed on 2004 are the SimplePHOX.[29] As the name gives away, the selling point is their very simple preparation. Reaction between a chiral amino alcohol (obtained from an amino acid) and 2-hydroxy-2-methylpropionic acid affords the corresponding oxazonyl alcohol. Then, deprotonation and reaction with a chlorophosphine affords the ligand.

Both catalysts gave excellent results in the hydrogenation of new alkene substrates with conversions and ee's up to 99%. [17]

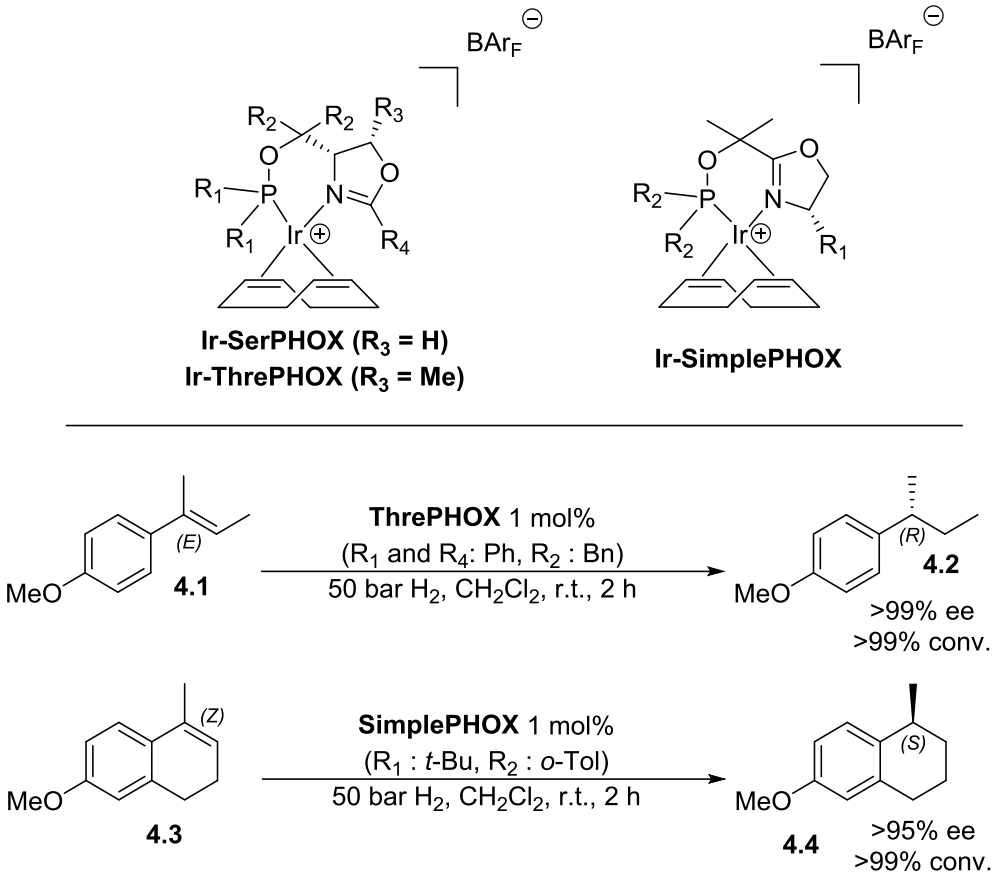

Figure 4. *The SerPHOX, the ThrePHOX and the SimplePHOX Ir catalysts. New alkenes could be reduced with excellent results.*

In pursue of achieving a more similar coordination sphere to the Crabtree's catalyst, Pfaltz developed another noteworthy type of catalysts derived from pyridine and quinolone. [30] These complexes proved to be useful in the asymmetric hydrogenation of purely alkyl-substituted olefins and furans.[31]

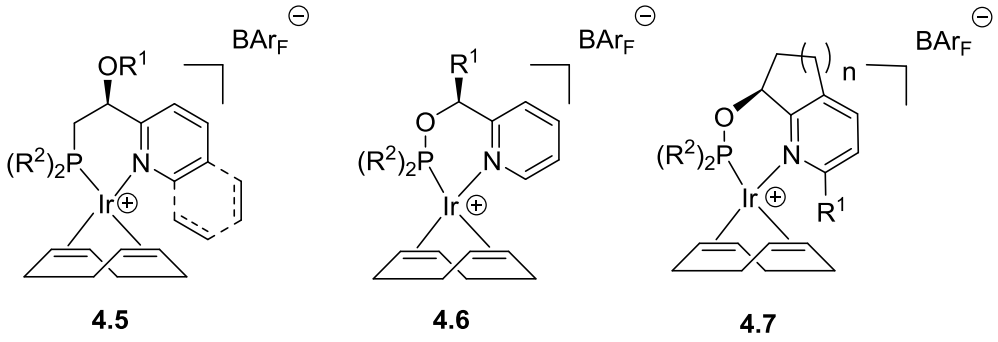

Figure 5. *Pyridine and quinolones derived Pfaltz's complexes.*

4.1.1.3. Other P,N catalysts

Chiral P,N-Iridium catalysts have arisen a lot of interest from many research groups. This caused many new other complexes of the kind to show up. Herein we are reporting a few noteworthy examples.

Andersson and co-workers, between 2004 and 2006,[32–34] studied and developed new P,N ligands that contain a rigid bicyclic backbone and a oxazole or a thiazole moiety. Also, a norbornane-oxazoline one. These ligands, once coordinated to Ir, perform at the same level as the best oxazoline-based complexes.

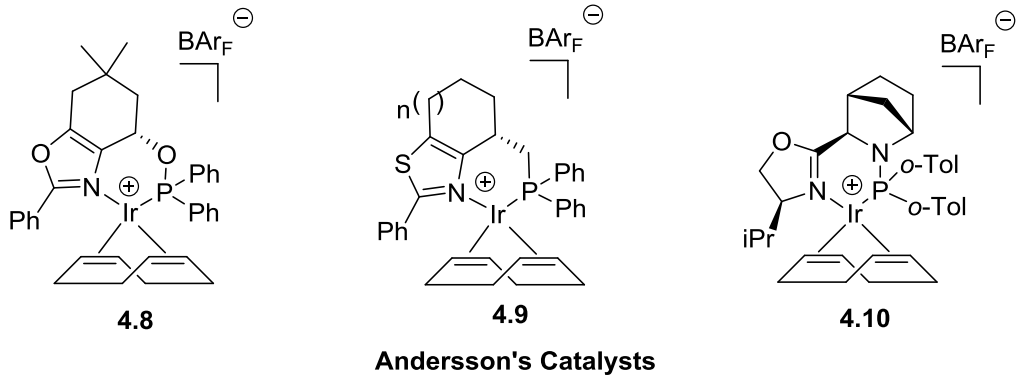

Figure 6. *Andersson's Ir-P,N catalysts.*

Knochel,[35] in 2003, developed another new pyridine-phosphine catalyst to hydrogenate methyl α-acetamidocinnamates with ee's up to 97%, as shown in Figure 7.

Zhou developed in 2006 a new ligand that he named SIPHOX.[36] This phosphine-oxazoline ligand contains a rigid and bulky spirobiindane backbone. Once coordinated to Ir, with BAr_F^- as counteranion, the complex is efficient for example in the asymmetric hydrogenation of *N*-aryl imines.

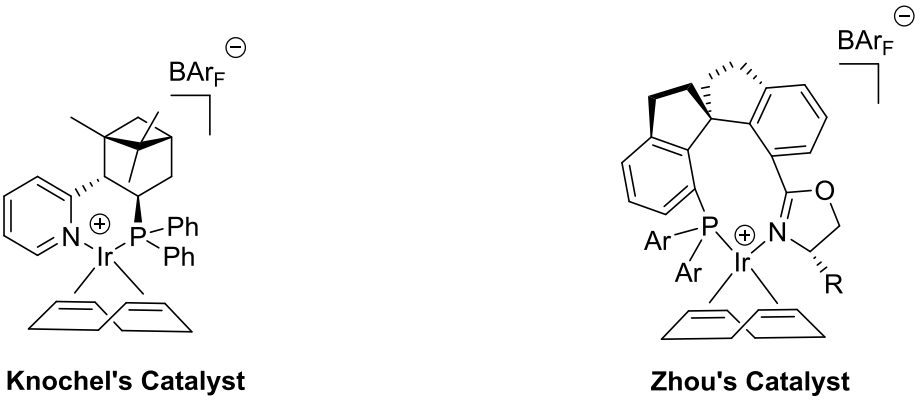

Figure 7. *Knochel's and Zhou's Ir catalysts.*

In 2009 Dieguez, Andersson and Borner joined forces to develop a library of up to 96 phosphite oxazoline ligands.[37] Those ligands are formed out of a SerPHOX or ThrePHOX derived backbone plus different chiral biarylphosphinites. With Ir as metal and BAr_F^- as counteanion, they hydrogenated for instance a series of aryl-alkyl substituted terminal alkenes.

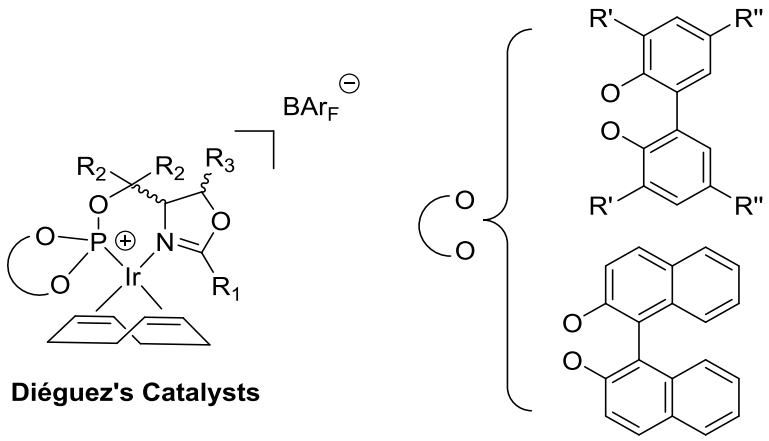

Figure 8. *Diéguez's Ir / Phosphite oxazoline catalysts.*

Finally, Burgess reported in 2003 a new Iridium catalyst.[38] The catalyst contains the common oxazoline moiety and, although the P-group has been replaced by a heterocyclic carbene, we deemed necessary to make allusion to this complex. The catalyst has been used in the hydrogenation of bis and monoarylalkenes, allylic alchohols, enoates and more.[39]

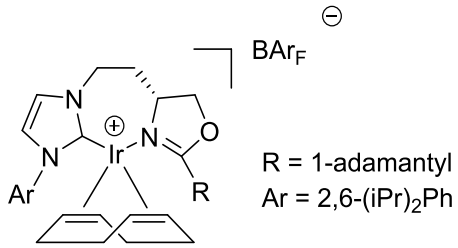

Burgess's Catalyst

Figure 9. *The Burgess's catalyst. A P,Carbene-Ir complex.*

Many other P,N ligands have been coordinated to Ir and used for asymmetric catalysis. However, we cannot discuss them all in the present work. Instead, we will move on to the MaxPHOX family of catalysts. They have been developed in our group and are fundamental in this PhD thesis.[40]

4.1.1.4. The MaxPHOX catalysts

As explained before in Chapter 1, our group developed a methodology to synthesize chiral aminophosphines by S_N2@P reaction between an amine and the chiral synthon *tert*-butylmethylphosphinous acid borane. Applying this procedure, S. Orgué reported the synthesis of the MaxPHOX ligand **4.11** and its coordination to Ir. The complexation is a 3-step procedure; first there is the deprotection with neat pyrrolidine. This cyclic amine proved to be a better reagent for deprotection than, for example, the well-known DABCO basically due to purification issues. Once the phosphine is deprotected, the pyrrolidine can be removed under high vacuum. The borane protected pyrrolidine byproduct formed is not volatile, but it does not affect the procedure and can be purified straightforwardly at the end of the synthesis. The free ligand, under N_2 atmosphere, is resolubilized with CH_2Cl_2 and then $[IrCl(cod)]_2$ is added. After 1 h, $NaBAr_F$ is added and the reaction is left stirring for another hour. The catalyst, with BAr_F^- as counteranion, can be easily purified by silica column with hexanes / CH_2Cl_2.

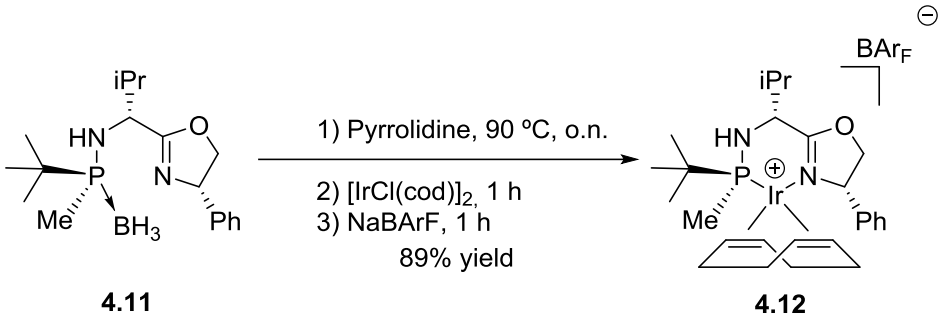

Figure 10. *The 3 step procedure for the coordination with Ir.*

The Ir-MaxPHOX catalysts bear 3 independent chiral centers; one is the P unit and the other two are located in the C-backbone. For one type of Ir-MaxPHOX catalyst (same substituents) there are 4 possible diastereoisomers. As the C-backbone chiral groups can be easily changed (Ph, Bn, iPr, *t*-Bu, etc), the possible combinations are many. Hence, one of the strongpoints of this family of catalysts is the possibility to fine-tune the complex until the asymmetric catalysis proceeds as desired.

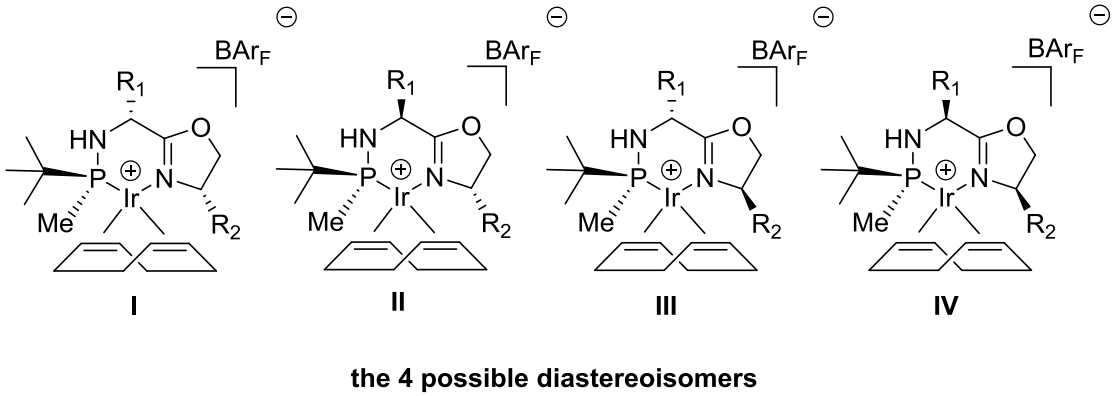

Figure 11. *There are four diastereoisomers for one Ir-MaxPHOX catalyst. The other 4 stereoisomers would be the corresponding enantiomers.*

Nevertheless, S. Orgué's methodology failed to afford any MaxPHOX ligand but ligand **4.11**. During the present PhD thesis we designed a new synthetic route and created

a small family of MaxPHOX ligands and their corresponding complexes that will be described in Chapter 5. We have used the Ir-MaxPHOX family to asymmetrically hydrogenate the following substrates;

a) *N*-aryl imines (Chapter 6)
b) *N*-alkyl imines (Chapter 7)
c) Cyclic Enamides (Chapter 8)

Next we will report some of the most important and best results for each type of substrate.

4.2. Asymmetric hydrogenation of *N*-aryl imines

4.2.1. Best reported results to the date

The catalytic asymmetric hydrogenation of imines is a very important methodology to obtain chiral amines.[41–43] These amines can be used as key building blocks for synthesizing drugs and other fine chemistry compounds. *N*-aryl imines are usually easier to synthesize and more stable than other imines (e.g. *N*-alkyl imines). The results obtained on the asymmetric hydrogenation of *N*-aryl imines are also generally better in terms of conversion and ee than for other imines. Taking all this into account, is not surprising that these compounds have been used as benchmark substrates.

There are many successful examples for catalytic asymmetric hydrogenations of *N*-aryl imines. However, in this work we are only highlighting a few noteworthy examples. We selected acetophenone *N*-phenyl imine as our basic, model substrate. In Figure 12 we report some of the best and latest results obtained for this asymmetric hydrogenation.

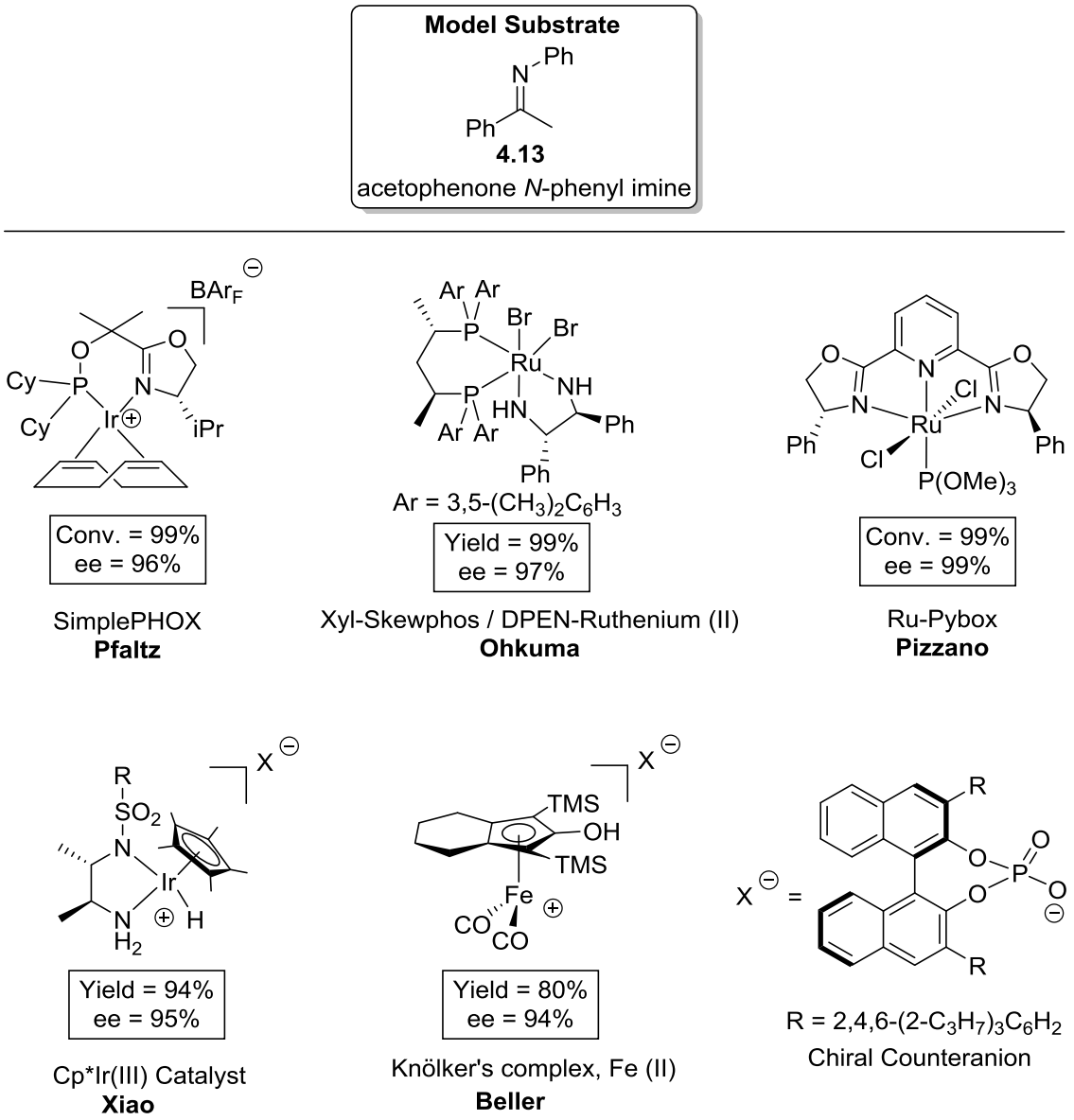

Figure 12. *Some relevant catalysts for the asymmetric hydrogenation of N-aryl imines.*

In 2008, J. Xiao reported the hydrogenation of the model imine with 94% yield and 95% ee.[44] He employed a chiral iridium catalyst aided by a chiral phosphate counteranion. In 2011, Beller reported 80% yield and 94% ee by using a similar procedure.[45] Although the methodology resembles Xiao's, Beller's employs a non-chiral iron catalyst, which is a greener metal. The chirality resides solely on the counteranion.

In 2010 Pfaltz studied these imines with different Ir-P,N catalysts.[46] With his own catalyst, the SimplePHOX, he obtained complete conversion and 96% ee on the

hydrogenation of the model substrate. This reaction had to be conducted at -20 ºC in order to obtain the maximum possible ee.

Later on, in 2012, Ohkuma reported a methodology that employs the complex Xyl-Skewphos / DPEN-Ruthenium (II).[47] With this complex they obtained 99% yield and up to 97% ee on the hydrogenation of the model compound.

The most recent successful attempt was reported by Pizzano in 2015.[48] Using Ru complexes bearing both a pybox (2,6-bis(oxazoline)pyridine) and a monodentate phosphite ligand. He reported full conversion and complete control over the ee at 20 bar of H_2 and 60 ºC.

4.2.2. Mechanism

4.2.2.1. Pfaltz's Iridacycle

As in the present PhD thesis we have attempted the asymmetric hydrogenation of *N*-aryl imines with the Ir-MaxPHOX catalysts, we are centering this Section on the hydrogenation mechanism with P,N-Ir catalysts. The mechanism has been deeply debated over the years. However, it was not until recently (in 2013) that Pfaltz's group experimentally identified a key catalytic intermediate; an iridiacycle.[49] This has guided other groups on their respective computational studies and it seems like finally there is a well-supported and defined hydrogenation mechanism.

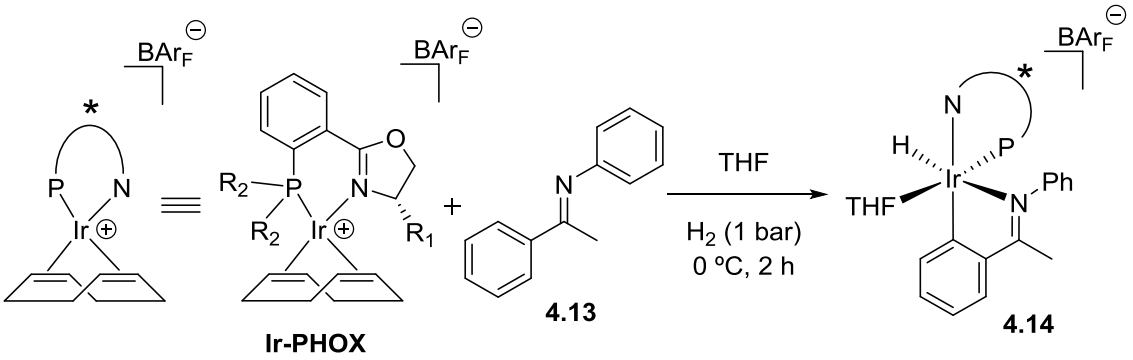

Figure 13. *Pfaltz reported the existence of a key iridacycle intermediate in the hydrogenation of N-aryl imines with the Ir-PHOX catalysts.*

Pfaltz identified an iridacycle that is formed when an Ir-P,N catalyst (like the Ir-PHOX or the SimplePHOX) is reacted with an *N*-aryl ketimine in presence of H_2 (Figure 13). The Ir-P,N is activated (COD is removed) and the imine undergoes a C–H activation that leads to the formation of the iridacycle intermediate. Pfaltz managed to obtain an X-Ray structure of an iridacycle, further confirming his discovery. In this 2013 publication there are two key experiments that shed light on the hydrogenation of imines mechanism;

a) Pfaltz pondered if this intermediate is actually a key part of the hydrogenation mechanism or just an inactive species outside the catalytic cycle in equilibrium with an active catalytic intermediate. If the iridacycle is truly a key, active component of the catalytic cycle; does it react via reduction of the cyclometalated imine, with reductive elimination of the saturated amine, or is the imine part of the true catalyst and remains attached to the metal during the whole catalytic cycle?

To answer these questions Pfaltz proposed a simple, key experiment. He was able to isolate the more stable but inactive Cl-iridacycle **4.15** (Figure 14). By adding $NaBAr_F$ to the media, the counteranion is exchanged and the catalysis proceeds again. So, he isolated iridacycle **4.15** and added it to a solution of $NaBAr_F$ and imine **4.16** in CH_2Cl_2 under a H_2 atmosphere. The catalysis proceeded as expected and amine **4.17** was obtained with the expected ee. No trace of imine **4.13**, used to form the initial Cl-iridacycle, or the corresponding reduced amine **4.18** were detected. This proves that the metal-chelated imine is not labile and does not dissociate from the metal during the whole catalysis and consequently plays an active role in the catalytic cycle.

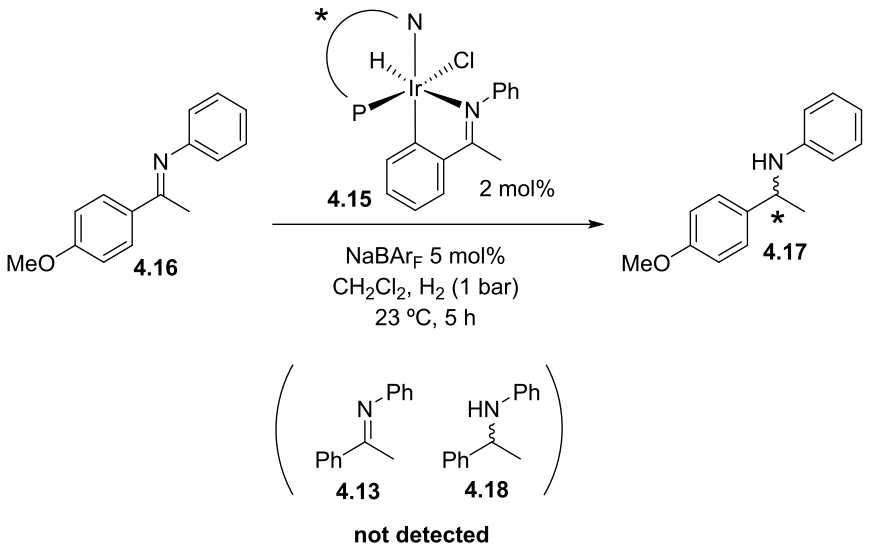

Figure 14. *Catalysis employing* ***4.15*** *as catalyst. Imine* ***4.13*** *or amine* ***4.18*** *were not detected.*

b) The second pivotal experiment in Pfaltz's 2013 paper is the reduction of **4.19**. This type of *N*-aryl imines of dialkyl ketones are very problematic to hydrogenate properly with Crabtree-like catalysts. Pfaltz theorized this was due to the impossibility for this substrates to undergo a C–H activation and form the iridacycle (the alkylic ring is formed out of C sp^3 and not C sp^2). By using imine **4.13** as additive, the conversion and the ee obtained surprisingly increased. This indicates that the cyclometalated species is a much more efficient catalyst that the non-cyclometalated one, further proving the relevance of this intermediate in the catalytic cycle.

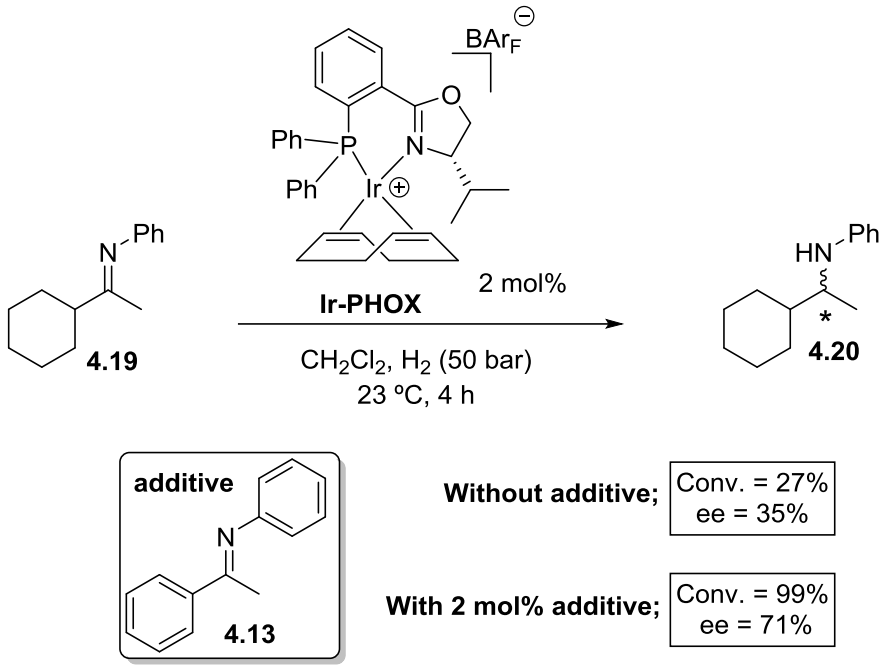

Figure 15. *Hydrogenation of N-aryl imines of dialkyl ketones such as* ***4.19*** *using* ***4.13*** *as additive.*

4.2.2.2. Computational studies considering the iridacycle

There are many computational papers claiming or supporting different mechanisms for the hydrogenation of *N*-aryl imines with Ir-P,N catalysts. However, once Pfaltz iridacycle was identified, the reports to the date had to be revised. In 2018, Norrby, Wiest and Andersson published a study taking into account Pfaltz's discovery.[50] They proposed three different Ir^{III} / Ir^{V} mechanisms for the hydrogenation of model substrate **4.13** with one of Andersson's Ir-P,N complexes; an outer sphere one and two inner sphere mechanisms. All three mechanisms takes into account the iridacycle species. The inner sphere proposals consisted in a C-Migration vs a N-Migration. After doing the pertinent calculations, they concluded that the Outer Sphere mechanism is more energetically plausible than any of the Inner Sphere ones. Also this model predicts an ee and a configuration for the product that matches the experimental results.

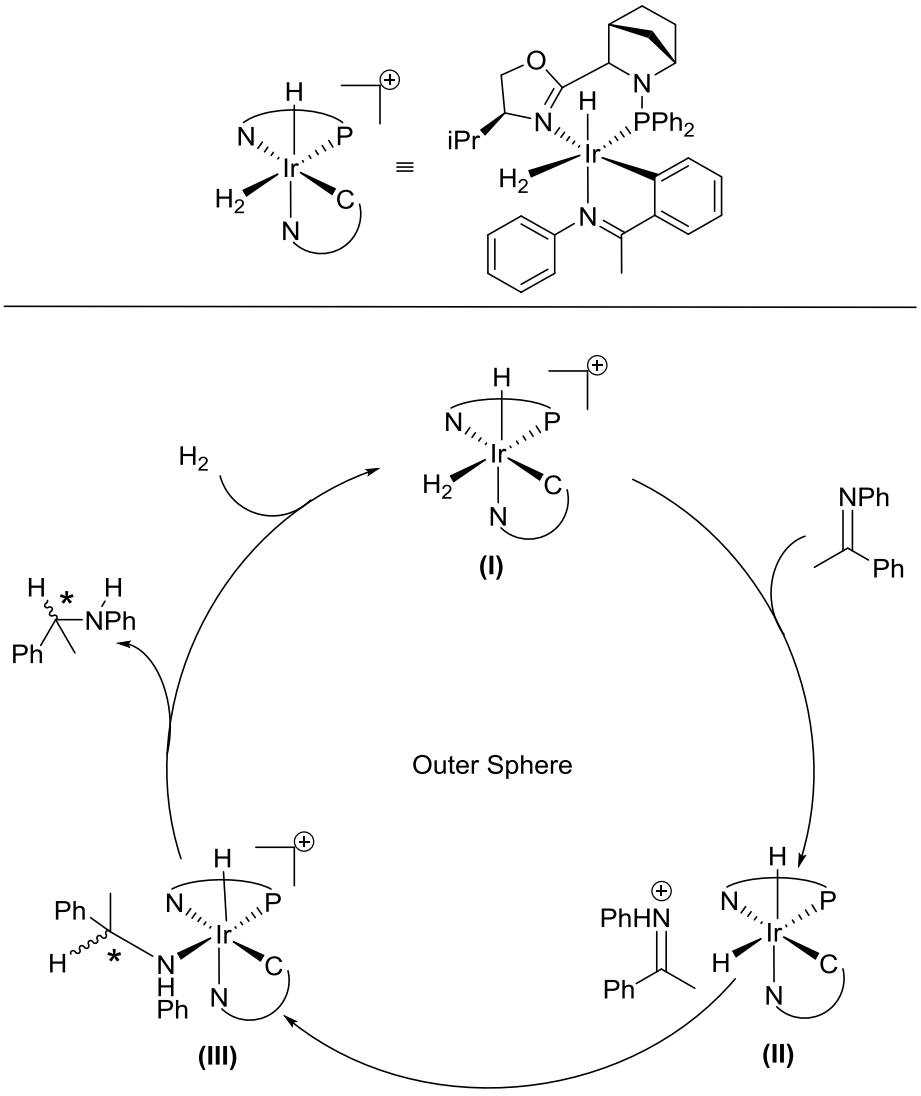

Figure 16. *Norrby-Wiest-Andersson's proposed Outer Sphere mechanism for the hydrogenation of N-aryl imines with Crabtree-like catalysts.*

4.3. Asymmetric hydrogenation of *N*-alkyl imines

4.3.1. Best reported results to the date

The asymmetric catalytic reduction of *N*-alkyl imines to the corresponding amines is no easy task. Compared to *N*-aryl imines, they are less stable. More importantly, they are also more basic and nucleophilic, which can be problematic as they might interfere with the catalyst and consequently jeopardize the whole catalysis.

There have not been as many attempts to hydrogenate *N*-alkyl imines as with *N*-aryl imines and very few have been successful. For the following background report we have picked acetophenone *N*-methyl imine **4.21** as a model substrate.

In 1996, Buchwald and co-workers reported a very efficient enantioselective imine hydrosilylation using a Ti catalyst.[51] The ee's for the obtained amines went up to 99%. It is the only methodology to the date that claims complete control over the enantioselectivity of the amine. The only drawbacks for this procedure are its poor atom economy and the difficult synthesis of the Ti catalyst. Also, this approach did not perform well with bulky imines. However, Buchwald overcame this shortcoming by using different amines as additives, as he reported in a follow up publication in 1998.[52]

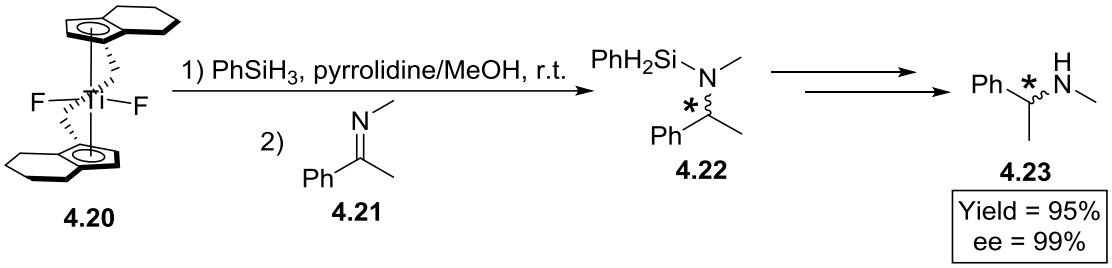

Figure 17. *Buchwald's reduction of* ***4.21*** *by hydrosilylation with Ti catalyst* ***4.20****.*

The second best results obtained for the reduction of this substrates were published by B. List in 2015.[53] His group employed an organocatalytic approach to hydrogenate with up to 91% ee the model substrate acetophenone *N*-methyl imine **4.21**. To do so, the reaction had to be conducted in the presence of Boc_2O. Otherwise the catalyst underwent product inhibition by the freshly formed amine. With Boc_2O in the media, the reduced imine is protected in situ and does not interfere with the catalyst. The method required long reaction times (up to two days), very specific conditions and 5% catalyst loading.

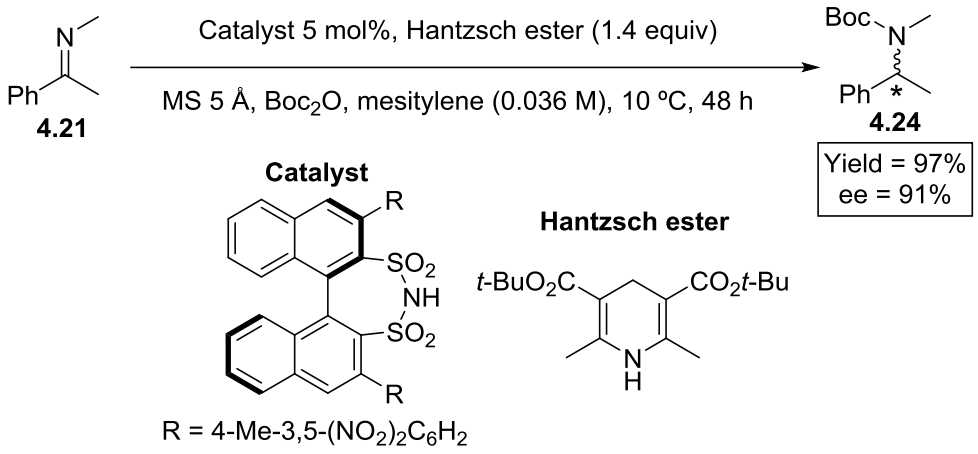

Figure 18. *B. List's reduction of* ***4.21*** *by organocatalysis.*

The results obtained by direct metal catalyzed hydrogenation with these imines are few and unexceptional. Hydrogenation with a Ru-BINAP-DPEN catalyst provided with 71% of ee (Figure 19). This result is reported in a patent.[54] Pfaltz obtained 58% ee and full conversion when using up to 4 mol% of Ir-PHOX and 100 bars of H_2.[24]

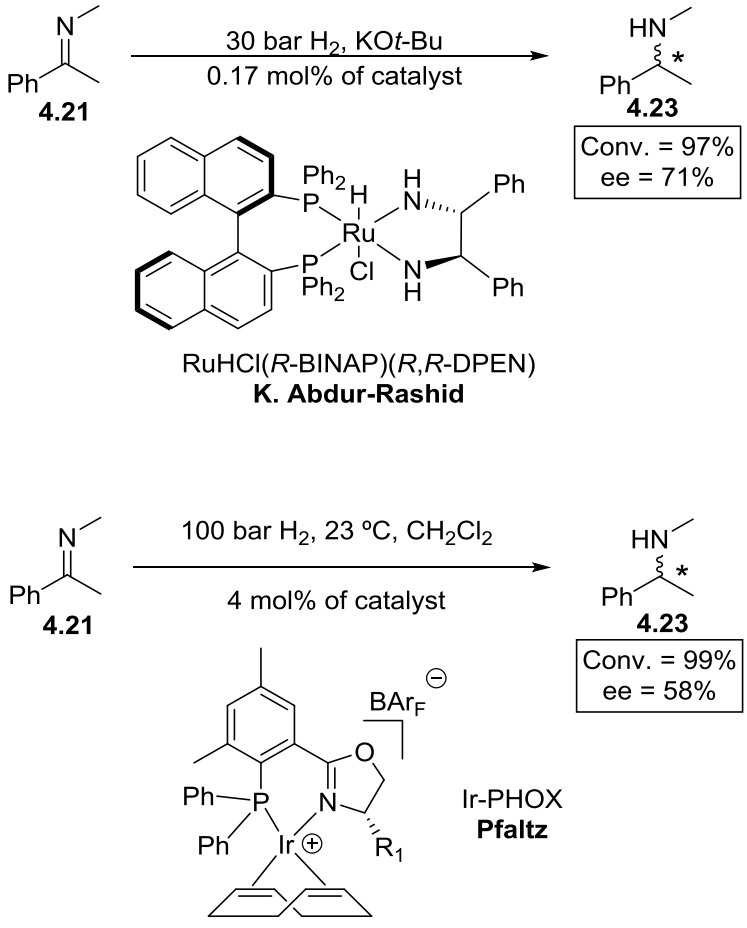

Figure 19. *Attempts to the direct metal catalyzed hydrogenation of* ***4.21****.*

4.4. Asymmetric hydrogenation of cyclic enamides

4.4.1. Best reported results to the date

Asymmetric reduction of enamides is another relevant manner to obtain chiral amines. If we had to classify cyclic enamides as chelating or non-chelating substrates for catalytic hydrogenations, they would fall into the first category. The enamide moiety can direct the substrate and therefore helps with the chirality transfer. Considering this, it is logical that Ru or Rh have been the metals of choice so far. Nevertheless, no one has obtained complete control over the enantioselectivity yet.

4.4.1.1. Cyclic β-enamides hydrogenation

There have been many attempts to asymmetrically hydrogenate cyclic β-enamides. We are next reporting the five most notable ones.

Bruneau[55] and Ratovelomanana[56] employed a Ru-BINAP and a Ru-SYNPHOS system, respectively. They reported 90% and 95% ee on the hydrogenation of the model substrate *N*-(3,4-dihydronaphthalen-2-yl)acetamide, respectively.

Reek, on 2006, reported an ee of 94% using a supramolecular Rh-catalyst.[57] Pizzano, in 2013, used a combination of Rh and a phosphine-phosphinite ligand that afforded an ee of 93% for the aforementioned model substrate, *N*-(3,4-dihydronaphthalen-2-yl)acetamide.[58] That same year, Tang and co-workers also reported the hydrogenation of *N*-(3,4-dihydronaphthalen-2-yl)acetamide with 96% of ee using a Rh-catalyst with the ligand WingPhos that conforms a deep chiral pocket.[59]

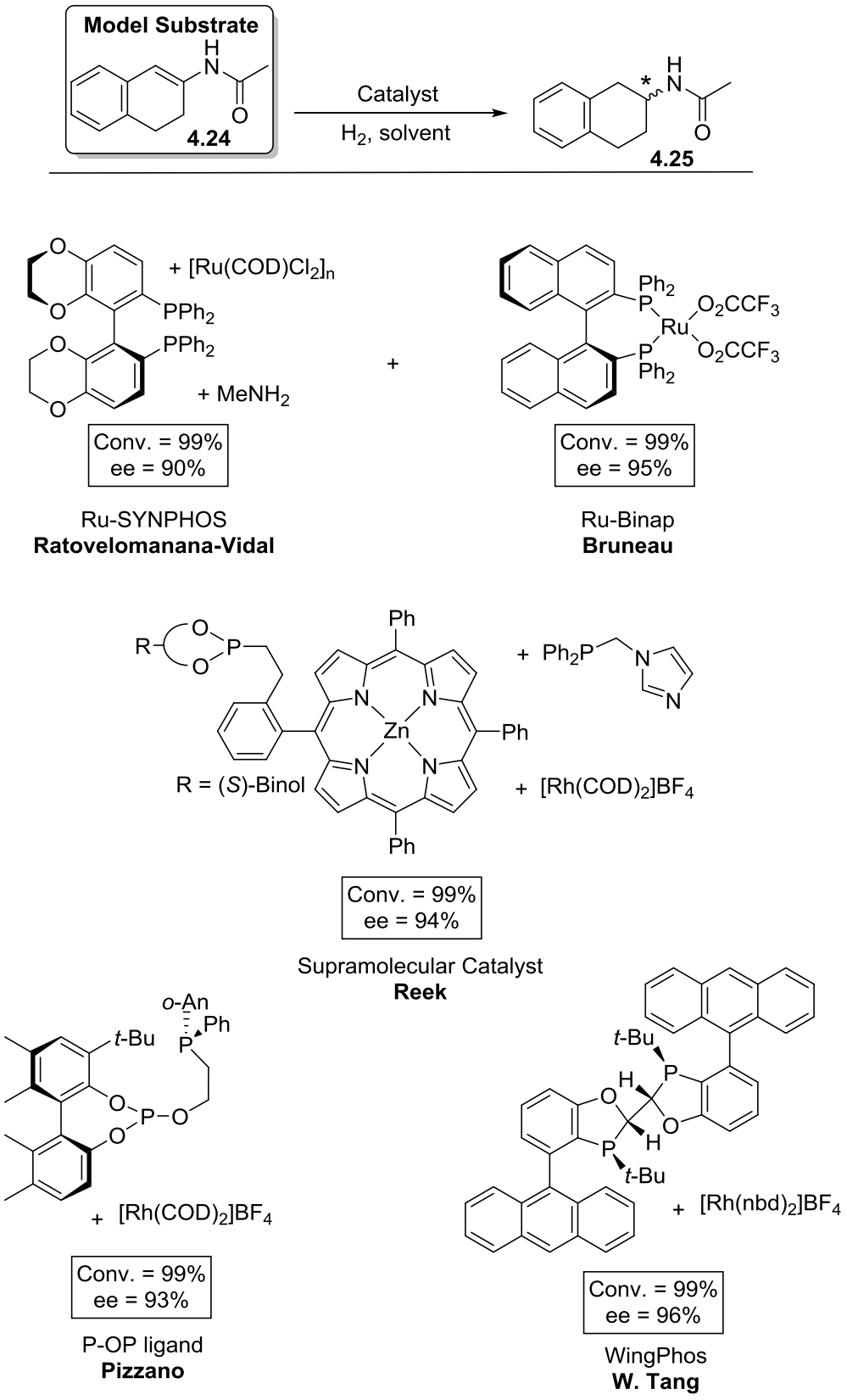

Figure 20. *Hydrogenation of cyclic β-enamides.*

4.4.1.2. Cyclic α-enamides hydrogenation

Some attempts have also been reported at the hydrogenation of cyclic α-enamides. Feringa in 2005 obtained an ee of 98% for the hydrogenation of the model substrate *N*-(3,4-dihydronaphthalen-1-yl)acetamide.[60] He employed MorfPHOS; a BINOL derived phosphoramidite in combination with Rh.

X. Zhang also reported a 98% of enantiomeric excess using Rh-PennPhos for the same substrate in 1999.[61]

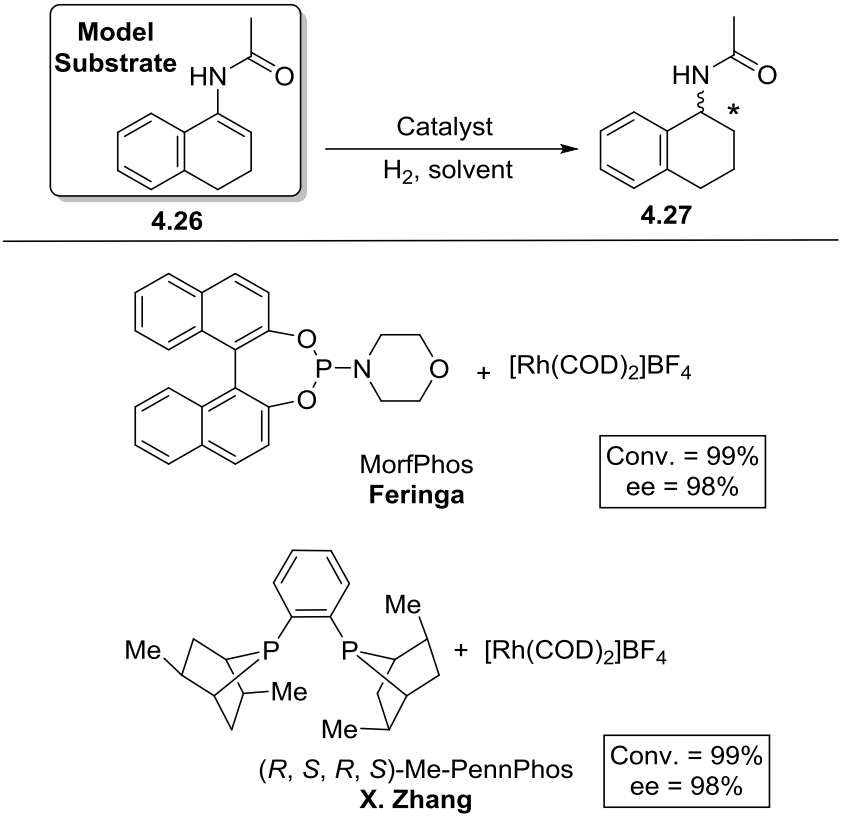

Figure 21. *Hydrogenation of cyclic* α*-enamides.*

It is noteworthy that, although there are very high ee's reported for both cyclic α and β-enamides, no one ever managed to achieve complete control over the reaction enantioselectivity. Also, the catalysts that perform well for cyclic α-enamides, do not function properly with β-enamides, and the other way around. So, there is still a need for a catalytic system that completely controls the enantioselectivity and works for both cyclic α- and β-enamides.

4.5. Asymmetric hydrogenation of non-functionalized alkenes

4.5.1. Best reported results to the date

To enantioselectively hydrogenate an olefin lacking coordinating groups that chelate to the metal and direct the catalysis is no easy task. As we previously explained, P,P based ligands coordinated to metals like Rh or Ru, are often proficient in the hydrogenation of functionalized olefins. When it comes to selectively hydrogenating minimally or even non-functionalized double bonds, the P,N based ligands coordinated to Ir usually perform better.

We believe that the Ir-MaxPHOX catalysts can afford very good results in the hydrogenation of this kind of non-functionalized alkenes. In consequence, we initiated a collaboration with the group of Prof. Diéguez, which are experts in the field.

4.5.2. Mechanism

In regard to the mechanism, there has been many proposals over the years. A few years ago there was a discrepancy about what mechanism was the correct one; the Ir^{I}/Ir^{III} or the Ir^{III}/Ir^{V} mechanism. The Ir^{I}/Ir^{III} mechanism was an analogy to the alkene hydrogenation with Rh mechanism and was supported, among others, by Chen.[62] Meanwhile, Andersson[63] and Burgess[64] proved computationally that the Ir^{III}/Ir^{V} mechanism was the more energetically favored of the two.

In 2014, Pfaltz proved experimentally the Ir^{III}/Ir^{V} over the Ir^{I}/Ir^{III} one.[65] To do so, his group identified a previously elusive iridium dihydride alkene complex (intermediate **A**, Figure 22). They studied the intermediate and experimentally observed that it requires H_2 (g) from the media (in red) in order to hydrogenate and release the catalyst-bound alkene (in green). This event agrees with an Ir^{III}/Ir^{V} mechanism. For an Ir^{I}/Ir^{III} mechanism, the identified intermediate could reduce and release the alkane without requiring more H_2 from the media.

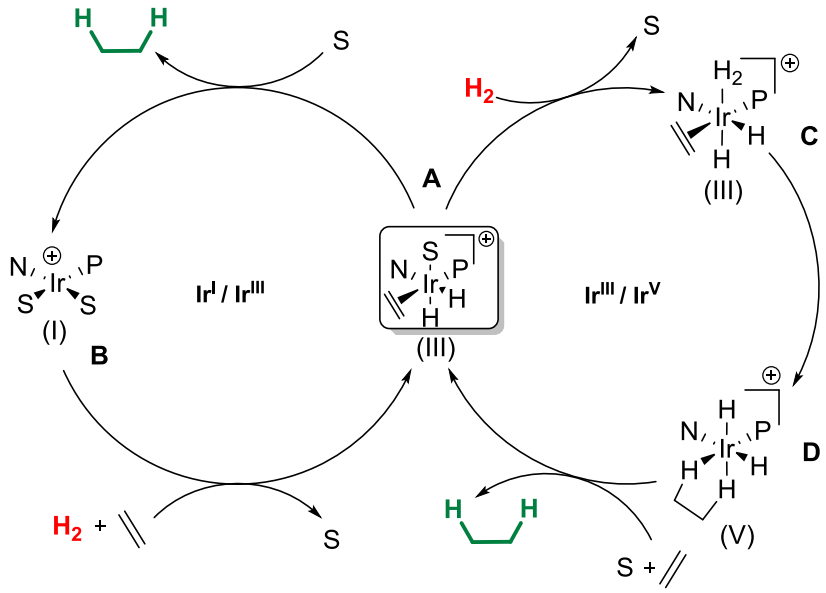

Figure 22. *By isolating and studying intermediate* ***A****, Pfaltz could prove the* $Ir^{III/V}$ *mechanism over the* $Ir^{I/III}$ *mechanism.*

Pfaltz studied intermediate (**III**) by NMR and observed two possible ways by which the alkene could coordinate to the metal center. These two isomers are in fast equilibrium and afford different reduced enantiomers. Interestingly, the predominant isomer does not afford the main enantiomer observed experimentally, but the minor one. While the minor of the two isomers affords the principal reduced enantiomer. It seems like the major pathway proceeds through a minor intermediate, analogous to the mechanism of the hydrogenation of acetamidoacrylates with chiral Rh-P,P complexes.

M. Diéguez[66] and K. H. Hopmann[67] separately proved computationally that, out of the two possible Ir^{III}/Ir^{V} mechanisms that were proposed, the Metathesis (Meta) mechanism and the Migratory Insertion (MI) mechanism, the second one was the most energetically viable (Figure 23).

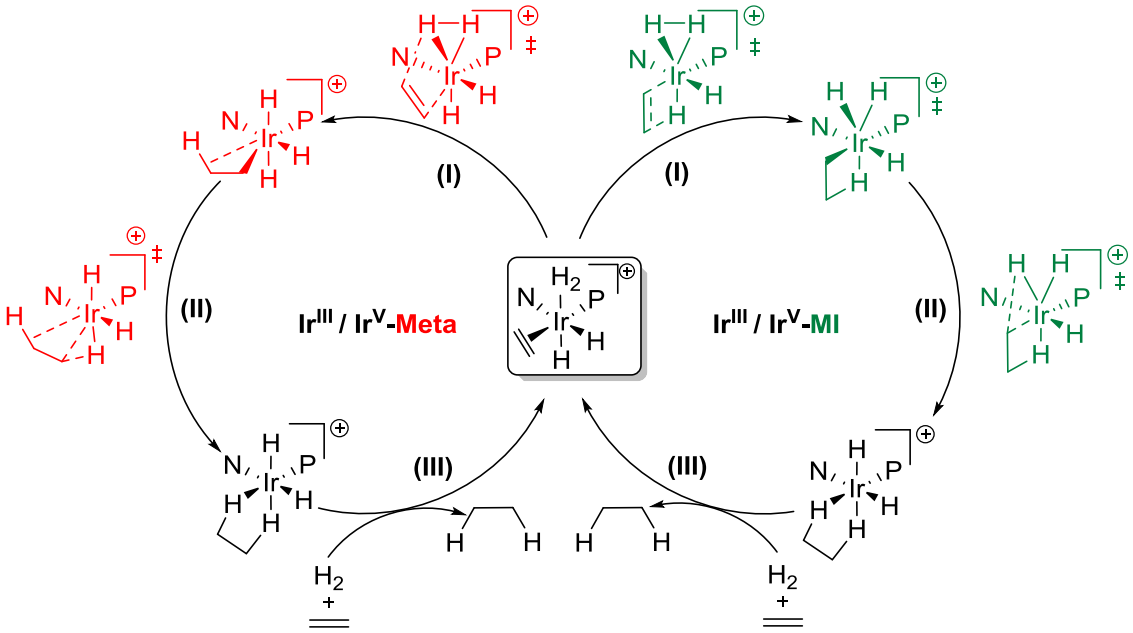

Figure 23. *Diéguez's representation of the $Ir^{III/V}$-MI and the $Ir^{III/V}$-Meta mechanisms. MI is more viable than Meta.*

In Figure 24 we present an alkene Ir-P,N hydrogenation mechanism taking all the previous discoveries into account.

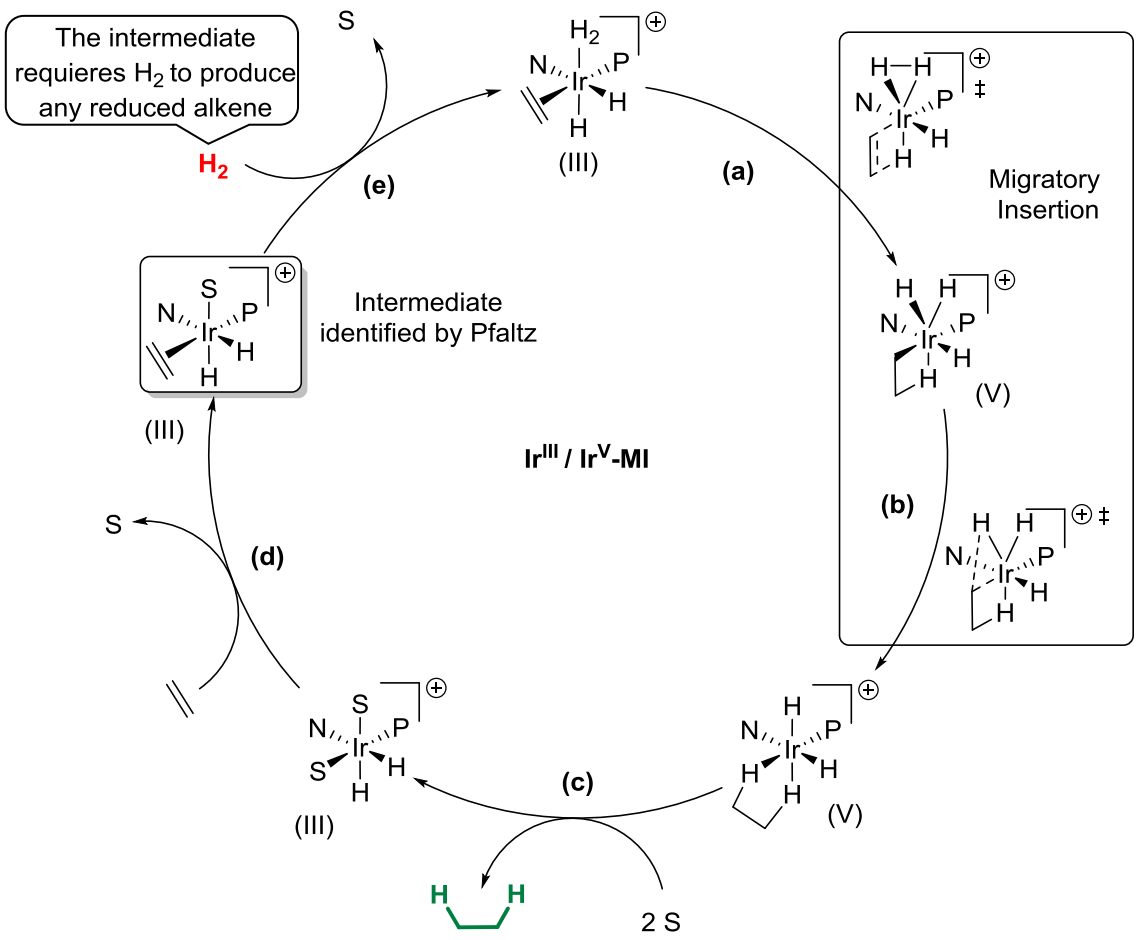

Figure 24. *Mechanism for the hydrogenation of non-functionalized alkenes with Crabtree-type catalysts.*

4.6. References

[1] H.-J. F. H.-U. Blaser, *Asymmetric Catalysis on Industrial Scale: Challenges, Approaches and Solutions*, Wiley, **2010**.

[2] P. Etayo, A. Vidal-Ferran, *Chem. Soc. Rev. Chem. Soc. Rev* **2013**, *42*, 728–754.

[3] P. G. Andersson, I. J. Munslow, *Modern Reduction Methods*, Wiley, **2008**.

[4] A. Börner, *Phosphorus Ligands in Asymmetric Catalysis*, Wiley, **2008**.

[5] J. J. Verendel, O. Pàmies, M. Diéguez, P. G. Andersson, *Chem. Rev.* **2014**, *114*, 2130–2169.

[6] W. Tang, X. Zhang, *Chem. Rev.* **2003**, *103*, 3029–3070.

[7] T. P. Dang, H. B. Kagan, *J. Chem. Soc. D* **1971**, 481.

[8] H. B. Kagan, Dang-Tuan-Phat, *J. Am. Chem. Soc.* **1972**, *94*, 6429–6433.

[9] M. D. Fryzuk, B. Bosnich, *J. Am. Chem. Soc.* **1977**, *99*, 6262–6267.

[10] B. D. Vineyard, W. S. Knowles, M. J. Sabacky, G. L. Bachman, D. J. Weinkauff, *J. Am. Chem. Soc.* **1977**, *99*, 5946–5952.

[11] A. Miyashita, A. Yasuda, H. Takaya, K. Toriumi, T. Ito, T. Souchi, R. Noyori, *J. Am. Chem. Soc.* **1980**, *102*, 7932–7934.

[12] M. J. Burk, *J. Am. Chem. Soc.* **1991**, *113*, 8519–8521.

[13] M. J. Burk, J. E. Feaster, W. A. Nugent, R. L. Harlow, *J. Am. Chem. Soc.* **1993**, *115*, 10125–10138.

[14] W. Tang, X. Zhang, *Angew. Chem. Int. Ed.* **2002**, *41*, 1612–1614.

[15] T. Imamoto, K. Sugita, K. Yoshida, *J. Am. Chem. Soc.* **2005**, *127*, 11934–11935.

[16] W. Tang, B. Qu, A. G. Capacci, S. Rodriguez, X. Wei, N. Haddad, B. Narayanan, S. Ma, N. Grinberg, N. K. Yee, et al., *Org. Lett.* **2010**, *12*, 176–179.

[17] S. J. Roseblade, A. Pfaltz, *Acc. Chem. Res.* **2007**, *40*, 1402–1411.

[18] D. H. Woodmansee, A. Pfaltz, *Chem. Commun.* **2011**, *47*, 7912.

[19] J. A. Osborn, R. R. Schrock, *J. Am. Chem. Soc.* **1971**, *93*, 2397–2407.

[20] R. R. Schrock, J. A. Osborn, *J. Am. Chem. Soc.* **1976**, *98*, 2134–2143.

[21] R. H. Crabtree, H. Felkin, G. E. Morris, *J. Organomet. Chem.* **1977**, *141*, 205.

[22] R. H. Crabtree, A. Gautier, G. Giordano, T. Khan, *J. Organomet. Chem.* **1977**, *141*, 113.

[23] R. Crabtree, *Acc. Chem. Res.* **1979**, *12*, 331–337.

[24] P. Schnider, G. Koch, R. Pretot, G. Wang, F. M. Bohnen, C. Kriiger, A. Pfaltz, *Chem. Eur. J.* **1997**, *3*, 887–892.

[25] A. Lightfoot, P. Schnider, A. Pfaltz, *Angew. Chem. Int. Ed.* **1998**, *37*, 2897–2899.

[26] A. Pfaltz, J. Blankenstein, R. Hilgraf, E. Hörmann, S. McIntyre, F. Menges, M. Schönleber, S. P. Smidt, B. Wüstenberg, N. Zimmermann, *Adv. Synth. Catal.* **2003**, *345*, 33–43.

[27] S. P. Smidt, N. Zimmermann, M. Studer, A. Pfaltz, *Chem. - A Eur. J.* **2004**, *10*, 4685–4693.

[28] J. Blankenstein, A. Pfaltz, *Angew. Chem. Int. Ed.* **2001**, *40*, 4445.

[29] S. P. Smidt, F. Menges, A. Pfaltz, *Org. Lett.* **2004**, *6*, 2023–2026.

[30] W. J. Drury, N. Zimmermann, M. Keenan, M. Hayashi, S. Kaiser, R. Goddard, A. Pfaltz, *Angew. Chem. Int. Ed.* **2004**, *43*, 70–74.

[31] S. Kaiser, S. P. Smidt, A. Pfaltz, *Angew. Chem. Int. Ed.* **2006**, *45*, 5194–5197.

[32] A. Trifonova, J. S. Diesen, C. J. Chapman, P. G. Andersson, **2004**, 1–38.

[33] K. Källström, C. Hedberg, P. Brandt, A. Bayer, P. G. Andersson, *J. Am. Chem. Soc.* **2004**, *126*, 14308–14309.

[34] C. Hedberg, K. Källström, P. Brandt, L. K. Hansen, P. G. Andersson, *J. Am. Chem. Soc.* **2006**, *128*, 2995–3001.

[35] T. Bunlaksananusorn, K. Polborn, P. Knochel, *Angew. Chem. Int. Ed.* **2003**, *42*, 3941–3943.

[36] S. F. Zhu, J. B. Xie, Y. Z. Zhang, S. Li, Q. L. Zhou, *J. Am. Chem. Soc.* **2006**, *128*, 12886–12891.

[37] J. Mazuela, J. J. Verendel, M. Coll, B. Schäffner, A. Börner, P. G. Andersson, O. Pàmies, M. Diéguez, *J. Am. Chem. Soc.* **2009**, *131*, 12344–12353.

[38] M. C. Perry, X. Cui, M. T. Powell, D. R. Hou, J. H. Reibenspies, K. Burgess, *J. Am. Chem. Soc.* **2003**, *125*, 113–123.

[39] Y. Zhu, K. Burgess, *Acc. Chem. Res.* **2012**, *45*, 1623–1636.

[40] S. Orgué, A. Flores-Gaspar, M. Biosca, O. Pàmies, M. Diéguez, A. Riera, X. Verdaguer, *Chem. Commun.* **2015**, *51*, 17548–17551.

[41] J. H. Xie, S. F. Zhu, Q. L. Zhou, *Chem. Rev.* **2011**, *111*, 1713–1760.

[42] N. Fleury-Brégeot, V. de la Fuente, S. Castillón, C. Claver, *ChemCatChem* **2010**, *2*, 1346–1371.

[43] K. H. Hopmann, A. Bayer, *Coord. Chem. Rev.* **2014**, *268*, 59–82.

[44] C. Li, C. Wang, B. Villa-marcos, J. Xiao, **2008**, 14450–14451.

[45] S. Zhou, S. Fleischer, K. Junge, M. Beller, *Angew. Chem. Int. Ed.* **2011**, *50*, 5120–5124.

[46] A. Baeza, A. Pfaltz, *Chem. - A Eur. J.* **2010**, *16*, 4003–4009.

[47] N. Arai, N. Utsumi, Y. Matsumoto, K. Murata, K. Tsutsumi, T. Ohkuma, *Adv. Synth. Catal.* **2012**, *354*, 2089–2095.

[48] E. Menéndez-Pedregal, M. Vaquero, E. Lastra, P. Gamasa, A. Pizzano, *Chem. - A Eur. J.* **2015**, *21*, 549–553.

[49] Y. Schramm, F. Barrios-Landeros, A. Pfaltz, *Chem. Sci.* **2013**, *4*, 2760.

[50] B. Tutkowski, S. Kerdphon, E. Limé, P. Helquist, P. G. Andersson, O. Wiest, P.

O. Norrby, *ACS Catal.* **2018**, *8*, 615–623.

[51] X. Verdaguer, U. Lange, M. . Reding, S. L. Buchwald, *J. Am. Chem. Soc.* **1996**, *118*, 6784–6785.

[52] X. Verdaguer, U. E. W. Lange, S. L. Buchwald, *Angew. Chem. Int. Ed.* **1998**, *37*, 1103–1107.

[53] V. N. Wakchaure, P. S. J. Kaib, M. Leutzsch, B. List, *Angew. Chem. Int. Ed. Engl.* **2015**, *54*, 11852–6.

[54] K. Abdur-Rashid, *Asymmetric Imine Hydrogenation Processes*, **2005**, WO 2005/056513 Al.

[55] J. L. Renaud, P. Dupau, A.-E. Hay, M. Guingouain, P. H. Dixneuf, C. Bruneau, *Adv. Synth. Catal.* **2003**, *345*, 230–238.

[56] C. Pautigny, C. Debouit, P. Vayron, T. Ayad, V. Ratovelomanana-Vidal, *Tetrahedron: Asymmetry* **2010**, *21*, 1382–1388.

[57] X. Bin Jiang, L. Lefort, P. E. Goudriaan, A. H. M. De Vries, P. W. N. M. Van Leeuwen, J. G. De Vries, J. N. H. Reek, *Angew. Chem. Int. Ed.* **2006**, *45*, 1223–1227.

[58] I. Arribas, M. Rubio, P. Kleman, A. Pizzano, *J. Org. Chem.* **2013**, *78*, 3997–4005.

[59] G. Liu, X. Liu, Z. Cai, G. Jiao, G. Xu, W. Tang, *Angew. Chem. Int. Ed.* **2013**, *52*, 4235–4238.

[60] H. Bernsmann, M. Van Den Berg, R. Hoen, A. J. Minnaard, G. Mehler, M. T. Reetz, J. G. De Vries, B. L. Feringa, *J. Org. Chem.* **2005**, *70*, 943–951.

[61] Q. Jiang, D. Xiao, Z. Zhang, P. Cao, X. Zhang, *Angew. Chem. Int. Ed.* **1999**, *38*, 516–518.

[62] R. Dietiker, P. Chen, *Angew. Chem. Int. Ed.* **2004**, *43*, 5513–5516.

[63] P. Brandt, C. Hedberg, P. G. Andersson, *Chem. - A Eur. J.* **2003**, *9*, 339–347.

[64] X. Cui, Y. Fan, M. B. Hall, K. Burgess, *Chem. - A Eur. J.* **2005**, *11*, 6859–6868.

[65] S. Gruber, A. Pfaltz, *Angew. Chem. Int. Ed.* **2014**, *53*, 1896–1900.

[66] J. Mazuela, P.-O. Norrby, P. G. Andersson, O. Pàmies, M. Diéguez, *J. Am. Chem. Soc.* **2011**, *133*, 13634–13645.

[67] K. H. Hopmann, A. Bayer, *Organometallics* **2011**, *30*, 2483–2497.

Chapter 5

Synthesis of the Ir-MaxPHOX Catalysts

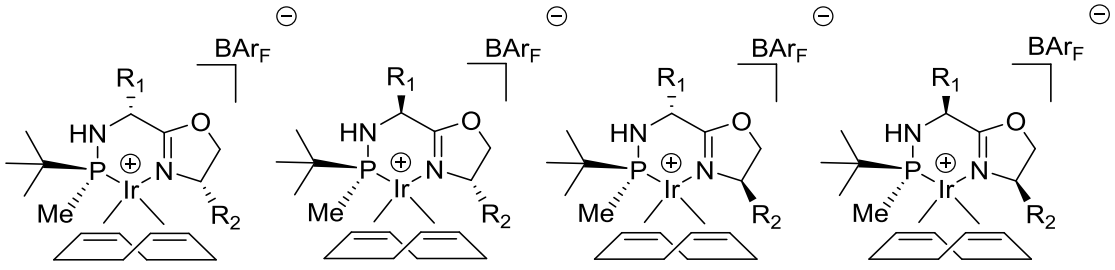

5.1. A new route to synthesize MaxPHOX ligands

At the beginning of the present doctoral thesis, our group had just developed a new Ir-P*,N catalyst for which we had high expectations, the Ir-MaxPHOX catalyst. Our objective was to create a small family of Ir-MaxPHOX catalysts that could adapt to the requirements of each specific substrate. In Chapter 1 we reported the synthesis of **5.5**, developed by S. Orgué in her PhD thesis.[1]

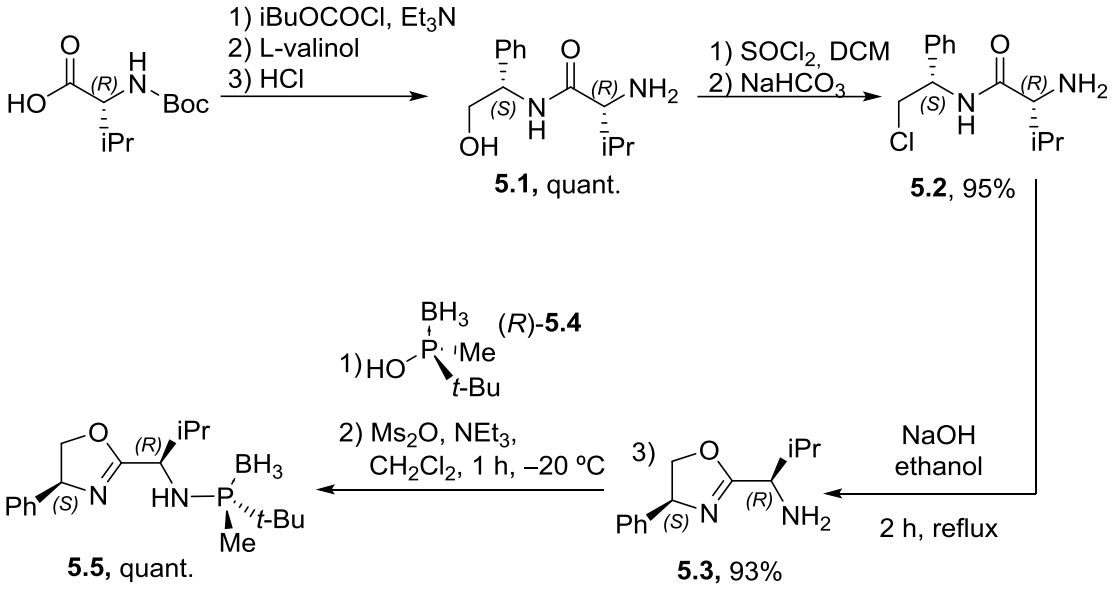

Figure 1. *S. Orgué's original MaxPHOX ligand synthesis. This synthesis fails to afford other MaxPHOX ligands with different configurations and bulky groups other than* ***5.5****.*

This route first prepares a chiral amino oxazoline[2,3] and then uses it as a nucleophile in the S_N2@P reaction with the chiral synthon **5.4** to obtain the final ligand. However, when we attempted to expand the methodology and synthesize other MaxPHOX ligands with different bulky groups and configurations, we did not succeed. The route depicted in the Figure 1, which is effective for producing compound **5.5**, is not reliable for other ligands containing different substituents. Many byproducts were observed during the synthesis at the chlorination step with $SOCl_2$ and at the oxazoline cyclization step with NaOH. The S_N2@P reaction with the chiral phosphorous synthon **5.4** requires the amino oxazoline to be rather pure. Both the chlorinated compounds, such as **5.2,** and the oxazolines, such as **5.3,** are difficult to purify by flash chromatography

and cannot be easily crystallized. If we had to create a small family of ligands and catalysts we needed an efficient, clean and, above all, robust route.

One of the main byproducts that we observed during the ligand synthesis was the cyclic sulfuramidite in Figure 2. We suspected that the amino moiety reacts with an intramolecular nucleophilic attack and forms the eight membered ring byproduct.

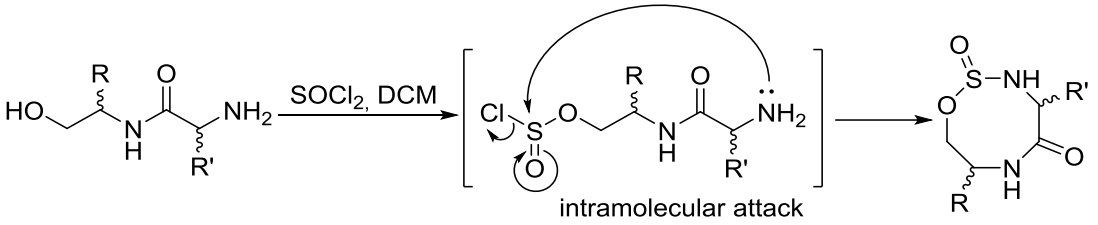

Figure 2. *Intramolecular nucleophilic attack. Formation of cyclic sulfuramidite byproduct.*

In order to avoid this secondary reaction we came up with the idea to couple the phosphorous synthon to the rest of the chiral C-backbone early on in the route. This way the chiral phosphorous unit would act as a protecting group to the reactive amino moiety.

The new route consisted on first reacting amino alcohol **5.6** with phosphinous acid **5.4**. This aminophosphine could next be activated with $SOCl_2$ and then cyclized using basic conditions to afford the final aminophosphine-oxazoline ligand. The S_N2@P reaction with the chiral amino alcohol was successful. The desired amino phosphines **5.7** were obtained with yields that ranged from low to excellent. The yields were largely influenced by the solubility of the amino alcohols. The amino phosphines obtained were very stable and could be purified in a very straightforward manner by SiO_2 column. For most cases, just with a thorough "work-up" with base and acid we could obtain the product pure enough.

The next step was the activation with $SOCl_2$. This reaction did not proceed as expected. We intended to isolate the chlorinated compound, to later cyclize it under strong basic conditions and form the oxazoline. However, what we obtained was the already cyclized compound. Due to the phosphorous unit attached, the chlorinated compound cyclizes and forms the oxazoline unit much more easily. The $NaHCO_3$ saturated solution used during the "work-up" step to neutralize the HCl formed during the reaction is enough

to induce the cyclization and afford the aminophosphino-oxazoline ligand. This step is very clean and the amino oxazolines **5.8** are generally obtained with enough purity. However, if a higher purity is required, they can be purified via flash chromatography.

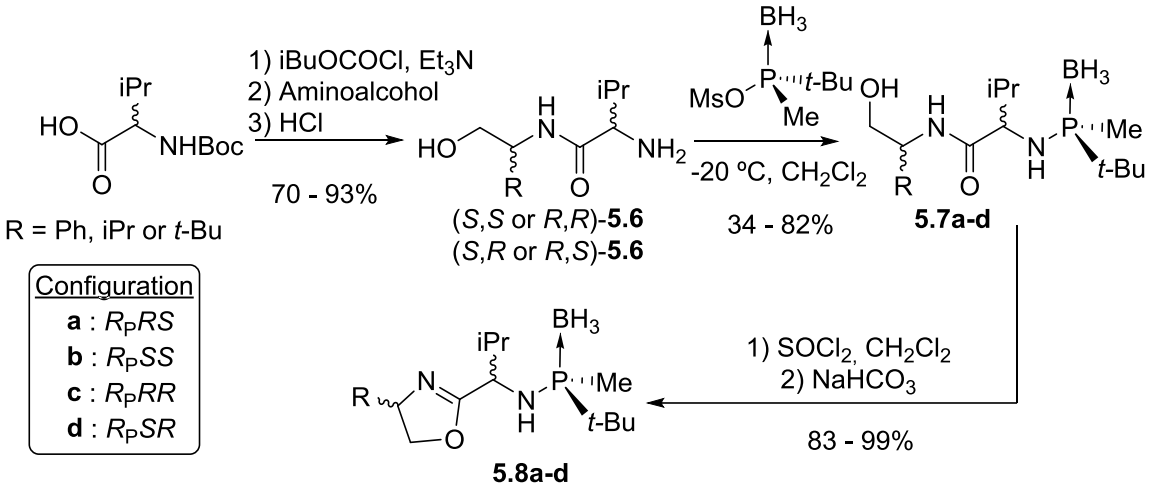

Figure 3. *New route for the MaxPHOX ligands synthesis. Although many MaxPHOX ligands with different substituents have been synthesized in this manner, in this Figure we only present the synthesis for the MaxPHOX ligands that correspond to the catalysts in Figure 5. For each step of the synthesis there are 4 configurations (**a-d**) and 3 different substituents for the R group (Ph, iPr or t-Bu).*

The method employed to coordinate the MaxPHOX ligands to Ir is the same as reported by S. Orgué in her PhD thesis (Figure 4). The complexation consists in a 3-step procedure; first there is the deprotection with neat pyrrolidine. This cyclic amine proved to be a better deprotection reagent than for example the well-known DABCO, basically due to purification issues. Once the phosphine is deprotected, the pyrrolidine can be removed by heating the solution under high vacuum. The borane protected pyrrolidine byproduct formed is not volatile, but it does not affect the rest of the procedure and can be purified straightforwardly at the end of the synthesis with a short flash chromatography. The free ligand, always under N_2 atmosphere, is resolubilized with CH_2Cl_2 and then $[IrCl(cod)]_2$ is added. After 1 h, $NaBAr_F$ is added and the reaction is left stirring for another hour. The catalyst, with BAr_F^- as counteranion, can be easily purified by silica column with hexanes / CH_2Cl_2.

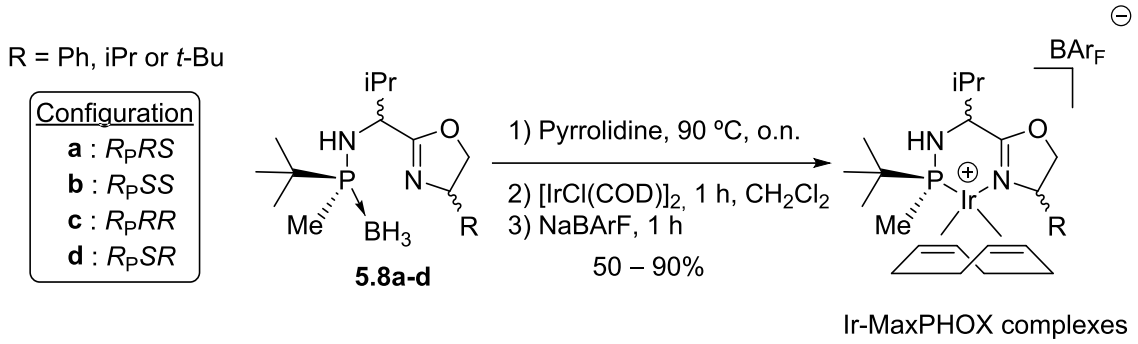

Figure 4. *Ligand coordination to Ir for the Ir-MaxPHOX represented in Figure 5.*

5.2. A small catalyst library

Using this methodology we managed to synthesize a small library of ligands and the corresponding Ir catalysts (Figure 5). Although several other MaxPHOX ligands and catalysts with different substituents have been synthesized in this manner, we are not describing them because they do not play a relevant role in the reduction of the substrates studied in this work and would only interfere with the storyline.

To correctly understand the small library in Figure 5, first we have to focus on the catalyst structure. As depicted in the Figure bellow, the Ir-MaxPHOX catalysts contain 3 independent chiral centers that can be substituted with different bulky groups. This means that for a given catalyst (same groups) we can synthesize up to 8 stereoisomers ($2^{n^{o}\text{chiral centers}} = 2^3 = 8$ stereoisomers). However, we can only have 4 possible diastereoisomers. The other 4 stereoisomers would be their enantiomers.

We named the 3 chiral units present in the catalyst the P, the ARM and the TAIL units, respectively. A quick study of a few catalysts showed us that the ARM unit has a bigger impact on the ee than the TAIL unit, probably because it is closer to the reacting site. In order to maintain the library relatively small, we only varied the ARM unit (Ph, iPr and *t*-Bu), while the TAIL and P units remained fixed (iPr and *t*-Bu/Me, respectively). Nevertheless, the premise that the ARM plays a more important role than the TAIL on the product's ee, while true for many substrates, like the ones reported in this PhD thesis, might be untrue for other cases.

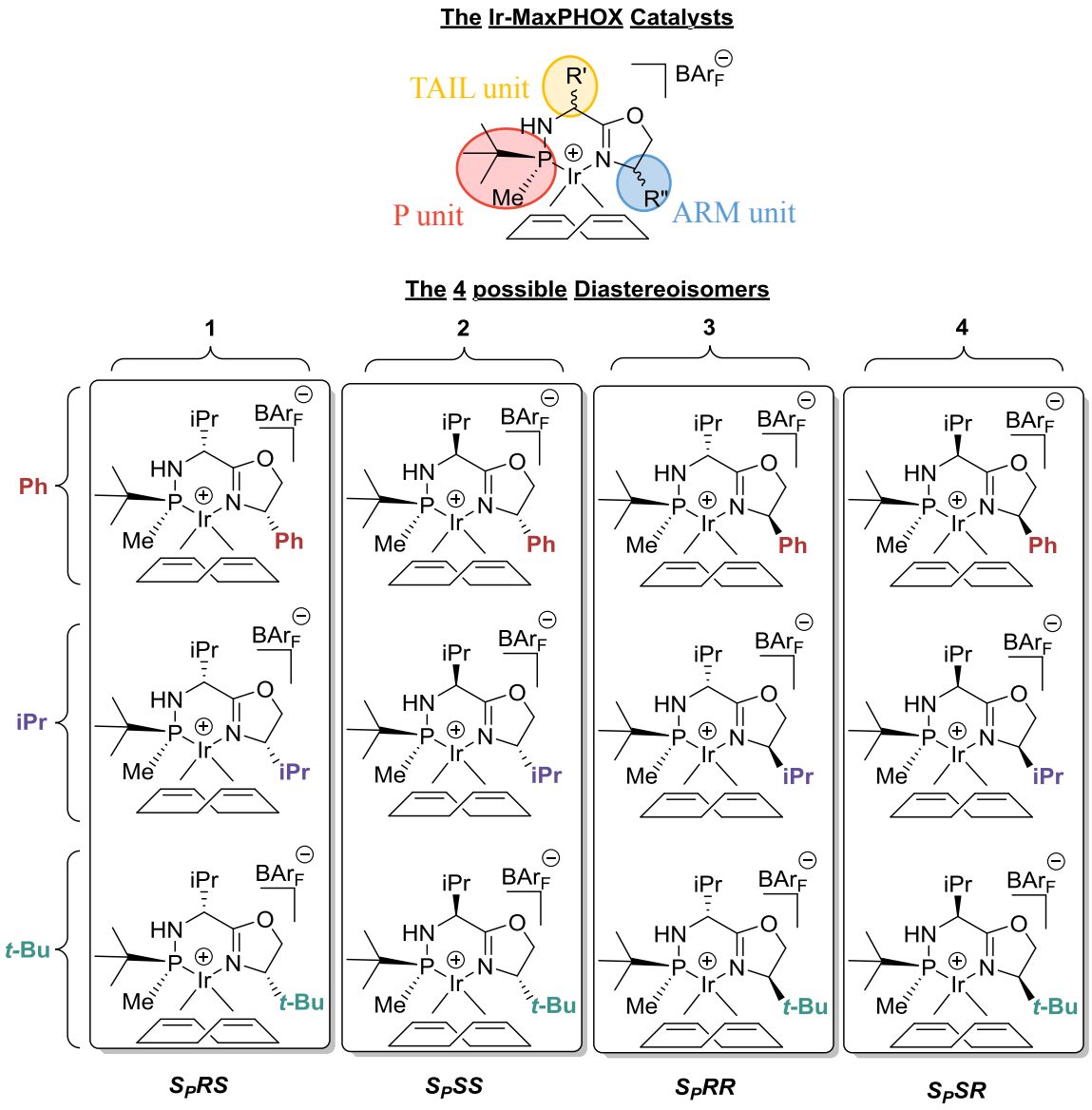

Figure 5. *A small library of Ir-MaxPHOX catalysts. Each column contains catalysts with the same configuration. Each row contains catalysts with the same substituents.*

In summary, the library depicted above contains up to 12 catalysts. For each of the 4 diastereoisomers, there are 3 different versions with either Ph, iPr or *t*-Bu groups as the ARM unit. During the present PhD thesis, to describe these 12 Ir-MaxPHOX complexes we are going to use a number (1 to 4) to indicate the catalyst configuration and Ph, iPr or *t*-Bu to indicate the ARM's substituent. For example, the top-left complex would be the **1Ph** catalyst (Figure 5). This nomenclature is valid for every chapter of the present work.

5.3. Conclusions

In the present Chapter we designed a novel route to synthesize MaxPHOX ligands. This new methodology is robust and versatile; we can vary at will the substituents at the ARM and TAIL positions, along with their configuration, to synthesize the desired ligand. With 3 independent chiral units, the MaxPHOX ligands can be fine-tuned to best fit the specifics of each substrate.

In this Chapter we report a small family of 12 different Ir-MaxPHOX catalysts (Figure 5) that will be applied in the hydrogenation of challenging substrates such as imines[4–6] (Chapters 6 & 7) and cyclic enamides[7–10] (Chapter 8).

5.4. References

[1] S. Orgué, A. Flores-Gaspar, M. Biosca, O. Pàmies, M. Diéguez, A. Riera, X. Verdaguer, *Chem. Commun.* **2015**, *51*, 17548–17551.

[2] P. Västilä, I. M. Pastor, H. Adolfsson, *J. Org. Chem.* **2005**, *70*, 2921–2929.

[3] I. M. Pastor, P. Västilä, H. Adolfsson, *Chem. - A Eur. J.* **2003**, *9*, 4031–4045.

[4] K. H. Hopmann, A. Bayer, *Coord. Chem. Rev.* **2014**, *268*, 59–82.

[5] N. Fleury-Brégeot, V. de la Fuente, S. Castillón, C. Claver, *ChemCatChem* **2010**, *2*, 1346–1371.

[6] J. H. Xie, S. F. Zhu, Q. L. Zhou, *Chem. Rev.* **2011**, *111*, 1713–1760.

[7] J. L. Renaud, P. Dupau, A.-E. Hay, M. Guingouain, P. H. Dixneuf, C. Bruneau, *Adv. Synth. Catal.* **2003**, *345*, 230–238.

[8] C. Pautigny, C. Debouit, P. Vayron, T. Ayad, V. Ratovelomanana-Vidal, *Tetrahedron: Asymmetry* **2010**, *21*, 1382–1388.

[9] I. Arribas, M. Rubio, P. Kleman, A. Pizzano, *J. Org. Chem.* **2013**, *78*, 3997–4005.

[10] X. Bin Jiang, L. Lefort, P. E. Goudriaan, A. H. M. De Vries, P. W. N. M. Van Leeuwen, J. G. De Vries, J. N. H. Reek, *Angew. Chem. Int. Ed.* **2006**, *45*, 1223–1227.

Chapter 6

P-Stereogenic and Non P-Stereogenic Ir-MaxPHOX in the Asymmetric Hydrogenation of *N*-Aryl Imines

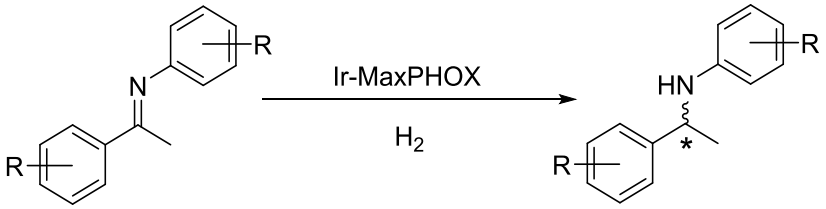

E. Salomó, P. Rojo, P. Hernández-Lladó, A. Riera, X. Verdaguer, *J. Org. Chem.* **2018**, *83*, 4618–4627.

6.1. Introduction: Asymmetric hydrogenation of *N*-aryl imines

The hydrogenation of imines via asymmetric catalysis is a key method to prepare chiral amines. These substrates can later be useful as chiral building blocks for fine chemical, agrochemical or pharmaceutical industries. Taking this into account, it is not surprising the interest in designing new more efficient methods that completely reduce the imines while controlling the enantioselectivity of the obtained amine.[1–3] However, to do so is not an easy task.

It is well-known that Ir-P,N catalysts perform well in the hydrogenation of *N*-aryl imines.[4,5] For example, Pfaltz reported very good results when employing one of his Ir-P,N catalysts, the SimplePHOX.[6] In the previous Chapter we prepared a new family of Ir-P*,N catalysts for which we had high expectations; the Ir-MaxPHOX. We hypothesized that these novel catalysts could afford good results on the hydrogenation of *N*-aryl imines.

6.2. Synthesis of *N*-aryl imines

Probably the most straightforward manner to synthesize an imine is by condensation between a primary amine and a ketone/aldehyde.[7–9] This reaction produces H_2O, so a desiccant is required to shift the equilibrium towards the products. Molecular sieves suffice when the reagents are very reactive. However, due to the low nucleophilicity of aryl amines, the synthesis of *N*-aryl imines often requires a much stronger desiccant, like $TiCl_4$.

Catalytic hydrogenation substrates must be very pure. Purification with SiO_2 column produces decomposition on imines. Thus, crystallization and/or distillation are usually the methods of choice.

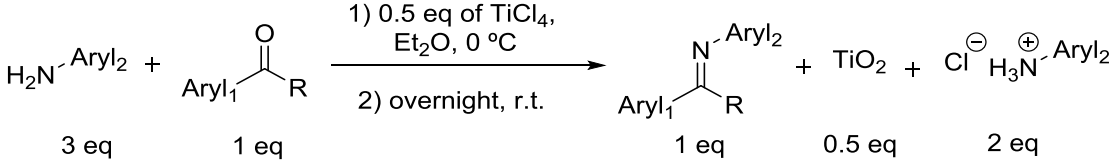

Figure 1. *Synthesis of N-aryl imines using $TiCl_4$ as desiccant.*

6.3. Hydrogenation of *N*-aryl imines with the Ir-MaxPHOX catalysts

The 12 different Ir-MaxPHOX catalysts described in Chapter 5 were tested on the chosen model substrate acetophenone *N*-phenylimine **6.1**. The reactions were conducted under the conditions described below. The results obtained are summarized in Figure 2.

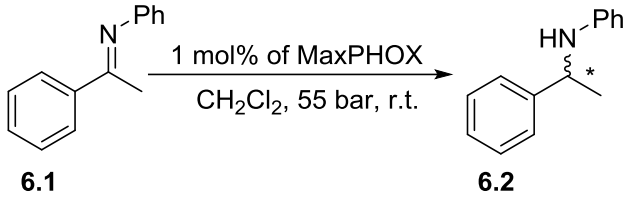

6.1 **6.2**

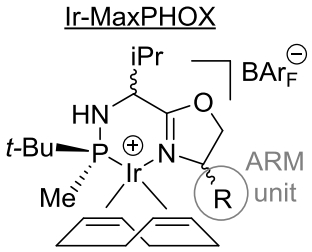

R	Ir-MaxPHOX Catalysts			
	S*P*RS	***S*P*SS***	***S*P*RR***	***S*P*SR***
	1	**2**	**3**	**4**
Ph	60% ee	12% ee	43% ee	47% ee
iPr	89% ee	37% ee	65% ee	85% ee
tBu	79% ee	53% ee	53% ee	77% ee

R	**S**	**ee(%)**
		0–25
		25–50
		50–75
		75–100

Figure 2. *Ee values for the hydrogenation of* ***6.1****. Screening for the best Ir-MaxPHOX catalyst. Conversion was complete for all cases.*

The best results were obtained for catalysts with configurations ***S*P*RS*** and ***S*P*SR***. The isopropyl group on the ARM position provided the best results. Pfaltz and co-workers also observed with their Ir-P,N catalysts that an iPr group on the oxazoline usually helped increasing the ee. Complex **1iPr** gave the highest enantiomeric excess (89% ee) and **4iPr** the second best (85% ee) but with the opposite product configuration. Catalysts **1iPr** and **4iPr** would be enantiomers of each other, except that the chirality at phosphorus is inverted. This result suggests that the stereochemical configuration at phosphorus had a limited impact on the selectivity. On the other hand, we observed that the configuration

of the chiral center on the backbone of the ligand had a major effect on the selectivity. Catalysts **2iPr** and **3iPr**, while having the same configuration at the P-center and oxazoline with respect **1iPr** and **4iPr,** provided much lower selectivity. We called this phenomenon the "tail effect". We believe this behavior is associated with conformational changes within the Ir-P,N six-membered ring chelate.

6.3.1. The non P-stereogenic Ir-MaxPHOX

Most of the Ir-P,N ligands described so far in the literature do not contain a P-stereogenic unit. Some of them afford very good results in various asymmetric hydrogenations. Based on this facts, we believe that the ARM unit in the Ir-MaxPHOX catalysts is a very important part of it. Nevertheless, in our opinion, the chiral P unit, which is also close to the reacting site, plays an important role too. To prove this theory, we aimed for the synthesis of a non P-stereogenic version of the Ir-MaxPHOX catalysts (Figure 3). To replace the chiral P unit for a non stereogenic one would cut down to 4 the number of possible stereoisomers for one given catalyst ($2^{n^{o}\text{chiral centers}} = 2^4 = 4$ stereoisomers). Consequently, only 2 diastereoisomers are possible for a given catalyst.

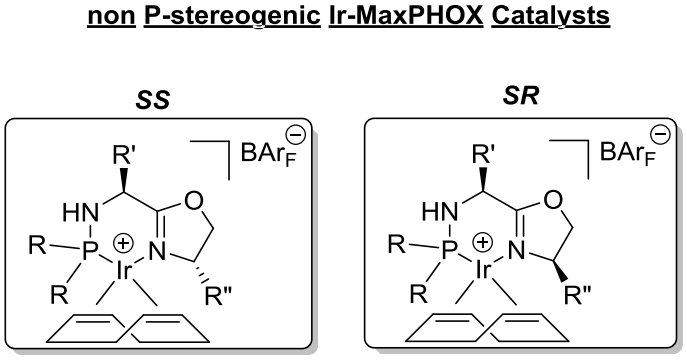

Figure 3. *The two possible configurations for a non P-stereogenic Ir-MaxPHOX.*

Our first synthetic approach consisted in reacting a chlorophosphine with a chiral aminoalcohol and then protecting the free P with $BH_3 \cdot SMe_2$ in situ (Figure 4). Next, by cyclization we could obtain the non P-MaxPHOX ligand. However, diphenylchlorophosphine and di(*o*-tolyl)chlorophosphine were too reactive and many byproducts were detected. The purification was very complicated and none of the two

aminophosphines **6.3** and **6.4** could be obtained pure. As we tried the following two reactions, the cyclization and the coordination to Ir, more byproducts were observed. The desired products were detected in very small quantities and could not be isolated properly. On the other hand, tBu_2PCl did not react at all with the chiral amine. In fact, we have not managed to obtain the corresponding aminophosphine **6.5** despite many different attempts.

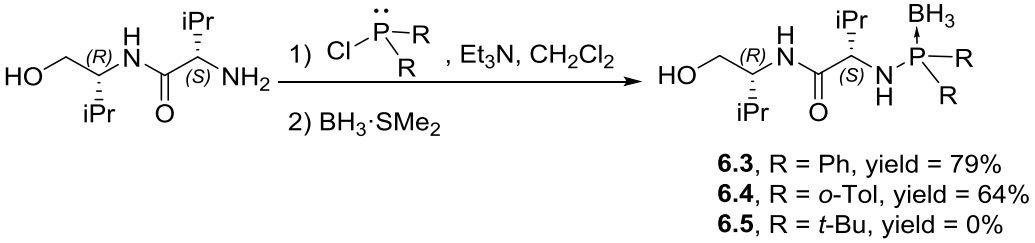

Figure 4. *Nucleophilic attack onto different chlorophosphines followed by reaction in situ with BH_3·SMe_2.*

When we attempted the reaction with chlorodicyclohexylphosphine we again obtained the corresponding aminophosphine along some byproducts. However, the two following reactions, the oxazoline cyclization and coordination to Ir, occurred in a clean manner and the purifications were more straightforward. At the end we were able to obtain both MaxPHOX ligands and the respective Ir-catalysts pure and with acceptable yields. The synthesis weak step was the coupling between the C-backbone and the P-unit. In order to increase the step's yield, we designed a route using phosphinous acid borane **6.7** (Figure 5). As we know from *tert*-butylmethylphosphinous acid borane (Chapter 5), these compounds after activation with methansulfonic anhydride can react cleanly with nucleophiles. We expected **6.7** to behave in the same fashion. To synthesize **6.7** we treated chlorodicyclohexylphosphine as depicted in Figure 5. First the chlorophosphine was protected with BH_3·SMe_2 in THF. Then we added NaOH in H_2O / THF. H_2O is not nucleophile enough to react properly and NaOH without H_2O as solvent is not soluble enough. Bellow we depict the total synthesis for the two non P-stereogenic Ir-MaxPHOX catalysts diastereoisomers (*S*,*S*)-**6.10** and (*S*,*R*)-**6.10**.

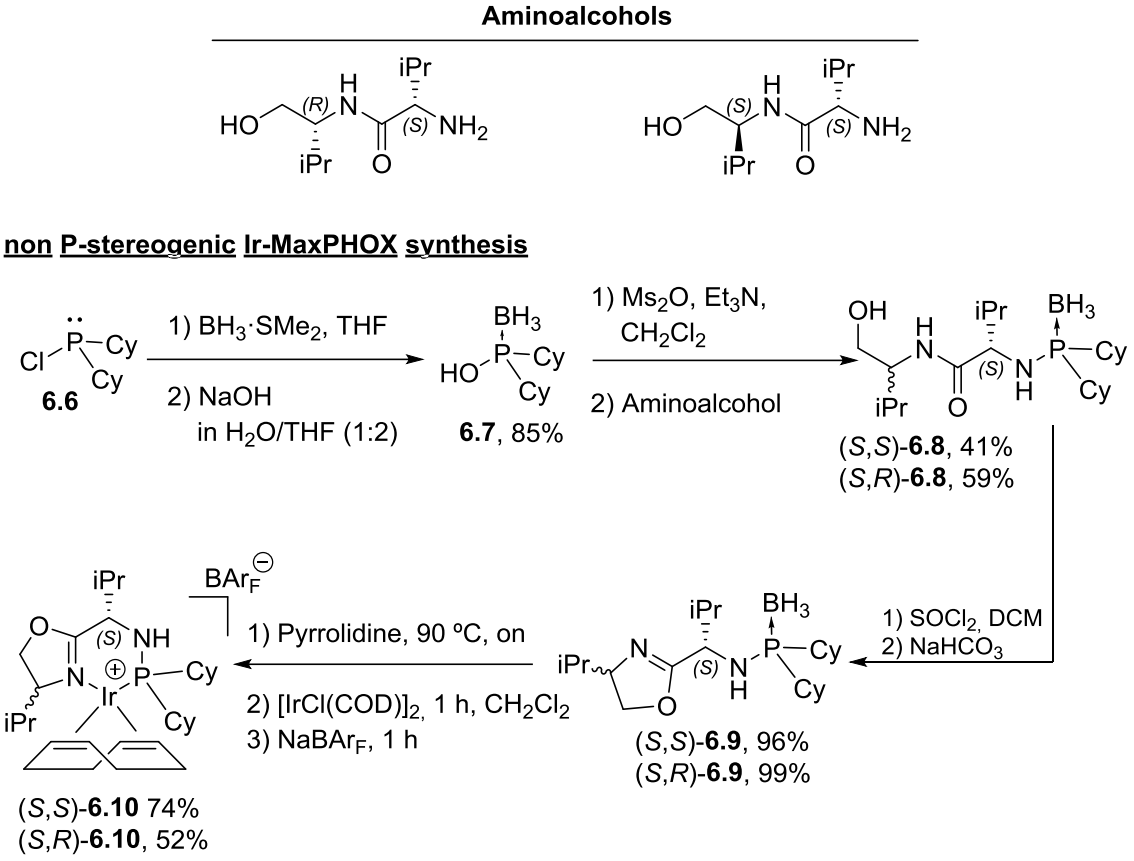

Figure 5. *Synthesis of the non P-stereogenic Ir-MaxPHOX catalysts* ***6.10****. The non P-stereogenic and the P-stereogenic versions were tested against each other.*

We tested the non P-stereogenic versions of the Ir-MaxPHOX ((*S*,*S*)-**6.10** and (*S*,*R*)-**6.10**) in the hydrogenation of **6.1** so we could compare their performace against the P-stereogenic version and get more insight on the importance of the stereogenic P unit. These two catalysts afforded 57% and 81% ee for the reduced product. The best ee obtained this way is inferior to the best one obtained with the P-stereogenic Ir-MaxPHOX. We concluded that the chiral P-unit, although is not crucial, helps to achieve higher ee's and is an important part of the catalysts.

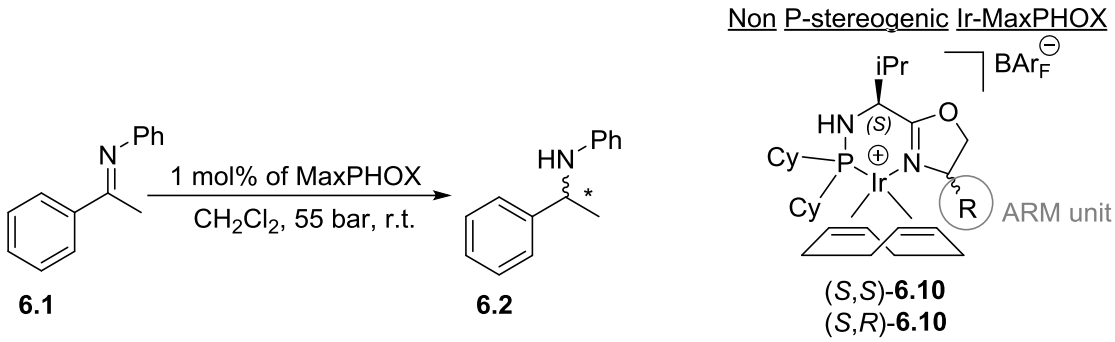

R	Non P-stereogenic Ir-MaxPHOX Catalysts	
	SS	***SR***
iPr	57% ee	81% ee

R	***S***	**ee(%)**
		0–25
		25–50
		50–75
		75–100

Figure 6. *Ee values for the hydrogenation of acetophenone N-phenylimine* ***6.1*** *with non P-stereogenic Ir-MaxPHOX. Conversion was complete for all cases.*

6.3.2. Influence of H_2 pressure, solvent and temperature

In Table 1 we report the most important results for the optimization of the hydrogenation of **6.1** with the Ir-MaxPHOX catalysts.

Table 1. Influence of H_2 pressure, solvent and temperature on the hydrogenation of **6.1**

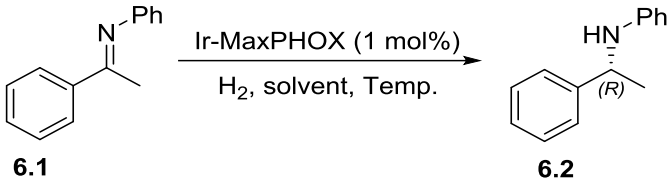

6.1 **6.2**

Entry	**Ir-MaxPHOX**	**H_2 (bar)**	**Solvent**	**Temp. (ºC)**	**Conv. (%)[c]**	**ee (%)[d]**
1	**1iPr**	55	CH_2Cl_2	r.t.	100	89
2	**1iPr**	3	CH_2Cl_2	r.t.	100	90
3	**1iPr**	balloon[a]	CH_2Cl_2	r.t.	100	90
4	**1iPr**	3	EtOAc	r.t.	100	66
5	**1iPr**	3	MeOH	r.t.	100	45
6	**1iPr**	3	Toluene	r.t.	100	85
7	**1iPr**	balloon[a]	CH_2Cl_2	0	100	93
8	**1iPr**	balloon[a]	CH_2Cl_2	–20	100	96
9[b]	**4iPr**	balloon[a]	CH_2Cl_2	r.t.	8	--

a) Equivalent to atmospheric H_2 pressure. b) 72 h reaction c) Conversion was determined by ^1H NMR analysis of the crude reaction mixture. d) The ee value was determined by HPLC analysis on a chiral stationary phase.

We studied the influence of hydrogen pressure, solvent and temperature on the reaction outcome. Selectivity was relatively insensitive to the reaction pressure. In this regard, a pressure reduction from 55 bar to 3 bar produced only a slight increase in the enantiomeric excess (from 89 to 90% ee, Table 1, entries 1 and 2). The pressure was even reduced to the atmospheric pressure of H_2 (balloon), giving the same results with respect to conversion and selectivity (Table 1, entry 3). Switching the reaction solvent from CH_2Cl_2 to greener and more coordinating solvents like EtOAc or MeOH caused a dramatic drop in selectivity (Table 1, entries 4 and 5). A reduction in the reaction temperature enhanced the selectivity. Thus, at 0 ºC and atmospheric H_2 pressure, the imine was reduced with 94% ee. Lowering the temperature even more, to –20 ºC, afforded the reduced amine with 96% ee (Table 1, entries 7 and 8). We wondered if by optimizing the reaction conditions, catalyst **4iPr** would perform better than **1iPr.** We observed that

under the optimized conditions **4iPr** was considerably less active since after 72 h only 8% conversion was achieved. This demonstrates that while the chirality on phosphorous does not directly influence greatly the selectivity, it has a great impact on the catalyst activity.

6.3.3. Counteranion study

We wanted to study the influence that different counteranions have over the catalyst reactivity.[6,10] We attempted the synthesis of Ir-MaxPHOX 1iPr catalyst with $BF_4^-$and Cl^- counteranions instead of BAr_F^-(ligand with configuration S_PRS). BF_4^- is a smaller and coordinates more strongly than BAr_F^-, and Cl^- even more than BF_4^-. We based the syntheses on the one developed for [IrMaxPHOX(COD)](BAr_F).

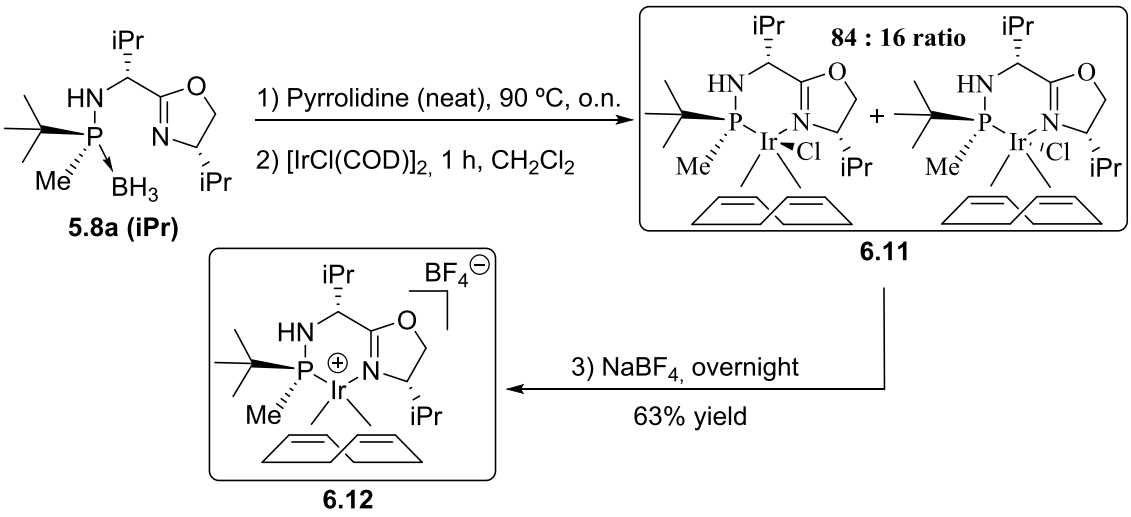

Figure 7. *Synthesis of Ir-MaxPHOX catalysts with $Cl^-$and BF_4^- as counteranions. The configuration of the catalysts is the same as for* ***1iPr*** *(S_PRS).*

First we deprotected the phosphine overnight with neat pirrolidine. The next day, we coordinated the ligand to Ir, by adding $[Ir(COD)Cl]_2$. To obtain [Ir(Cl)MaxPHOX(COD)] we stopped the reaction at this point. To obtain [IrMaxPHOX(COD)](BF_4) we added $NaBF_4$ to the solution, so the Cl^- counteranion would exchange with BF_4^-.

Cl^-proved to be too coordinating to be a good counteranion. By ^{31}P-NMR, we detected two phosphorous species in an 84:16 ratio. Attempts to separate these two

species were unfruitful. We theorized these were two different diastereoisomers caused by the strong coordination of the Cl atoms to the Ir center (Figure 7). The [IrMaxPHOX(COD)](BF_4) was purified by flash chromatography and further crystallization.

We tested complexes 6.11 and 6.12 in the hydrogenation of 6.1 (Table 2). The [Ir(Cl)MaxPHOX(COD)] is not active in catalysis. It seems that the Cl atom strongly binds to the metal, blocks a necessary coordination side and impedes any reactivity, rendering the complex useless. As for the [IrMaxPHOX(COD)](BF_4) the catalysis proceeded with full conversion but only 41% ee.

Table 2. Influence of counteranion with Ir-MaxPHOX **1iPr** on the hydrogenation of **6.1**

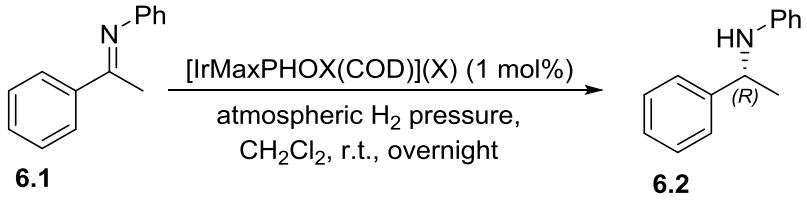

6.1 **6.2**

Entry	**Counteranion (X)**	**Conv. (%)**	**ee (%)**
1	BAr_F	100	90
2	BF_4	100	41
3	Cl	0	--

a) Reactions carried out with a H_2 filled balloon b) Conversion was determined by ^1H NMR analysis of the crude reaction mixture. c) The ee value was determined by HPLC analysis on a chiral stationary phase.

We considered interesting to compare the reaction rates with catalysts [IrMaxPHOX(COD)](BF_4) and [IrMaxPHOX(COD)](BAr_F). We studied the reaction of both catalysts at atmospheric H_2 pressure. We took samples of the crude at different times and analyzed them with HPLC analysis. As we can see in Figure 8, both reactions went to full conversion, but at different rates. Reaction with [IrMaxPHOX(COD)](BAr_F) was faster and conversion was complete within an hour. However, reaction with [IrMaxPHOX(COD)](BF_4) needed 3 hours to achieve full conversion. In conclusion, the best counteranion for the Ir-MaxPHOX is BAr_F^-.

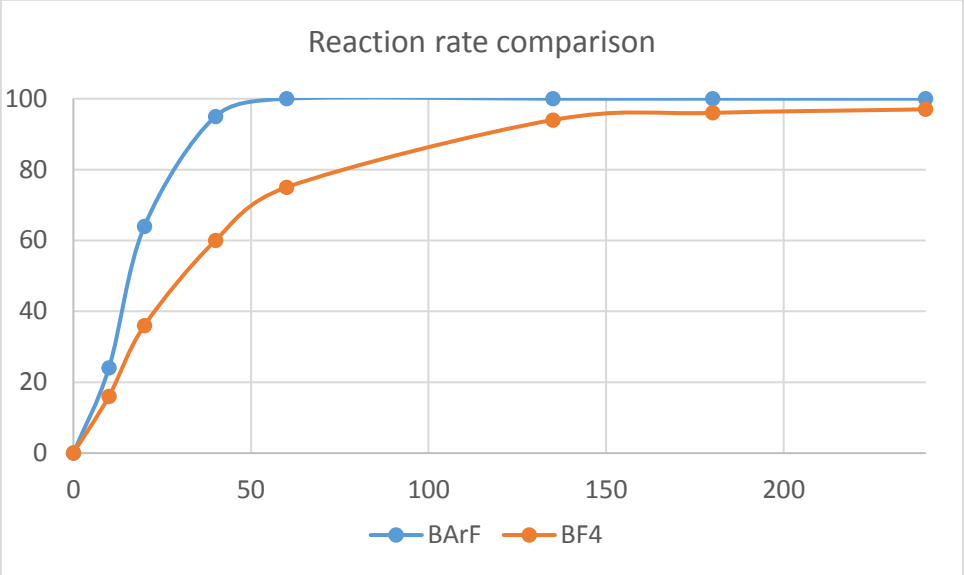

Figure 8. *Reaction rate comparison between [IrMaxPHOX(COD)](BAr$_F$) and [IrMaxPHOX(COD)](BF$_4$).*

6.3.4. Reaction scope

Once the reaction parameters were optimized, we proceeded to assess the scope of the hydrogenation with catalyst **1iPr** with various *N*-aryl imines. Both imines **I1** and **I2** contain a MeO– donor group on the Ph, at the *para* and the *meta* positions respectively. Reduction of **I1** and **I2** proceeded with 95% and 92% ee, respectively. However, **I3**, which has a MeO– group at the *orto* position of the Ph, was hydrogenated with only 28% ee. The low ee is probably due to the E/Z ratio of the starting imine and the influence of the MeO group which is very close to the double bond of the substrate. The *N*-phenyl imines **I4** (contains a Cl– substituent at the *para* position of the Ph) and **I5** (imine derived from 2-acetonaphthone) were both reduced with 94% ee. **I5** required more catalyst loading and H_2 pressure due to solubility issues. Imine **I6** is derived from propiophenone instead of acetophenone. It was reduced with a low enantiomeric excess (ee = 74%). This inferior selectivity is most likely due to a less favorable E/Z ratio of the starting imine. Imines **I7**, **I8** and **I9** contain different substituents on the N-Ph group. **I7** has a donor MeO– group at the *orto* postion. **I8** and **I9** contain methyl substituents at the *meta* and the *para* positions of the *N*-Ph respectively. All three of them were reduced with excellent selectivities (90-95% ee). On the other hand, imines **I10**, **I11** and **I12** possess substituents

on the *N*-Ph gro*up* close to the reacting site (*orto* positions). This affects the ee for **I10** (one MeO– substituent) and **I11** (one methyl) and the conversion for **I12** (methyls at both orto positions). The ee for imine **I13**, with methyls at both the Ph's *meta* positions, is lower than expected, probably because of the steric hindrance too. *N*-benzyl imines do not react in the same manner as *N*-aryl imines. Prove of that are imines **I14** and **I15**, with lower than expected conversions and ee's. In Chapter 7 we provide more insight into the reduction of *N*-bemzyl imines with Ir-MaxPHOX catalysts. Cyclic imine **I16** is probably not reactive enough as it is a very stable quinoline. On the other hand, we suspect five membered cyclic imine **I17** is too nucleophilic and interferes with the catalyst. Oxime **I18** and carbazones **I19** and **I20** do not react at all with our catalysts.

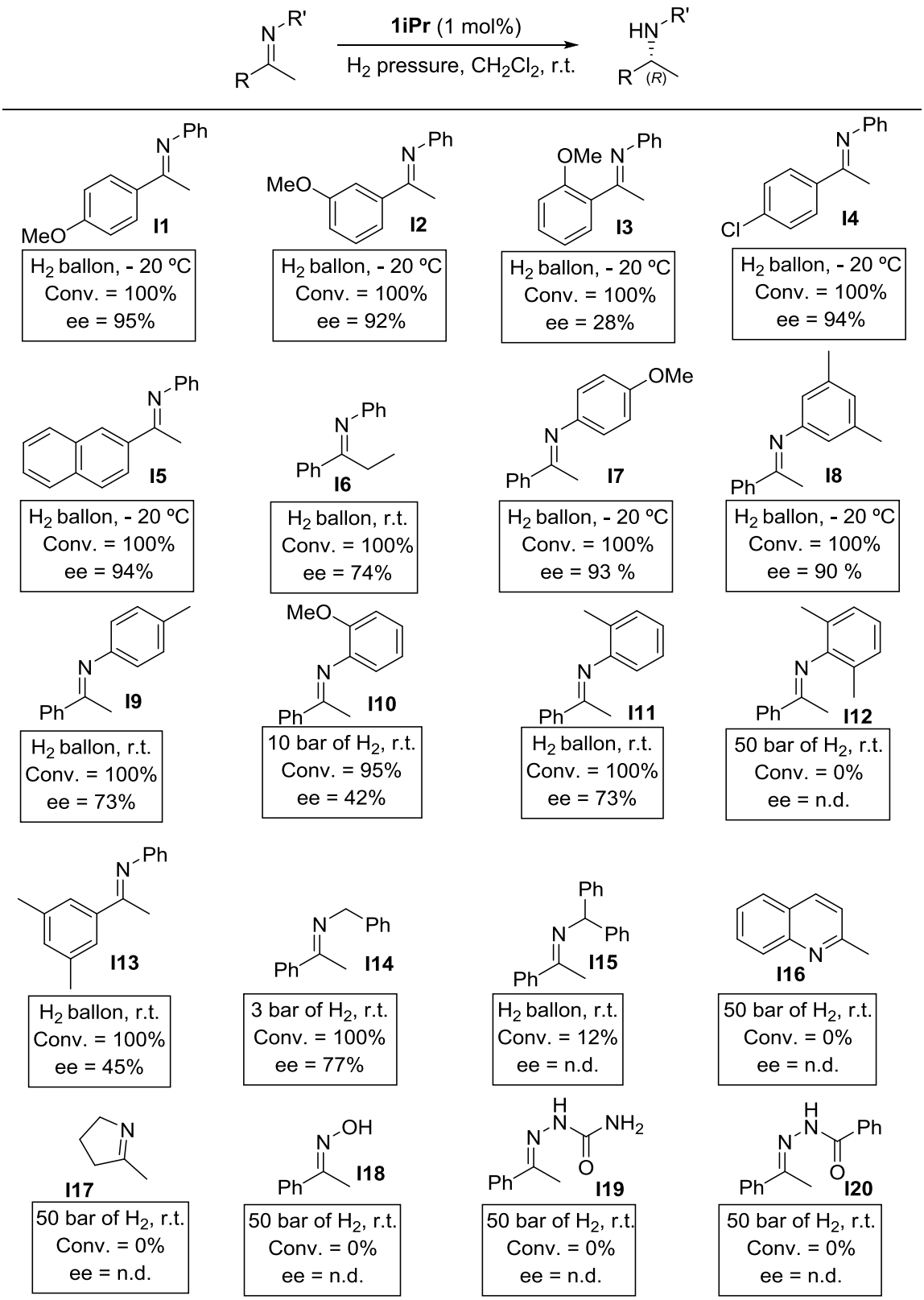

Figure 9. *a) Reduction of **I5** was carried out with 2 mol% of catalyst loading and 3 bar of H_2. b) Catalyst **1iPr** (S_PRS) afforded the amines as the (R) enantiomer. c) The configuration was determined by optical rotation analysis or analogy. d) Unexpectedly, **I14** afforded the (S) enantiomer.*

6.4. MaxPHOX iridacycles

As reported in the Chapter 4, Pfaltz and co-workers have recently shown that an imine iridacycle is the actual catalyst when using Ir–P,N complexes.[11] To further increase knowledge of the true catalytic system, we questioned whether these intermediates were also involved in our Ir–MaxPHOX system. The first steps towards this possible MaxPHOX iridacycles were taken using catalyst ***ent*-3iPr**. This is because ***ent*-3iPr** is the most stable, easy and cheap to produce catalyst from the ones we have synthesized so far. Once the methodology and conditions were optimized, we carried on the same study with catalyst ***ent*-1iPr**, which is the best catalyst for the hydrogenation of *N*-aryl imines.

Complexes ***ent*-1iPr** and ***ent*-3iPr** were reacted under hydrogen atmosphere with acetophenone *N*-phenylimine in THF (Figure 10). The solvent was evaporated with a N_2 current and the crude was treated with a mixture 1:1 SiO_2/LiCl in EtOAc. This afforded the corresponding cyclometallated iridium hydride neutral complexes **6.13** and **6.14**. These complexes were isolated as a pale yellow solids by silica gel chromatography. ^{1}H and ^{31}P NMR analysis confirmed compounds **6.13** and **6.14** as diastereomerically pure compounds. A single signal for the Ir–H was observed at –19.76 ppm (d, J_P = 26 Hz) and –19.62 ppm (d, J_P = 23 Hz) for **6.13** and **6.14**, respectively. It should be noted that heteroleptic octahedral complexes such as these, in principle, can provide various diastereomers. It is therefore remarkable that in this case a single stereoisomer is generated.

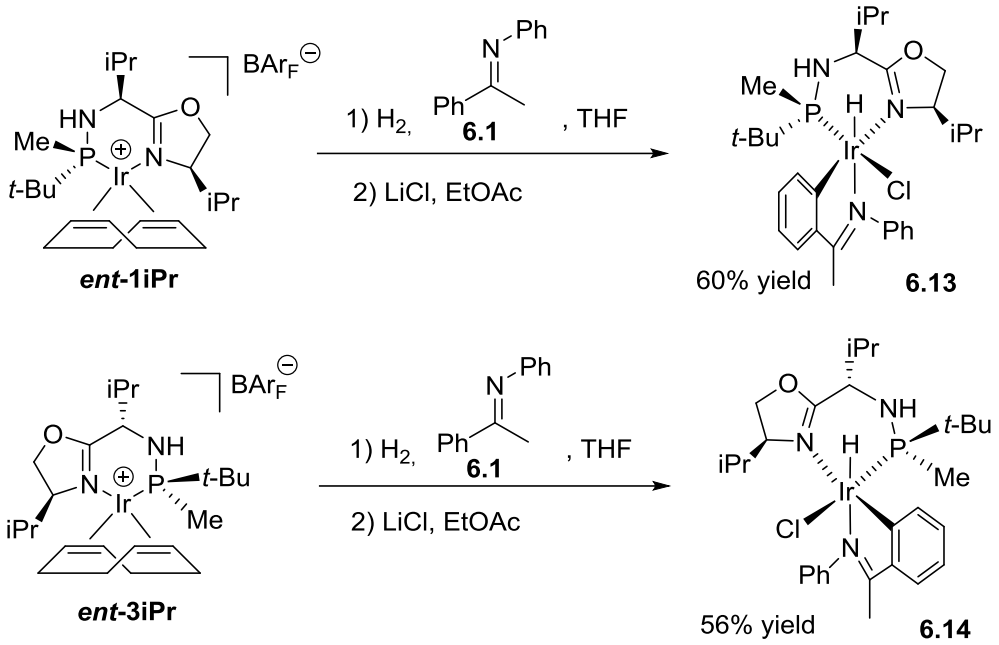

Figure 10. *Synthesis of MaxPHOX-imine iridacycles.*

Compounds **6.13** and **6.14** were crystalized from a hexanes / CH_2Cl_2 mixtures to obtain single crystals for X-ray analysis. The resulting solid state structures are shown in Figure 11. As expected, the iridium (III) in these structures display octahedral coordination. The phosphino-oxazoline ligand and the cyclometallated imine ligand are perpendicular to each other, with the oxazoline nitrogen atom *trans* vs the phenyl ring. The chiral center of the oxazoline fragment seems to control the coordination of the imine nitrogen. In both complexes, the *N*-phenyl group is positioned away from the isopropyl substituent of the oxazoline ring. Finally, the hydride and chloride ligands are *cis* to each other and *trans* to the imine nitrogen and phosphine ligands respectively. It is noteworthy that **6.13** and **6.14**, if the P and the TAIL configurations are not taken into account, are pseudoenantiomers to each other.

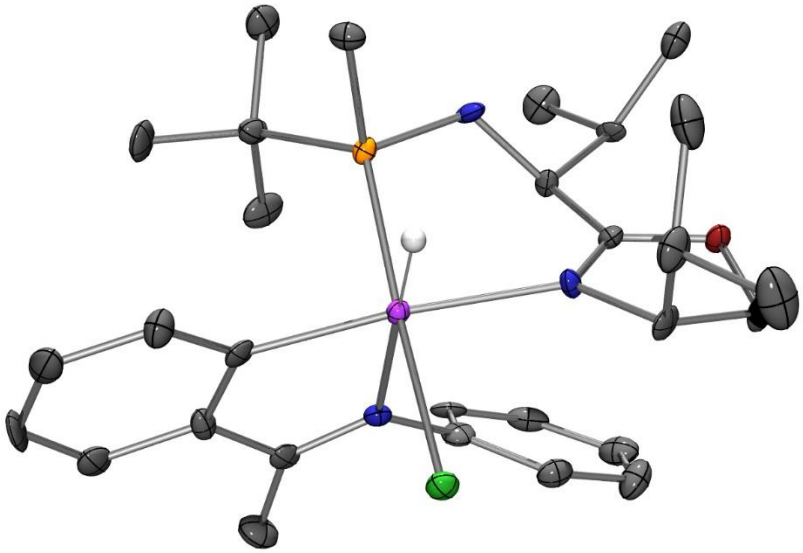

6.13

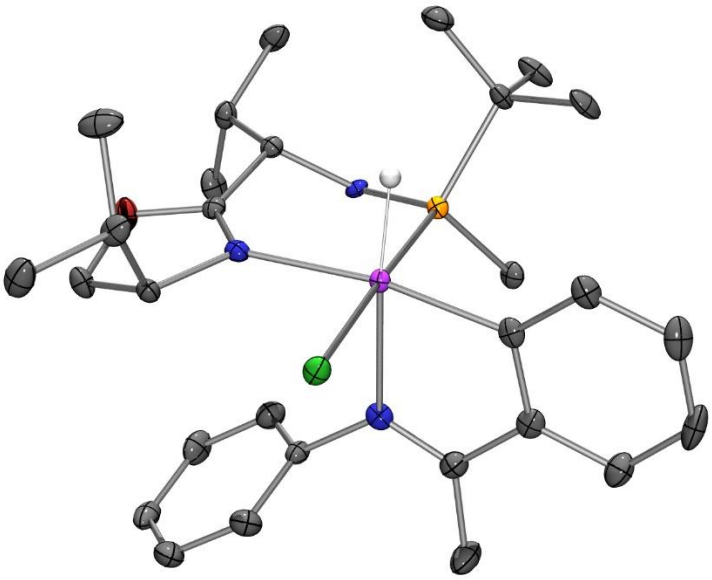

6.14

Figure 11. *X-ray structures of iridacycles* ***6.13*** *and* ***6.14****. Ortep diagram shows ellipsoids at 50% probability. Only the hydrogen atom attached to iridium has been drawn.*

To verify whether the isolated imine iridacycles can be used as precatalysts, compound **6.13** was tested in the hydrogenation of imines. Thus, we treated 1 mol% of **6.13** with 2 equivalents of $NaBAr_F$ in order to produce the active catalyst by counter ion exchange (Figure 12). The use of this mixture as catalyst reduced imine **6.1** with 60% conversion and 91% ee. Obtaining nearly the same ee as when using Ir-MaxPHOX (Table

1, Entry 3) strongly suggests that the cationic cyclometallated complex arising from chloride abstraction of **6.13** is an active species in the catalytic cycle.

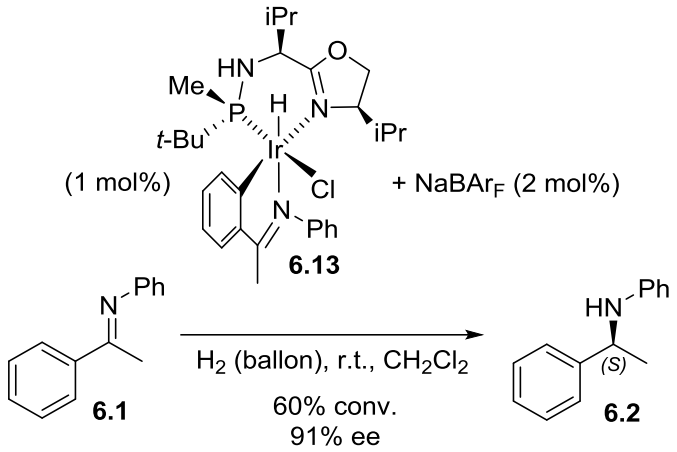

Figure 12. *Using iridacycle **6.13** as precatalyst in the hydrogenation of imines.*

This experiment has not been carried out with iridacycle **6.14** due to the low ee obtained with catalyst ***ent-3iPr*** in the hydrogenation of **6.1**.

6.5. Mechanistic considerations

6.5.1. Introduction

In 2013 Pfaltz and co-workers identified an iridacycle intermediate that is key for the hydrogenation of imines with Ir-P,N catalysts.[11] Later, in 2018, Norrby and co-workers proposed a mechanism for the hydrogenation of *N*-aryl imines with an Andersson's Ir-P,N catalyst that takes into account the iridacycle and that correctly predict the stereochemical outcome (Figure 13).[12]

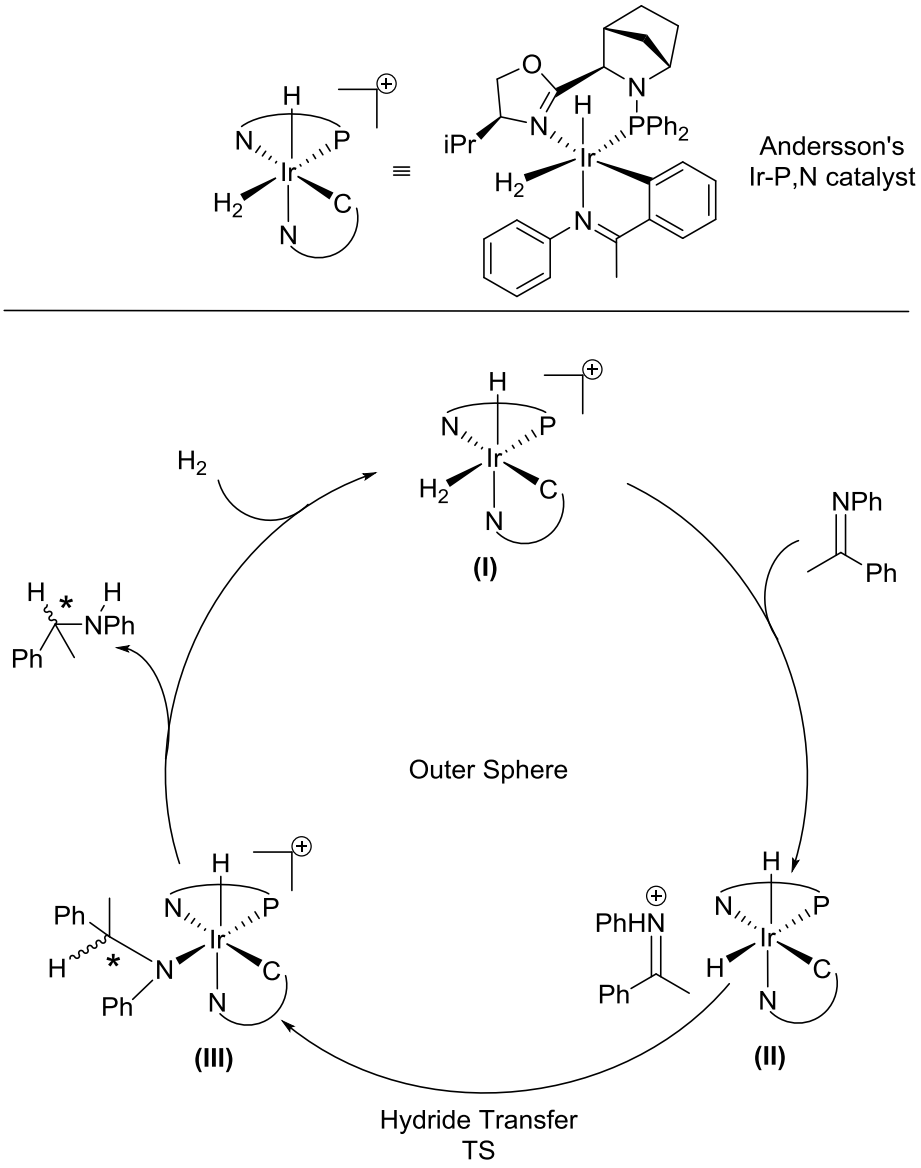

Figure 13. *Norrby-Wiest-Andersson's proposed Outer Sphere mechanism for the hydrogenation of N-aryl imines with Crabtree-like catalysts. The product stereochemistry is defined in the Hydride Transfer TS.*

6.5.2. Equilibrium between iridacycles

Analyzing the X-ray structures of both iridacycles **6.13** and **6.14** (prepared from catalysts ***ent*-1iPr** and ***ent*-3iPr**, respectively) we observed that the TAIL and the P unit seem to be far away from the reacting center. However, we obtained rather different selectivities in the hydrogenation of model imine **6.1** with only varying the configuration of the TAIL or the P unit. Thus, we concluded that the P unit and the TAIL do play a

relevant role in the reaction's outcome. To explain this behavior, we propose two concurrent effects. First, we believe that the TAIL and P units, although might not interact directly the substrate, can cause small conformation differences on the reacting site and consequently on the selectivity.

If we take a look at the reacting sites of complexes **6.13** and **6.14** (Figure 14), we can observe that for complex **6.13** the oxazoline ring is slightly tilted upward and the *N*-phenyl ring of the cyclometalated imine is parallel to it. On the other hand, for complex **6.14** both the oxazoline and the *N*-phenyl ring are almost perpendicular to the Ir−imine metallacycle in the pseudo-enantiomeric reacting site. These conformational differences of the oxazoline ring and, consequently the *N*-phenyl group, are ultimately governed by the configuration of the P unit and the TAIL and should lead to a difference in selectivity between catalysts ***ent*-1iPr** and ***ent*-3iPr**.

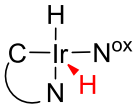

From Ir-MaxPHOX ***ent*-1iPr**

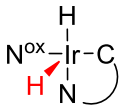

From Ir-MaxPHOX ***ent*-3iPr**

A) Reacting site for complex **6.13**

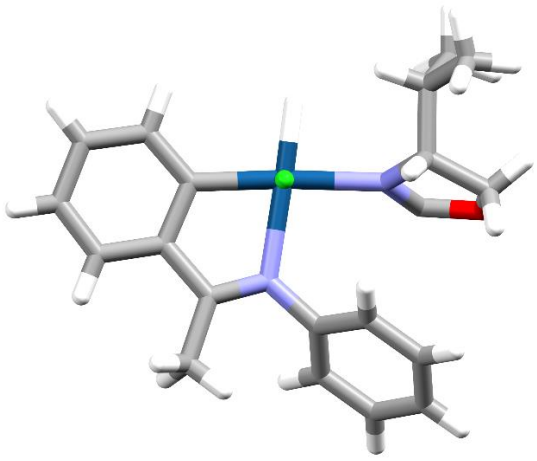

B) Reacting site for complex **6.14**

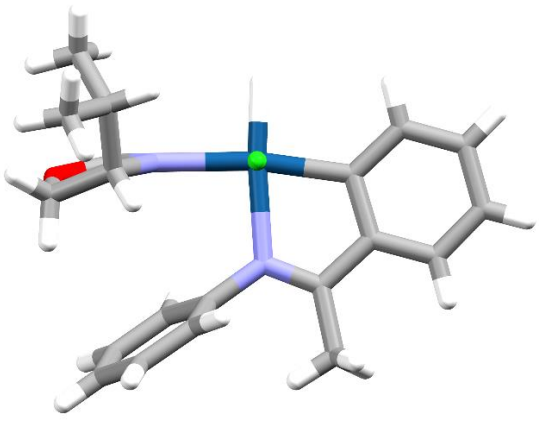

Figure 14. *Reacting sites for complexes **6.13** and **6.14**, as extracted from the corresponding X-ray structures. The phosphine and ligand backbone have been deleted for clarity. View along the Cl−Ir bond axis (green dot). The green dot also corresponds to the hydride transferred in the stereodetermining step.*

On the other hand, we consider that an equilibrium between iridacyles **IV** and **V** (Figure 15), which contain a vacant coordination site, might be possible. It is reasonable to think that the coordination of H_2 to either one of them would result in a different selectivity outcome. The two X-Ray neutral iridacycle structures obtained ([IrH(Cl)(MaxPHOX)(imine)] **6.13** and **6.14** present the stereochemistry of **IV** (vacant coordination site *trans* to the P or cyclometalated phenyl group *cis* to the P). Pfaltz reported the X-ray crystal structure of an $[IrH(THF)(PHOX)(imine)]^+$ complex, where the cyclometalated phenyl group is *trans* to the P (as in **V**) and which, upon removal of the solvent molecule, provides a complex with the same stereochemistry at the metal as **V**.[11]

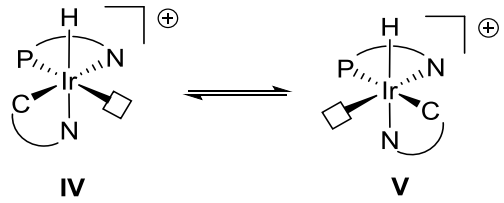

Figure 15. *Equilibrium between iridacycles **IV** and **V** with a vacant coordination site.*

To see if this hypothesis was feasible we performed some basic computational calculations. We calculated the equilibrium geometry for intermediates **IV(H)-*ent*-1iPr** and **V(H)-*ent*-1iPr** (Ir-MaxPHOX ***ent*-1iPr**). We considered the corresponding dihydride intermediates as viable surrogates of **IV** and **V**. Moreover, the dihydride intermidiates are the proposed hydride transfer species in the putative stereodetermining step.[12] The core structure employed was extracted from an X-Ray of iridacycle **6.13**. Calculations were performed with Spartan 16 (DFT, RM06 functional with 6-31G* & LANL2DZ basis set).

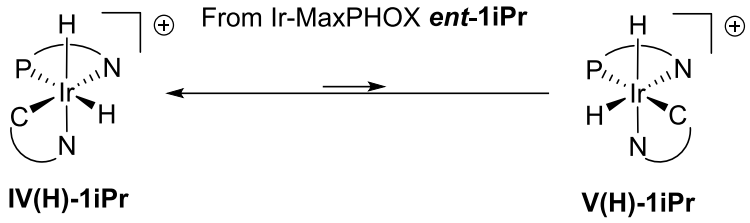

IV(H)-*ent*-1iPr; cyclometalated Ph group *cis* to the P

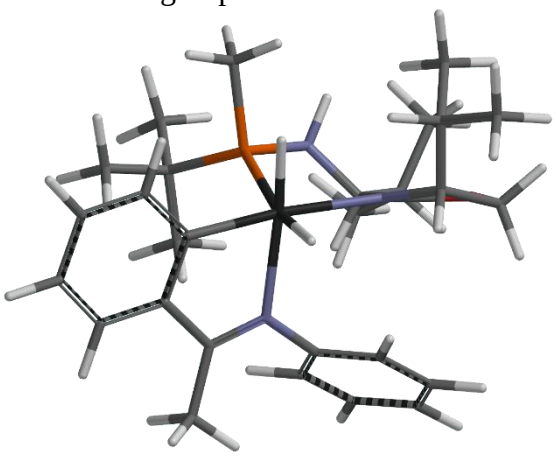

0.00 Kcal / mol

V(H)-*ent*-1iPr; cyclometalated Ph group *trans* to the P

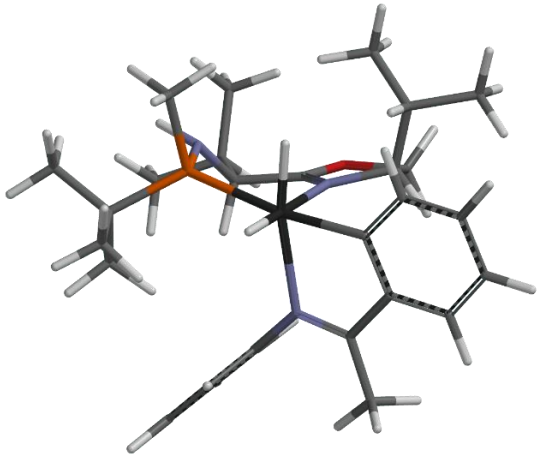

5.62 Kcal / mol

Figure 16. *a) The two possible configurations for the iridacycle dihydride (catalyst* ***ent-1iPr****). Conformation* ***IV(H)-ent-1iPr*** *is thermodynamically favored with respect to* ***V(H)-ent-1iPr****. b) Calculations were performed with Spartan 16 using RM06 functional with the 6-31G* & LANL2DZ basis set.*

As we can appreciate, **IV(H)-*ent*-1iPr** is 5.62 Kcal / mol more stable than **V(H)-*ent*-1iPr**. From a thermodynamically point of view we can predict that this equilibrium would be completely shifted towards **IV(H)-*ent*-1iPr**.

To gain further insight on the reaction, we carried out an analogous study with catalyst ***ent*-3iPr** (Figure 17).

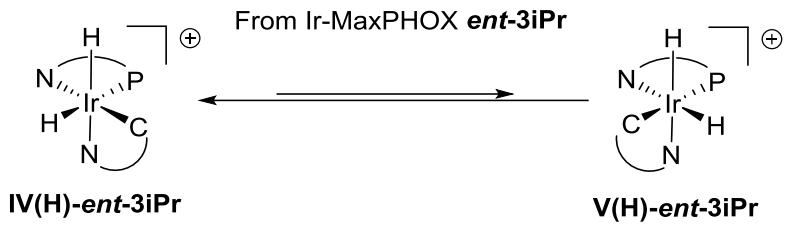

IV(H)-*ent*-3iPr; cyclometalated Ph group *cis* to the P

V(H)-*ent*-3iPr; cyclometalated Ph group *trans* to the P

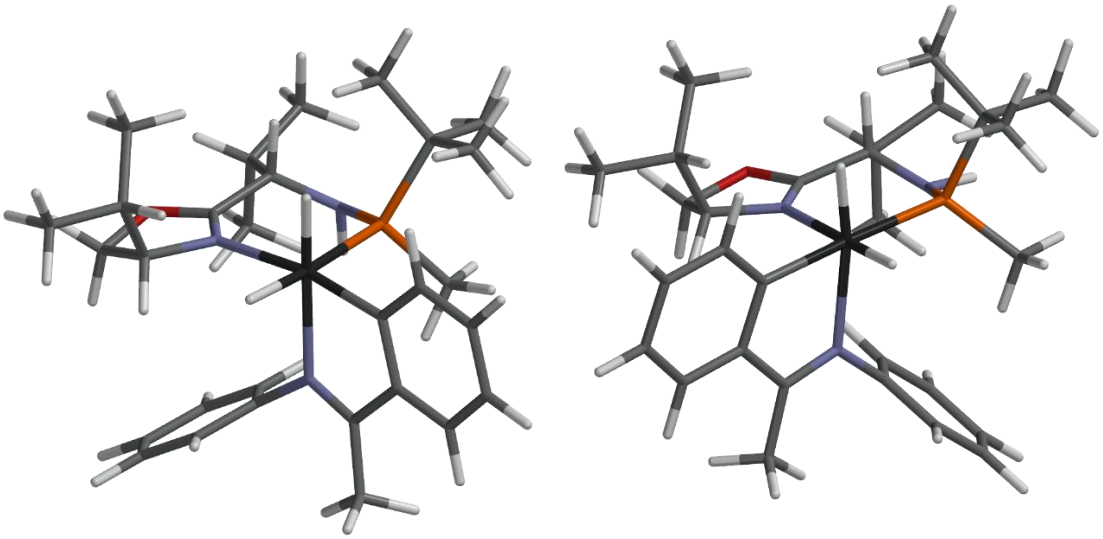

0.00 Kcal / mol

0.88 Kcal / mol

Figure 17. *a) The two possible configurations for the iridacycle dihydride (catalyst* ***ent-3iPr****). Conformation* ***IV(H)-ent-3iPr*** *is thermodynamically favored with respect to* ***V(H)-ent-3iPr****. b) Calculations were performed with Spartan 16 using RM06 functional with the 6-31G* & LANL2DZ basis set.*

As we can observe, although **IV(H)-*ent*-3iPr** is 0.88 Kcal / mol more stable than **V(H)-*ent*-3iPr** and this equilibrium would be slightly shifted towards **IV(H)-*ent*-3iPr**, the energy difference between the two configurations is smaller than between **IV(H)-*ent*-1iPr** and **IV(H)-*ent*-1iPr**. Considering the proposed equilibrium happens during a catalysis, this could partially explain why the selectivity of the reduced amine with catalyst ***ent*-3iPr** is lower than with ***ent*-1iPr** (65% ee vs. 89% ee)

We want to stress that these calculations are just a rough approach. To be sure if this equilibrium is responsible for the reduced selectivity with ***ent*-3iPr**, a full mechanistic study taking into account all intermediates and TSs should be carried out.

6.5.3. Model for the Hydride Transfer stereodetermining step

In 2018, Norrby-Wiest-Andersson reported calculations for the transition state in which the hydride is transferred to the iminium cation and the stereochemistry of the reduced amine is determined. The authors highlight some interactions between the iminium cation and the iridacycle that allow to explain the stereochemistry observed experimentally.

Considering the similarities between the catalyst that Norrby and co-workers use in their study (Andersson's Ir-P,N catalyst) and the Ir-MaxPHOX catalysts employed in the present chapter, we decided to apply the same model to our catalytic system. In Figure 18 we depict the two possible iminium cation approaches to the reacting site for the hydride transfer. This model uses catalyst **ent-1iPr**.

The iminium cation approach that yields the major enantiomer (*S*) is favored by a π– π interaction (Figure 18, **in green**) that is not present in the approach that yields the minor enantiomer (*R*).

For the *R* product yielding approach there is an interaction between the phenyl group of the iminium cation (C–Ph) and the bulky oxazoline that causes additional steric strain (Figure 18, **in red**). On the other hand, for the *S* product yielding approach the methyl group of the iminium carbon is oriented towards the oxazoline and the steric strain is less.

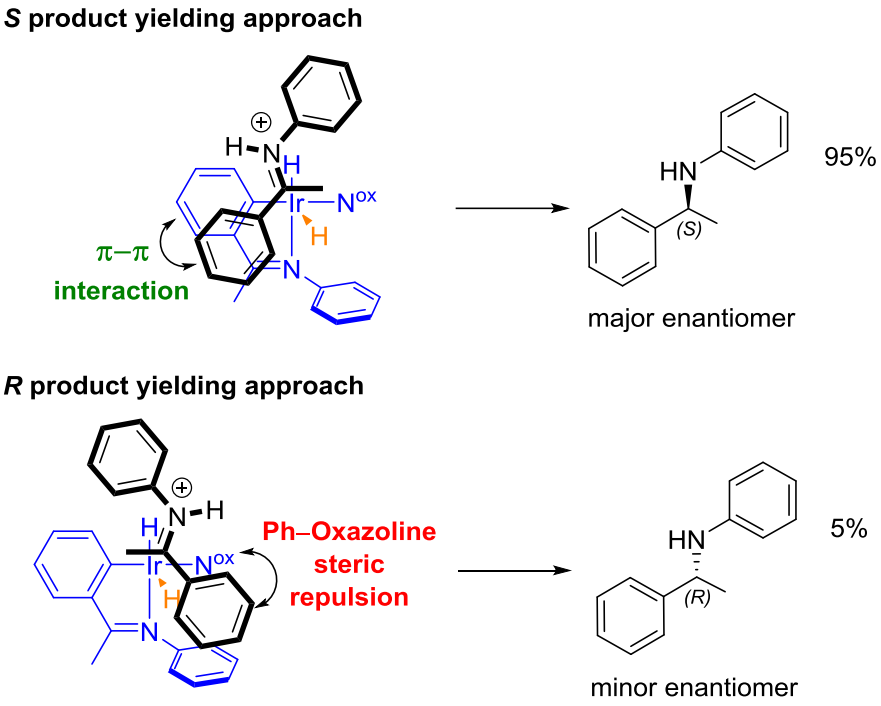

Figure 18. *Model for the hydride transfer transition state for Ir-MaxPHOX* ***ent-1iPr*** *iridacycle in which the stereochemistry of the reduced product is defined. The hydride transferred to the substrate is highlighted in orange. Positive interactions are highlighted in green and negative in red. The enantiomeric ratio corresponds to a catalysis in CH_2Cl_2, at 55 bar of H_2, r.t. and 1 mol% of catalyst* ***ent-1iPr****.*

The present model is in agreement with the absolute configuration obtained when employing Ir-MaxPHOX catalysts.

6.6. Conclusions

From a small family of P-stereogenic Ir-MaxPHOX precatalysts, we pinpointed complex **1iPr,** which shows activity and selectivity that matches the best Ir–P,N systems in the hydrogenation of *N*-aryl imines. Catalyst **1iPr** hydrogenated them with up to 96% ee at atmospheric pressure of hydrogen and low temperature. Non P-stereogenic Ir-MaxPHOX versions provided lower selectivity. The nature of the counteranion greatly influenced the reaction outcome; smaller counteranions (e.g. BF_4) afforded slower reactions and reduced enantiomeric excesses.

The catalyst species used were cationic iridium complexes that have an imine molecule from the substrate incorporated *via* cyclometalation. Cyclometalated

[IrHCl(MaxPHOX)(imine)] complexes **6.13** and **6.14** were prepared from ***ent*-1iPr** *and* ***ent*-3iPr**, isolated and characterized by X-ray crystallography. Chloride exchange with $NaBAr_F$ on **6.13** provided a functional catalytic system with the same level of selectivity as that obtained with catalyst ***ent*-1iPr**.

With some basic and primal calculations we determined that the dihydride Ir-MaxPHOX iridacycles are more stable when the cyclometalated Ph group is positioned *cis* to the P unit. The energy difference is bigger for the *cis*/*trans* ***ent*-1iPr** iridacycle stereoisomers than for the ***ent*-3iPr** iridacycle stereoisomers. This could explain the higher ee obtained in the reduction of *N*-aryl imines with catalyst ***ent*-1iPr** with respect to ***ent*-3iPr**. Although we consider these calculations a starting point, to truly comprehend this possible equilibrium we would need to take into consideration each step and transition state between the two configurations.

Finally, the model developed by Norrby-Wiest-Andersson was able to predict the stereochemistry for the reduced amines with catalyst ***ent*-1iPr**.

6.7. References

[1] K. H. Hopmann, A. Bayer, *Coord. Chem. Rev.* **2014**, *268*, 59–82.

[2] N. Fleury-Brégeot, V. de la Fuente, S. Castillón, C. Claver, *ChemCatChem* **2010**, *2*, 1346–1371.

[3] J. H. Xie, S. F. Zhu, Q. L. Zhou, *Chem. Rev.* **2011**, *111*, 1713–1760.

[4] C. Moessner, C. Bolm, *Angew. Chem. Int. Ed.* **2005**, *44*, 7564–7567.

[5] A. Trifonova, J. S. Diesen, C. J. Chapman, P. G. Andersson, **2004**, 1–38.

[6] A. Baeza, A. Pfaltz, *Chem. - A Eur. J.* **2010**, *16*, 4003–4009.

[7] X. Verdaguer, U. E. W. Lange, M. T. Reding, S. L. Buchwald, *J. Am. Chem. Soc.* **1996**, *118*, 6784–6785.

[8] P. Schnider, G. Koch, R. Pretot, G. Wang, F. M. Bohnen, C. Kriiger, A. Pfaltz, *Chem. Eur. J.* **1997**, *3*, 887–892.

[9] Y. Liu, H. Du, *J. Am. Chem. Soc.* **2013**, *135*, 6810–6813.

[10] S. P. Smidt, N. Zimmermann, M. Studer, A. Pfaltz, *Chem. - A Eur. J.* **2004**, *10*, 4685–4693.

[11] Y. Schramm, F. Barrios-Landeros, A. Pfaltz, *Chem. Sci.* **2013**, *4*, 2760.

[12] B. Tutkowski, S. Kerdphon, E. Limé, P. Helquist, P. G. Andersson, O. Wiest, P. O. Norrby, *ACS Catal.* **2018**, *8*, 615–623.

Chapter 7

MaxPHOX iridacycles on the asymmetric hydrogenation of *N*-alkyl imines

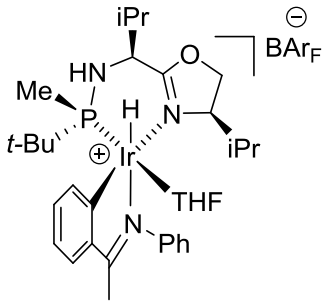

E. Salomó, A. Gallen, A. Grabulosa, A. Riera, X. Verdaguer *(submitted*)

7.1. Introduction: Catalytic asymmetric hydrogenation of *N*-alkyl imines

Many relevant pharmaceutical and agrochemical substances contain chiral amines. As we explained in Chapter 6, hydrogenation of imines via asymmetric catalysis is a key method to prepare chiral amines.[1–3] In Chapter 6 we employed the Ir-MaxPHOX catalyst to hydrogenate *N*-aryl imines. The results obtained were excellent. However, when it comes to hydrogenate *N*-alkyl imines, traditional Ir–P,N catalysts such as Ir-MaxPHOX do not perform well.[4] Theoretically, the great basicity of the resulting *N*-alkyl amines can interact with the catalyst and even deactivate it.[5] Nonetheless, the enantioselective reduction of *N*-alkyl imines is very attractive because it would directly furnish the corresponding *N*-alkyl amines (**I1**). Some examples of relevant substances containing chiral *N*-alkyl amines are depicted in Figure 1.

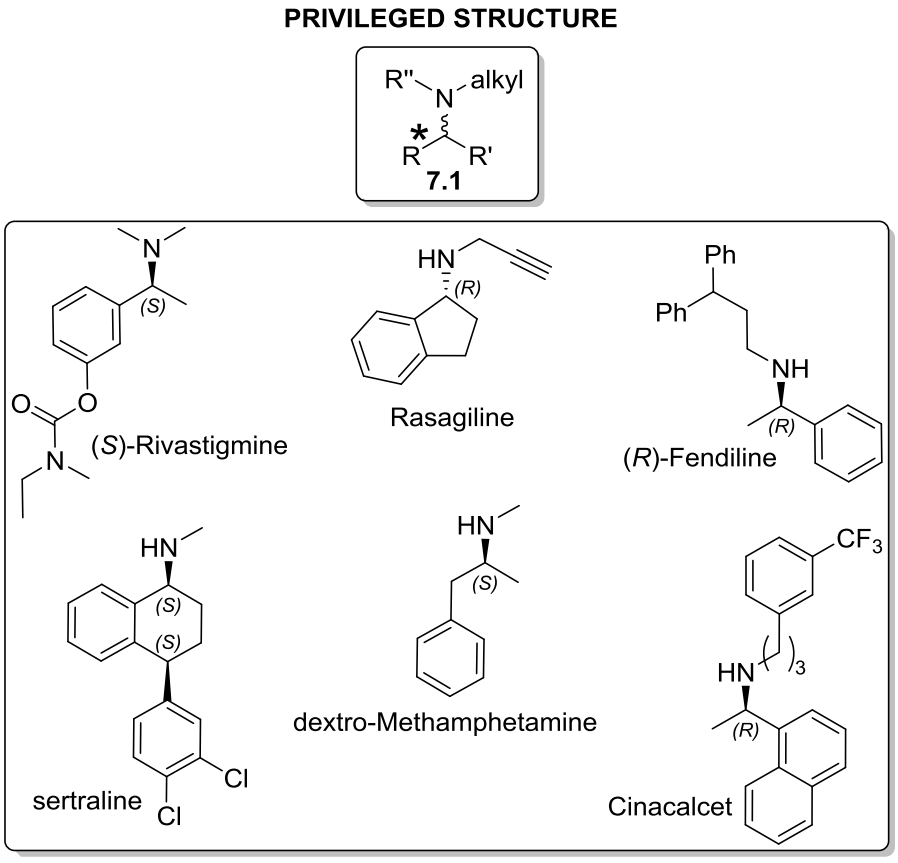

Figure 1. *Chiral N-alkyl amines are present in many relevant substances.*

As we reported in Chapter 4, there are not many approaches to reduce *N*-alkyl imines enantioselectively.[5,6] Furthermore, there is no proper method to do so by organometallic catalytic hydrogenation. Consequently, a successful method employing Ir-MaxPHOX catalysts would be groundbreaking.

7.2. Synthesis of *N*-alkyl imines

There are several methods to synthesize *N*-alkyl imines. In analogy to what we reported in Chapter 6 for the synthesis of *N*-aryl imines, the reaction between a ketone and an amine with a desiccant works efficiently. For some small and nucleophilic amines, such as methyl or ethylamine, the reaction goes to completion by just using a mild desiccant such as molecular sieves. However, for bigger and more hindered amines (like propyl amine), a stronger desiccant, like $TiCl_4$, is often required. [5]

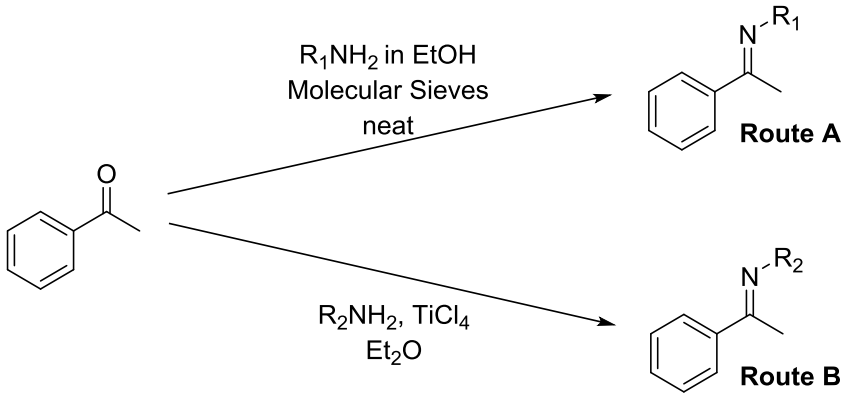

Figure 2. *The two routes we employed to synthesize N-alkyl imines. Route A for small nucleophilic amines. Route B for bigger and more hindered amines.*

The imines obtained with Route A can be obtained pure enough with just filtering the molecular sieves and evaporating all the volatiles (the amines are volatile too). For Route B, distillation is usually the method of choice for purifying. Sometimes, if the imines is crystalline enough, it can be purified by crystallization.

N-alkyl imines are relatively easier to synthesize than for example *N*-aryl imines. Nevertheless, they are more reactive than their arylic analogs and therefore have to be carefully stored and handled.

7.3. Hydrogenation of *N*-alkyl imines with Ir-MaxPHOX catalysts

7.3.1. Firsts steps toward the hydrogenation of *N*-alkyl imines

We selected acetophenone *N*-methylimine **I1** as a model substrate. Imine **I1** is very easy to produce and the corresponding amine is rather basic and nucleophilic. We rationalized that if we could properly reduce it, it would be possible to expand the methodology to other *N*-alkyl imines. As catalysts for the study, we selected the 4 basic iPr/iPr Ir-MaxPHOX catalysts in Figure 3 since in the hydrogenation of *N*-aryl imines the catalysts containing iPr on the ARM position afforded the best results.

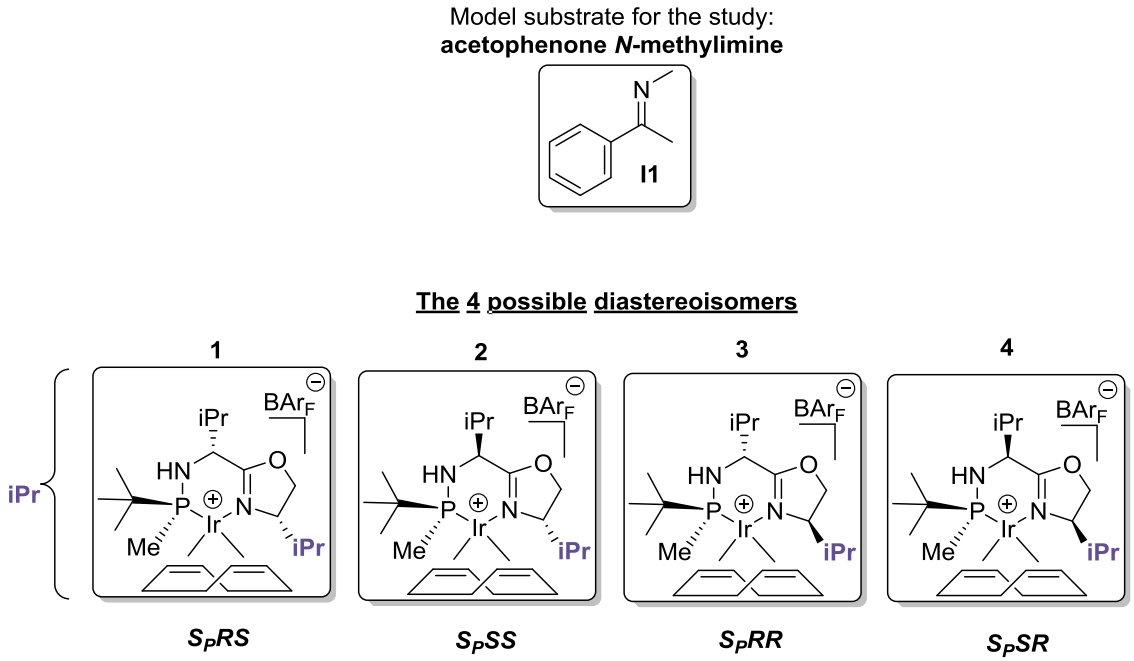

Figure 3. *The model substrate acetophenone N-methylimine and the Ir-MaxPHOX catalysts employed in this study; the 4 iPr/iPr diastereoisomers.*

In our first attempts we used 1 mol% of Ir-MaxPHOX in CH_2Cl_2 with 3 bars of H_2. The results obtained were not satisfactory (Figure 4). Conversions were lower than expected (even at 3 H_2 bars) and the ee's were very low and did not follow a clear trend.

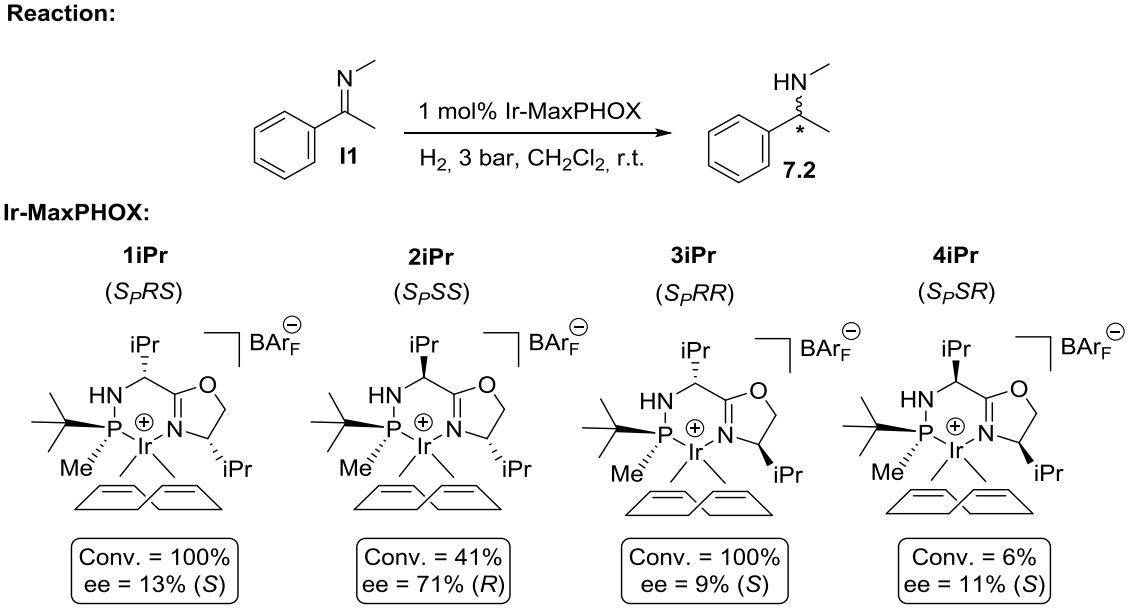

Figure 4. *a) Hydrogenation of acetophenone N-methylimine with the 4 selected Ir-MaxPHOX catalysts b) Conversion was determined by ^{1}H NMR analysis of the crude reaction mixture. c) Unless otherwise noted, the ee value was determined by HPLC or GC analysis of the corresponding trifluoroacetamides on a chiral stationary phase.*

As explained in Chapters 4 and 6, Pfaltz and co-workers detected an iridacycle that is crucial for the reduction of *N*-aryl imines when using Ir-PHOX type catalysts.[7] We also detected these complexes when using our Ir-MaxPHOX catalysts. We proved that they were the true catalytic species and vital in the hydrogenation process. We decided to study the formation of these metallocycles with *N*-alkyl imines too in hope of shedding some light on why the hydrogenation was not proceeding as expected.

7.3.2. ^{1}H- and ^{31}P-NMR analyses to detect iridacycles

We thought of using ^{1}H and ^{31}P NMR to develop a quick, simple and efficient method to study the formation of iridacycles with *N*-alkyl imines. We selected *N*-aryl imine **A0** in Figure 5 to develop the technique as we knew that it forms cyclometallated

compounds with Ir-MaxPHOX catalysts (Chapter 6). We selected catalyst **1iPr** because it was the best catalyst in the hydrogenation of *N*-aryl imines in Chapter 6. After various attempts we designed and optimized the method depicted in Figure 5.

The first step formed the iridacycle in a solvent coordinating enough to stabilize it but no so much that thwarts its formation. Then, by addition of ACN-d_3 we obtained **7.3**. We carefully evaporated all volatiles as the presence of non-deuterated THF would not allow us to perform ^{1}H NMR analyses. We dissolved the crude in ACN-d_3 and obtained ^{1}H and ^{31}P NMR spectra. All the employed ACN was deuterated. This way the spectra were cleaner and easier to analyze.

Probably the most characteristic signal in these substances ^{1}H NMR was the hydride peak. It appeared at very high fields (around –20 ppm) as a doublet provoked by coupling with the P atom.[7] As we can see in Figure 5, the spectra is rather clean. There was only one hydride signal, which means the formation of the iridacycle happened in a selective manner. Only one phosphorous species was detected in the ^{31}P NMR. This further confirmed the purity of the formed iridacycle.

When we applied the same analytic procedure but using *N*-methyl imine **I1**, the NMR's we obtained were less clear (Figure 6). Many signals were detected in the hydride and phosphorous zones. This proves that the acetophenone *N*-methyl imine **I1** does not selectively afford a clean iridacycle. These intermediate are key components for the catalysis and its absence partially explains the unsatisfactory results obtained for the hydrogenation of this substrates.

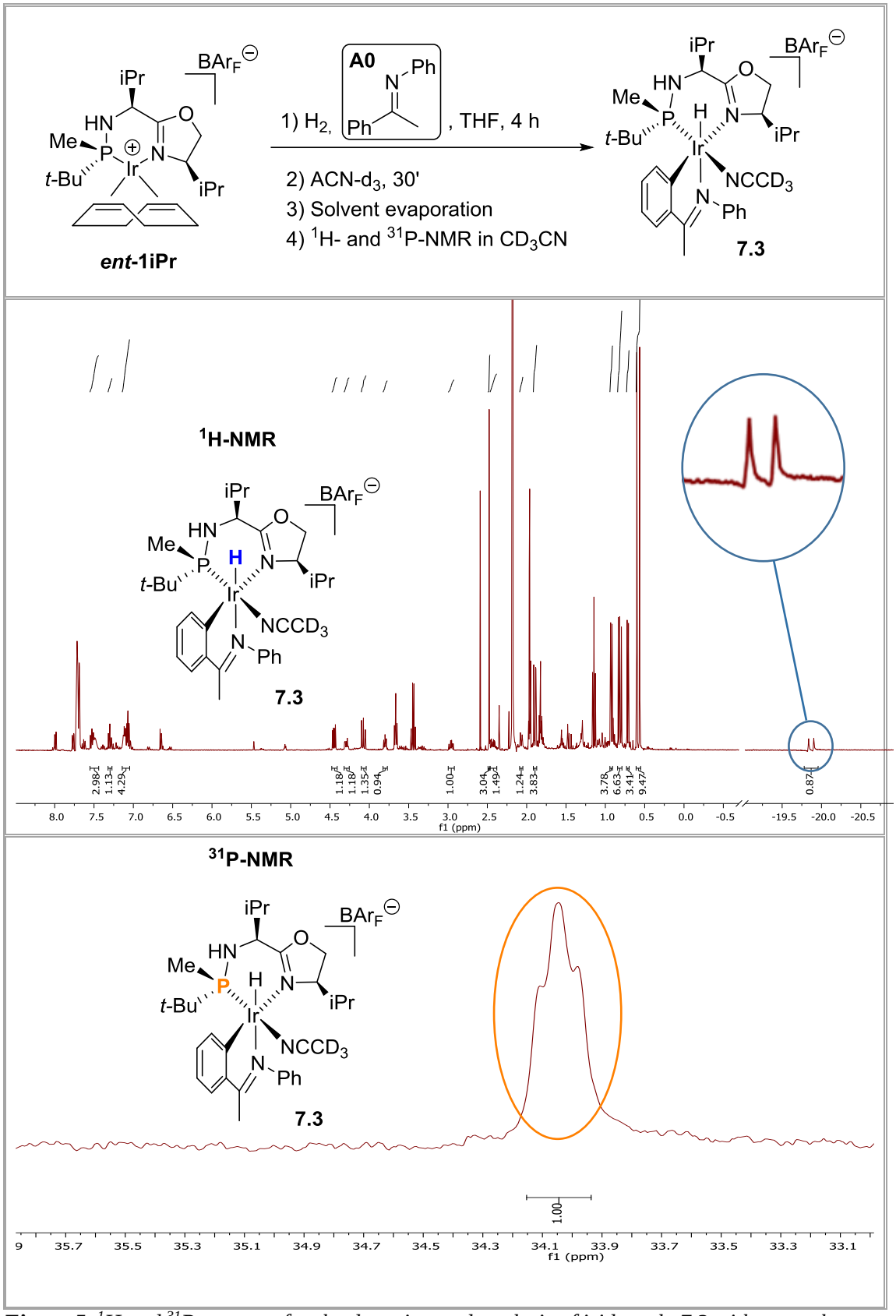

Figure 5. *^{1}H and ^{31}P spectras for the detection and analysis of iridacycle* ***7.3*** *with acetophenone N-phenyl imine* ***A0****.*

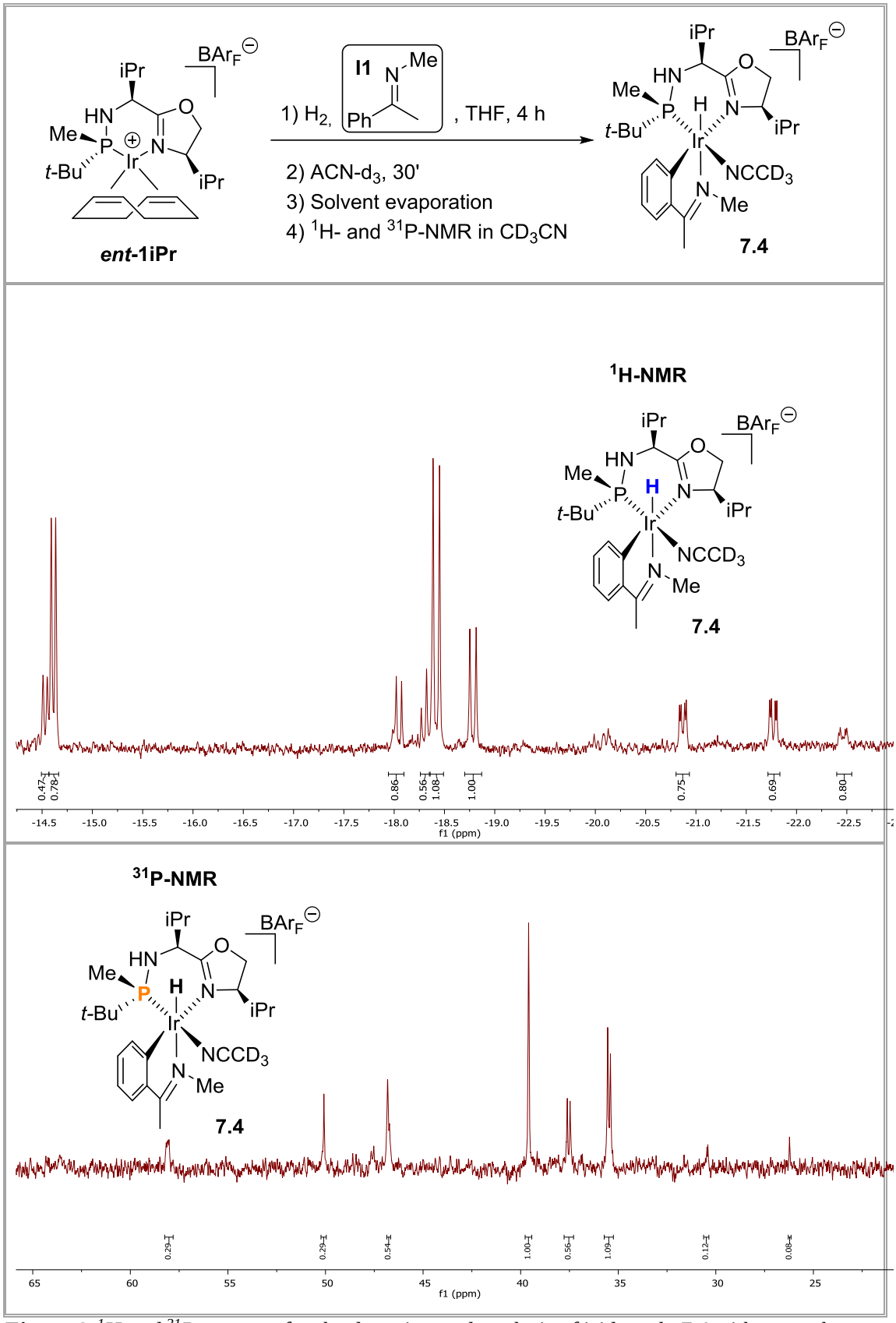

Figure 6. *^{1}H and ^{31}P spectras for the detection and analysis of iridacycle **7.4** with acetophenone N-methyl imine **I1**.*

7.3.3. *N*-aryl imines as additives

Considering the results in Section 7.3.2, we decided to employ *N*-aryl imine **A0** as an additive for the catalyses. We hoped that **A0** would form a proper iridacycle with the corresponding Ir-MaxPHOX catalyst and catalyze the reduction of *N*-alkyl imines.

On our first attempt we mixed all the reagents together and charged the reactor with 3 bars of H_2. There was no improvement respecting the analogous catalyses without additive. We theorized that the *N*-alkyl imine **I1** (or the corresponding amine **7.2**) interacted with the catalyst before the iridacycle could be constituted.

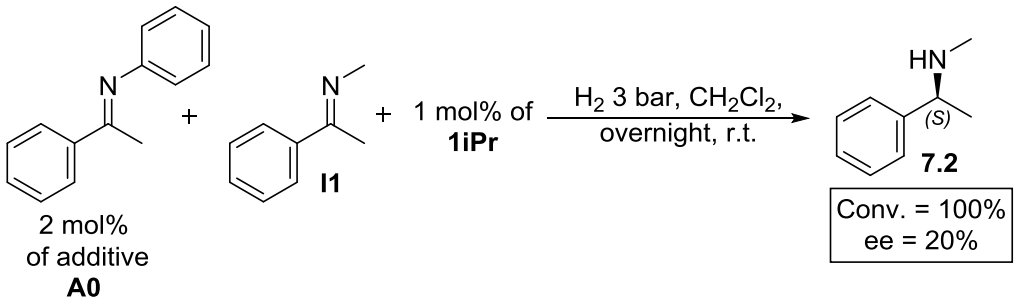

Figure 7. *Hydrogenation of acetophenone N-methylimine conducted by mixing all reagents at the beginning. The ee did not substantially improve (from 13% to 20% ee).*

We tried to preform the iridacycle by reacting the *N*-aryl imine additive and the Ir-MaxPHOX catalyst under 3 bars of H_2 for 30 min. Then we added the *N*-alkyl imine substrate. The outcome was dramatically different; both the conversion and the ee increased drastically for all cases. The results obtained resemble the ones obtained for the hydrogenation of *N*-aryl imines with Ir-MaxPHOX catalysts. The best results (conversion and ee) were also obtained with catalyst **1iPr**. Apparently, the iridacycle, once formed, is robust enough and does not suffer from deactivation.

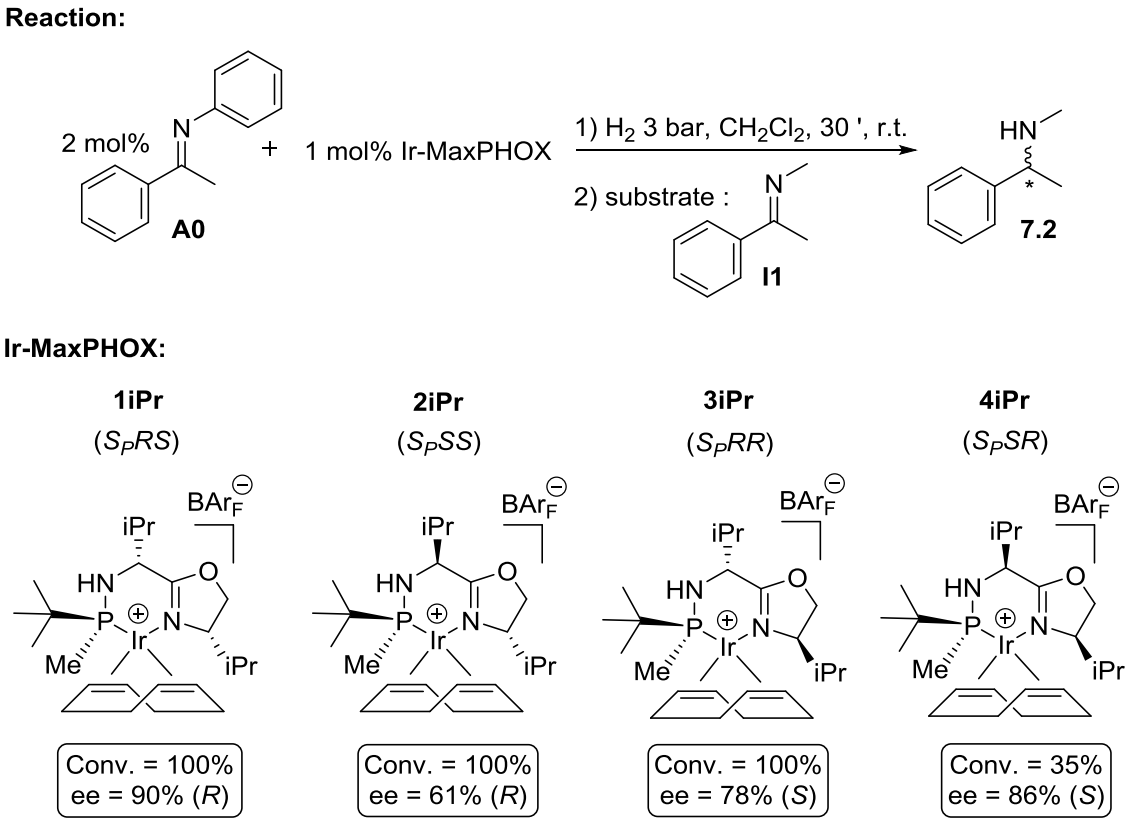

Figure 8. *a) Hydrogenation of acetophenone N-methylimine with the 4 selected Ir-MaxPHOX catalysts using* ***A0*** *as additive and preforming the iridacycle b) Conversion was determined by* ^{1}H *NMR analysis of the crude reaction mixture. c) Unless otherwise noted, the ee value was determined by HPLC or GC analysis of the corresponding trifluoroacetamides on a chiral stationary phase.*

7.3.4. Optimization of the additive

The results so far have proved that the true catalyst for these reactions is actually an iridacycle. So, the imine employed as additive is part of the catalytic species. Theoretically a different imine would furnish a different catalyst and affect the outcome of the catalysis. We decided to test different *N*-aryl imines as additives with the intention to increase the ee. In Figure 9 we depict all the additives we studied. The conversions and ee's obtained are summarized in Table 1.

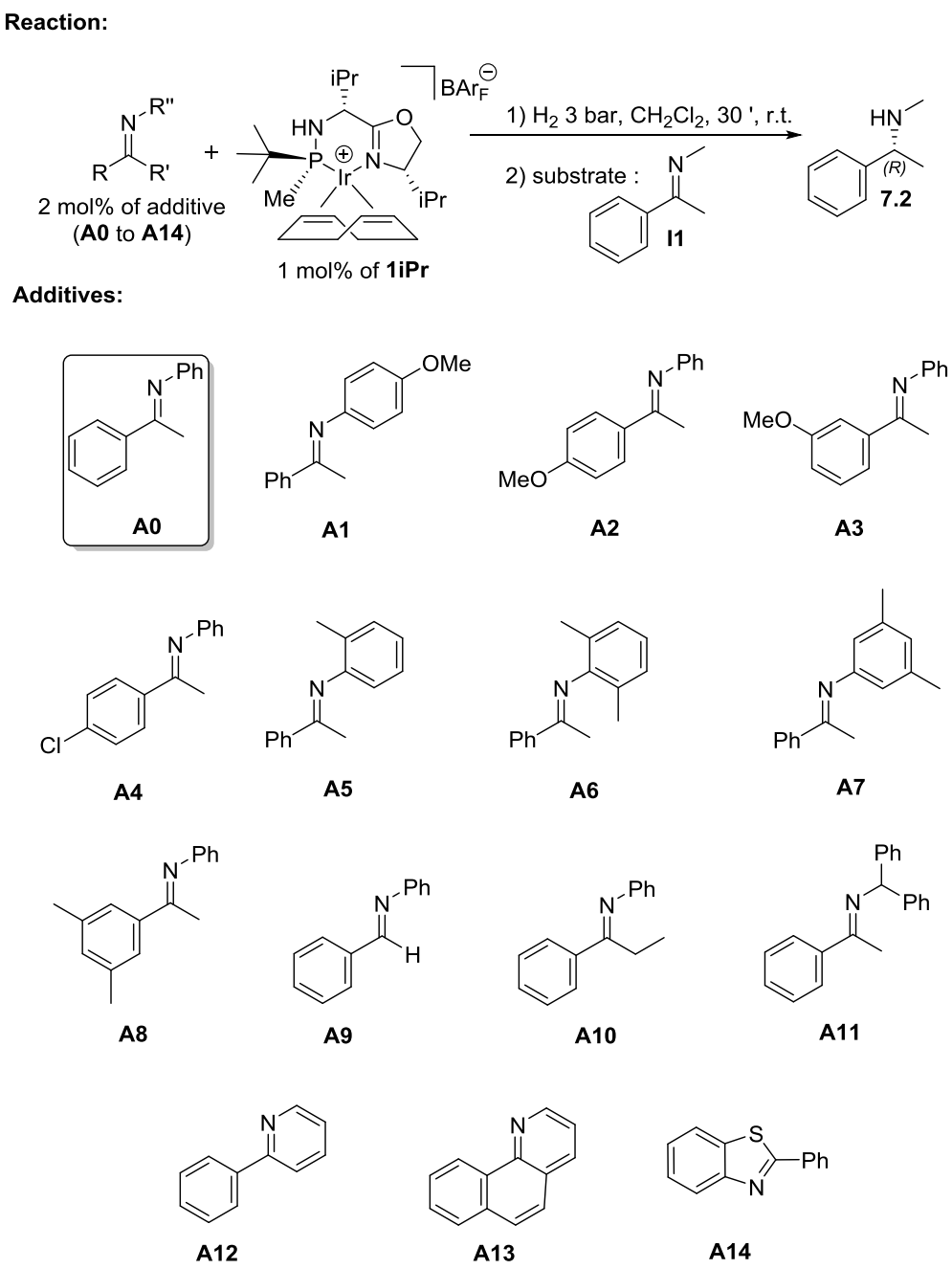

Figure 9. *Screening for new additives to use in the hydrogenation of N-alkyl imines.*

Table 1. Influence of different additives on the catalysis

Entry	**Additive**	**Conversion (%)**	**ee (%)**
1	**A0**	100%	90% (*R*)
2	**A1**	100%	88% (*R*)
3	**A2**	100%	87% (*R*)
4	**A3**	100%	83% (*R*)
5	**A4**	49%	60% (*R*)
6	**A5**	100%	82% (*R*)
7	**A6**	36%	40% (*R*)
8	**A7**	100%	87% (*R*)
9	**A8**	100%	62% (*R*)
10	**A9**	16%	n.d.
11	**A10**	100%	85% (*R*)
12	**A11**	50%	49% (*R*)
13	**A12**	33%	24% (*R*)
14	**A13**	52%	57% (*R*)
15	**A14**	43%	46% (*R*)

a) Conversion was determined by ^{1}H NMR analysis of the crude reaction mixture. b) The ee value was determined by HPLC analysis of the corresponding trifluoroacetamide on a chiral stationary phase

With **A0** we obtained full conversion and 90% ee. Additives **A1**–**A4** contain electrowithdrawing and electrodonating groups at the aromatic rings. The electrodonating MeO– groups decreased the ee's respect of **A0** by a few points, whilst the electrowithdrawing Cl– group provoked a significant decrease in both conversion and ee. Imines **A5–A8** have methyl groups on the aromatic positions. We hoped that the steric hindrance would help to improve the ee, but instead it decreased (ee's between 40 and 87%). Compounds **A9** and **A10** had different groups than methyl on the benzylic position. Neither of them improved the ee of 90% obtained with **A0**. The additives **A11**–**A14** were compounds with similar structures to **A0** that we tested hoping that they would furnish a

proper iridacycle. However, the conversions and ee's obtained were worse than with **A0**. After analyzing these results we selected **A0** as the best additive for the hydrogenations.

7.3.5. Reaction scope

With the selected catalyst (**1iPr**) and additive (**A0**), we proceeded to assess the scope of the hydrogenation with various *N*-alkyl imines (Figure 10). We observed that low temperatures increased the ee. Consequently, the temperature was optimized for each substrate. Imine **I1** was reduced with 92% ee. Imines **I2** and **I3**, which possess electrodonating groups, seemed to be less reactive. The reaction for these had to be conducted at room temperature and the ee's for the corresponding amines were 91 and 89%, respectively. Imines **I4**, **I5** and **I6** contain electrowithdrawing groups. The temperature could be decreased up to –10 ºC to afford 95, 94 and 93% of ee for the reduction of each imine, respectively. These results suggest that electrowithdrawing groups activate these imines for the catalysis. Cyclic imine **I7** was also hydrogenated with an ee of 89% at –10 ºC. The good results obtained with imines **I8**, **I9** and **I10** indicate that substrates with different *N*-alkyl groups from methyl can also be reduced with excellent ee's. For substrate **I11** the ee was not as high as expected at room temperature and it was not studied at low temperatures. Substrate **I12** is a very difficult substrate to hydrogenate as it is does not contain any aromatic substituent that can stabilize the imine. Consequently this is a very unstable imine and its reactivity is hard to control. The hydrogenation result, although is not impressive, is better than the one obtained without using imines **A0** as additive. This again prove that the iridacycle intermediate is key for the hydrogenation of imines (**I12** cannot form an iridacycle as the cyclohexane ring does not contain any Csp2 atoms). **I13** and **I14** are very difficult to hydrogenate. For **I13** we managed 38% and for **I14** we obtained no conversion at all. We believe the stronger nucleophilic behavior of **I14** is what thwarts the reaction. The conversion for **I15** was very low due to solubility issues. **I16** was also studied in Chapter 6. The hydrogenation using a Ir-MaxPHOX catalyst with 55 bar of H_2 did not afford any product. If imine **A0** is used as additive, the conversion increases to 10% with only 3 bars of H_2. Further studies will be carried on with this class of substances. **I17** was very problematic to analyze by HPLC or GC; we could not find a method with which we could quantify precisely the

two enantiomeric signals. We previously studied the hydrogenation of **I18** in Chapter 6. Without employing any additive we obtained the *S* enantiomer with an ee of 77%. When using additive **A0** the *R* enantiomer was obtained with 86%. The use of an additive improves slightly the ee, but not to exceptional levels. However, what it is very interesting is that the configuration of the obtained amine is different. This indicates that the reaction mechanism is completely different when a proper iridacycle is formed. We have in mind to further study this type of substrates along with the reaction mechanism in the future.

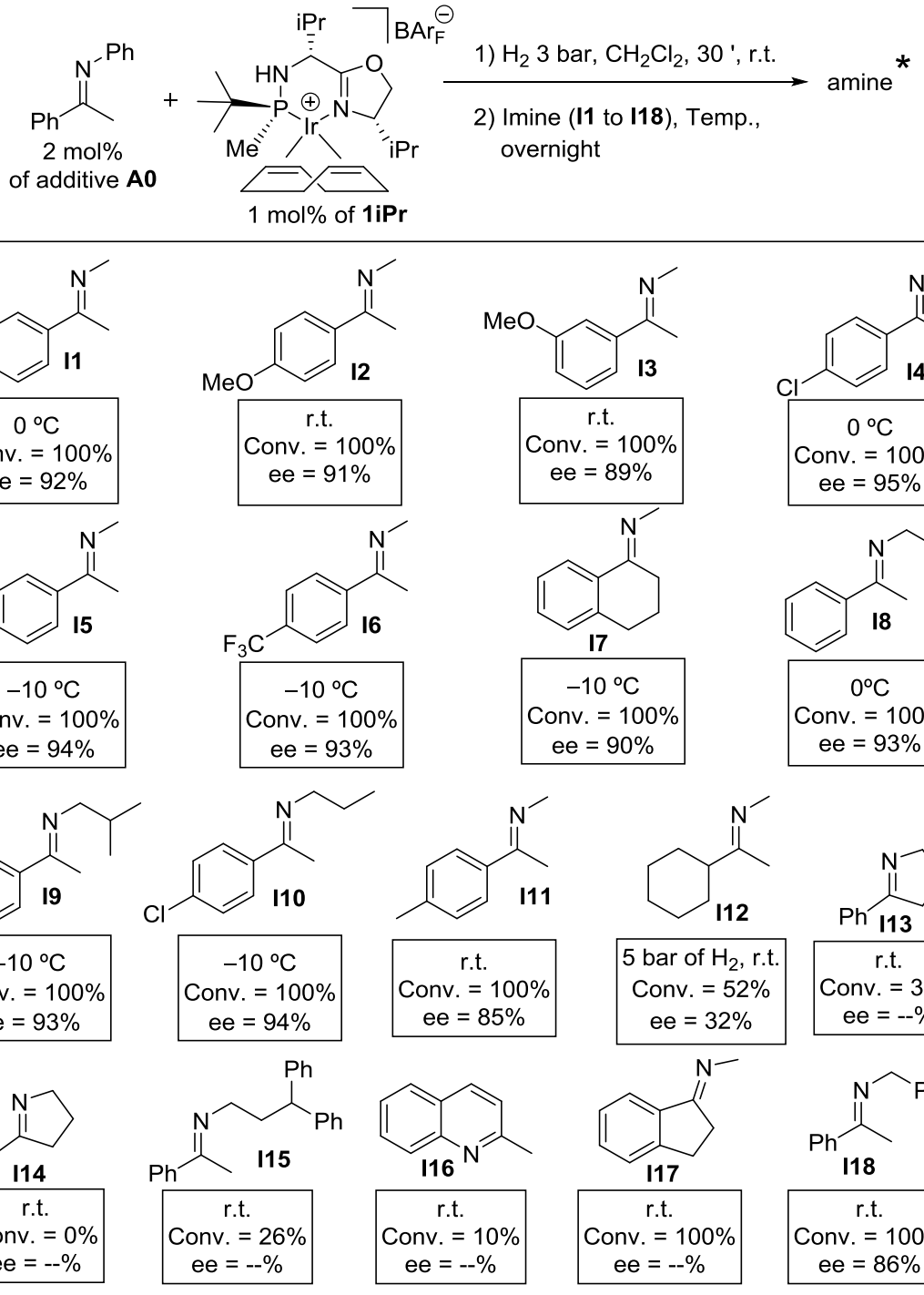

Figure 10. *a) Scope for the hydrogenation on N-alkyl imines with Ir-MaxPHOX* ***1iPr*** *using additive* ***A0****. Catalyst* ***1iPr*** *(SPRS) with additive* ***A0*** *afforded the amines as the (R) enantiomer. The configuration was determined by optical rotation analysis or analogy. b) Conversion was determined by* ^{1}*H NMR analysis of the crude reaction mixture. c) Unless otherwise noted, the ee value was determined by HPLC or GC analysis of the corresponding trifluoroacetamides on a chiral stationary phase d) The ee value of* ***I16*** *was determined by HPLC analysis of the corresponding acetamide.*

7.3.6. Reaction performance with base and/or nucleophiles in the media

The result obtained with **I14** in Section 7.3.5 led us to believe that the nucleophilicity and/or the basicity of the substrates/products might interfere with the catalytic system. We studied the reaction in Table 2 with some amines present in the media in order to observe how the catalytic system would be affected. We added the corresponding base (**B1**-**B4**) along with the *N*-alkyl imine after preforming the iridacycle.

Table 2. Study of the effect of amines on the catalytic system

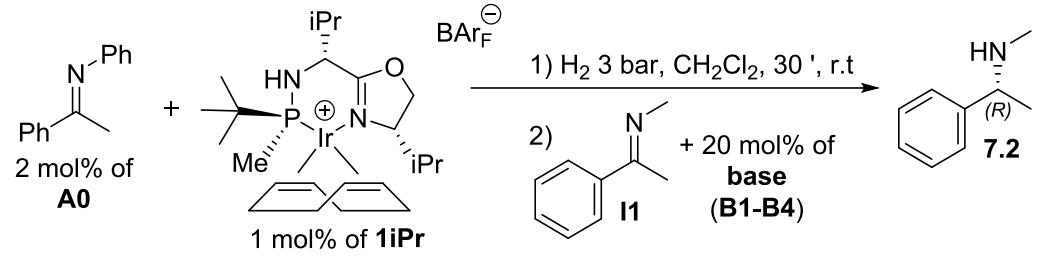

Base:

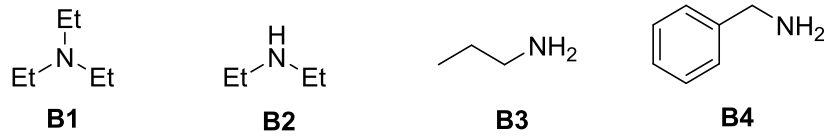

Entry	Base	Conv. (%)	ee (%)
1	**B1**	100	89 (*R*)
2	**B2**	100	90 (*R*)
3	**B3**	0	--
4	**B4**	0	--

a) Conversion was determined by ^{1}H NMR analysis of the crude reaction mixture. b) The ee value was determined by HPLC analysis of the corresponding trifluoroacetamide on a chiral stationary phase

The addition of a tertiary or a secondary amine such as **B1** or **B2** (Entries 1 and 2) does not affect the reaction. On the other hand, more nucleophilic amines such as **B3** or **B4** (Entries 3 and 4) affect drastically the conversion. It seems that the catalytic system can tolerate basicity to a certain degree. However, nucleophilic substances can interfere with the catalytic system in a dramatic manner, probably by coordinating to the catalyst.

Another experiment on the same line is depicted in Figure 11. Cyclic imine **I14** is more nucleophilic than *N*-aryl or *N*-alkyl imines such as acetophenone *N*-phenylimine or

acetophenone *N*-methylimine. When adding imine **I14** to the reaction mixture (Figure 11) we did not detect any reduced amine for any imines. We also observed than the addition of **B5** after 10' stops the catalysis completely (Conv. = 40%). We concluded that some imines (or their reduced amines) are too nucleophilic and interact with the catalytic system, either if we preform the iridacycle (Figure 11, Reaction 2) or if we do not (Figure 11, Reaction 1).

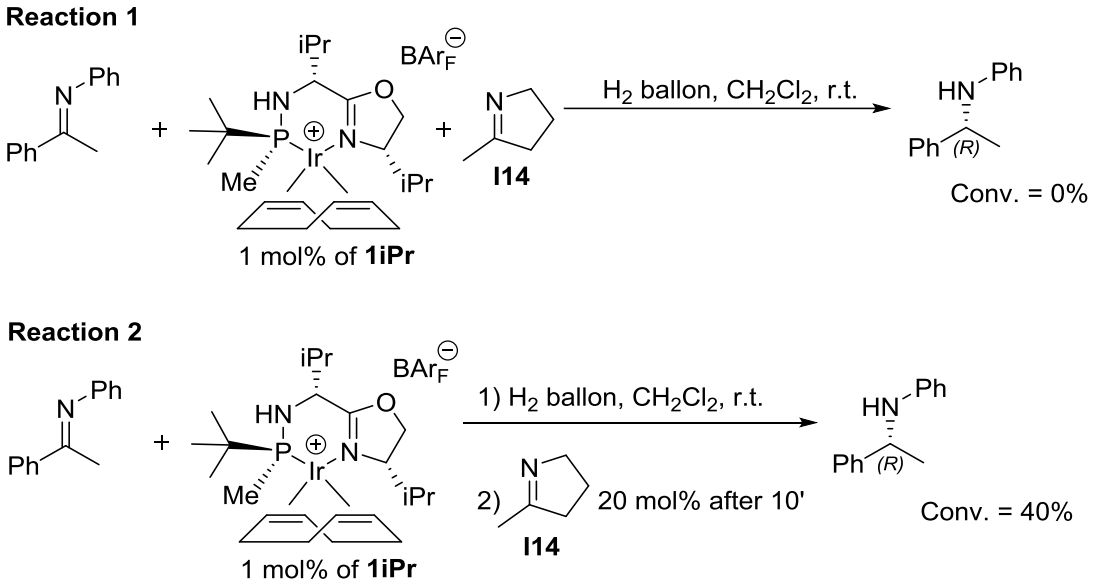

Figure 11. *Study of the effect of nucleophilic imines on the catalytic system.*

7.4. Isolation of a stable iridacycle-catalyst *(in collaboration with A. Gallén)*

The in situ formation of the iridacycle (Ir-MaxPHOX + *N*-aryl imine) and later addition of the desired *N*-alkyl ketimine is an effective methodology. Nevertheless, to have a more reliable and robust method that could be applied if needed in large scale procedures, we aimed for a version of the iridacycle that could be isolated, even stored, and used directly in hydrogenations as a catalyst when needed.

Neutral iridacycles like **7.5** can be isolated as we have demonstrated in Chapter 6. However, these compounds had to be treated with $NaBAr_F$ for them to be catalytically active.[7] Consequently, we aimed for a cationic catalyst such as complexes **7.7**-**7.10**, with BAr_F^- as counteranion and with a ligand (L) that occupies and protects the coordination site of the iridacyle but also is labile enough to leave a free coordination site during a

catalysis. With this purpose, complex ***ent*-1iPr** was reacted, in the presence of hydrogen, with *N*-aryl imine (**A0**) and the resulting complex treated with several stabilizing ligands (**X, in orange**) (Figure 12). We studied the addition of up to four different ligands (**X**) by ^{1}H and ^{31}P NMR and in all cases only one stereoisomer of the corresponding cationic octahedral Ir(III) complexes **7.7**-**7.10** was detected.

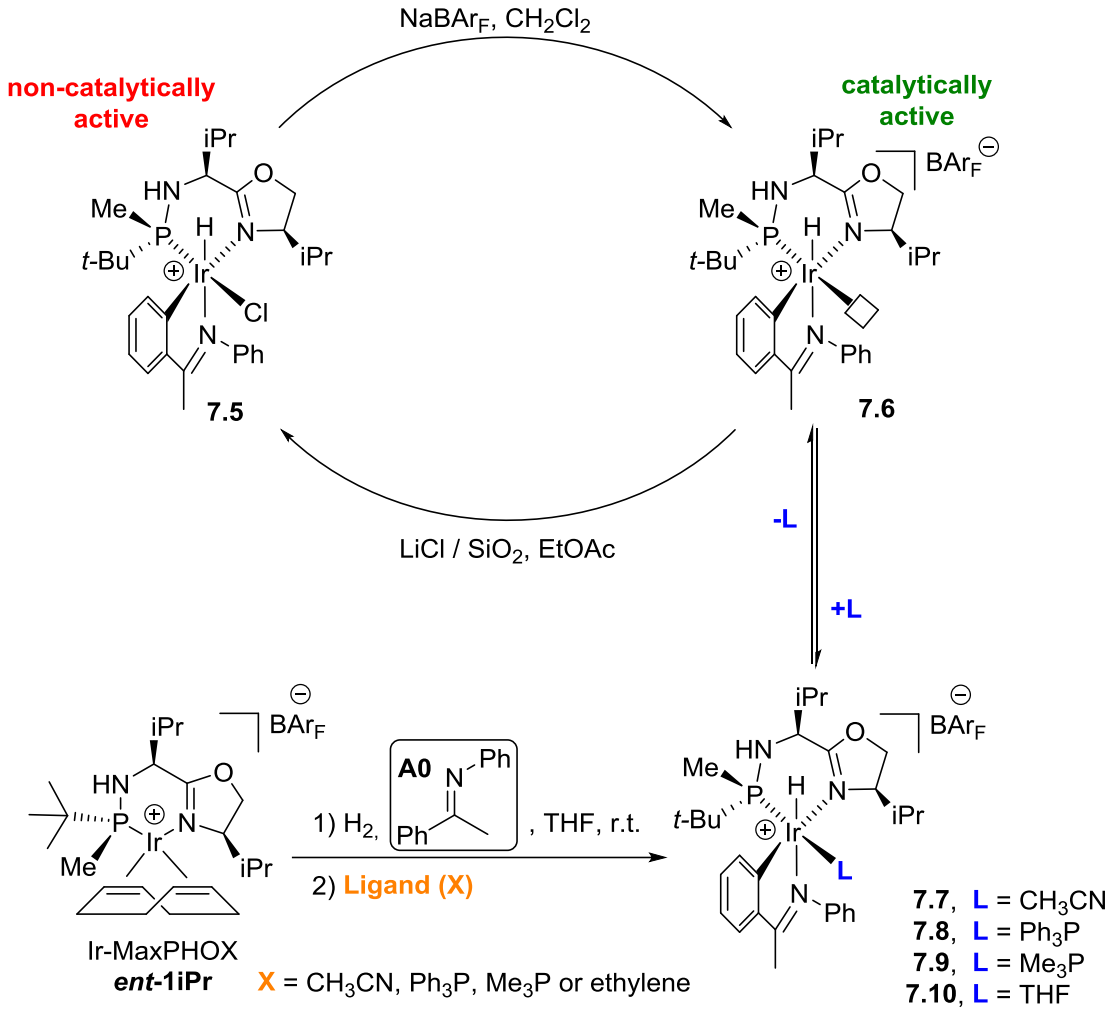

Figure 12. *Synthesis of a new iridacycle-catalyst. Screening for the most suited Ligand (L).*

Surprisingly, complex **7.10** did not contain an ethylene ligand but a solvent THF molecule instead. As expected, complex **7.10** could be synthesized without the addition of ethylene. Nevertheless, the resulting complex is of lower purity, as determined by ^{1}H NMR spectroscopy. We hypothesized that ethylene assists in the isomerization of intermediate unsaturated species to yield the final compound **7.10** with a THF molecule as ligand (**L**).

Complexes **7.7**-**7.10** were pure enough to be used in a preliminary catalysis test without first purifying and isolating them. Iridacycle **7.7** gave full conversion but the ee decreased compared with the in situ version. It seems like even traces of ACN in solution can influence the catalysis. Complex **7.8** gave no conversion at all. We rationalized that the ligand was too strongly bound to the metal and did not allow for the catalysis to happen. Catalysts **7.9** and **7.10** afforded full conversions and the ee's were the same as in the in situ version of the catalysis (Table 1, Entry 1).

Table 3. Hydrogenation of **I1** with different iridacycles as catalysts

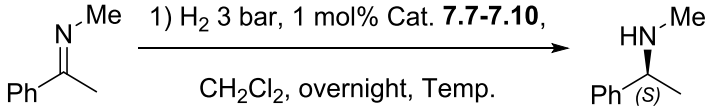

I1 **7.2**

Entry	**Catalyst**	**Temp. (ºC)**	**Conv. (%)**	**ee (%)**
1	In situ reaction	r.t.	100	90 (*S*)
2	**7.7**	r.t.	100	85 (*S*)
3	**7.8**	r.t.	0	-
4	**7.9**	r.t.	100	90 (*S*)
5	**7.10**	r.t.	100	91 (*S*)
6	**7.9**	0 ºC	0	--
7	**7.10**	0 ºC	100	91 (*S*)

a) The complexes were isolated by crystallization

As **7.9** and **7.10** offered the best results at room temperature, we attempted to purify and isolate them by crystallization/precipitation. We were very pleased to see that both catalysts were air-stable solids that can be used outside a glovebox and stored in a N_2 purged vial for several days. However, when running catalysis at low temperatures, in order to increase the ee's, we observed that **7.10** is much more active than **7.9**; the hydrogenation at 0 ºC with **7.9** did not afford any product while with **7.10** the conversion was complete (Entries 6 and 7). Consequently, we selected **7.10** as our new catalyst.

7.4.1. Study of the scope of iridacycle-catalyst 7.10 *(in collaboration with A. Gallén)*

To be useful, the new isolated catalyst **7.10** had to offer at least the same results obtained with the in situ version of the hydrogenation. So, employing catalyst **7.10** we reproduced the reduction of some of the best results obtained in the hydrogenation of *N*-alkyl imines in the substrate scope in Section 7.3.5. The results with this new iridacycle and the reaction in situ are compared in Table 4.

Table 4. Scope comparison between "in situ reaction (***ent*-1iPr**+**A0**)" and "Cat. **7.10**"

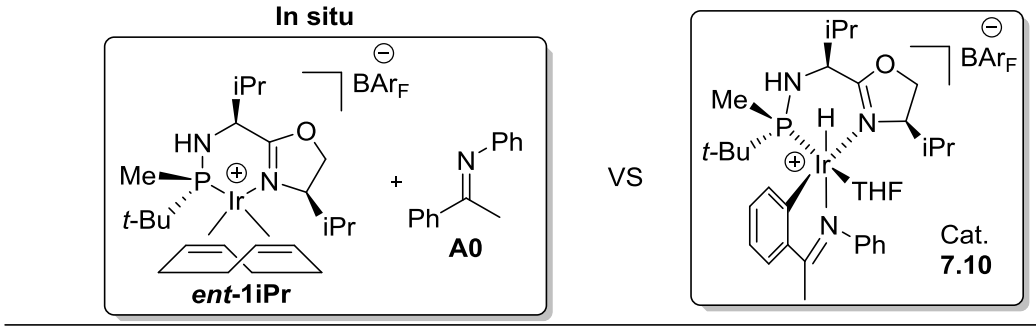

Imines:

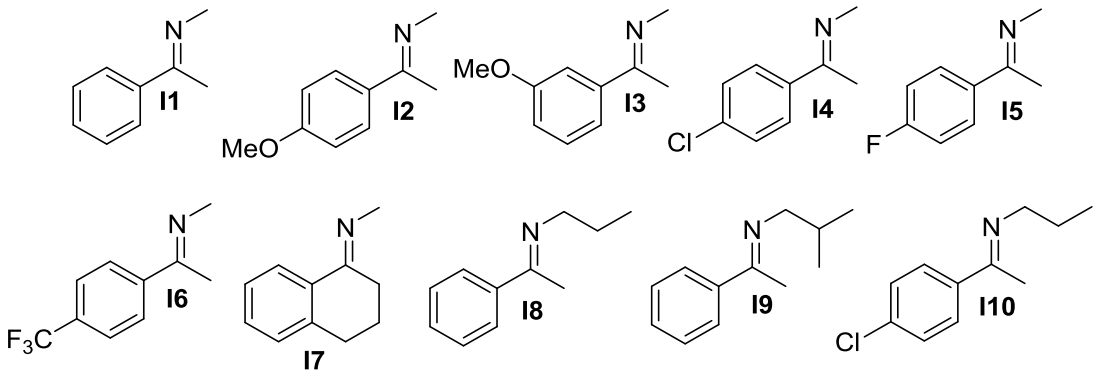

Entry	**imine**	**Temp. (ºC)**	**In situ**	**Cat. 7.10**
1	**I1**	0	92% ee (*S*)	91% ee (*S*)
2	**I2**	r.t.	90% ee (*S*)	91% ee (*S*)
3	**I3**	r.t.	89% ee (*S*)	89% ee (*S*)
4	**I4**	0	95% ee (*S*)	94% ee (*S*)
5	**I5**	–10	94% ee (*S*)	93% ee (*S*)
6	**I6**	–10	93% ee (*S*)	93% ee (*S*)
7	**I7**	–10	90% ee (*S*)	89% ee (*S*)
8	**I8**	0	93% ee (*S*)	92% ee (*S*)
9	**I9**	–10	94% ee (*S*)	93% ee (*S*)
10	**I10**	–10	93% ee (*S*)	94% ee (*S*)

a) Full conversion was obtained in all cases. b) Temperatures are the same as in the hydrogenations in Figure 10. c) Conversion was determined by ^{1}H NMR analysis of the crude reaction mixture. d) Unless otherwise noted, the ee value was determined by HPLC or GC analysis of the corresponding trifluoroacetamides on a chiral stationary phase.

As shown in Table 4 the results are practically the same. This proves that catalyst **7.10** is a viable option as an iridacycle-catalyst for the hydrogenation of *N*-alkyl imines.

7.5. Model for the Hydride Transfer stereodetermining step

In the same manner as with *N*-aryl imines in Chapter 6, Norrby and co-workers's model can predict the stereochemical outcome for the reduction of *N*-alkyl imines with Ir-MaxPHOX iridacycles.[8]

In Figure 13 we depict the two possible iminium cation approaches to the reacting site for the hydride transfer. The iminium cation approach that yields the major enantiomer is favored by a π– π interaction (Figure 13, **in green**) that is not present in the TS that yields the minor enantiomer. There is an interaction between the phenyl group of the iminium cation (C–Ph) and the bulky oxazoline that causes additional steric strain for the *S* product yielding approach (Figure14, **in red**). On the other hand, for the *R* product yielding approach (Figure14) the methyl group of the iminium carbon is oriented towards the oxazoline and the steric strain is lesser. Norrby and co-workers, who designed the model for *N*-aryl imines, claim that there is a favorable π–CH interaction between the iminium cation's phenyl group (N–Ph) and the iPr group of the oxazoline. This interaction is obviously not possible for *N*-alkyl imines.

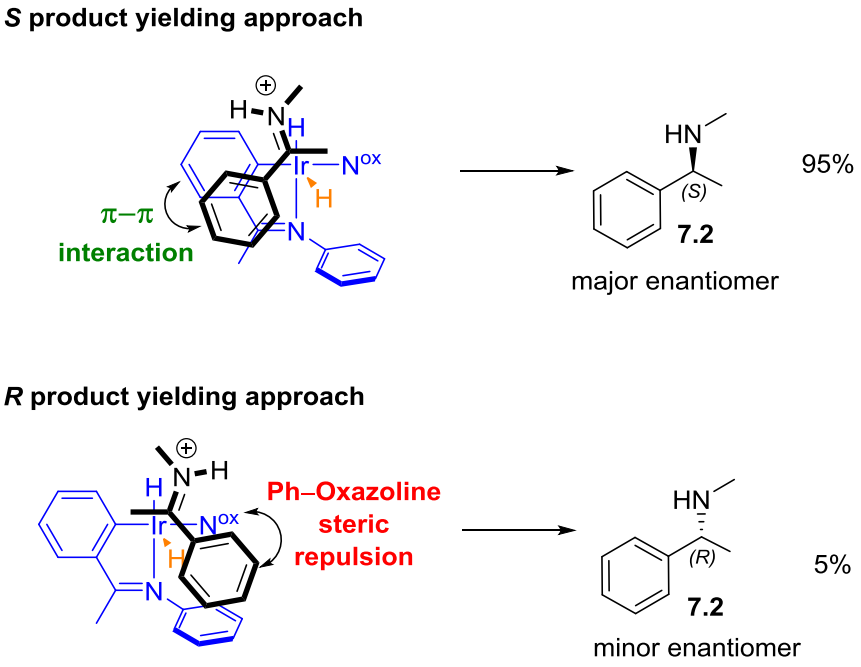

Figure 13. *Model for the Hydride Transfer transition state for Ir-MaxPHOX iridacycle (**ent-1iPr+A0**) in which the stereochemistry of the reduced product is defined. The hydride transferred to the substrate is highlighted in orange. Positive interactions are highlighted in green and negative in red. The enantiomeric ratio corresponds to a catalysis in CH_2Cl_2, at 3 bar of H_2, r.t. with 1 mol% of catalyst **7.10**.*

The model proposed for the Hydride Transfer TS is in agreement with our experimental results when employing catalyst **7.10** for the hydrogenation of *N*-alkyl imine **I1**.

7.6. Conclusions

We successfully hydrogenated with full conversions and excellent ee's different challenging *N*-alkyl imines. To do so, it was crucial to take into consideration the importance of the imine-iridacycles in the hydrogenation of imines. By using acetophenone *N*-phenylimine as an additive, we were able to form a proper iridacycle in situ that could catalyze the reduction of *N*-alkyl imines and overcome the catalyst deactivation issue. With this methodology, we studied the scope of the reaction with different *N*-alkyl imines (Figure 10).

In order to obtain a more robust and practical methodology, we aimed for a new iridacyle-catalyst that could be isolated, stored and used directly in a catalytic hydrogenation. We looked for an ideal ligand that could stabilize the iridacycle and at the same time be labile enough to allow the catalysis to happen. We found in ethylene the perfect match to our needs. We managed to isolate an air-stable iridacycle and studied its scope with different *N*-alkyl ketimines. The results obtained with **7.10** are at the same level to the ones obtained by performing the reaction in situ (Table 4). To the best of our knowledge, the results obtained in terms of conversion and ee are the best in the direct asymmetric hydrogenation of *N*-alkyl imines so far. We believe this new kind of iridacycle-catalyst holds a great potential.

Finally, we applied Norrby's model to predict the reaction's stereochemical outcome. The experimental results are in agreement to the model's prediction.

7.7. References

[1] K. H. Hopmann, A. Bayer, *Coord. Chem. Rev.* **2014**, *268*, 59–82.

[2] N. Fleury-Brégeot, V. de la Fuente, S. Castillón, C. Claver, *ChemCatChem* **2010**, *2*, 1346–1371.

[3] J. H. Xie, S. F. Zhu, Q. L. Zhou, *Chem. Rev.* **2011**, *111*, 1713–1760.

[4] P. Schnider, G. Koch, R. Pretot, G. Wang, F. M. Bohnen, C. Kriiger, A. Pfaltz, *Chem. Eur. J.* **1997**, *3*, 887–892.

[5] V. N. Wakchaure, P. S. J. Kaib, M. Leutzsch, B. List, *Angew. Chem. Int. Ed. Engl.* **2015**, *54*, 11852–6.

[6] X. Verdaguer, U. E. W. Lange, M. T. Reding, S. L. Buchwald, *J. Am. Chem. Soc.* **1996**, *118*, 6784–6785.

[7] Y. Schramm, F. Barrios-Landeros, A. Pfaltz, *Chem. Sci.* **2013**, *4*, 2760.

[8] B. Tutkowski, S. Kerdphon, E. Limé, P. Helquist, P. G. Andersson, O. Wiest, P. O. Norrby, *ACS Catal.* **2018**, *8*, 615–623.

Chapter 8

Highly Enantioselective Iridium-Catalyzed Hydrogenation of Cyclic Enamides

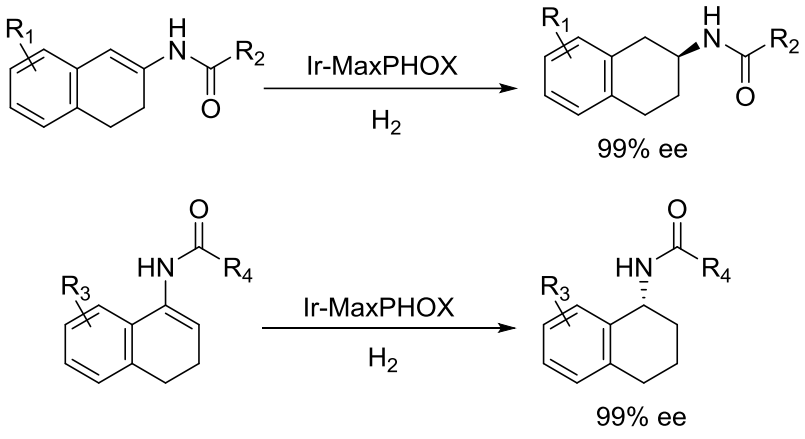

E. Salomó, S. Orgué, A. Riera, X. Verdaguer, *Angew. Chem. Int. Ed.* **2016**, *55*, 7988–7992

8.1. Introduction: Catalytic asymmetric hydrogenation of cyclic α- and β-enamides

As we explained in previous chapters, chiral amines are present in many relevant substrates. Among the different routes to obtain these structures, asymmetric hydrogenation of enamides is a well stablished method. In this Chapter we focused in the reduction of cyclic both α- and β-enamides, which are challenging substrates to hydrogenate selectively. Nevertheless, they are very interesting as they can afford valuable substrates such as Rotigotine,[1] Terutroban,[2] Nepicastat[3] or Robalzotan[4] among others.

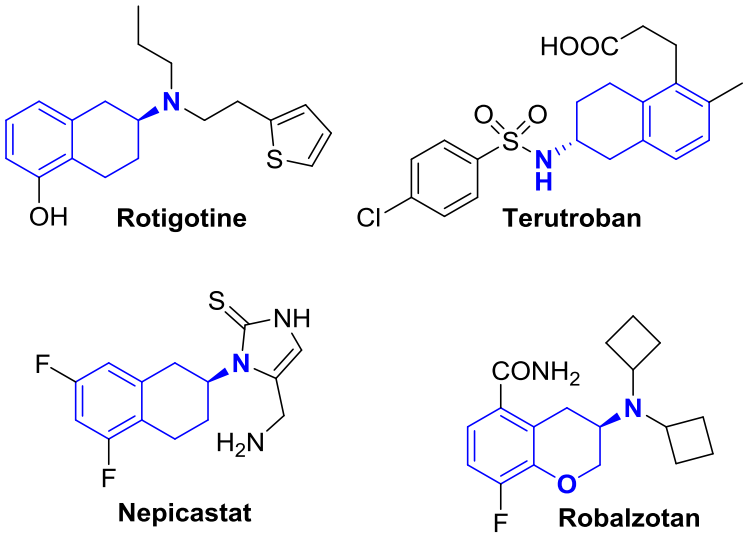

Figure 1. *Some relevant chiral amines derived from cyclic β-enamides.*

Usually the hydrogenation of these substrates has been attempted with Rh or Ru catalysts.[5–9] However, in the present Chapter we are reporting the reduction of these compounds with our Ir-MaxPHOX catalysts.

8.2. Synthesis of cyclic enamides

8.2.1. Synthesis of cyclic α-enamides

To synthesize cyclic α-enamides we applied two different methodologies. In Route A initially an oxime is formed by treating the corresponding ketone with

hydroxylamine, which reacts in a nearly quantitatively manner. The second step consists in a reductive acylation with Ac_2O and a reducing agent. The reducing agents can be for instance $Cr(OAc)_2$, $Ti(OAc)_3$ or Fe, being this last one in fact the most commonly employed.[10–15] The procedure, although effective, requires high temperatures and iron, which makes the process tedious and not practical as large quantities of inorganic salts must be removed with a slow filtration. As an alternative to this procedure, Reeves and co-workers presented Route B, which is a 3-step one-pot procedure.[16] First the imine is formed, aided by $Ti(OiPr)_4$. The titanium compound captures the H_2O formed during the imine formation and shifts the equilibrium towards the imine. This reaction can be carried on at room temperature. Then by using base and acetic anhydride, the enamide is readily formed. The major problem with this methodology is the formation of insoluble titanium oxides. Reeves and co-workers employed EDTE (Figure 2) to overcome this setback. EDTE coordinates with titanium and forms a water-soluble complex that can be removed with a simple aqueous wash during the work-up, thus avoiding a problematic filtration.

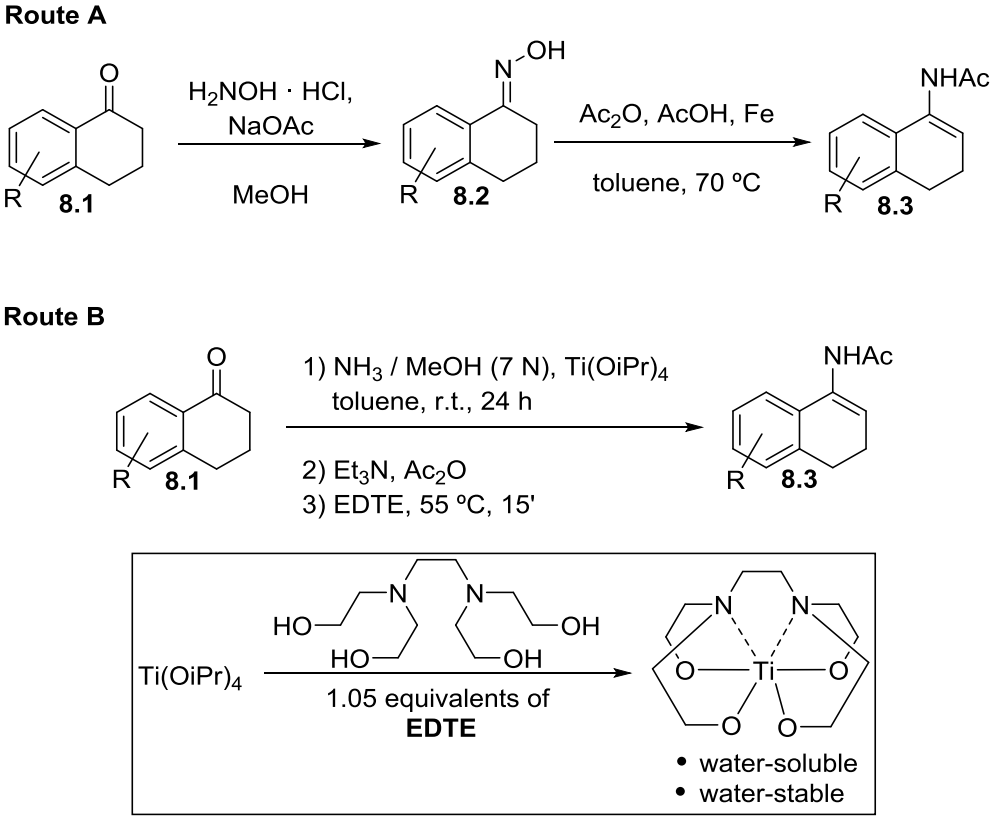

Figure 2. *Synthesis of cyclic α-enamides.*

8.2.2. Synthesis of cyclic β-enamides

To synthesize cyclic β-enamides we used the methodology depicted in Figure 3.[5,17] The tetralone is reacted with an amide (*p*-TsOH as acid catalyst) in toluene at reflux. It is necessary to employ a Dean-Stark system so the water produced can be removed and the equilibrium shifts to the enamides.

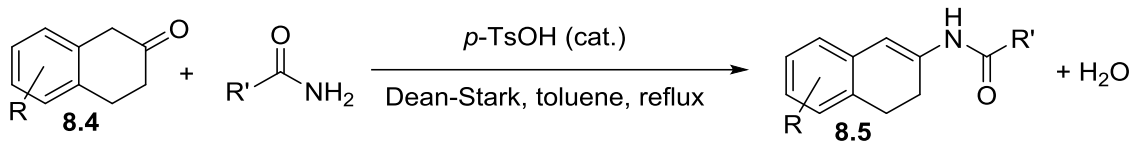

Figure 3. *Synthesis of cyclic* β*-enamides.*

Both cyclic α- and β-enamides have to be very pure so the catalyses proceed as well as possible. The enamides can be purified by flash SiO_2 column. Nevertheless, a second purification by crystallization is often required.

8.3. Enamide hydrogenation with Ir-MaxPHOX

8.3.1. Catalyst screening

We have employed the Ir-MaxPHOX catalysts in Figure 4 for this study. At that time, we had only synthesized the 8 catalysts depicted in Figure 4 (**2Ph**, **3Ph**, **2*t*-Bu** and **3*t*-Bu** had yet to be synthesized). As we will explain in the present Section we did not consider necessary to synthesize any other Ir-MaxPHOX for this study because we had already found two excellent catalysts among these 8 complexes.

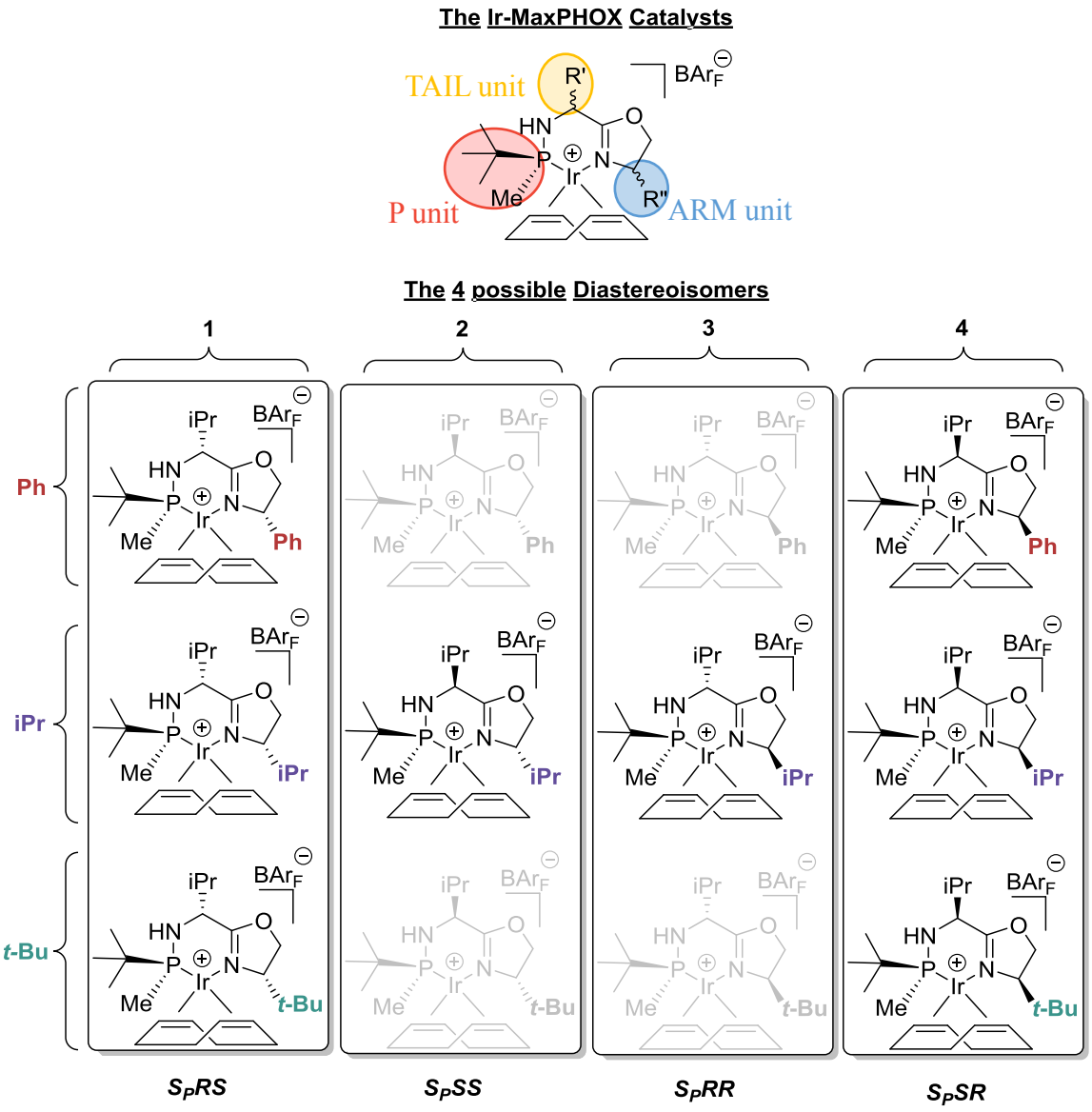

Figure 4. *A small library of Ir-MaxPHOX catalysts. Each column contains catalysts with the same configuration. Each row contains catalysts with the same substituents.*

The 8 different Ir-MaxPHOX complexes in Figure 4 were tested on model substrate cyclic β-enamide **8.6**. The reactions were conducted with 1 mol% of MaxPHOX catalyst, at 55 bar of H_2 pressure at room temperature in CH_2Cl_2 overnight. The results obtained are summarized in Figure 5.

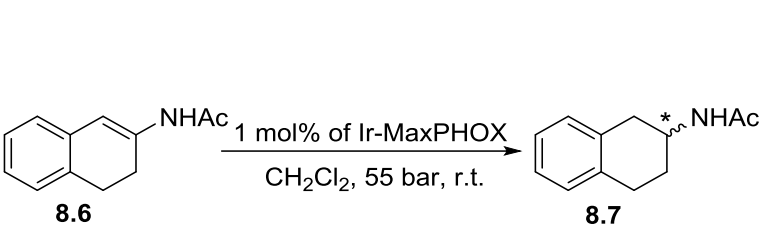

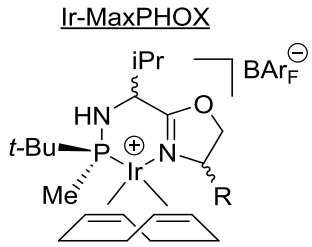

R	Ir-MaxPHOX Catalysts			
	S*P*RS	***S*P*SS***	***S*P*RR***	***S*P*SR***
	1	**2**	**3**	**4**
Ph	58% (*S*)			94% (*S*)
iPr	3% (*R*)	67% (*S*)	96% (*S*)	97% (*S*)
***t*-Bu**	75% (*R*)			99% (*S*)

R	S	ee(%)
		0–25
		25–50
		50–75
		75–100

Figure 5. *Ee values for the hydrogenation of* ***8.6****. Screening for the best Ir-MaxPHOX catalyst. Conversion was complete for all cases.*

The best results were obtained with catalysts **4iPr** and **4*t*-Bu** (97% and 99% ee, respectively). Although results with catalyst **4*t*-Bu** are slightly better, it has to be taken into account that **4iPr** is much more economic to produce.

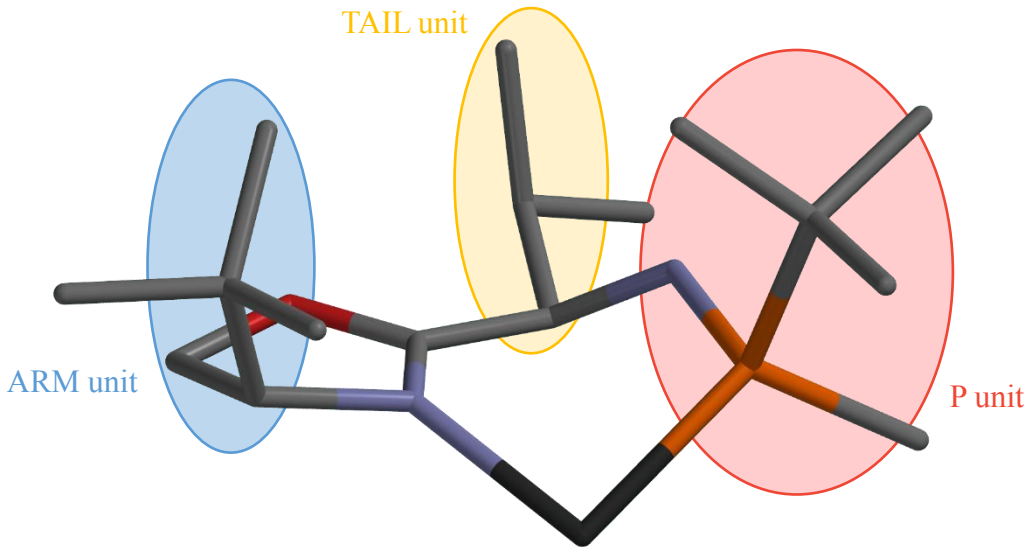

Figure 6. *Partial image of an X-Ray of catalyst* ***4t-Bu****. All substituents (ARM, TAIL and P-unit) are facing the same side of the Ir-ligand six membered chelate.*

If we focus on the four **iPr** complexes (**1iPr-4iPr**) we can observe that for **1iPr** we obtain nearly a racemic product and the ee increases as we advance towards **4iPr** configuration, for which the control over the ee is nearly total (ee = 97%). We can explain this phenomenon with a match/mismatch effect. It seems that for **4iPr** all 3 substituents (ARM, TAIL and P-unit) are directed towards the same side of the six membered iridium-ligand chelate (Figure 6) and work towards the formation of the same enantiomer. However, **3iPr**'s TAIL unit is oriented contrary to the two other substituents. The TAIL unit is further away from the Ir-reacting site and its mismatch effect is small (from 97% to 96% ee). Catalyst **2iPr** has the ARM unit aimed contrary to the two other units (TAIL and P-unit). As the ARM is closer to the reacting site than the TAIL, it has a bigger impact on the ee. This would explain the lower ee for **2iPr** compared to **3iPr** (67% and 96% respectively). Finally, **1iPr** has the ARM and TAIL units oriented contrary to the P-unit. This mismatch effect causes the reduced product to be obtained in a nearly racemic manner (ee = 3%). For this configuration, ***S*ₚ*RS***, bigger substituents at the ARM position (*t*-Bu for **1*t*-Bu**) causes the ee to increase towards the *R* enantiomer, while smaller substituents (Ph for **1Ph**) affords mainly the *S* reduced product. We understand that the ARM and the TAIL units for complexes with ***S*ₚ*RS*** configuration induce the formation of the *R* enantiomer. Thus, having bulkier substituents in these positions (**1*t*-Bu**) causes the ee to increase in that direction, while having smaller substituents (**1Ph**) in these positions makes the influence of the P-unit more relevant, shifting the selectivity back towards the *S* configuration. This same phenomena happens with configuration ***S*ₚ*SR***. However, for this configuration we have a match situation and all substituents work towards the formation of the same enantiomer (the *S* enantiomer). That is why having bulkier substituents cause the selectivity to increase towards the *S* enantiomer (**4Ph** < **4iPr** < **4*t*-Bu**, 94% < 97% < 99% ee's respectively).

The approach we took for the reduction of cyclic α-enamides is analogous. We tested the 8 Ir-MaxPHOX catalysts on model substrate **8.8**. We found in **4iPr** and **4*t*-Bu** our best options (95% and 97% ee, respectively).

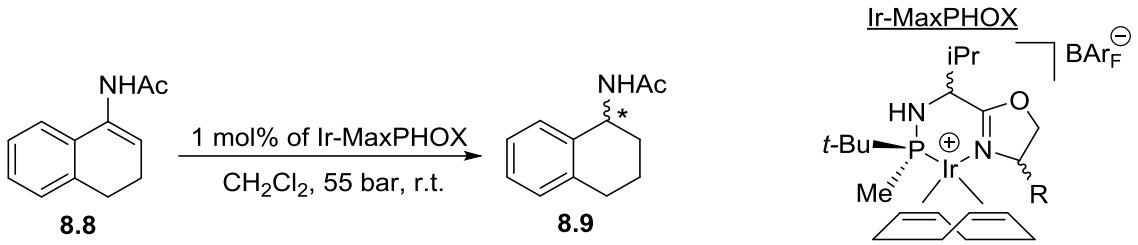

R	Ir-MaxPHOX Catalysts			
	S*ₚ*RS	***S*ₚ*SS***	***S*ₚ*RR***	***S*ₚ*SR***
	1	**2**	**3**	**4**
Ph	87% (*S*)			87% (*R*)
iPr	82% (*S*)	Conv. 87% 67% (*R*)	78% (*R*)	95% (*R*)
***t*-Bu**	Conv. 95% 33% (*S*)			97% (*R*)

R	S	ee(%)
		0–25
		25–50
		50–75
		75–100

Figure 7. *Ee values for the hydrogenation of* ***8.8****. Screening for the best Ir-MaxPHOX catalyst. Conversion was complete for all cases.*

In this experiment, we again observe a match/mismatch effect. Apparently, the ARM and the P-unit of the catalysts with configuration ***S*ₚ*SR*** work towards the formation of the same enantiomer. That is why the bulkier the substituent in the arm position, the higher the ee obtained for the reduced product (**4Ph** < **4iPr** < **4*t*-Bu**, 87% < 95% < 97% ee's respectively). However, again the ee's decrease and shift towards the other enantiomer (*S*) as we advance to the left in Figure 7. The configuration ***S*ₚ*RS*** affords the product with the opposite configuration (*S*). Nevertheless, for these 3 catalysts the bulkiness of the ARM substituent negatively affects the products selectivity (**1Ph** > **1iPr** > **1*t*-Bu**, 87% < 82% < 33% ee's respectively).

8.3.2. Influence of H2 pressure and solvent

In Table 1 we report the most important results for the optimization of the hydrogenation of **8.6** with Ir-MaxPHOX catalysts. We did not optimize the reaction with Ir-MaxPHOX **4*t*-Bu** as we already obtained complete conversion and control over the ee with it.

We studied the reduction of **8.6** at different H_2 pressures: 55, 10 and 3 bars. We observed that as the H_2 pressure decreases, the ee increases. We studied different solvents: CH_2Cl_2, EtOAc, MeOH and THF. We observed that at 3 bars all solvents but THF afforded the reduced product with complete control over the ee. Nevertheless, the conversion w not complete in MeOH. We were particularly pleased to observe that the reaction at low H_2 pressures (3 bar) in EtOAc is completely enantioselective (Entry 6), as EtOAc is more environmentally friendly than CH_2Cl_2.

Table 1. Influence of H_2 pressure and solvent with **4iPr** on the hydrogenation of **8.6**

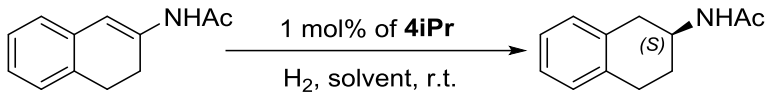

8.6 **8.7**

Entry	**Solvent**	**H_2 (bar)**	**Conv. (%)**	**ee (%)**
1	CH_2Cl_2	55	100	97 (*S*)
2	CH_2Cl_2	10	100	99 (*S*)
3	CH_2Cl_2	3	100	99 (*S*)
4	EtOAc	55	100	95 (*S*)
5	EtOAc	10	100	96 (*S*)
6	EtOAc	3	100	99 (*S*)
7	MeOH	55	100	96 (*S*)
8	MeOH	10	100	99 (*S*)
9	MeOH	3	96	99 (*S*)
10	THF	55	100	95 (*S*)
11	THF	10	100	94 (*S*)
12	THF	3	100	95 (*S*)

a) Conversion was determined by ^{1}H NMR analysis of the crude reaction mixture. b) The ee value was determined by HPLC analysis on a chiral stationary phase.

In Table 2 we report the most important results for the optimization of the hydrogenation of **8.1** with catalysts Ir-MaxPHOX **4iPr** and **4*t*-Bu**. We studied the reduction with both **4iPr** and **4*t*-Bu** Ir-MaxPHOX catalysts. We carried on the reaction at 3 bars of H_2, because we have observed (Table 1) that the ee increases as the H_2 pressure is lowered. The reaction in CH_2Cl_2 afforded complete control over the selectivity with both catalysts (Entries 1 and 5). Opposite to what we observed in Table 1, EtOAc is not a good solvent for this particular substrate. Conversions in EtOAc and in THF were very low (Entries 2, 4, 6 and 8). On the other hand, the reaction in MeOH affords excellent selectivity for both Ir-MaxPHOX catalysts (Entries 3 and 7). However, conversion is not complete in either reaction. We believe the low conversions observed with solvents other than CH_2Cl_2 are due to the poor solubility of the enamide **8.8** in these.

Table 2. Influence of solvent with **4iPr** or **4*t*-Bu** on the hydrogenation of **8.8**

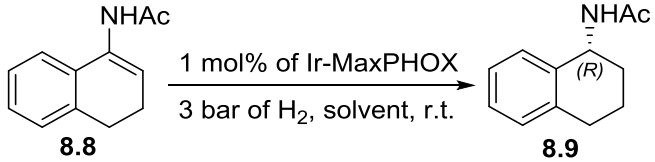

8.8 **8.9**

Entry	**Solvent**	**Ir-MaxPHOX**	**Conv. (%)**	**ee (%)**
1	CH_2Cl_2	**4iPr**	99	99
2	EtOAc	**4iPr**	15	--
3	MeOH	**4iPr**	93	99
4	THF	**4iPr**	25	--
5	CH_2Cl_2	**4*t*-Bu**	99	99
6	EtOAc	**4*t*-Bu**	15	--
7	MeOH	**4*t*-Bu**	62	98
8	THF	**4*t*-Bu**	25	--

a) Conversion was determined by ^{1}H NMR analysis of the crude reaction mixture. b) The ee value was determined by HPLC or GC analysis on a chiral stationary phase.

8.3.3. Reaction scope

In Table 3 we wanted to study the scope for the Ir-MaxPHOX catalysts on the reduction of cyclic α- and β-enamides. Each studied enamide had to be approached

differently. By optimizing the H_2 pressure, the solvent and selecting either catalyst **4iPr** or catalyst **4*t*-Bu**, we managed to obtain full conversion and attained complete control over the ee for all the substrates.

Table 3. Reaction scope for different cyclic α- or β-enamides

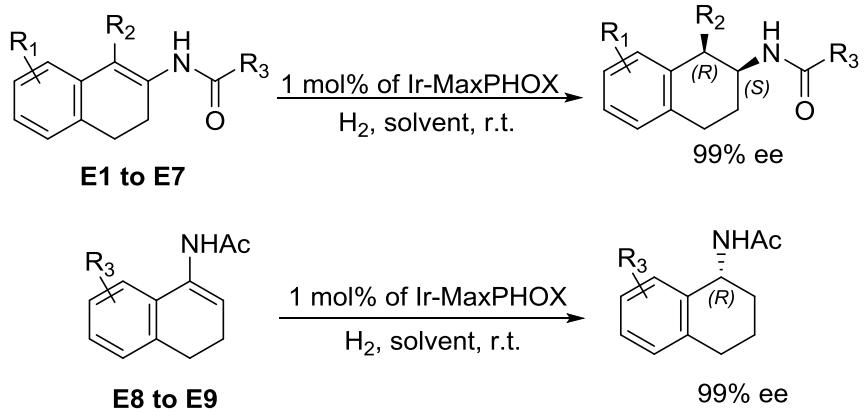

enamides (E1-E9):

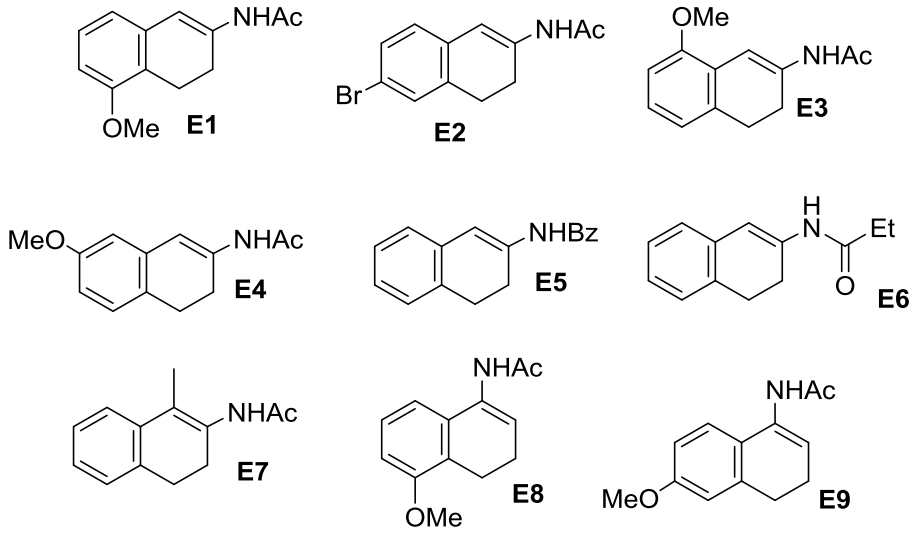

Entry	Enamide	Ir-MaxPHOX	Solvent	H_2 (bar)	Conv. (%)	ee (%)
1	**E1**	**4*t*-Bu**	CH_2Cl_2	55	100	99 (*S*)
2	**E1**	**4iPr**	CH_2Cl_2	55	80	99 (*S*)
3	**E1**	**4iPr**	MeOH	3	94	99 (*S*)
4	**E1**	**4iPr**	EtOAc	3	100	99 (*S*)
5	**E2**	**4*t*-Bu**	CH_2Cl_2	55	100	99 (*S*)

6	**E2**	**4iPr**	CH_2Cl_2	55	100	97 (*S*)
7	**E2**	**4iPr**	CH_2Cl_2	3	100	82 (*S*)
8	**E2**	**4iPr**	MeOH	3	0	--
9	**E2**	**4iPr**	EtOAc	3	100	99 (*S*)
10	**E3**	**4*t*-Bu**	CH_2Cl_2	55	100	99 (*S*)
11	**E3**	**4iPr**	CH_2Cl_2	55	100	97 (*S*)
12	**E3**	**4iPr**	CH_2Cl_2	3	100	99 (*S*)
13	**E3**	**4iPr**	EtOAc	3	100	99 (*S*)
14	**E4**	**4*t*-Bu**	CH_2Cl_2	55	100	96 (*S*)
15	**E4**	**4*t*-Bu**	CH_2Cl_2	3	100	99 (*S*)
16	**E4**	**4iPr**	CH_2Cl_2	55	100	95 (*S*)
17	**E4**	**4iPr**	CH_2Cl_2	3	100	99 (*S*)
18	**E4**	**4iPr**	MeOH	3	83	n.d.
19	**E4**	**4iPr**	EtOAc	3	100	99 (*S*)
20	**E5**	**4*t*-Bu**	CH_2Cl_2	55	100	93 (*S*)
21	**E5**	**4iPr**	CH_2Cl_2	55	100	92 (*S*)
22	**E5**	**4*t*-Bu**	CH_2Cl_2	3	100	99 (*S*)
23	**E5**	**4iPr**	CH_2Cl_2	3	100	99 (*S*)
24	**E6**	**4*t*-Bu**	CH_2Cl_2	3	100	99 (*S*)
25	**E7**	**4*t*-Bu**	CH_2Cl_2	55	100	82 (*S*)
26	**E7**	**4*t*-Bu**	CH_2Cl_2	3	100	99 (*S*)
27	**E8**	**4*t*-Bu**	CH_2Cl_2	55	100	88 (*R*)
28	**E8**	**4*t*-Bu**	CH_2Cl_2	3	100	98 (*R*)
29	**E8**	**4*t*-Bu**	EtOAc	3	100	99 (*R*)
30	**E9**	**4*t*-Bu**	CH_2Cl_2	55	100	89 (*R*)
31	**E9**	**4iPr**	CH_2Cl_2	55	100	19 (*R*)
32	**E9**	**4*t*-Bu**	CH_2Cl_2	3	100	99 (*R*)

a) The best result for each substrate is highlighted in yellow. b) Conversion was determined by ^{1}H NMR analysis of the crude reaction mixture. c) The ee value was determined by HPLC or GC analysis on a chiral stationary phase.

β-enamide **E1** was obtained with 99% ee in Entries 1, 2, 3 and 4. However, the conversion in CH_2Cl_2 is not complete at high pressures with catalyst **4iPr**. That is why we studied EtOAc and MeOH as alternative solvents. We were pleased to discover that at 3 bars the conversion is complete in both solvents. In Entries 5 to 9 we studied enamide **E2**. We achieved full control over the ee with catalyst **4*t*-Bu** in CH_2Cl_2. Nevertheless, reaction in EtOAc at 3 bars of H_2 also afforded complete control over the selectivity and in comparison this is a milder and more convenient reaction. Enamide **E3** was hydrogenated with 99% ee when employing catalyst **4*t*-Bu** in CH_2Cl_2 at 55 bar of pressure and also when conducting the reaction at 3 bar of H_2, both in CH_2Cl_2 and EtOAc (Entries 10 to 13). **E4** was reduced with 99% ee when using either catalyst **4iPr** or **4*t*-Bu** in CH_2Cl_2 at 3 bar of pressure (Entries 15 and 17). Also, in EtOAc at 3 bar of H_2 and with catalyst **4iPr** (Entry 19). For cyclic β-enamide **E5** (Entries 20 to 23) the reduced product was obtained with 99% ee for both catalysts at 3 bar of pressure in CH_2Cl_2. Other solvents were not tested as we believe that with the previous hydrogenated substrates we had provided with enough evidence to consider EtOAc and in some cases MeOH as viable solvents. **E6** was reduced with complete control over the ee with catalyst **4*t*-Bu** in CH_2Cl_2 at 3 bar of pressure (Entry 24). Enamide **E7** contains a tetrasubstituted double bond which makes the asymmetric catalysis more difficult. When hydrogenating **E7** two vicinal stereocenters are formed. Although only the *cis* isomer is formed, the ee for it with catalyst **4*t*-Bu** at 55 bar of H_2 is inferior to what we expected (Entry 25). However, we observed that decreasing the pressure has a huge positive impact on the ee; at 3 bar of pressure, the ee increased from 82% to 99% (Entry 26).

Although there are some good results reported in the literature on the asymmetric hydrogenation of either α- or β-enamides, so far no one has managed to reduce both type of substrates with good selectivities with the same catalytic system. We were pleased to see that with the Ir-MaxPHOX catalysts (Ir-MaxPHOX **4*t*-Bu**) we could attain a good control over the ee in the asymmetric reduction of either α- or β-enamides. When employing catalyst **4*t*-Bu** at 3 bar of H_2 in CH_2Cl_2, **E8** was reduced with 88% of ee (Entry 27). When the reduction was conducted at 3 bar, the ee increased to 98% (Entry 28). When the reaction was carried on in EtOAc the control over the ee was complete (Entry 29). Another example would be the reduction of the α-cyclic enamide **E9**. At 55 bar of H_2 in CH_2Cl_2, catalysts **4*t*-Bu** and **4iPr** afforded the reduced product with 89% and 19%

ee. We focused in catalyst **4*t*-Bu** and we observed that when reducing the pressure down to 3 bar the product amide was obtained with 99% ee.

Besides the cyclic α- and β-enamides reported in Table 3 we studied other substrates containing the enamide moiety. However, the results obtained were not as good. Although substrate **E10** is very similar to the cyclic β-enamides hydrogenated so far, no good control over the ee was achieved with any of the studied Ir-MaxPHOX (Entries 1 to 4). Enamide **E11** is a five-membered ring cyclic enamide for which the control over the ee was not good at high pressures (Entry 5) and at low H_2 pressure the conversion was very low (Entry 6). Enamide **E12** is derived from the 4-chromanone. Although it is very similar to the cyclic α-enamides hydrogenated so far, it seems that the substitution of a CH_2 by an O atom has a huge impact on the catalysis because the ee's obtained were low (Entry 7). Enamide **E13** which should be highly reactive (1,1-disubstituted double bond) was reduced at high pressures with only 81% conversion. Moreover, the ee obtained was low (34%). Finally, enamides **E14**, **E15** and **E16**, which afforded excellent results in the hydrogenation with Rh-MaxPHOS, did not react at all with Ir-MaxPHOX.[18] It seems that the CO_2Me group affects negatively the catalysis with Ir-MaxPHOX.

Table 4. Reaction scope for different enamides

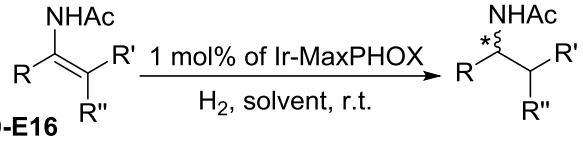

E10-E16

Enamides:

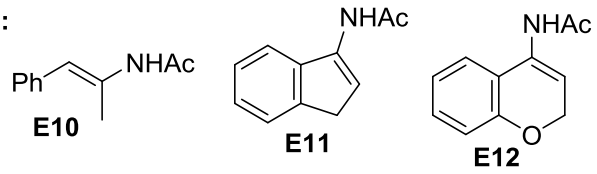

E10

E11

E12

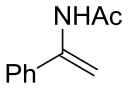

E13

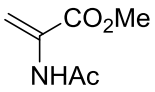

E14

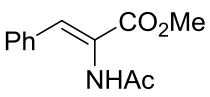

E15

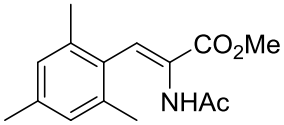

E16

Entry	**enamide**	**Ir-MaxPHOX**	**Solvent**	**H_2 (bar)**	**Conv. (%)**	**ee (%)**
1	**E10**	**1iPr**	CH_2Cl_2	55	100	1
2	**E10**	**2iPr**	CH_2Cl_2	55	83	11
3	**E10**	**3iPr**	CH_2Cl_2	55	100	17
4	**E10**	**4iPr**	CH_2Cl_2	55	100	6
5	**E11**	**4*t*-Bu**	CH_2Cl_2	55	100	69
6	**E11**	**4*t*-Bu**	CH_2Cl_2	3	20	n.d.
7	**E12**	**4*t*-Bu**	CH_2Cl_2	55	100	8
8	**E13**	**4iPr**	CH_2Cl_2	55	81	34
9	**E14**	**4iPr**	CH_2Cl_2	55	0	--
10	**E15**	**4iPr**	CH_2Cl_2	55	0	--
11	**E16**	**4iPr**	CH_2Cl_2	55	0	--

a) Conversion was determined by ^1H NMR analysis of the crude reaction mixture. b) The ee value was determined by HPLC or GC analysis on a chiral stationary phase.

8.4. Mechanistic considerations

As we have previously mentioned, the hydrogenation of enamides such as the ones studied in this Chapter has usually been attempted with Rh or Ru catalysts. Ir-P*,N

catalysts such as the ones we have employed (Ir-MaxPHOX) are not the usual choice. Consequently, the knowledge on the mechanism for the catalysis is limited.

Bolm reported in 2016 a mechanism for the hydrogenation of α,β-unsaturated ketones with Ir-P,N catalysts (Figure 8), which is the closest mechanistic study we could find in the literature.[19] Although there are obvious differences, we believe that the mechanism for the hydrogenation of cyclic α- or β-enamides with the Ir-MaxPHOX catalysts share a key feature such as the coordination of the carbonyl moiety to the metal center that directs the alkene coordination.

Bolm's mechanism depicts the octahedral complex **I** (Figure 8) which has the unsaturated ketone coordinated in a bidentate manner. Both the olefin and the carbonyl of the ketone are coordinated *cis* to the P unit. Then, via two migratory insertions of the hydride *trans* to the P atom, we obtain the reduced ketone. First, there is a hydride insertion to the β position and secondly to the α position.

While the accepted mechanism for the Ir catalyzed hydrogenation of non-functionalized olefins predicts that the double bond coordination happens *trans* to the phosphorous, in this case the reaction seems to occur with the alkene coordinated *cis* to the P and away from the N-ligand. The key step in Bolm's proposed mechanism is the oxidative addition of H_2, that is much more favorable when it occurs *trans* to the phosphine.

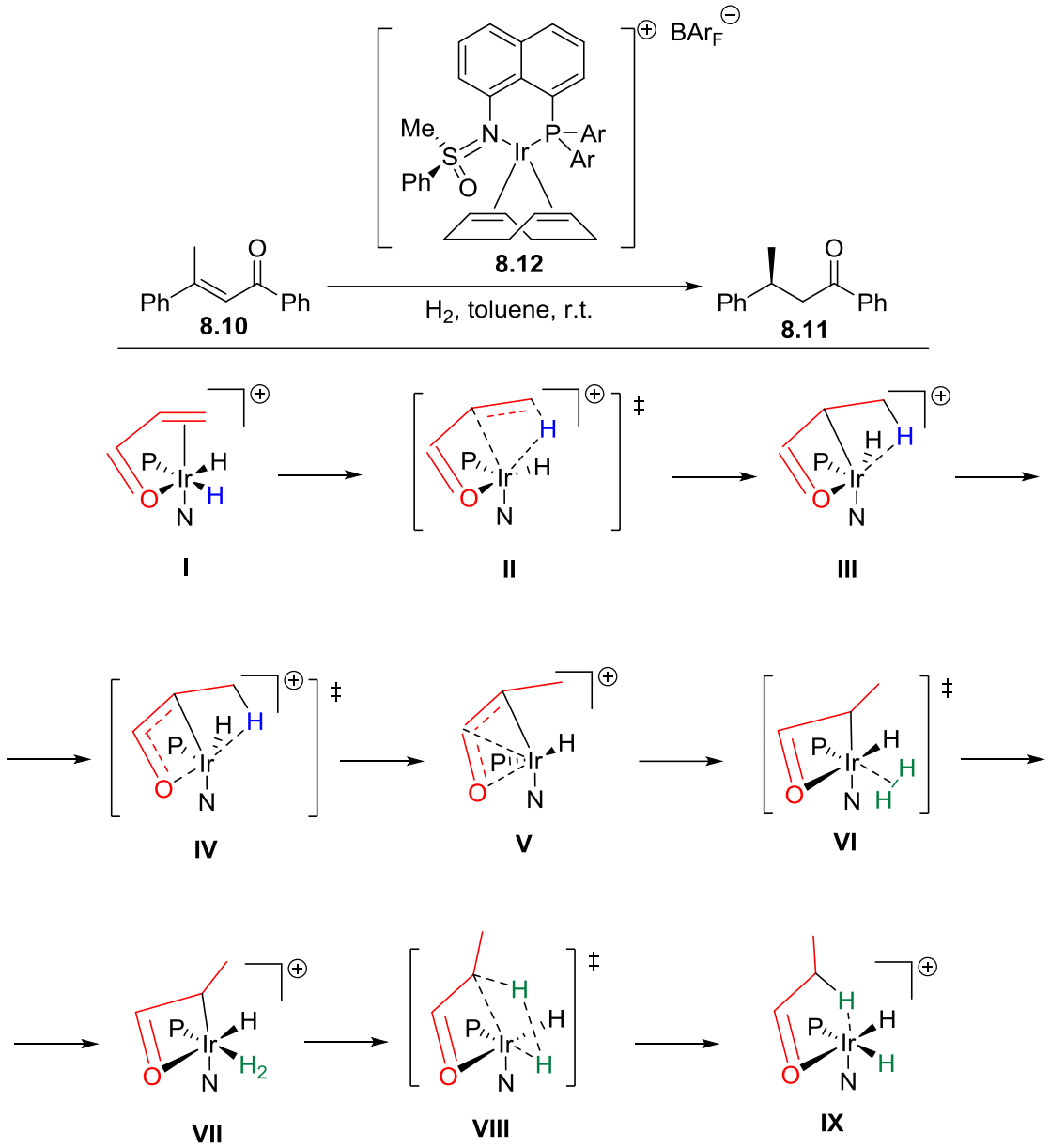

Figure 8. *Bolm's Ir^{III}-mechanism for the hydrogenation of α,β-unsaturated ketones with Ir-P,N catalysts.*

We theorized that the cyclic β-enamides that we have studied in the present Chapter might coordinate to the Ir-MaxPHOX in a similar fashion. We envisioned 4 different ways in which β-enamide **8.6** could coordinate to the metal center (Figure 9). As previously explained (Figure 6), the substituents in catalyst **4*t*-Bu** are all oriented towards the same face of the six-membered ring of the Ir-ligand chelate. As this face is very sterically hindered, we believe that the carbonyl of the β-enamide would coordinate

mainly to the other face away from the *t*-Bu groups. The enamide's double bond could then coordinate *cis* or *trans* to the phosphorous. In either situation the alkene can coordinate though the *pro-S* or the *pro-R* face, depending on how the double bond is oriented. To see which coordination is the preferred one, we calculated the equilibrium geometry for the 4 possibilities with the program Spartan 16 (DFT, RM06 functional with 6-31G* & LANL2DZ basis set). The initial structure for the calculation was extracted from an X-Ray of the catalyst **4*t*-Bu**.

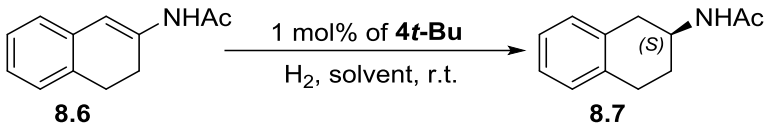

8.6 **8.7**

A) P-*trans* coordination to afford the *S* product

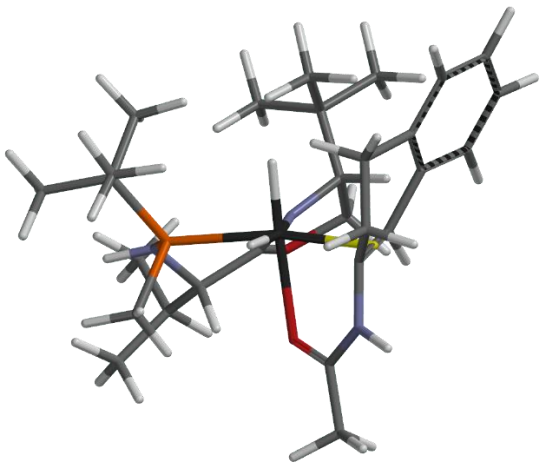

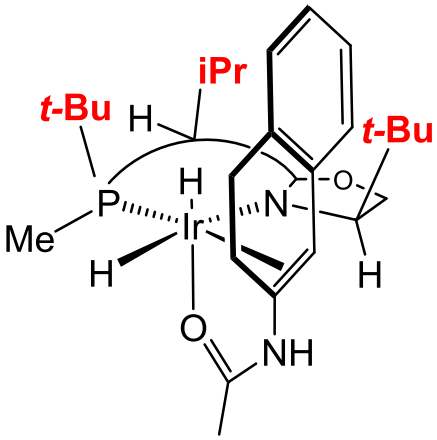

0.0 Kcal / mol

B) P-*trans* coordination to afford the *R* product

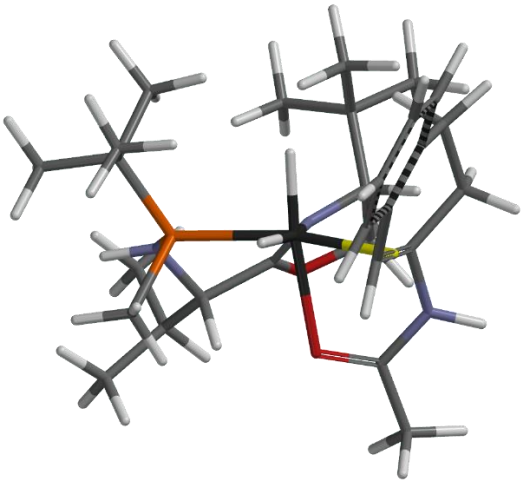

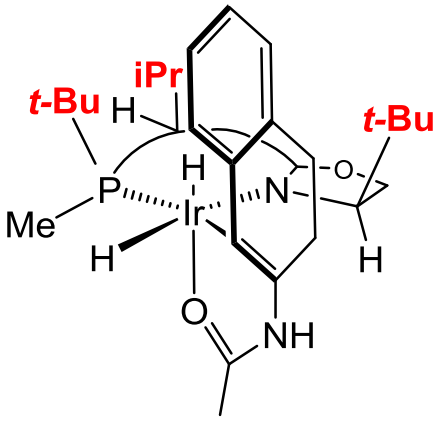

5.37 Kcal / mol

C) P-*cis* coordination to afford the *S* product

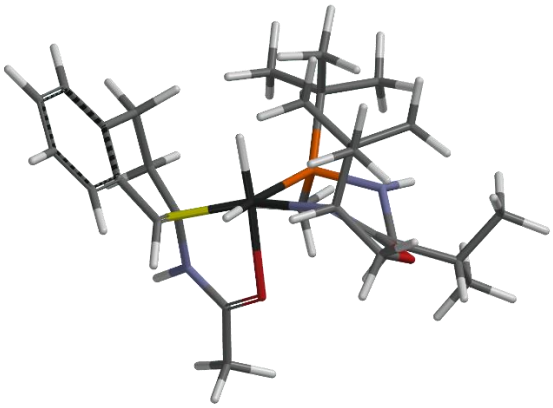

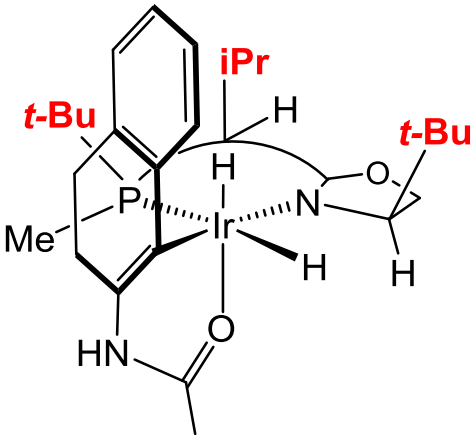

10.57 Kcal / mol

D) P-*cis* coordination to afford the *R* product

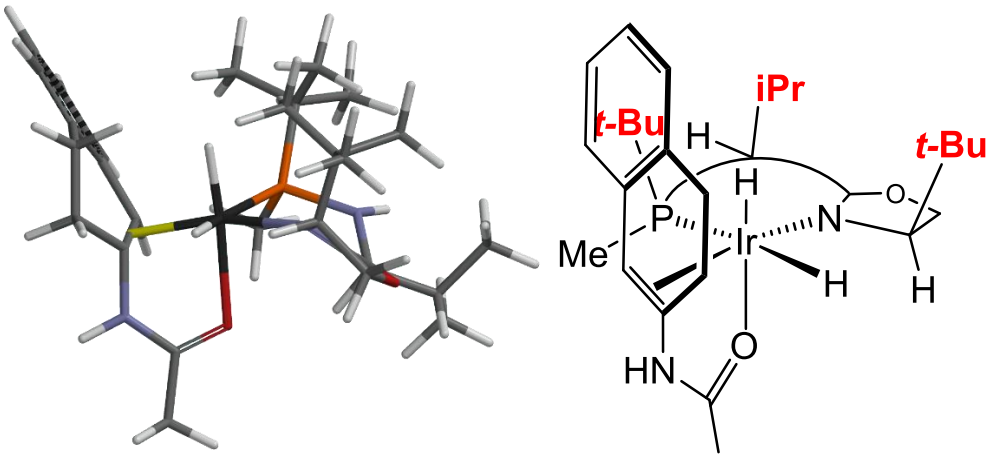

6.30 Kcal / mol

Figure 9. *a) Four different coordinations for the β-enamide–**4t-Bu** complex. b) Calculations were performed with Spartan 16 using RM06 functional with the 6-31G* & LANL2DZ basis set.*

These calculations showed that the alkene prefers to coordinate *trans* to the phosphine in proximity with the oxazoline group. The most favored coordination is the one that leads to the *S* product, which is the one observed experimentally. In this structure, the *t*-Bu group of the oxazoline faces the phenyl ring of the substrate; most probably an attractive π–CH interaction stabilizes this intermediate.

Despite these calculations might suggest that the olefin coordination takes place *trans* to the P and *cis* to the oxazoline, we cannot rule out that, as proposed by Bolm and co-workers, *cis* coordination leads to a more favorable transition state. We encounter a similar situation in Halpern's classic mechanism for the Rh-catalyzed asymmetric hydrogenation.[20] The dependence of the enantioselectivity with the H_2 pressure we found in the present system points also in that direction since lower H_2 pressures provide higher selecitivities, as with the Rh-catalyzed hydrogenation of alkenes, suggesting that H_2 is involved in the stereodetermining step, which should be further along on in the reaction pathway.

8.5. Conclusions

We have shown that the Ir-MaxPHOX catalyst system provides the highest selectivity reported to date for the reduction of cyclic enamides derived from α- and β-tetralones, outperforming Ru and Rh catalysts. These results indicate that iridium catalysts can be also proficient in the reduction of alkenes bearing metal-coordinating groups. For the present system, selectivity was pressure-dependent; in most cases, lowering the hydrogen pressure to 3 bar resulted in an increase in enantioselectivity. Moreover, the process can be carried out in environmentally friendly solvents, such as methanol and ethyl acetate, with no loss of selectivity for most situations.

Bolm reported in 2016 a mechanism for the hydrogenation of α,β-unsaturated ketones with Ir-P,N catalysts. By analogy, we proposed 4 different structures for the coordination of **8.6** with catalyst **4*t*-Bu**. By means of DFT calculations we determined that out of the four, the most stable structure is the one with the enamide coordinated *trans* to the P atom, in a position that would afford the (*S*) reduced product. These facts are in concordance with the results obtained experimentally. In order to be able to state a mechanism, a full computational mechanistic study will be carried out in the near future.

8.6. References

[1] J. J. Chen, D. M. Swope, K. Dashtipour, K. E. Lyons, *Pharmacotherapy* **2009**, *29*, 1452–1467.

[2] J. I. Osende, D. Shimbo, V. Fuster, M. Dubar, J. J. Badimon, *J. Thromb. Haemost.* **2004**, *2*, 492–498.

[3] W. C. Stanley, B. Li, D. W. Bonhaus, L. G. Johnson, K. Lee, S. Porter, K. Walker, G. Martinez, R. M. Eglen, R. L. Whiting, et al., *Br. J. Pharmacol.* **1997**, *121*, 1803–1809.

[4] D. A. Drossman, M. Danilewitz, J. Naesdal, C. Hwang, J. Adler, D. G. Silberg, *Am. J. Gastroenterol.* **2008**, *103*, 2562–2569.

[5] J. L. Renaud, P. Dupau, A.-E. Hay, M. Guingouain, P. H. Dixneuf, C. Bruneau, *Adv. Synth. Catal.* **2003**, *345*, 230–238.

[6] C. Pautigny, C. Debouit, P. Vayron, T. Ayad, V. Ratovelomanana-Vidal, *Tetrahedron: Asymmetry* **2010**, *21*, 1382–1388.

[7] I. Arribas, M. Rubio, P. Kleman, A. Pizzano, *J. Org. Chem.* **2013**, *78*, 3997–4005.

[8] X. Bin Jiang, L. Lefort, P. E. Goudriaan, A. H. M. De Vries, P. W. N. M. Van Leeuwen, J. G. De Vries, J. N. H. Reek, *Angew. Chem. Int. Ed.* **2006**, *45*, 1223–1227.

[9] G. Liu, X. Liu, Z. Cai, G. Jiao, G. Xu, W. Tang, *Angew. Chem. Int. Ed.* **2013**, *52*, 4235–4238.

[10] R. B. Boar, J. F. McGhie, M. Robinson, D. H. R. Barton, D. C. Horwell, R. V. Stick, *J. Chem. Soc. Perkin Trans. 1* **1975**, 1237.

[11] D. H. R. Barton, S. Z. Zard, *J. Chem. Soc. Chem. Commun.* **1985**, 1098.

[12] M. J. Burk, G. Casy, N. B. Johnson, *J. Org. Chem.* **1998**, *63*, 6084–6085.

[13] G. Zhu, A. L. Casalnuovo, X. Zhang, *J. Org. Chem.* **1998**, *63*, 8100–8101.

[14] Z. Hang, C. P. Vandenbossche, S. G. Koenig, S. P. Singh, R. P. Bakale, *Org. Lett.* **2008**, *10*, 505–507.

[15] Z. H. Guan, Z. Y. Zhang, Z. H. Ren, Y. Y. Wang, X. Zhang, *J. Org. Chem.* **2011**, *76*, 339–341.

[16] J. T. Reeves, Z. Tan, Z. S. Han, G. Li, Y. Zhang, Y. Xu, D. C. Reeves, N. C. Gonnella, S. Ma, H. Lee, et al., *Angew. Chem. Int. Ed.* **2012**, *51*, 1400–1404.

[17] P. Dupau, P. Le Gendre, C. Bruneau, P. H. Dixneuf, *Synlett* **1999**, *1999*, 1832–1834.

[18] E. Cristóbal-Lecina, P. Etayo, S. Doran, M. Revés, P. Martín-Gago, A. Grabulosa, A. R. Costantino, A. Vidal-Ferran, A. Riera, X. Verdaguer, *Adv. Synth. Catal.* **2014**, *356*, 795–804.

[19] J. Engel, S. Mersmann, P. O. Norrby, C. Bolm, *ChemCatChem* **2016**, *8*, 3099–3106.

[20] J. Halpern, *Science (80-.).* **1982**, *217*, 401–407.

Experimental Section

General Considerations

Non-aqueous reactions were carried out under nitrogen atmosphere. Dry THF, Et_2O and CH_2Cl_2 were obtained from a Solvent Purification System (SPS PS-MD-3). Other anhydrous solvents were purchased from Aldrich. Commercially available reagents were purchased from Aldrich, TCI America, Strem Chemicals and/ or Acros Organics and were used with no further purification. All reactions were monitored by TLC analysis using Merck 60 F_{254} silica gel on aluminum sheets. Silica gel chromatography was performed by using 35–70 mm silica or an automated chromatography system (Combiflash®, Teledyne Isco).

Aluminum Sheets of Merck Silica gel 60 F_{254} were used for Thin Layer Chromatography. Used revelators were:

- UV 254 nm
- Anisaldehyde: 92 mL of 4-methoxybenzaldehyde, 3.8 mL of glacial acetic acid, 338 mL of ethanol (98%) and 12.5 mL of H_2SO_4 (98%)
- Phosphomolybdic: 23 g of phosphomolybdic acid in 400 mL of ethanol (98%)
- $KMnO_4$: 3 g of $KMnO_4$, 20 g of K_2CO_3, 300 mL of H_2O and 5 mL of NaOH 5% aqueous.

Molecular sieves activation (both powder and pellets) was carried out by heating in sand bath (300–350 ºC) under high vacuum during 7–10 hours. Then the activated sieves were kept under vacuum in an oven at 140 ºC.

For low temperature baths, mixtures of CO_2/acetone have been used for –78 ºC to –30 ºC, and ice-water for 0 ºC. For more than 5 hours reactions Cryocool CC-100 system and IPA as solvent have been used.

NMR spectra were recorded at room temperature on a Varian Mercury 400, Varian Mercury 500, Bruker 300 or Bruker 600. ^{1}H NMR and ^{13}C NMR spectra were referenced either to relative internal TMS or to residual solvent peaks. ^{31}P NMR spectra were referenced to phosphoric acid. Signal multiplicities in the ^{13}C spectra were assigned by DEPT and HSQC experiments. The following abbreviations were used to define the

multiplicities: s, singlet; d, doublet; t, triplet; q, quadruplet; p, quintuplet; m, multiplet; br, broad signal. The chemical shifts are expressed in ppm and the coupling constants (*J*), in hertz (Hz). ^{19}F NMR spectra were referenced by the spectrometer without any external pattern.

IR spectra were recorded in a Thermo Nicolet Nexus FT-IR apparatus, either by preparing a KBr pastille or by depositing a film of the product on a NaCl window. Absorptions are given in wavenumbers (cm^{-1}).

Melting points were recorded in a Büchi M-540 apparatus without recrystallization of the final solids.

Optical rotations were measured at room temperature (25 °C) using a Jasco P-2000 iRM-800 polarimeter. Concentration is expressed in g / 100 mL. The solvent is defined for each case in brackets. The cell sized 10 cm long and had 1 mL of capacity. Measuring λ was 589 nm, which corresponds to a sodium lamp.

Mass spectrometry were recorded in a Hewlett-Packard 5988 A using EI, CI or ES techniques and High Resolution Mass Spectrometry were recorded in a LTQ-FT Ultra (Thermo Scientific) using Nanoelectrospray technique at the Mass Spectrometry Core Facility from the IRB Barcelona.

HPLC analysis were carried out using a Hewlett-Packard 1050 equipment and GC chromatography was performed on a Agilent Technologies 6890N with a FID detector by Enantia S.L. Conditions of each analysis are specified in each case.

Experimental Section for Chapter 2

Efficient Preparation of
(*S*)- and (*R*)-*tert*-Butylmethylphosphine Borane:
A Novel Entry to Important P-Stereogenic Ligands

E. Salomó, S. Orgué, A. Riera, X. Verdaguer, *Synthesis.* **2016**, *48*, 2659–2663.

(*R*)-*tert*-Butylmethylphosphine borane, (*R*)-2.1.[1,2]

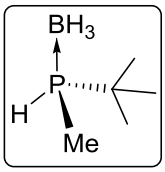

A solution of (*R*)-*tert*-butyl(methyl)phosphinous acid borane (*R*)-**2.8** (200mg, 1.50 mmol) and methansulfonic anhydride (313 mg, 1.80 mmol) in CH_2Cl_2 (6 mL) was cooled to –20 °C. To this solution, anhydrous *N*-methylmorpholine (205 µL, 1.87 mmol) was slowly added, and the mixture was stirred 1.5 h at –20 °C. A solution of $[Bu_4N][BH_4]$ (1.15 g, 4.5 mmol) in 2 mL of CH_2Cl_2 was slowly added and the mixture was further stirred 2 h at –20 °C. After this time, consumption of the starting material was observed by TLC. The reaction was quenched by slow addition of HCl (1 M in H_2O). The organic layer was separated and the aqueous phase was extracted twice with CH_2Cl_2. The combined extracts were washed with brine (5 mL), dried over $MgSO_4$ and concentrated on a rotary evaporator under reduced pressure. Purification by short column chromatography (SiO_2, isocratic hexanes/CH_2Cl_2, 6:4) yielded 154 mg (88%, 99% ee) of pure (*R*)-**2.1** as a colorless semisolid.

[α]D: – 4.5 (c 0.60, $CHCl_3$). **^{1}H NMR (400 MHz, $CDCl_3$) δ;** 4.40 (dm, J_P = 355 Hz, 1H, HP), 1.31 (dd, J = 11 and 6 Hz, 3H, CH_3), 1.21 (d, J_P = 15 Hz, 9H, tBu), 0.48 (br q, J_B = 96 Hz, 3H, BH_3) ppm. **^{31}P NMR (202 MHz, $CDCl_3$) δ;** 11.7 (q, J_B = 48 Hz) ppm.

Enantiomeric excess determination for (*R*)-2.1: Optical purity for (*R*)-**2.1** was determined by derivatization to the corresponding benzyl phosphine which was analyzed by chiral HPLC.

(*R*)-Benzyl-*tert*-butylmethylphosphine borane.[1]

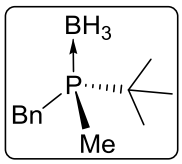

A sample of (*R*)-**2.1** (34 mg, 0.31 mmol) was dissolved in anhydrous THF (3 mL) and cooled to –78 °C. Then *n*-BuLi (0.250 mL, 0.39 mmol, 1.6 M in hexanes) was slowly added at –78 °C. The mixture was left stirring for 50 min. At low temperature, benzyl bromide (37 µL, 0.31 mmol) was then added. The reaction was left to warm to room temperature and left to stir overnight. The mixture was then quenched by addition of NH_4Cl at 0 °C. The mixture was extracted thrice with EtOAc. The combined extracts were washed with brine, dried over $MgSO_4$ and

concentrated on a rotary evaporator under reduced pressure. The benzyl-*tert*-butylmethylphosphine borane was obtained pure as a white solid (99%).

^{1}H NMR (400 MHz, $CDCl_3$) δ; 7.15 – 7.35 (m, 5H, Ph), 2.90 – 3.11 (m, 2H, CH_2), 1.21 (d, *J* = 14 Hz, 9H, *t*Bu), 1.04 (d, *J* = 10 Hz, 3H, CH_3), 0.09 – 0.85 (m, 3H, BH_3) ppm. **HPLC:** Daicel Chiralcel OD-H; heptane/iPrOH = 9:1, 0.5 mL/min, 210 nm, t_S= 18.6 min, t_R = 20.6 min.

(*S*)-*tert*-Butyl(methyl)phosphinous acid borane, (*S*)-2.8[3]

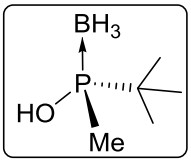

^{1}H NMR (400 MHz, $CDCl_3$) δ; 0.53 (qd, *J* = 94, 15 Hz, 3H BH_3), 1.17 (d, J_P = 14 Hz, 9H), 1.45 (d, J_P = 9 Hz, 3H) ppm.

(*S*,*S*)-2,3-Bis(*t*-butylmethylphosphino)quinoxaline[4]

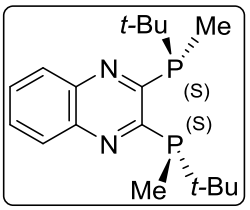

^{1}H NMR (400 MHz, $CDCl_3$) δ; 8.10 (dd, *J* = 6, 4 Hz, 2H), 7.72 (dd, *J* = 6, 3 Hz, 2H), 1.43 (t, *J* = 3 Hz, 6H), 1.02 (t, *J* = 6 Hz, 18H) ppm.

REFERENCES

[1] T. Miura, H. Yamada, S. Kikuchi, T. Imamoto, *J. Org. Chem.* **2000**, *65*, 1877–1880.

[2] K. Nagata, S. Matsukawa, T. Imamoto, *J. Org. Chem.* **2000**, *65*, 4185–4188.

[3] S. Orgué, A. Flores-Gaspar, M. Biosca, O. Pàmies, M. Diéguez, A. Riera, X. Verdaguer, *Chem. Commun.* **2015**, *51*, 17548–17551.

[4] T. Imamoto, K. Sugita, K. Yoshida, *J. Am. Chem. Soc.* **2005**, *127*, 11934–11935.

Experimental Section for Chapter 3

Dialkylammonium *tert*-Butylmethylphosphinites:

Stable Intermediates for the Synthesis of P-Stereogenic Ligands

E. Salomó, A. Prades, A. Riera, X. Verdaguer, *J. Org. Chem.* **2017**, *82*, 7065–7069.

(*R*)-*tert*-butyl(methyl)phosphinous acid borane, 3.1[1]

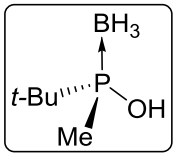

^{1}H NMR (400 MHz, $CDCl_3$) δ; 0.53 (qd, J = 94, 15 Hz, 3H BH_3), 1.17 (d, J_P = 14 Hz, 9H), 1.45 (d, J_P = 9 Hz, 3H) ppm.

(*S*)-*tert*-butyl(methyl)aminophosphine borane, 3.3[2]

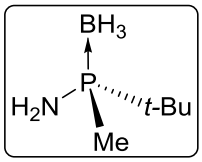

^{1}H NMR (400 MHz, $CDCl_3$) δ; 0.47 (qd, J = 80 and 16 Hz, BH_3), 1.14 (d, J_P = 14 Hz, 9H), 1.35 (d, J_P = 9 Hz, 3H), 1.74 (br, 1H, NH) ppm.

General Method 1: Synthesis of 3.7, 3.8 and 3.9 using 3.1

Phosphinous acid (*S*)-**3.1** was placed in a vial (15 mg, 0.11mmol) and solved in TBME (0.5 mL). The corresponding base (1 eq, 0.11 mmol) was added dropwise via a syringe. The resulting precipitate was filtered and dried under a stream of nitrogen.

Diethylammonium (*S*)-*tert*-butyl(methyl)phosphinite borane, **3.7**

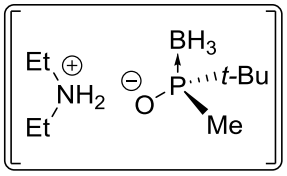

Following **GM1**, phosphinous acid (*S*)-**3.1** was placed in a vial (15 mg, 0.11mmol) and solved in TBME (0.5 mL). Diethylamine (12 µL, 0.11 mmol) was added dropwise via a syringe. The resulting crystalline precipitate was filtered and dried under a stream of nitrogen.

White solid. **Yield:** 87% (20 mg). **M_P:** 151 – 153ºC. **$[\alpha]_D$:** –22.1 (c 0.50, $CHCl_3$). **IR (KBr/NaCl) υ_{max}:** 3424, 2966, 2349, 1628 and 997 cm^{-1}. **^{1}H NMR (400 MHz, $CDCl_3$) δ;** 9.08 (br s, 2H), 2.97 – 2.81 (m, 4H), 1.33 (t, J = 7 Hz, 6H), 1.16 (d, J_P = 8 Hz, 3H), 1.06 (d, J_P = 13 Hz, 9H), 0.73 – 0.03 (m, 3H, BH_3) ppm. **^{13}C NMR (101 MHz, $CDCl_3$) δ;** 42.4 (2 x CH_2), 30.8 (d, J_P = 41 Hz, C), 24.6 (d, J_P = 3 Hz, 3 x CH_3), 13.8 (d, J_P = 33 Hz, CH_3), 12.0 (2 x CH_3) ppm.**^{31}P NMR (202 MHz, $CDCl_3$) δ;** 90.1 – 87.9 (m, P–BH_3).

HRMS (ESI-positive mode): calc. for $[C_4H_{12}N]^+$: 74,0964, found 74.0965. **HRMS (ESI-negative mode):** calc. for $[C_5H_{15}OBP]^-$: 133.0959, found 133.0959.

Diisopropylammonium (*S*)-*tert*-butyl(methyl)phosphinite borane, 3.8

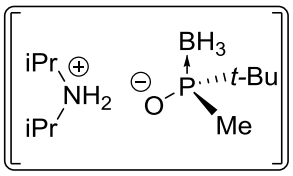

Following **GM1**, phosphinous acid (*S*)-**3.1** was placed in a vial (15 mg, 0.11mmol) and solved in TBME (0.5 mL). Diisopropylamine (16 µL, 0.11 mmol) was added dropwise via a syringe. The resulting crystalline precipitate was filtered and dried under a stream of nitrogen.

White solid. **Yield:** 81% (21 mg). M_P: 136.5 – 138.0ºC. $[\alpha]_D$: +3.2 (c 0.56, $CHCl_3$). **IR (KBr/NaCl) υ_{max}:** 3439, 2923, 2860, 2388 and 2342 cm^{-1}. **^{1}H NMR (400 MHz, $CDCl_3$) δ;** 7.43 (br s, 1H), 3.27 – 3.16 (m, 2H), 1.29 (d, J = 6 Hz, 12H), 1.22 (d, J_P = 9 Hz, 3H), 1.09 (d, J_P = 13 Hz, 9H), 0.79 – 0.01 (m, 3H, BH_3) ppm. **^{13}C NMR (101 MHz, $CDCl_3$) δ;** 46.6 (2 x CH), 30.9 (d, J_P = 43 Hz, C), 24.6 (3 x CH_3), 21.0 (d, J_P = 11 Hz, 4 x CH_3), 13.3 (d, J_P = 35 Hz, CH_3) ppm. **^{31}P NMR (202 MHz, $CDCl_3$) δ;** 92.4 – 90.2 (m, P–BH_3) ppm. **HRMS (ESI-positive mode):** calc. for $[C_6H_{16}N]^+$: 102.1278, found 102.1277. **HRMS (ESI-negative mode):** calc. for $[C_5H_{15}OBP]^-$: 133.0959, found 133.0959.

Dicyclohexylammonium (*S*)-*tert*-butyl(methyl)phosphinite borane, 3.9

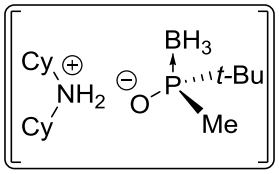

Following **GM1**, phosphinous acid (*S*)-**3.1** was placed in a vial (15 mg, 0.11mmol) and solved in TBME (0.5 mL). Dicyclohexylamine (22 µL, 0.11 mmol) was added dropwise via a syringe. The resulting crystalline precipitate was filtered and dried under a stream of nitrogen.

White solid. **Yield:** 87% (32 mg). **M_P:** 143 – 144ºC. **$[\alpha]_D$:** +8.8 (c 0.34, $CHCl_3$). **IR (KBr/NaCl) υ_{max}:** 3419, 2939, 2857, 2347 and 1619 cm^{-1}. **^{1}H NMR (400 MHz, $CDCl_3$) δ;** 7.57 (br s, 2H), 2.94 – 2.80 (m, 2H), 2.09 – 1.95 (m, 4H), 1.85 – 1.74 (m, 4H), 1.68 – 1.60 (m, 2H), 1.51 – 1.33 (m, 4H), 1.31 – 1.12 (m, 6H), 1.20 (d, J_P = 9 Hz, 3H), 1.08 (d, J_P = 13 Hz, 9H), 0.84–0.03 (m, 3H, BH_3) ppm. **^{13}C NMR (101 MHz, $CDCl_3$) δ;** 53.6 (2 x CH), 31.4 – 31.2 (4 x CH_2), 30.9 (d, J_P = 43 Hz, C), 25.3 – 24.9 (6 x CH_2), 24.6 (d, J_P = 3 Hz, 3 x CH_3), 13.4 (d, J_P = 36 Hz, CH_3) ppm. **^{31}P NMR (202 MHz, $CDCl_3$) δ;** 91.4 – 89.1 (m, P–BH_3) ppm. **HRMS (ESI-positive mode):** calc. for $[C_{12}H_{24}N]^+$: 182.1905,

found 182.1903. **HRMS (ESI-negative mode):** calc. for $[C_5H_{15}OBP]^-$: 133.0959, found 133.0959.

ONE-POT LARGE SCALE SYNTHESIS OF (*R*)-3.8 FROM (*S*,*R*)-3.10

(1*S*,2*R*)-1-(*tert*-butyl(methyl)phosphinoamino)-2,3-dihydro-1H- inden-2-ol, 3.10[3]

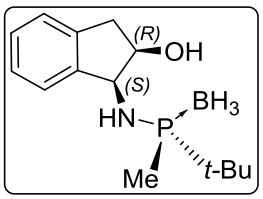

^{1}H NMR (400 MHz, $CDCl_3$) δ; 0.20-1.08 (m, BH_3), 1.29 (d, J_P = 14 Hz, 9H), 1.47 (d, J_P = 9 Hz, 3H), 2.11-2.30 (m, 2H), 2.91 (dd, *J* = 17, 1 Hz, 1H), 3.11 (dd, *J* = 17, 5 Hz, 1H), 4.51 (td, *J* = 5, 1 Hz, 1H), 4.78 (td, *J* = 10, 5 Hz, 1H), 7.24-7.32 (m, 3H), 7.35-7.41 (m, 1H) ppm.

50 g (189 mmol, 1 eq) of **3.10** were placed in a reactor with a magnetic stirrer and a condenser. Then the system was purged with N_2. Then 500 mL of MeOH (10 V) and 250 mL of H_2O (5 V) were added in this order. The reaction was then cooled to 0 ºC and 77 mL of concentrated H_2SO_4 (756 mmol, 4 eq) were added dropwise. The mixture was stirred at reflux temperature for 15 h (oil bath: 80 ºC). The reaction can be easily followed by TLC. Longer reaction times are not desirable due to possible oxidation of the product. 500 mL of H_2O were then added. This way, MeOH can be safely removed under reduced pressure at 25 ºC without increasing the H_2SO_4 concentration, which would lead to oxidative reactions of the product. The aqueous layer was extracted three times with TBME (200 mL + 4 x 100 mL, 4 V + 4 x 2 V). The combined organic layers were washed with water (200 mL + 3 x 100 mL, 4 V + 3 x 2 V) until the washings were no longer acidic (around pH 6). Stripping was carried out to remove possible water traces and also reaching approximately 5V of TBME. 53 mL of iPr_2NH (378 mmol, 2 eq) were then added dropwise to the organic layer over 15 min. Precipitation of the solid was observed. The slurry solution was stirred at 0 ºC for 1h and then filtered and washed with TBME to afford 36 g (82%, 155 mmol) of **3.8** as a white crystalline solid. The mother liquors can be concentrated further through evaporation and filtered again to afford more product (up to 5% more).

S_N2@P REACTIONS WITH THE SALT SURROGATE 3.8.

General Method 2: S_N2@P reactions with 3.8.

Methanesulfonic anhydride (1.0 – 1.2 eq.) was solved in CH_2Cl_2 under N_2 atmosphere and cooled to –20 ºC. A solution of the phosphinous acid salt **3.8** in CH_2Cl_2 under N_2 atmosphere was slowly added dropwise. Anhydrous NEt_3 (2.0 eq.) was then added dropwise. The reaction was stirred for 1.5 h at –20ºC. The corresponding amine/reducing agent (0.5 – 3 eq.) was added and the solution was stirred overnight at –20ºC. NaOH (1 M) was added to quench the reaction and the mixture was allowed to warm to room temperature. The mixture was extracted with CH_2Cl_2. The organic layer was washed with NaOH (1M) and/or HCl (1M) when deemed useful to purify the crude product. The organic layer was dried with $MgSO_4$ and filtered, and the solvent was removed under reduced pressure. When required, the crude was purified by flash chromatography (SiO_2, hexanes:EtOAc).

(*R*)-*tert*-butyl(methyl)phosphanamine borane, 3.3[2]

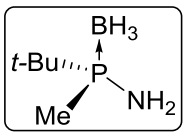

Following the **GM2**, 73 mg of methanesulfonic anhydride (0.41 mmol, 1.2 eq.), 80 mg of **3.8** (0.34 mmol, 1 eq.), 95 µL of NEt_3 (0.68 mmol, 2 eq.) and 5 mL of CH_2Cl_2 were used. NH_3 was bubbled through the solution for 5 min, then the flow was removed and the reaction stirred for 10 min. H_2O was added to quench the reaction. The mixture was extracted with CH_2Cl_2 to afford 46 mg (99%, 0.34 mmol) of **3.3** as a white wax, which was not further purified (*ee* 98%).
^{1}H NMR (400 MHz, $CDCl_3$) δ; 1.76 (s, 2H), 1.35 (d, J_P = 9 Hz, 3H), 1.14 (d, J_P = 14 Hz, 9H), 0.86–0.08 (m, 3H, BH_3) ppm. **GC:** *β*-DEX (30 m), 130ºC, 1 mL/min, t_R(+) = 14.5 min, t_R (–) = 14.9 min.

(*S*)-*tert*-butyl(methyl)phosphine borane, 3.12[4,5]

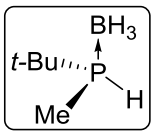

Following the **GM2**, 128 mg of methanesulfonic anhydride (0.71 mmol, 1.05 eq), 160 mg of **3.8** (0.68 mmol, 1 eq), 150 µL of *N*-methylmorpholine (1.36 mmol, 2 eq) and 8 mL of CH_2Cl_2 were used. 525 mg (2.04 mmol, 3 eq) of nBu$_4$NBH$_4$ in 2 mL of CH_2Cl_2 were added dropwise and the solution was stirred for 2 hours at –20ºC. NaOH (1 M) was added to quench the reaction. The mixture was

extracted with CH_2Cl_2. This afforded, after purification by flash chromatography (SiO_2, hexanes/EtOAc), 64 mg (80%, 0.54 mmol) of **3.12** as a white waxy solid (*ee* = 99%).

^{1}H NMR (400 MHz, $CDCl_3$) δ; 4.40 (dm, J_P = 355 Hz, 1H), 1.31 (dd, J = 11, 6 Hz, 3H), 1.21 (d, J_P = 15 Hz, 9H), 0.48 (br q, J_B = 96 Hz, 3H, BH_3) ppm.

Enantiomeric excess determination for 3.12: Optical purity for **3.12** was determined by derivatization to the corresponding benzyl phosphine, which was analyzed by chiral HPLC.

(*S*)-Benzyl-*tert*-butylmethylphosphine borane.[4,5]

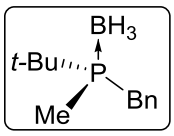

A sample of (*S*)-**3.12** (34 mg, 0.31 mmol) was dissolved in anhydrous THF (3 mL) and cooled to –78 °C. Then *n*-BuLi (0.250 mL, 0.39 mmol, 1.6 M in hexanes) was slowly added at –78 °C. The mixture was left stirring for 50 min. At low temperature, benzyl bromide (37 µL, 0.31 mmol) was then added. The reaction was left to warm to room temperature and left to stir overnight. The mixture was then quenched by addition of NH_4Cl at 0 °C. The mixture was extracted thrice with EtOAc. The combined extracts were washed with brine, dried over $MgSO_4$ and concentrated on a rotary evaporator under reduced pressure. The benzyl-*tert*-butylmethylphosphine borane was obtained pure as a white solid (99%). Spectroscopic data was in agreement with the literature.

^{1}H NMR (400 MHz, $CDCl_3$) δ; 7.15 – 7.35 (m, 5H, Ph), 2.90 – 3.11 (m, 2H, CH_2), 1.21 (d, J = 14 Hz, 9H, *t*Bu), 1.04 (d, J = 10 Hz, 3H, CH_3), 0.09 – 0.85 (m, 3H, BH_3) ppm. **HPLC:** Daicel Chiralcel OD-H; heptane/iPrOH = 9:1, 0.5 mL/min, 210 nm, t_S= 18.6 min, t_R = 20.6 min.

(*R*)-1-*tert*-butyl-1-methyl-*N*-(pyridin-2-ylmethyl)phosphinamine borane, 3.13[1]

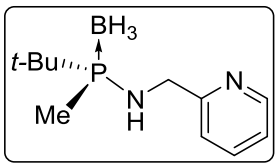

Following the **GM2**, 64 mg of methanesulfonic anhydride (0.36 mmol, 1.05 eq), 80 mg of **3.8** (0.34 mmol, 1 eq.), 95 µL of NEt_3 (0.68 mmol, 2 eq.) and 4 mL of CH_2Cl_2 were used. 2-Picolylamine (105 µL, 1.02 mmol, 3 eq.) was added and the solution was stirred overnight at –20ºC. This afforded 64 mg (84%, 0.29 mmol) of **3.13** as a white solid (*ee* = 99%) after purification by flash chromatography (SiO_2, hexanes/EtOAc).

^{1}H NMR (400 MHz, $CDCl_3$) δ; 8.56 – 8.44 (m, 1H), 7.66 (td, *J* = 8, 2 Hz, 1H), 7.30 – 7.27 (m, 1H), 7.21 – 7.15 (m, 1H), 4.42 – 4.30 (m, 1H), 4.30 – 4.19 (m, 1H), 2.80 (br s, 1H), 1.33 (d, J_P = 9 Hz, 3H), 1.14 (d, J_P = 14 Hz, 9H), 0.96–0.07 (m, 3H, BH_3) ppm. **HPLC:** CHIRALCEL OJ. Heptane:EtOH: 90:10-0.2% DEA, 0.50 mL/min, λ= 210 nm. t_R (–) = 12.9 min, t_R (+) = 13.6 min.

(*S*)-1-*tert*-butyl-1-methyl-*N*-(2-thiophenylmethyl)phosphinamine borane, 3.14[1]

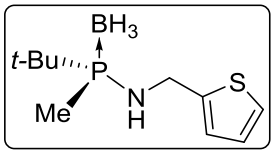

Following the **GM2**, 64 mg of methanesulfonic anhydride (0.36 mmol, 1.05 eq.), 80 mg of **3.8** (0.34 mmol, 1 eq.), 95 µL of NEt_3 (0.68 mmol, 2 eq.) and 4 mL of CH_2Cl_2 were used. 2-Thiophenemethylamine (105 µL, 1.02 mmol, 3 eq.) was added and the solution was stirred overnight at –20ºC. After purification by flash chromatography (SiO_2, hexanes/EtOAc), 66 mg (85%, 0.29 mmol) of **3.14** as a white solid was obtained (*ee* = 99%).

^{1}H NMR (400 MHz, $CDCl_3$) δ; 7.23 – 7.20 (m, 1H), 6.96 – 6.93 (m, 2H), 4.47 – 4.37 (m, 1H), 4.37 – 4.23 (m, 1H), 1.86 (br s, 1H), 1.36 (d, J_P = 9 Hz, 3H), 1.15 (d, J_P = 14 Hz, 9H), 0.95 – 0.13 (m, 3H, BH_3) ppm. **HPLC:** CHIRALCEL OJ. Heptane:EtOH: 80:20-0.2% DEA, 0.50 mL/min, λ= 210 nm. t_R (–) = 14.7 min, t_R (+) = 15.9 min.

(*S*)-1-*tert*-butyl-1-methyl-*N*-((*R*)-1-phenylethyl)phosphanamine borane, 3.15[1]

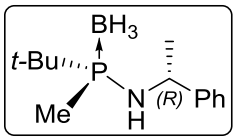

Following the **GM2**, 64 mg of methanesulfonic anhydride (0.36 mmol, 1.05 eq.), 80 mg of **3.8** (0.34 mmol, 1 eq.), 95 µL of NEt_3 (0.68 mmol, 2 eq.) and 4 mL of CH_2Cl_2 were used. (*R*)-(1)-phenylethylamine (132 µL, 1.02 mmol, 3 eq.) was added and the solution was stirred overnight at –20ºC. After purification by flash chromatography (SiO_2, hexanes/EtOAc), 66 mg (83%, 0.28 mmol) of **3.15** as a white solid was obtained (*de* 98%, as determined by ^{1}H NMR).

^{1}H NMR (400 MHz, $CDCl_3$) δ; 7.37 – 7.20 (m, 5H), 4.50 – 4.41 (m, 1H), 1.81 (br d, *J* = 9 Hz, 1H)), 1.46 (d, *J* = 7 Hz. 3H), 1.24 (d, J_P = 9 Hz, 3H), 1.07 (d, J_P = 14 Hz, 9H), 0.96–0.12 (m, 3H, BH_3) ppm.

(*S*)-1-*tert*-butyl-1-methyl-*N*-((*S*)-1-phenylethyl)phosphanamine borane, 3.16[1]

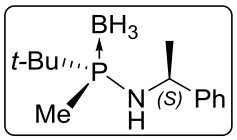

Following the **GM2**, 64 mg of methanesulfonic anhydride (0.36 mmol, 1.05 eq), 80 mg of **3.8** (0.34 mmol, 1 eq.), 95 µL of NEt_3 (0.68 mmol, 2 eq.) and 4 mL of CH_2Cl_2 were used. (*S*)-(1)-phenylethylamine (132 µL, 1.02 mmol, 3 eq.) were added and the solution was stirred overnight at –20ºC. The work-up afforded 70 mg (88%, 0.30 mmol) of **3.16** as a white solid which was not further purified (*de* 98%, as determined by ^{1}H NMR).

^{1}H NMR (400 MHz, $CDCl_3$) δ; 7.48 – 7.14 (m, 5H), 4.53 – 4.48 (m, 1H), 1.74 (br d, *J* = 9 Hz, 1H)), 1.44 (d, *J* = 7 Hz. 3H), 1.20 (d, J_P = 9 Hz, 3H), 1.11 (d, J_P = 14 Hz, 9H), 0.96–0.11 (m, 3H, BH_3) ppm.

(*S*)-2-(((*S*)-*tert*-butyl(methyl)phosphanyl)amino)-N-((*S*)-1-hydroxy-3-methylbutan-2-yl)-3-methylbutanamide borane, 3.17[6]

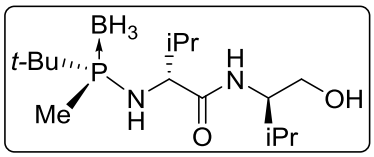

Following the **GM2**, 73 mg of methanesulfonic anhydride (0.41 mmol, 1.2 eq.), 80 mg of **3.8** (0.34 mmol, 1 eq.), 95 µL of NEt_3 (0.68 mmol, 2 eq.) and 4 mL of CH_2Cl_2 were used. (*S*)-2-Amino-N-((*S*)-1-hydroxy-3-methylbutan-2-yl)-3-methylbutanamide (206 mg, 1.02 mmol, 3 eq.) was added and the solution was stirred overnight at –20ºC. Work-up and purification by flash chromatography (SiO_2, hexanes/EtOAc) afforded 96 mg (93%, 0.32 mmol) of **3.17** as a white solid. (*de* >95%, as determined by ^{1}H NMR).

^{1}H NMR (400 MHz, $CDCl_3$) δ; 6.13 (br s, 1H), 3.77 – 3.64 (m, 3H), 3.49 (ddd, *J* = 11, 9, 7 Hz, 1H), 2.21 (dd, *J* = 11, 5 Hz, 1H), 2.01 – 1.84 (m, 2H), 1.27 (d, J_P = 9 Hz, 3H), 1.15 (d, J_P = 14 Hz, 9H), 1.01 – 0.95 (m, 12H), 0.81 – 0.06 (m, 3H, BH_3) ppm.

(*S*,*S*)-N^1,N^2-bis(*tert*-butyl(methyl)phosphanyl)ethane-1,2-diamine bisborane, 3.18.

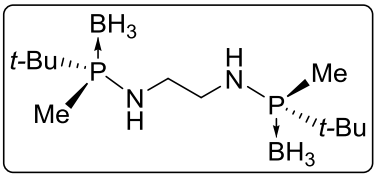

Following the **GM2**, 128 mg of methanesulfonic anhydride (0.71 mmol, 1.05 eq.), 160 mg of **3.8** (0.68 mmol, 1 eq.), 189 µL of NEt_3 (1.36 mmol, 2 eq.) and 10 mL of CH_2Cl_2 were used. ethylenediamine (18 µL, 0.27 mmol, 0.4 eq.) were added and the solution was stirred overnight at –20ºC. This afforded, after purification by flash chromatography (SiO_2, hexanes/EtOAc), 52 mg (66%, 0.18 mmol) of **3.18** as a white solid. (*de* >95%, as determined by ^{1}H NMR).

White solid. **Yield :** 66% (52 mg). **Mp:** 123.5 – 124.5ºC. **[α]D:** +6.7 (c 0.23, $CHCl_3$). **IR (KBr/NaCl) υmax:** 3335, 2970, 2390, 2345 and 1467 cm^{-1}. **^{1}H NMR (400 MHz, $CDCl_3$) δ;** 3.16 – 2.97 (m, 4H), 1.68 (br s, 2H), 1.33 (d, *J* = 9 Hz, 6H), 1.12 (d, *J* = 14 Hz, 18H), 0.86–0.05 (m, 6H, 2 x BH_3) ppm. **^{13}C NMR (101 MHz, $CDCl_3$) δ;** 45.3 (d, *J* = 5 Hz, 2 x CH_2), 31.2 (d, *J* = 39 Hz, 2 x C,), 24.7 (d, *J* = 3 Hz, 6 x CH_3), 9.6 (d, *J* = 40 Hz, 2 x CH_3) ppm. **^{31}P NMR (202 MHz, $CDCl_3$) δ;** 72.3 – 70.0 (m, 2 x P–BH_3) ppm. **HRMS (ESI):** calc. for $[C_{12}H_{36}B_2N_2P_2 + H]^+$: 293.2609, found 293.2613.

(1*R*,2*R*)-*N*^{1},*N*^{2}-bis((*S*)-*tert*-butyl(methyl)phosphanyl)cyclohexane-1,2-diamine bisborane, 3.19

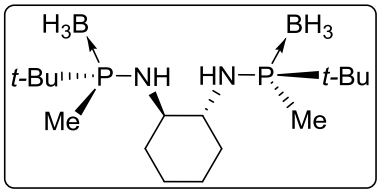

Following the **GM2**, 99 mg of methanesulfonic anhydride (0.55 mmol, 1 eq.), 130 mg of **3.8** (0.55 mmol, 1 eq.), 154 µL of NEt_3 (1.11 mmol, 2 eq.) and 6 mL of CH_2Cl_2 were used. (1*R*,2*R*)-cyclohexane-1,2-diamine (28 mg, 0.25 mmol, 0.45 eq.) were added dissolved in 3 mL of CH_2Cl_2 and the solution was stirred overnight at –20ºC. This afforded 78 mg (91%, 0.23 mmol) of a very pure solid crude. After further purification by column chromatography (SiO_2, hexanes/EtOAc), 66 mg (77%, 0.19 mmol) of **3.19** was obtained as a white solid. (*de* >95%, as determined by ^{1}H NMR).

White solid. **Yield:** 77% (66 mg). **MP:** 216.5 – 217.5ºC. **[α]D:** –3.9 (c 0.39, $CHCl_3$). **IR (KBr/NaCl) υmax:** 3305, 2926, 2362, 2339 and 1096 cm^{-1}. **^{1}H NMR (400 MHz, $CDCl_3$) δ;** 2.91 (br s, 2H), 2.12 (br d, *J* = 13 Hz, 2H), 1.68 – 1.52 (m, 4H), 1.36 – 1.13 (m, 4H), 1.33 (d, *J* = 9 Hz, 6H), 1.16 (d, *J* = 14 Hz, 18H), 0.84–0.03 (m, 6H, 2 x BH_3) ppm. **^{13}C NMR (101 MHz, $CDCl_3$) δ;** 57.8 (d, *J* = 7 Hz, 2 x CH), 36.1 (CH_2), 30.1 (d, *J* = 44 Hz, C), 24.7 (d, *J* = 3 Hz, 6 x CH_3), 24.4 (4 x CH_2), 11.8 (d, *J* = 32 Hz, 2 x CH_3) ppm. **^{31}P NMR (202 MHz, $CDCl_3$) δ;** 70.8 – 69.0 (m, 2 x P–BH_3) ppm. **HRMS (ESI):** calc. for $[C_{16}H_{42}B_2N_2P_2 + Na]^+$: 369.2907, found 369.2902.

N^1-((*S*)-tert-butyl(methyl)phosphanyl)-N^2-(2-(((*S*)-tert-butyl(methyl)phosphanyl) amino) ethyl)ethane-1,2-diamine bisborane, 3.20

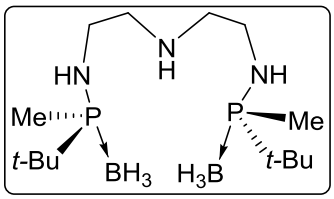

Following the **GM2**, 128 mg of Ms_2O (0.71 mmol, 1 eq.), 168 mg of **3.8** (0.71 mmol, 1 eq.), 199 µL of NEt_3 (1.42 mmol, 2 eq.) and 10 mL of CH_2Cl_2 were used. Diethylenetriamine (35 µL, 0.32 mmol, 0.45 eq.) was added and the solution was stirred overnight at –20ºC. This afforded, after purification by column chromatography (SiO_2, hexanes/EtOAc), 92 mg (84%) of **3.20** as a yellow wax. (*de* >95%, as determined by ^{1}H NMR).

Yellow wax. **Yield:** 94% (92 mg). **$[\alpha]_D$:** +11.4 (c 0.54, $CHCl_3$). **IR (KBr) υ_{max}:** 3353, 2928, 2866, 2364 and 2337 cm^{-1}. **^{1}H NMR (400 MHz, $CDCl_3$) δ;** 3.15 – 3.05 (m, 2H), 3.05 – 2.96 (m, 2H), 2.71 – 2.66 (m, 4H), 2.03 (br t, *J* = 6 Hz, 2H), 1.95 (br s, 1H), 1.30 (d, *J* = 9 Hz, 6H), 1.11 (d, *J* = 14 Hz, 18H), 0.86–0.03 (m, 6H, 2 x BH_3) ppm. **^{13}C NMR (101 MHz, $CDCl_3$) δ;** 50.8 (d, *J* = 5 Hz, 4 x CH_2), 42.8 (4 x CH_2), 31.2 (d, *J* = 39 Hz, C), 24.8 (d, *J* = 3 Hz, 6 x CH_3), 9.28 (d, *J* = 39 Hz, 2 x CH_3) ppm. **^{31}P NMR (202 MHz, $CDCl_3$) δ;** 70.7 – 68.9 (m, 2 x P–BH_3) ppm. **HRMS (ESI):** calc. for $[C_{14}H_{41}B_2N_3P + H]^+$: 336.3034, found 336.3035.

REFERENCES

[1] S. Orgué, A. Flores-Gaspar, M. Biosca, O. Pàmies, M. Diéguez, A. Riera, X. Verdaguer, *Chem. Commun.* **2015**, *51*, 17548–17551.

[2] M. Revés, C. Ferrer, T. León, S. Doran, P. Etayo, A. Vidal-Ferran, A. Riera, X. Verdaguer, *Angew. Chem. Int. Ed.* **2010**, *49*, 9452–9455.

[3] T. León, A. Riera, X. Verdaguer, *J. Am. Chem. Soc.* **2011**, *133*, 5740–5743.

[4] K. Nagata, S. Matsukawa, T. Imamoto, *J. Org. Chem.* **2000**, *65*, 4185–4188.

[5] T. Miura, H. Yamada, S. Kikuchi, T. Imamoto, *J. Org. Chem.* **2000**, *65*, 1877–1880.

[6] E. Salomó, S. Orgué, A. Riera, X. Verdaguer, *Angew. Chem. Int. Ed.* **2016**, *55*, 7988–7992.

Experimental Section for Chapter 5

Synthesis of the Ir-MaxPHOX Catalysts

SYNTHESIS OF THE Ir-MaxPHOX CATALYSTS

General Method 1: Synthesis of the chiral aminoalcohols.[1,2]

Et_3N (2 eq) and isobutylchloroformate (1.1 eq) were slowly added to a solution of the *N*-Boc-protected aminoacid (1 eq) in THF (0.13 M) at –30 ºC (white solid was observed when adding iBuOCOCl). The reaction mixture was stirred for 45 min at –30 ºC, and then the corresponding aminoalcohol (1.1 eq) was added. The resulting mixture was left stirring at room temperature overnight. Then the THF was removed under reduced pressure and the oily solid was dissolved in H_2O and EtOAc. The phases were separated and the aqueous layer was extracted twice with EtOAc. The organic layers were combined, dried over $MgSO_4$ and the solvent evaporated under reduced pressure. The crude obtained was dissolved in a 1:1 mixture of MeOH and HCl (3 M, aq) (0.1 M) and stirred overnight at room temperature. The MeOH was removed under vacuum and the resulting aqueous phase was extracted with EtOAc twice to remove impurities. Then EtOAc was added over the aqueous phase and it was basified using NaOH (40%, aq) at 0 ºC. The layers were separated and the aqueous phase was extracted thrice with EtOAc. The organic phases were combined, dried over $MgSO_4$ and the solvent was removed under reduced pressure to yield the deprotected aminoalcohols as white pure solids. These were used on the next steps without further purification.

The corresponding enantiomers of the amino alcohols described below were obtained in the same manner and with equal results.

(R)-2-amino-N-((S)-2-hydroxy-1-phenylethyl)-3-methylbutanamide, (*S,R)*-5.6Ph[1,2]

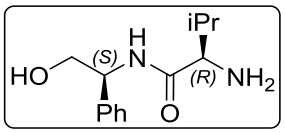

This compound is reported in the literature.

(R)-2-amino-N-((R)-2-hydroxy-1-phenylethyl)-3-methylbutanamide, (*R,R)*-5.6-Ph[1,2]

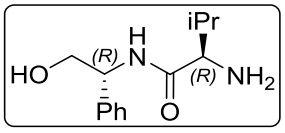

This compound is reported in the literature.

(*R*)-2-amino-N-((*S*)-1-hydroxy-3-methylbutan-2-yl)-3-methylbutanamide, (*S,R)*-5.6-iPr

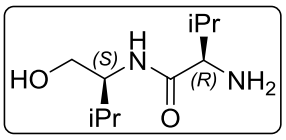

This compound was synthesized applying **GM1**.

White solid. **Yield:** 80% (1.29 g). **Mp:** 121 – 122 ºC. **[α]D:** +9.4 (c 1.19, $CHCl_3$). **IR (KBr) υmax:** 3277, 2961, 2871, 1640, 1562 cm^{-1}. **^{1}H NMR (400 MHz, $CDCl_3$) δ;** 7.58 (br s, 1H), 3.76 – 3.59 (m, 3H), 3.27 (d, J = 3.8 Hz, 1H), 2.40 – 2.28 (m, 1H), 1.99 – 1.85 (m, 1H), 1.01 (d, *J* = 7 Hz, 3H), 0.98 (d, *J* = 7 Hz, 3H), 0.95 (d, *J* = 7 Hz, 3H), 0.86 (d, *J* = 7 Hz, 3H) ppm. **^{13}C NMR (101 MHz, $CDCl_3$) δ;** 175.6 (C), 64.6 (CH_2), 60.3 (CH), 57.4 (CH), 30.9 (CH), 29.0 (CH), 19.7 (CH_3), 19.6 (CH_3), 18.6 (CH_3), 16.1 (CH_3) ppm. **HRMS (ESI):** calc for $[C_{12}H_{22}O_2N_2+H]^+$: 203.1754 found 203.1754.

(*S*)-2-amino-N-((*S*)-1-hydroxy-3-methylbutan-2-yl)-3-methylbutanamide, (*S,S)*-5.6-iPr

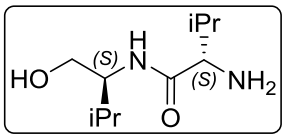

This compound was synthesized applying **GM1**.

White solid. **Yield:** 82% (1.32 g). **Mp:** 76 – 77 ºC. **[α]D:** –56.9 (c 1.21, $CHCl_3$). **IR (KBr) υmax:** 3331, 2963, 2872, 1630, 1548 cm^{-1}. **^{1}H NMR (400 MHz, $CDCl_3$) δ;** 7.66 (s, 1H), 3.78 – 3.59 (m, 3H), 3.30 (d, *J* = 4 Hz, 1H), 2.44 – 2.28 (m, 1H), 2.00 – 1.86 (m, 1H), 1.01 (d, *J* = 7 Hz, 3H), 0.97 (d, *J* = 7 Hz, 3H), 0.95 (d, *J* = 7 Hz, 3H), 0.84 (d, *J* = 7 Hz, 3H) ppm. **^{13}C NMR (101 MHz, $CDCl_3$) δ;** 175.7 (C), 64.6 (CH_2), 60.2 (CH), 57.2 (CH), 30.6 (CH), 28.9 (CH), 19.8 (CH_3), 19.7 (CH_3), 18.5 (CH_3), 16.0 (CH_3) ppm. **HRMS (ESI):** calc for $[C_{12}H_{22}O_2N_2+H]^+$: 203.1754 found 203.1754.

(*R*)-2-amino-N-((*S*)-1-hydroxy-3,3-dimethylbutan-2-yl)-3-methylbutanamide, (*S,R)*-5.6-*t*-Bu

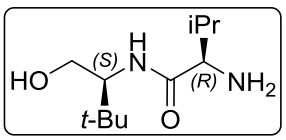

This compound was synthesized applying **GM1**.

White solid. **Yield:** 70% (2.43 g). **Mp:** 88.5–89.5 ºC. **[α]D:** +21.0 (c 0.52, $CHCl_3$). **IR (NaCl) υmax:** 3297, 2961, 2869, 1651, 1550 cm^{-1}. **^{1}H NMR (400 MHz, $CDCl_3$) δ** 8.05 (br s, 1H), 7.46 – 7.16 (m, 5H), 5.14 – 4.97 (m, 1H), 3.89 (d, *J* = 6 Hz, 2H), 3.33 (d, *J* = 4 Hz, 1H), 3.08 (s, 1H), 2.39 – 2.24 (m, 1H),

1.29 (br s, 1H), 0.99 (d, *J* = 7. Hz, 3H), 0.79 (d, *J* = 7 Hz, 3H) ppm. **^{13}C NMR (101 MHz, $CDCl_3$) δ;** 175.9 (C), 63.7 (CH_2), 60.3 (CH), 60.2 (CH), 33.3 (C), 30.9 (CH), 26.9 (3 x CH_3), 19.7 (CH_3), 16.0 (CH_3) ppm. **HRMS (ESI):** calc. for $[C_{11}H_{24}O_2N_2+H]^+$: 217.1911 found 217.1909.

(*S*)-2-amino-N-((*S*)-1-hydroxy-3,3-dimethylbutan-2-yl)-3-methylbutanamide, (*R,R)*-5.6-*t*-Bu

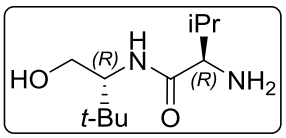

This compound is described in Maria Fernanda Céspedes Master thesis.

General Method 2: SN2@P reaction with synthon 5.4 and the chiral amino alcohols, 5.7

A solution of optically pure *tert*-butyl(methyl)phosphinous acid borane **5.4** (1 eq) and methansulfonic anhydride (1.2 eq) in CH_2Cl_2 (0.2M) was cooled to –20 ºC. To this solution, anhydrous NEt_3 (2.5 eq) was slowly added, and the mixture was stirred 1 h at –20 ºC. The corresponding amine (1.5 eq) was then added and the solution was stirred overnight at –20 ºC. NaOH (1 M) was added and the mixture was allowed to warm to room temperature. More CH_2Cl_2 was added and the organic layer was separated and washed once with NaOH (1 M). Then the organic layer was washed twice with HCl (1 M). Finally, the organic layer was concentrated under reduced pressure. When required, purification by column chromatography (SiO_2, hexanes:EtOAc) yielded the corresponding compounds as white solids.

(*R*)-*tert*-butyl(methyl)phosphinous acid borane, 5.4[3]

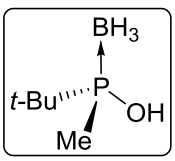

^{1}H NMR (400 MHz, $CDCl_3$) δ; 0.53 (qd, *J* = 94, 15 Hz, 3H BH_3), 1.17 (d, J_P = 14 Hz, 9H), 1.45 (d, J_P = 9 Hz, 3H) ppm.

(*S*)-2-(((*R*)-*tert*-butyl(methyl)phosphanyl)amino)-*N*-((*S*)-1-hydroxy-2-phenyl)-3-methylbutanamide borane, 5.7b-Ph

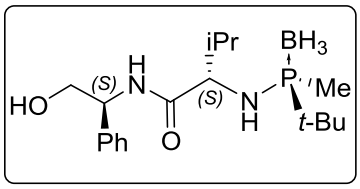

Compound **5.7b-Ph** was synthesized following **GM2**. White solid. **Yield:** 67% (350 mg). **M_P**= 171 – 172ºC. **$[\alpha]_D$** = +15.928 (c 0.65, $CHCl_3$). **IR (KBr/NaCl) υ_{max}:** 3326, 2960, 2381, 1645, 1220, 772 $cm^{-1.}$ **^{1}H NMR (400 MHz, $CDCl_3$) δ;** 7.41 – 7.23 (m, 5H), 6.50 (d, *J* = 8 Hz, 1H), 5.07 (dt, *J* = 8, 5 Hz, 1H), 3.89 (t, *J* = 5 Hz, 2H), 3.57 (td, *J* = 10, 7 Hz, 1H), 2.43 (t, *J* = 6 Hz, 1H), 2.17 (d, *J* = 10 Hz, 1H), 2.06 – 1.93 (m, 1H), 1.33 (d, *J* = 9 Hz, 3H), 1.06 – 0.96 (m, 12H), 0.94 (m, 6H), 0.73 – 0.03 (m, 3H, BH_3) ppm. **^{13}C NMR (101 MHz, $CDCl_3$) δ;** 173.7 (d, J_P = 2 Hz, C), 138.4 (C), 128.8 (CH), 127.9 (C), 126.8 (CH), 66.5 (CH_2), 62.9 (d, J_P = 2 Hz, CH), 55.9 (CH), 32.8 (d, J_P = 4 Hz, CH), 30.7 (d, J_P = 39 Hz, C), 24.4 (d, J_P = 3 Hz, 3x CH_3), 19.5 (CH_3), 18.2 (CH_3), 10.7 (d, J_P = 41 Hz, CH_3) ppm. **^{31}P NMR** (202 MHz, $CDCl_3$) δ 73.8 – 72.4 (m, *J* = 84 Hz) ppm. **HRMS (ESI):** calc. for $[C_{18}H_{34}O_2N_2BP+H]^+$: 353.2529, found: 353.2522

(*R*)-2-(((*R*)-*tert*-butyl(methyl)phosphanyl)amino)-N-((*R*)-1-hydroxy-2-phenyl)-3-methylbutanamide borane, 5.7c-Ph

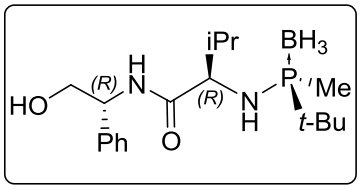

Compound **5.7c-Ph** was synthesized following **GM2**. This compound is described in Albert Cabré's PhD thesis.

(*S*)-2-(((*R*)-*tert*-butyl(methyl)phosphanyl)amino)-N-((*R*)-1-hydroxy-2-phenyl)-3-methylbutanamide borane, 5.7d-Ph

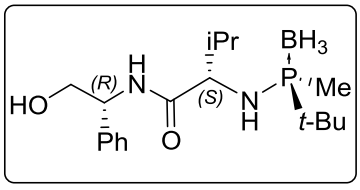

Compound **5.7d-Ph** was synthesized following **GM2**. White solid. **Yield:** 23% (170 mg). **M_P:** 123.5 – 124.5 ºC. **[α]D** –65.3 (c 0.37, $CHCl_3$). **IR (KBr) υ_{max}:** 3326, 2960, 2378, 1646, 1543cm^{-1}. **^{1}H NMR (400 MHz, $CDCl_3$) δ;** 7.40 – 7.26 (m, 4H), 7.25 – 7.22 (m, 1H), 5.24 – 5.15 (m, 1H), 4.69 (dd, *J* = 10, 9 Hz, 1H), 4.15 – 4.03 (m, 1H), 4.06 – 3.94 (m, 1H), 2.35 (d, *J* = 10 Hz, 1H), 2.08 – 1.98 (m, 1H), 1.33 (d, *J* = 9 Hz, 3H), 1.12 (d, *J* = 14 Hz, 12H), 1.01 (d, *J* = 7 Hz, 3H), 0.99 (d, *J* = 7 Hz, 3H), 0.85 – 0.11 (m, 3H, BH_3) ppm. **^{13}C NMR ($CDCl_3$, 101 MHz) δ;** 169.7 (d, J_P

= 3 Hz, C), 141.8 (C), 128.8 (2 x CH), 127.6 (CH), 126.6 (2 x CH), 75.1 (CH_2), 69.3 (CH), 56.8 (d, J_P = 3 Hz, CH), 33.8 (d, J_P = 4 Hz, CH), 31.4 (d, J_P = 37 Hz, C), 24.7 (d, J_P = 4 Hz, 3 x CH_3), 18.5 (d, J_P = 67 Hz, CH_3), 10.6 (d, J_P = 43 Hz, CH_3) ppm. **^{31}P NMR (162 MHz, $CDCl_3$) δ;** 75.2–69.9 (m, P–BH_3) ppm. **HRMS (ESI):** calc. for $[C_{18}H_{34}BN_2O_2P + H]^+$: 353.2524, found 353.2520.

(*R*)-2-(((*R*)-*tert*-butyl(methyl)phosphanyl)amino)-N-((*S*)-1-hydroxy-3-methylbutan-2-yl)-3-methylbutanamide borane, 5.7a-iPr

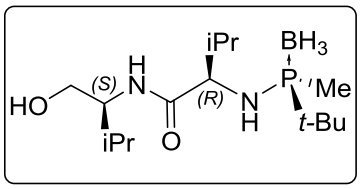

Compound **5.7a-iPr** was synthesized following **GM2**. White solid. **Yield:** 69% (230 mg). **Mp**: 128–129 ºC. **[α]$_D$:** –21.8 (c 0.68, $CHCl_3$). **IR (KBr) υ$_{max}$:** 3322, 2962, 2391, 1652, 1539 cm^{-1}. **^{1}H NMR (400 MHz, $CDCl_3$) δ;** 5.87 (br s, 1H), 3.80 – 3.72 (m, 2H), 3.71 – 3.64 (m, 1H), 3.40 (dt, *J* = 11, 8 Hz, 1H), 2.62 (br s, 1H), 2.11 (dd, *J* = 11, 5 Hz, 1H), 1.96 – 1.83 (m, 2H), 1.31 (d, J_P = 9 Hz, 3H), 1.15 (d, J_P = 14 Hz, 9H), 1.01 – 0.93 (m, 12H), 0.81 – 0.06 (m, 3H, BH_3) ppm. **^{13}C NMR (101 MHz, $CDCl_3$) δ;** 175.0 (C), 63.9 (CH_2), 63.3 (CH), 57.4 (CH), 32.8 (d, J_P = 8 Hz, CH), 30.57 (d, J_P = 46 Hz, C), 28.9 (CH), 24.3 (d, J_P = 3 Hz, 3 x CH_3), 19.7 (CH_3), 19.6 (CH_3), 18.9 (CH_3), 18.6 (CH_3), 10.4 (d, J_P = 33 Hz, CH_3) ppm. **^{31}P NMR (202 MHz, $CDCl_3$) δ;** 71.1 (m, P–BH_3) ppm. **HRMS (ESI):** calc. for $[C_{15}H_{36}BN_2O_2P + H]^+$: 319.2680, found 319.2680.

(*S*)-2-(((*R*)-*tert*-butyl(methyl)phosphanyl)amino)-N-((*S*)-1-hydroxy-3-methylbutan-2-yl)-3-methylbutanamide borane, 5.7b-iPr

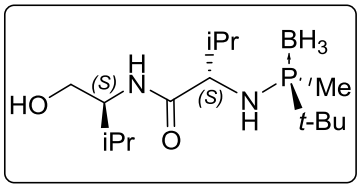

Compound **5.7b-iPr** was synthesized following **GM2**. White solid. **Yield:** 34% (104 mg). **Mp**: 111–112 ºC. **[α]$_D$:** –47.3 (c 0.84, $CHCl_3$). **IR (KBr) υ$_{max}$:** 3310, 2956, 2377, 1645, 1539cm^{-1}. **^{1}H NMR (400 MHz, $CDCl_3$) δ;** 6.06 (br s, 1H), 3.77 – 3.61 (m, 3H), 3.55 (td, *J* = 10, 6 Hz, 1H), 2.65 (br s, 1H), 2.22 (br d, *J* = 10 Hz, 1H), 2.05 – 1.85 (m, 2H), 1.35 (d, J_P = 9 Hz, 3H), 1.12 (d, J_P = 14 Hz, 9H), 0.99 – 0.91 (m, 12H), 0.81 – 0.06 (m, 3H, BH_3) ppm. **^{13}C NMR (101 MHz, $CDCl_3$) δ;** 173.2 (d, J_P = 2 Hz, C), 63.0 (CH_2), 61.8 (CH), 56.6 (CH), 31.7 (d, J_P = 4 Hz, CH), 29.8 (d, J_P = 39 Hz, C), 27.8 (CH), 23.5 (d, J_P = 3 Hz, 3 x CH_3), 18.5 (CH_3), 18.4 (CH_3), 17.9 (CH_3), 17.1 (CH_3), 9.6 (d, J_P = 40 Hz, CH_3) ppm. **^{31}P NMR(202 MHz, $CDCl_3$) δ;** 74.0– 71.7

(m, P–BH_3) ppm. **HRMS (ESI):** calc. for $[C_{15}H_{36}BN_2O_2P + H]^+$: 319.2680, found 319.2681.

(*R*)-2-(((*R*)-*tert*-butyl(methyl)phosphanyl)amino)-N-((*R*)-1-hydroxy-3-methylbutan-2-yl)-3-methylbutanamide borane, 5.7c-iPr

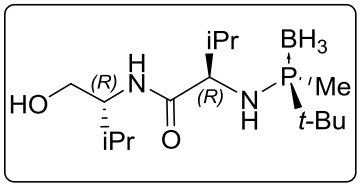

Compound **5.7c-iPr** was synthesized following **GM2**. White solid. **Yield:** 82% (261 mg). **Mp**: 114–115 ºC. **[α]$_D$:** +17.4 (c 0.97, $CHCl_3$). **IR (KBr) υ$_{max}$:** 3316, 2962, 2381, 1649, 1537 cm^{-1}. **^{1}H NMR (400 MHz, $CDCl_3$) δ;** 6.13 (br s, 1H), 3.77 – 3.64 (m, 3H), 3.49 (ddd, *J* = 11, 9, 7 Hz, 1H), 2.21 (dd, *J* = 11, 5 Hz, 1H), 2.01 – 1.84 (m, 2H), 1.27 (d, J_P = 9 Hz, 3H), 1.15 (d, J_P = 14 Hz, 9H), 1.01 – 0.95 (m, 12H), 0.81 – 0.06 (m, 3H, BH_3) ppm.. **^{13}C NMR (101 MHz, $CDCl_3$) δ;** 174.7 (C), 63.8 (CH_2), 62.8 (CH), 57.4 (CH), 33.1 (d, J_P = 8 Hz, CH), 30.5 (d, J_P = 46 Hz, C), 28.9 (CH), 24.4 (d, J_P = 3 Hz, 3 x CH_3), 19.5 (CH_3), 19.5 (CH_3), 18.9 (CH_3), 18.5 (CH_3), 10.4 (d, J_P = 32 Hz, CH_3) ppm. **^{31}P NMR(202 MHz, $CDCl_3$) δ;** 72.5 – 69.9 (m, P–BH_3) ppm. **HRMS (ESI):** calc. for $[C_{15}H_{36}BN_2O_2P + H]^+$: 319.2680, found 319.2669.

(*S*)-2-(((*R*)-*tert*-butyl(methyl)phosphanyl)amino)-N-((*R*)-1-hydroxy-3-methylbutan-2-yl)-3-methylbutanamide borane, 5.7d-iPr

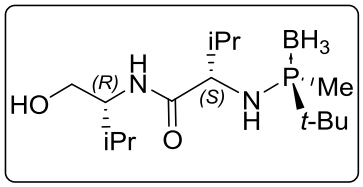

Compound **5.7d-iPr** was synthesized following **GM2**. White solid. **Yield:** 60% (644 mg). **Mp**: 120 – 121 ºC. **[α]$_D$:** –2.36 (c 0.70, $CHCl_3$). **IR (KBr) υ$_{max}$:** 3344 2962, 2381, 1651, 1529 cm^{-1}. **^{1}H NMR (400 MHz, $CDCl_3$) δ;** 6.04 (br d, *J* = 8 Hz, 1H), 3.75 – 3.69 (m, 1H), 3.67 (br s, 1H), 3.66 (br s, 1H), 3.55 – 3.46 (m, 1H), 2.30 (br d, *J* = 10 Hz, 1H), 1.98 – 1.84 (m, 2H), 1.33 (d, J_P = 9 Hz, 3H), 1.12 (d, J_P = 14 Hz, 9H), 0.99 – 0.92 (m, 12H), 0.81 – 0.06 (m, 3H, BH_3) ppm. **^{13}C NMR (101 MHz, $CDCl_3$) δ;** 174.3 (d, J_P = 2 Hz, C), 63.7 (CH_2), 63.1 (d, J_P = 2 Hz, CH), 57.5 (CH), 32.8 (d, J_P = 4 Hz, CH), 30.7 (d, J_P = 39 Hz, C), 28.9 (CH), 24.5 (d, J_P = 3 Hz, 3 x CH_3), 19.6 (CH_3), 19.5 (CH_3), 18.9 (CH_3), 18.2 (CH_3), 11.1 (d, J_P = 42 Hz, CH_3) ppm. **^{31}P NMR(202 MHz, $CDCl_3$) δ;** 74.1 – 72.1 (m, P–BH_3) ppm. **HRMS (ESI):** calc. for $[C_{15}H_{36}BN_2O_2P + H]^+$: 318.2680, found 319.2669.

(*R*)-2-(((*R*)-*tert*-butyl(methyl)phosphanyl)amino)-N-((*S*)-1-hydroxy-3,3-dimethylbutan-2-yl)-3-methylbutanamide borane, 5.7a-*t*-Bu

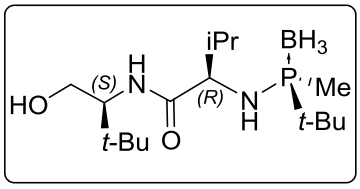

Compound **5.7a-*t*-Bu** was synthesized following **GM2**. White solid. **Yield:** 69% (230 mg). **Mp**: 140 – 141 ºC. **[α]D:** –9.2 (c 0.98, $CHCl_3$). **IR (KBr) υ_{max}:** 3256, 2961, 2354, 1644, 1564 cm^{-1}. **^{1}H NMR (400 MHz, $CDCl_3$) δ;** 5.95 (br d, *J* = 9 Hz, 1H), 3.90–3.77 (m, 2H), 3.65–3.57 (m, 1H), 3.51–3.44 (m, 1H), 2.72 (br s, 1H), 2.22–2.13 (m, 1H), 1.95–1.86 (m, 1H), 1.31 (d, *J* = 9 Hz, 3H), 1.13 (d, J_P = 14 Hz, 9H), 0.99–0.94 (m, 15H), 0.84–0.03 (m, 3H, BH_3) ppm. **^{13}C NMR (101 MHz, $CDCl_3$) δ;** 175.6 (C), 63.5 (CH), 63.3 (CH_2), 60.3 (CH), 33.4 (3 x CH_3), 32.9 (d, J_P = 8 Hz, CH), 30.7 (d, *J* = 47 Hz, C), 27.2 (3 x CH_3), 24.5 (d, J_P = 3 Hz, 3 x CH_3), 19.9 (CH_3), 18.7 (CH_3), 10.5 (d, J_P = 33 Hz, CH_3) ppm. **^{31}P NMR (202 MHz, $CDCl_3$) δ;** 70.3 – 71.8 (m, P–BH_3) ppm. **HRMS (ESI):** calc. for $[C_{16}H_{38}BN_2O_2P + H]^+$: 333.2837, found 333.2836.

(*S*)-2-(((*R*)-*tert*-butyl(methyl)phosphanyl)amino)-N-((*S*)-1-hydroxy-3,3-dimethylbutan-2-yl)-3-methylbutanamide borane, 5.7b-*t*-Bu

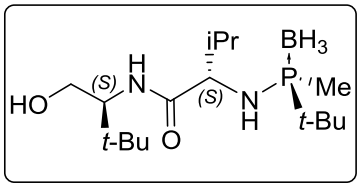

Compound **5.7b-*t*-Bu** was synthesized following **GM2**. This compound is described in Albert Cabré's PhD thesis.

(*R*)-2-(((*R*)-*tert*-butyl(methyl)phosphanyl)amino)-N-((*R*)-1-hydroxy-3,3-dimethylbutan-2-yl)-3-methylbutanamide borane, 5.7c-*t*-Bu

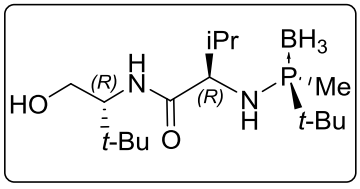

Compound **5.7c-*t*-Bu** was synthesized following **GM2**. This compound is described in Albert Cabré's PhD thesis.

(*S*)-2-(((*R*)-*tert*-butyl(methyl)phosphanyl)amino)-*N*-((*R*)-1-hydroxy-3,3-dimethylbutan-2-yl)-3-methylbutanamide borane, 5.7d-*t*-Bu

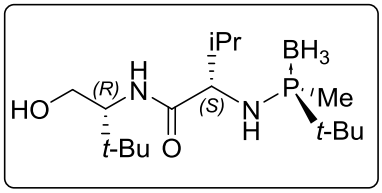

Compound **5.7d-*t*-Bu** was synthesized following **GM2**. White Solid. **Yield:** 63% (336 mg). **Mp**: 122–123 ºC. **[α]D:** +7.3 (c 1.00, $CHCl_3$). **IR (KBr) υ_{max}:** 3348, 2962, 2381, 1658, 1526 cm^{-1}.**^{1}H NMR (400 MHz, $CDCl_3$) δ;** 5.98 (br d, *J* = 9 Hz, 1H), 3.86–3.70 (m, 2H), 3.64–3.49 (m, 2H), 2.70 (br s, 1H), 2.30 (br d, *J* = 10 Hz, 1H), 1.91 (hept, *J* = 7 Hz, 1H), 1.32 (d, J_P = 9.0 Hz, 3H), 1.11 (d, J_P = 14 Hz, 9H), 0.96 (d, *J* = 7 Hz, 3H), 0.96 (s, 9H), 0.93 (d, *J* = 7 Hz, 3H), 0.84–0.06 (m, 3H, BH_3) ppm. **^{13}C NMR (101 MHz, $CDCl_3$) δ;** 174.8 (d, J_P = 2 Hz, C), 63.4 (CH_2), 63.2 (d, J_P = 3 Hz, CH), 60.3 (CH), 33.6 (C), 32.9 (d, J_P = 4 Hz, CH), 30.8 (d, J_P= 39 Hz, C), 27.2 (3 x CH_3), 24.6 (d, J_P = 3 Hz, 3 x CH_3), 19.8 (CH_3), 18.2 (CH_3), 11.3 (d, J_P = 41 Hz, CH_3) ppm. **^{31}P NMR (162 MHz, $CDCl_3$) δ;** 72.1–74.5 (m, P–BH_3) ppm. **HRMS (ESI):** calc. for $[C_{16}H_{38}BN_2O_2P + H]^+$: 333.2837, found 333.2844.

General Method 3: Synthesis of phosphino-oxazolines, 5.8

The corresponding aminophosphane (**5.7**) (1 eq) was dissolved in CH_2Cl_2 (0.08 M) and $SOCl_2$ (2.4 eq) was added drop wise at 0 ºC. The solution was stirred 4 h at room temperature. The solution was then cooled down to 0 ºC and $NaHCO_3$ saturated aqueous solution was added slowly until pH 8-9. The mixture was left stirring for 15 min at room temperature. The two phases were separated and the aqueous phase was extracted twice with CH_2Cl_2. The combined organic layers were washed with brine. The organic layer was dried over $MgSO_4$ and concentrated on a rotary evaporator under reduced pressure. When required, purification by column chromatography (SiO_2, hexanes:EtOAc) yielded the desired products as white solids or colourless oils.

(*R*)-1-*tert*-butyl-1-methyl-*N*-((*R*)-2-methyl-1-((*S*)-4-phenyl-4,5-dihydrooxazol-2-yl)propyl)phosphanamine borane, 5.8a-Ph[3]

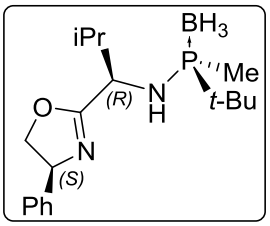

This compound is described in Sílvia Orgué's PhD thesis.

(*R*)-1-*tert*-butyl-1-methyl-*N*-((*S*)-2-methyl-1-((*S*)-4-phenyl-4,5-dihydrooxazol-2-yl)propyl)phosphanamine borane, 5.8b-Ph

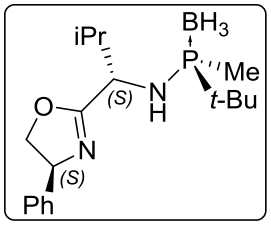

Compound **5.8b-Ph** was synthesized following **GM3**.

White solid. **M_P**= 48 – 49 ºC; **$[\alpha]_D$** = –46.9 (c 0.78, $CHCl_3$). **IR (KBr) υ_{max}:** 3347, 2962, 2380, 1660, 1138 cm^{-1}. **^{1}H NMR (400 MHz, $CDCl_3$) δ;** 7.37 – 7.30 (m, 2H), 7.32 – 7.24 (m, 3H), 5.24 – 5.13 (m, 1H), 4.71 – 4.62 (m, 1H), 4.17 (t, *J* = 9 Hz, 1H), 4.09 – 3.98 (m, 1H), 2.29 (d, *J* = 11 Hz, 1H), 2.09 – 1.95 (m, 1H), 1.34 (d, J_P = 9 Hz, 3H), 1.11 (d, J_P = 14 Hz, 9H), 1.00 (d, *J* = 7 Hz, 3H), 0.97 (d, *J* = 7 Hz, 3H), 0.80 – 0.06 (m, P–BH3) ppm. **^{13}C NMR (101 MHz, $CDCl_3$) δ;** 169.3 (d, *J* = 3 Hz, C), 141.6 (C), 128.6 (2 x CH), 127.6 (CH), 126.7 (2 x CH), 74.9, 69.4, 56.8 (d, *J* = 3 Hz, CH), 33.6 (d, J_P = 3 Hz, CH), 31.3 (d, *J* = 37 Hz, C), 24.7 (d, J_P = 3 Hz, 3 x CH_3), 18.8 (CH_3), 18.0 (CH_3), 10.5 (d, J_P = 42 Hz, CH_3) ppm. **^{31}P NMR (162 MHz, $CDCl_3$) δ;** 73.8 – 72.6 (m, *J* = 81 Hz, P–BH_3) ppm. **HRMS (ESI):** calc. for $[C_{18}H_{33}ON_2BP]^+$: 335.2418, found: 335.2416.

(*R*)-1-*tert*-butyl-1-methyl-*N*-((*R*)-2-methyl-1-((*R*)-4-phenyl-4,5-dihydrooxazol-2-yl)propyl)phosphanamine borane, 5.8c-Ph

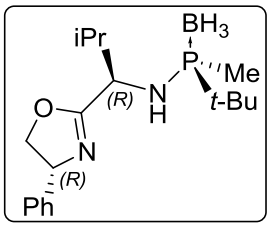

Compound **5.8c-Ph** was synthesized following **GM3**.

This compound is described in Albert Cabré's PhD thesis

(*R*)-1-*tert*-butyl-1-methyl-*N*-((*S*)-2-methyl-1-((*R*)-4-phenyl-4,5-dihydrooxazol-2-yl)propyl)phosphanamine borane, 5.8d-Ph

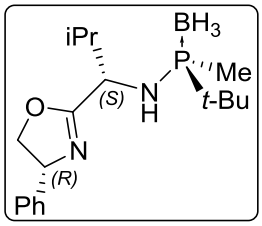

Compound **5.8d-Ph** was synthesized following **GM3**.

Waxy solid. **Yield:** 70% (67 mg). **[α]D:** –34.31 (c 0.43, $CHCl_3$). **IR (KBr) υmax:** 3344, 2965, 2380, 1661, 1466 cm^{-1}. **^{1}H NMR (400 MHz, $CDCl_3$) δ;** 7.40 – 7.26 (m, 4H), 7.25 – 7.22 (m, 1H), 5.24 – 5.15 (m, 1H), 4.69 (dd, *J* = 10, 9 Hz, 1H), 4.15 – 4.03 (m, 1H), 4.06 – 3.94 (m, 1H), 2.35 (d, *J* = 10 Hz, 1H), 2.08 – 1.98 (m, 1H), 1.33 (d, *J* = 9 Hz, 4H), 1.12 (d, *J* = 14 Hz, 9H), 1.01 (d, *J* = 7 Hz, 3H), 0.99 (d, *J* = 7 Hz, 3H), 0.80 – 0.06 (m, P–BH3) ppm. **^{13}C NMR (101 MHz, $CDCl_3$) δ;** 169.7 (d, J_P = 3 Hz, C), 141.8 (C), 128.8 (2 x CH), 127.6 (CH), 126.6 (2 x CH), 75.1 (CH_2), 69.3 (CH), 56.8 (d, J_P = 3 Hz, CH), 33.8 (d, J_P = 4 Hz, CH), 31.4 (d, J_P = 37 Hz, C), 24.7 (d, J_P = 3 Hz, 3 x CH_3), 18.8 (CH_3), 18,2 (CH_3), 10.6 (d, J_P = 43 Hz, CH_3) ppm. **^{31}P NMR (162 MHz, $CDCl_3$) δ;** 74.4 – 72.6 (m, P–BH_3) ppm. **HRMS (ESI):** calc. for $[C_{18}H_{32}BN_2OP+H]^+$: 335.2418, found 335.2400.

(*R*)-1-*tert*-butyl-N-((*R*)-1-((*S*)-4-(iso-propyl)-4,5-dihydrooxazol-2-yl)-2-methylpropyl)-1-methylphosphanamine borane, 5.8a-iPr

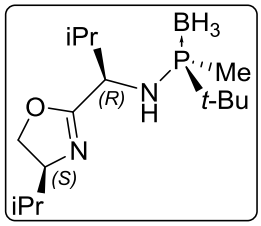

Compound **5.8a-iPr** was synthesized following **GM3**.

Colourless oil. **Yield:** 87% (66 mg). **[α]D:** –4.9 (c 0.96, $CHCl_3$). **IR (KBr) υmax:** 3331, 2962, 2379, 1666, 1467 cm^{-1}. **^{1}H NMR (400 MHz, $CDCl_3$) δ;** 4.33 – 4.25 (m, 1H), 3.94 (t, *J* = 8 Hz, 1H), 3.92 – 3.86 (m, 1H), 3.79 (td, *J* = 10, 6 Hz, 1H), 2.04 (br d, *J* = 10 Hz, 1H), 2.01 – 1.91 (m, 1H), 1.79 – 1.68 (m, 1H), 1.33 (d, J_P = 9 Hz, 3H), 1.15 (dd, J_P = 14, 1 Hz, 9H), 0.97 (d, *J* = 3 Hz, 3H), 0.96 (d, *J* = 3 Hz, 3H), 0.92 (d, *J* = 7 Hz, 3H), 0.88 (d, *J* = 7 Hz, 3H), 0.81 – 0.06 (m, 3H, BH_3) ppm. **^{13}C NMR (101 MHz, $CDCl_3$) δ;** 168.2 (C), 71.9 (CH), 70.4 (CH_2), 56.4 (CH), 33.0 (d, J_P = 6 Hz, CH), 32.5 (CH), 30.6 (d, J_P = 44 Hz, C), 24.6 (d, J_P = 3 Hz, 3 x CH_3), 19.2 (CH_3), 19.1 (CH_3), 18.3 (CH_3), 17.7 (CH_3), 9.8 (d, J_P = 33 Hz, CH_3) ppm. **^{31}P NMR(202 MHz, $CDCl_3$) δ;** 72.5 – 70.8 (m, P-BH_3) ppm. **HRMS (ESI):** calc. for $[C_{15}H_{34}BN_2OP+H]^+$: 301.2575, found 301.2571.

(*R*)-1-*tert*-butyl-N-((*S*)-1-((*S*)-4-(iso-propyl)-4,5-dihydrooxazol-2-yl)-2-methylpropyl)-1-methylphosphanamine borane, 5.8b-iPr

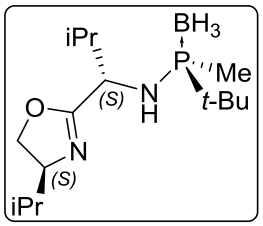

Compound **5.8b-iPr** was synthesized following **GM3**.

White Solid. **Yield:** 84% (71 mg). **Mp**: 55–56 ºC. **[α]$_D$:** –72.8 (c 0.86, $CHCl_3$). **IR (KBr) υ_{max}:** 3345, 2971, 2377, 1658, 1461 cm^{-1}. **^{1}H NMR (400 MHz, $CDCl_3$) δ;** 4.27 (dd, *J* = 10, 8 Hz, 1H), 3.99 (t, *J* = 8 Hz, 1H), 3.91 (td, *J* = 10, 5 Hz, 1H), 3.83 (dt, *J* = 10, 8 Hz, 1H), 2.31 (br d, *J* = 10 Hz, 1H), 2.04 – 1.87 (m, 1H), 1.74 – 1.58 (m, 1H), 1.33 (d, J_P = 9 Hz, 1H), 1.13 (d, J_P = 14 Hz, 3H), 0.99 (d, *J* = 7 Hz, 3H), 0.94 (d, *J* = 7 Hz, 3H), 0.90 (d, *J* = 7 Hz, 3H), 0.89 (d, *J* = 7 Hz, 3H), 0.81 – 0.06 (m, 3H, BH_3) ppm. **^{13}C NMR (101 MHz, $CDCl_3$) δ;** 168.0 (d, J_P = 3 Hz, C), 72.1 (CH), 70.8 (CH_2), 56.7 (d, J_P = 3 Hz, CH), 33.5 (d, J_P = 4 Hz, CH), 33.0 (CH), 31.3 (d, J_P = 37 Hz, C), 24.6 (d, J_P = 3 Hz, 3 x CH_3), 19.1 (CH_3), 18.7 (CH_3), 18.6 (CH_3), 17.8 (CH_3), 10.5 (d, J_P = 43 Hz, CH_3) ppm. **^{31}P NMR(202 MHz, $CDCl_3$) δ;** 73.7 – 71.5 (m, P-BH_3) ppm. **HRMS (ESI):** calc. for $[C_{15}H_{34}BN_2OP + H]^+$: 301.2575, found 301.2575.

(*R*)-1-*tert*-butyl-N-((*R*)-1-((*R*)-4-(iso-propyl)-4,5-dihydrooxazol-2-yl)-2-methylpropyl)-1-methylphosphanamine borane, 5.8c-iPr

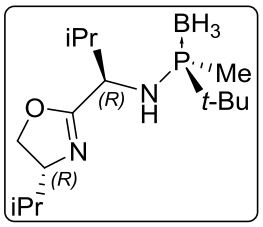

Compound **5.8c-iPr** was synthesized following **GM3**.

Colourless oil. **Yield:** 84% (118 mg). **[α]$_D$:** +63.6 (c 0.99, $CHCl_3$). **IR (KBr) υ_{max}:** 3331, 2962, 2380, 1665, 1466 cm^{-1}. **^{1}H NMR (400 MHz, $CDCl_3$) δ;** 4.27 (dd, *J* = 10, 8 Hz, 1H), 4.03 (t, *J* = 8 Hz, 1H), 3.93 – 3.81 (m, 2H), 2.12 – 1.98 (m, 2H), 1.81 – 1.66 (m, 1H), 1.37 (d, J_P = 9 Hz, 3H), 1.15 (d, J_P = 14 Hz, 9H), 0.98 (d, *J* = 7 Hz, 6H), 0.90 (d, *J* = 7 Hz, 3H), 0.88 (d, *J* = 7 Hz, 3H), 0.81 – 0.06 (m, 3H, BH_3) ppm. **^{13}C NMR (101 MHz, $CDCl_3$) δ;** 169.0 (C), 71.9 (CH), 70.9 (CH_2), 56.4 (CH), 32.8 (CH), 32.6 (d, J_P = 6 Hz, CH), 30.6 (d, J_P = 45 Hz, C), 24.5 (d, J_P = 3 Hz, 3 x CH_3), 19.4 (CH_3), 19.0 (CH_3), 18.5 (CH_3), 17.2 (CH_3), 10.2 (d, J_P = 33 Hz, CH_3) ppm. **^{31}P NMR (202 MHz, $CDCl_3$) δ;** 73.0 – 71.3 (m, P-BH_3) ppm. **HRMS (ESI):** calc. for $[C_{15}H_{34}BN_2OP + H]^+$: 301.2575, found 301.2565.

(*R*)-1-*tert*-butyl-N-((*S*)-1-((*R*)-4-(iso-propyl)-4,5-dihydrooxazol-2-yl)-2-methylpropyl)-1-methylphosphanamine borane, 5.8d-iPr

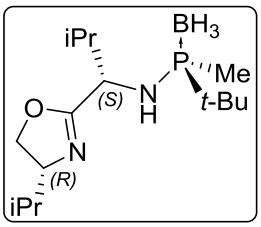

Compound **5.8d-iPr** was synthesized following **GM3**.

White Solid. **Yield:** 93% (86 mg). **Mp**: 55–56 ºC. **[α]$_D$:** –10.6 (c 1.02, $CHCl_3$). **IR (KBr) υ_{max}:** 3348, 2962, 2382, 1667, 1467 cm^{-1}. **^{1}H NMR (400 MHz, $CDCl_3$) δ;** 4.28 (dd, *J* = 9, 8 Hz, 1H), 3.96 – 3.91 (m, 1H), 3.90 – 3.82 (m, 2H), 2.25 (br d, *J* = 11 Hz, 1H), 2.00 – 1.85 (m, 1H), 1.79 – 1.64 (m, 1H), 1.33 (d, J_P = 9 Hz, 3H), 1.11 (d, J_P = 9.0 Hz, 9H), 0.97 (d, *J* = 7 Hz, 3H), 0.95 – 0.91 (m, 9H), 0.88 (d, *J* = 7 Hz, 3H), 0.81 – 0.06 (m, 3H, BH_3) ppm. **^{13}C NMR (101 MHz, $CDCl_3$) δ;** 167.9 (d, J_P = 2 Hz, C), 72.0 (CH), 70.5 (CH_2), 56.8 (d, J_P = 2 Hz, CH), 33.5 (d, J_P = 4 Hz, CH), 32.6 (CH), 31.3 (d, J_P = 37 Hz, C), 24.6 (d, J_P = 3 Hz, 3 x CH_3), 19.1 (CH_3), 18.8 (CH_3), 18.4 (CH_3), 18.0 (CH_3), 10.5 (d, J_P = 43 Hz, CH_3) ppm. **^{31}P NMR (202 MHz, $CDCl_3$) δ;** 74.6 – 71.4 (m, P-BH_3) ppm. **HRMS (ESI):** calc. for $[C_{15}H_{34}BN_2OP + H]^+$: 301.2575, found 301.2565.

(*R*)-1-*tert*-butyl-N-((*R*)-1-((*S*)-4-(tert-butyl)-4,5-dihydrooxazol-2-yl)-2-methylpropyl)-1-methylphosphanamine borane, 5.8a-*t*-Bu

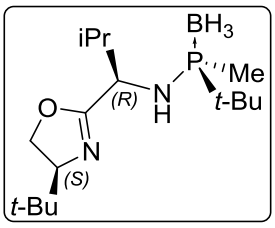

Compound **5.8a-*t*-Bu** was synthesized following **GM3**.

White Solid. **Yield:** 99% (667 mg). **Mp**: 55–56 ºC. **[α]$_D$:** –3.0 (c 1.00, $CHCl_3$). **IR (KBr) υ_{max}:** 3334, 2961, 2379, 1667, 1365 cm^{-1}. **^{1}H NMR (400 MHz, $CDCl_3$) δ;** 4.24 (dd, *J* = 10, 9 Hz, 1H), 3.99 (t, *J* = 9 Hz, 1H), 3.89 – 3.73 (m, 2H), 2.08 – 1.84 (m, 2H), 1.32 (d, J_P = 9 Hz, 3H), 1.14 (d, J_P = 14 Hz, 9H), 0.96 (d, *J* = 7 Hz, 3H), 0.91 – 0.86 (m, 12H), 0.83 – 0.01 (m, 3H, BH_3) ppm. **^{13}C NMR (101 MHz, $CDCl_3$) δ;** 168.5 (C), 75.7 (CH), 69.2 (CH_2), 56.5 (CH), 33.5 (C), 33.0 (d, J_P = 6 Hz, CH), 30.8 (d, J_P = 44 Hz, C), 26.2 (3 x CH_3), 24.7 (d, J_P = 3 Hz, 3 x CH_3), 19.4 (CH_3), 17.7 (CH_3), 10.0 (d, J_P = 33 Hz, CH_3) ppm. **^{31}P NMR (202 MHz, $CDCl_3$) δ;** 73.4 – 69.5 (m, P–BH_3) ppm. **HRMS (ESI):** calc. for $[C_{16}H_{36}BN_2OP + H]^+$: 315.2731, found 315.2733.

(*R*)-1-*tert*-butyl-N-((*S*)-1-((*S*)-4-(tert-butyl)-4,5-dihydrooxazol-2-yl)-2-methylpropyl)-1-methylphosphanamine borane, 5.8b-*t*-Bu

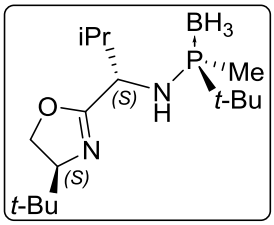

Compound **5.8b-*t*-Bu** was synthesized following **GM3**. This compound is described in Albert Cabré's PhD thesis

(*R*)-1-*tert*-butyl-N-((*R*)-1-((*R*)-4-(tert-butyl)-4,5-dihydrooxazol-2-yl)-2-methylpropyl)-1-methylphosphanamine borane, 5.8c-*t*-Bu

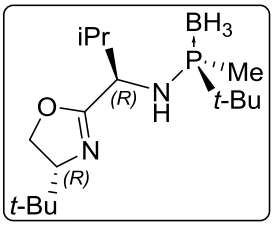

Compound **5.8c-*t*-Bu** was synthesized following **GM3**. This compound is described in Albert Cabré's PhD thesis

(*R*)-1-*tert*-butyl-N-((*S*)-1-((*R*)-4-(*tert*-butyl)-4,5-dihydrooxazol-2-yl)-2-methylpropyl)-1-methylphosphanamine borane, 5.8d-*t*-Bu

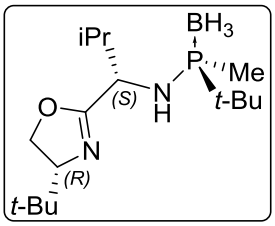

Compound **5.8d-*t*-Bu** was synthesized following **GM3**. White solid. **Yield:** 69% (182 mg). **Mp**: 84–85 ºC. **[α]D:** –11.3 (c 1.00, $CHCl_3$). **IR (KBr) υ_{max}:** 3349, 2960, 2384, 1669, 1365 cm^{-1}. **^{1}H NMR (400 MHz, $CDCl_3$) δ;** 4.23 (dd, *J* = 10, 9 Hz, 1H), 3.98 (dd, *J* = 10, 9 Hz, 1H), 3.92 – 3.77 (m, 2H), 2.41 – 2.22 (m, 1H), 2.00 – 1.86 (m, 1H), 1.32 (d, *J* = 9 Hz, 3H), 1.10 (d, *J* = 14 Hz, 9H), 0.94 (d, *J* = 7 Hz, 3H), 0.91 – 0.86 (m, 12H), 0.84 – 0.06 (m, 3H, BH_3) ppm. **^{13}C NMR (101 MHz, $CDCl_3$) δ;** 168.2 (C), 75.7 (CH), 69.2 (CH_2), 56.8 (d, J_P = 3 Hz, CH), 33.5 (d, J_P = 4 Hz, CH), 33.4 (C), 31.5 (d, J_P = 37 Hz, C), 26.2 (3 x CH_3) 24.7 (d, J_P = 3 Hz, 3 x CH_3), 19.0 (CH_3), 17.9 (CH_3), 10.8 (d, J_P = 43 Hz, CH_3) ppm.**^{31}P NMR (202 MHz, $CDCl_3$) δ;** 75.0 – 71.3 (m, P–BH_3) ppm. **HRMS (ESI):** calc. for $[C_{16}H_{36}BN_2OP + H]^+$: 315.2731, found 315.2730.

General Method 4: Preparation of Ir-MaxPHOX complexes

The corresponding borane protected ligand (**5.8**) (1 eq) was dissolved in freshly distilled pyrrolidine (0.06 M) and stirred for 16 h at 90 ºC. Afterwards, pyrrolidine was removed *in vacuo*. When no pyrrolidine remained, the crude was further dried under vacuum for 30 min at 50 ºC (the crude was under N_2 during all the procedure). A solution of $[Ir(COD)(Cl)]_2$ (0.5 eq) in CH_2Cl_2 (0.06 M) was added to the free ligand via cannula. The resulting mixture was stirred for 40 min at room temperature. $NaBAr_F$ (1 eq) was then added and the solution was stirred 1 h more at room temperature. The resulting crude was filtered through a small plug of silica gel, (first washed with Et_2O) under N_2, eluting with hexanes:CH_2Cl_2 (50:50 to 0:100). An orange fraction was collected and concentrated to yield the corresponding Ir complexes as deep orange solids.

The Ir-MaxPHOX Catalysts

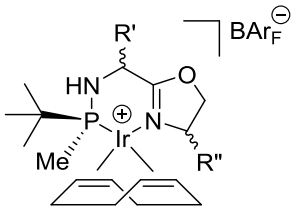

The 4 possible diastereoisomers

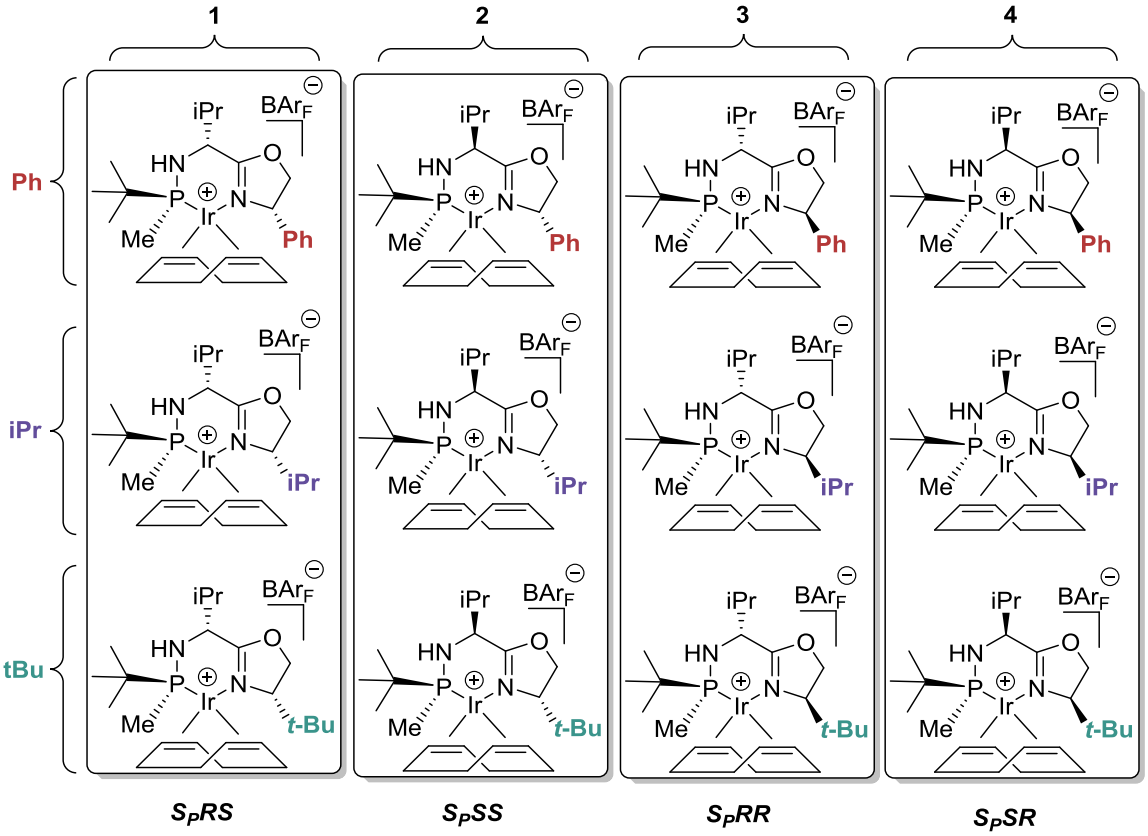

Ir-MaxPHOX catalyst 1Ph[3]

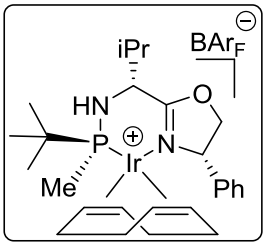

Compound **1Ph** was synthesized following **GM4**.

This compound is described in Sílvia Orgué's PhD thesis

Ir-MaxPHOX catalyst 2Ph

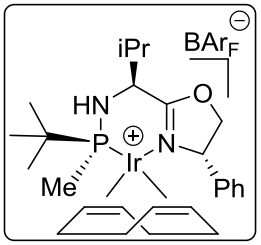

Compound **2Ph** was synthesized following **GM4**. This complex is unstable and decomposes easily.

Orange solid. **Yield:** 50% (131 mg). **M_P**= 130 – 131ºC. **$[\alpha]_D$** = +57.7 (c 0.65, CD_3Cl). **IR (KBr) υ_{max}:** 3408, 1635, 1277, 1125, 713 cm^{-1}. **^{1}H NMR (400 MHz, $CDCl_3$) δ**; 7.73 – 7.67 (m, 8H), 7.53 (s, 4H), 7.41 (qd, *J* = 5, 2 Hz, 3H), 7.18 – 7.10 (m, 2H), 5.03 (dd, *J* = 10, 5 Hz, 1H), 4.80 – 4.68 (m, 2H), 4.51 (dd, *J* = 9, 5 Hz, 1H), 4.30 (dd, 1H), 3.84 – 3.73 (m, 2H), 3.60 (dd, *J* = 7, 4 Hz, 1H), 2.28 – 2.09 (m, 2H), 2.12 – 1.95 (m, 2H), 1.97 – 1.85 (m, 2H), 1.74 (s, 4H), 1.29 (d, *J* = 8 Hz, 3H), 1.12 (d, *J* = 15 Hz, 9H), 1.14 – 1.07 (m, 6H) ppm. **HRMS (ESI):** calc. for $[C_{26}H_{41}IrN_2OP]^+$: 621,2580 found: 621.2574.

Ir-MaxPHOX catalyst 3Ph

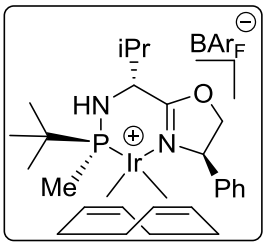

Compound **3Ph** was synthesized following **GM4**.

This compound is described in Albert Cabré's PhD thesis

Ir-MaxPHOX catalyst 4Ph

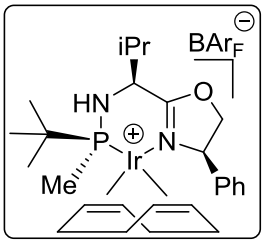

Compound **4Ph** was synthesized following **GM4**.

Orange solid. **Yield:** 22% (38 mg). **Mp**: 168 – 169 ºC. **$[\alpha]_D$:** –35.1 (c 0.31, $CHCl_3$). **IR (KBr) υ_{max}:** 2925, 1610, 1354, 1276, 1124 cm^{-1}. **^{1}H NMR (400 MHz, $CDCl_3$) δ;** 7.66 – 7.60 (m, 8H), 7.45 (s, 4H), 7.34 – 7.27 (m, 3H), 7.09 – 7.03 (m, 2H), 5.17 – 5.08 (m, 1H), 4.97 (dd, *J* = 10, 5 Hz, 1H), 4.81 – 4.63 (m, 3H), 3.99 – 3.90 (m, 1H), 3.53 – 3.39 (m, 1H), 3.44 – 3.34 (m, 1H), 2.50 – 2.37 (m, 1H), 2.21 – 1.87 (m, 6H), 1.75 – 1.57 (m, 2H), 1.41 (br s, 1H), 1.21 (d, *J* = 8 Hz, 3H), 1.04 – 0.94 (m, 6H), 0.84 (d, *J* = 15 Hz, 9H) ppm. **^{13}C NMR (101 MHz, $CDCl_3$) δ;** 175.5 (C), 161.7 (q, J_B = 50 Hz, 4 x C), 137.7 (C), 135 – 134.4 (m, 8 x CH), 129.9 (3 x CH), 129.4 – 128.3 (m, 8 x C), 126.8 (2 x CH), 124.5 (q, J_F = 273 Hz, 8 x CF_3), 117.4 (hept, J_F = 4 Hz, 4 x CH), 94.1 (d, J_P = 11 Hz, CH), 93.2 (d, J_P = 14 Hz, CH), 77.6 (CH_2), 67.7 (CH), 64.6 (CH), 58.2 (CH), 57.5 (CH), 36.3 (d, J_P = 42 Hz, C), 33.7 (CH_2), 31.3 (CH_2), 29.7 (CH_2), 28.8 (d, J_P = 9 Hz, CH), 28.0 (CH_2),

26.5 (d, J_P = 4 Hz, 3 x CH_3), 19.5 (CH_3), 16.8 (CH_3), 8.4 (d, J_P = 27 Hz, CH_3) ppm. **^{31}P NMR (162 MHz, $CDCl_3$) δ;** 62.4 (s) ppm. **HRMS (ESI):** calc. for $[C_{26}H_{41}IrN_2OP]^+$: 621.2580, found 621.2563.

Ir-MaxPHOX catalyst 1iPr

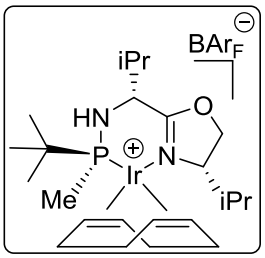

Compound **1iPr** was synthesized following **GM4**.

Orange solid. **Yield:** 84% (201 mg). **Mp**: 187.5 – 188.5 ºC. **[α]$_D$:** +61.9 (c 0.85, $CHCl_3$). **IR (KBr) υ$_{max}$:** 3417, 2969, 1604, 1348, 11271 cm^{-1}. **^{1}H NMR (400 MHz, $CDCl_3$) δ;** 7.72 – 7.66 (m, 8H), 7.53 (br s, 4H), 5.12 – 5.02 (m, 1H), 4.92 – 4.81 (m, 1H), 4.48 (dd, J = 10, 4 Hz, 1H), 4.27 (t, J = 10 Hz, 1H), 4.07 – 4.01 (m, 1H), 3.75 – 3.67 (m, 1H), 3.62 – 3.53 (m, 1H), 3.40 (ddd, J = 21, 10, 7 Hz, 1H), 2.80 – 2.67 (m, 1H), 2.30 – 1.98 (m, 7H), 1.97 – 1.76 (m, 3H), 1.34 (d, J_P = 8 Hz, 3H), 1.07 (d, J_P = 15 Hz, 9H), 1.00 (d, J = 7 Hz, 3H), 0.99 (d, J = 7 Hz, 3H), 0.89 (d, J = 7.0 Hz, 3H), 0.86 (d, J = 7 Hz, 3H) ppm. **^{13}C NMR (101 MHz, $CDCl_3$) δ;** 177.7 (d, J_P = 5 Hz, C), 161.7 (q, J_B = 50 Hz, 4 x C), 134.9 – 134.6 (m, 8 x CH), 129.5 – 128.2 (m, 8 x C), 124.5 (q, J_F = 273 Hz, 8 x CF_3), 117.4 (hept, J_F = 4 Hz, 4 x CH), 94.2 (d, J_P = 11 Hz, CH), 87.7 (d, J_P = 14 Hz, CH), 72.0 (CH), 70.5 (CH_2), 63.6 (CH), 60.7 (d, J_P = 5. Hz, CH), 58.1 (CH), 36.7 (d, J_P = 37 Hz, C), 35.2 (d, J_P = 5 Hz, CH), 32.6 (d, J_P = 3 Hz, CH_2), 31.8 (d, J_P = 3 Hz, CH_2), 30.6 (CH), 29.7 (d, J_P = 2 Hz, CH_2), 29.4 (CH_2), 25.5 (d, J_P = 4 Hz, 3 x (CH_3)), 19.1 (CH_3), 19.0 (CH_3), 18.9 (CH_3), 14.4 (CH_3), 8.4 (d, J_P = 35 Hz, CH_3) ppm. **^{31}P NMR(202 MHz, $CDCl_3$) δ;** 57.9 (s) ppm. **HRMS (ESI):** calc. for $[C_{23}H_{42}IrN_2OP]^+$: 587.2737, found 587.2735.

Ir-MaxPHOX catalyst 2iPr

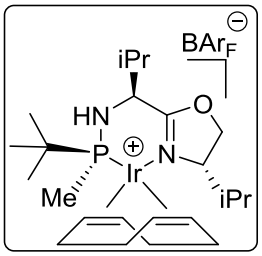

Compound **2iPr** was synthesized following **GM4**.

Orange solid. **Yield:** 90% (217 mg). **Mp**: 167 – 168 ºC. **[α]$_D$:** +72.6 (c 0.86, $CHCl_3$). **IR (KBr) υ$_{max}$:** 3410, 2965, 1610, 1361, 1270 cm^{-1}. **^{1}H NMR (400 MHz, $CDCl_3$) δ;** 7.75 – 7.67 (m, 8H), 7.53 (br s, 4H), 4.96 – 4.86 (m, 1H), 4.67 – 4.58 (m, 1H), 4.50 (dd, J = 10, 4 Hz, 1H), 4.28 (t, J = 10 Hz, 1H), 4.22 (br s, 1H), 3.98 (dt, J = 10, 4 Hz, 1H), 3.86 – 3.73 (m, 1H), 3.42 (ddd, J = 18, 10, 7 Hz, 1H), 2.37 – 2.24 (m, 1H), 2.23 – 2.00 (m, 6H), 1.97 – 1.92 (m, 1H), 1.91 – 1.84 (m, 1H), 1.77 – 1.66 (m, 2H), 1.41 (d, J_P = 7

Hz, 3H), 1.10 (d, J_P = 15 Hz, 9H), 1.08 (d, J = 7 Hz, 3H), 0.98 (d, J = 7.0 Hz, 3H), 0.91 (d, J = 7 Hz, 3H), 0.80 (d, J = 7 Hz, 3H) ppm. **^{13}C NMR (101 MHz, $CDCl_3$) δ;** 175.7 (C), 161.7 (q, J_B = 50 Hz, 4 x C), 134.8 (8 x CH), 129.39 – 128.27 (m, 8 x C), 124.5 (q, J_F = 273 Hz, 8 x CF_3), 117.4 (hept, J_F = 4 Hz, 4 x CH), 92.9 (d, J_P = 11 Hz, CH), 88.5 (d, J_P = 14 Hz, CH), 70.4 (CH_2), 69.6 (CH), 63.9 (CH), 60.1 (d, J_P = 4 Hz, CH), 57.6 (CH), 35.9 (d, J_P = 38 Hz, C), 35.0 (CH), 34.8 (CH_2), 31.7 (CH), 31.2 (CH_2), 30.6 (CH_2), 26.9 (CH_2), 25.8 (d, J_P = 4 Hz, 3 x CH_3), 20.1 (CH_3), 18.9 (CH_3), 18.6 (CH_3), 14.6 (CH_3), 12.3 (d, J_P = 32 Hz, CH_3) ppm. **^{31}P NMR(202 MHz, $CDCl_3$) δ;** 59.7 (s) ppm. **HRMS (ESI):** calc. for $[C_{23}H_{42}IrN_2OP]^+$: 587.2737, found 587.2742.

Ir-MaxPHOX catalyst 3iPr

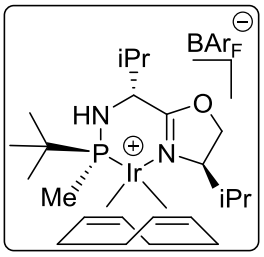

Compound **3iPr** was synthesized following **GM4**.

Orange solid. **Yield:** 81% (182 mg). **Mp**: 241 – 242 ºC. **[α]$_D$:** – 41.1 (c 0.55, $CHCl_3$). **IR (KBr) υ_{max}:** 3416, 2964, 1622, 1354, 1275 cm^{-1}. **^{1}H NMR (400 MHz, $CDCl_3$) δ;** 7.73 – 7.67 (m, 8H), 7.53 (br s, 4H), 4.84 – 4.75 (m, 1H), 4.67 – 4.59 (m, 1H), 4.54 (dd, J = 10, 4 Hz, 1H), 4.31 (t, J = 10 Hz, 1H), 3.88 (dt, J = 10, 4 Hz, 1H), 3.73 – 3.66 (m, 1H), 3.55 – 3.48 (m, 1H), 3.39 (ddd, J = 25, 10, 6 Hz, 1H), 2.42 – 2.31 (m, 3H), 2.27 – 2.16 (m, 3H), 2.15 – 2.02 (m, 2H), 1.85 – 1.75 (m, 1H), 1.74 – 1.62 (m, 2H), 1.34 (d, J_P = 8 Hz, 3H), 1.12 (d, J_P = 15 Hz, 9H), 1.04 (d, J = 7 Hz, 3H), 1.00 (d, J = 7 Hz, 3H), 0.89 (d, J = 7 Hz, 3H), 0.76 (d, J = 7 Hz, 3H) ppm. **^{13}C NMR (101 MHz, $CDCl_3$) δ;** 175.2 (d, J_P = 3 Hz, C), 161.7 (q, J_B = 50 Hz, 4 x C), 134.8 (8 x CH), 129.4 – 128.3 (m, 8 x C), 124.5 (q, J_F = 273 Hz, 8 x CF_3), 117.4 (hept, J_F = 4 Hz, 4 x CH), 92.6 (d, J_P = 13 Hz, CH), 92.0 (d, J_P = 11 Hz, CH), 70.1 (CH_2), 68.9 (CH), 63.8 (CH), 60.1 (d, J_P = 3 Hz, CH), 58.8 (CH), 40.0 (d, J_P = 6 Hz, CH), 36.2 (d, J_P = 42 Hz, C), 34.7 (d, J_P = 4 Hz, CH_2), 31.9 (CH), 30.7 (d, J_P = 2 Hz, CH_2), 30.4 (d, J_P = 3 Hz, CH_2), 27.1 (d, J_P = 2 Hz, CH_2), 26.4 (d, J_P = 4 Hz, 3 x (CH_3)), 20.2 (CH_3), 19.8 (CH_3), 18.4 (CH_3), 15.2 (CH_3), 10.8 (d, J_P = 29 Hz, CH_3) ppm. **^{31}P NMR(202 MHz, $CDCl_3$) δ;** 57.7 (s) ppm. **HRMS (ESI):** calc. for $[C_{23}H_{42}IrN_2OP]^+$: 587.2737, found 587.2716.

Ir-MaxPHOX catalyst 4iPr

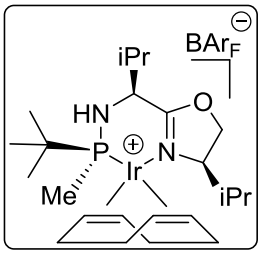

Compound **4iPr** was synthesized following **GM4**.

Orange solid. **Yield:** 60% (283 mg). **Mp**: 169 – 170 ºC. **[α]$_D$:** – 15.0 (c 0.62, $CHCl_3$). **IR (KBr) υ_{max}:** 3404, 2928, 1610, 1354, 1277 cm^{-1}. **^{1}H NMR (400 MHz, $CDCl_3$) δ;** 7.72 – 7.68 (m, 8H), 7.53 (br s, 4H), 4.92 – 4.84 (m, 1H), 4.68 – 4.60 (m, 1H), 4.57 (dd, *J* = 10, 4.0 Hz, 1H), 4.35 (t, *J* = 10 Hz, 1H), 3.97 – 3.85 (m, 2H), 3.65 – 3.52 (m, 2H), 2.49 – 2.38 (m, 1H), 2.38 – 2.28 (m, 1H), 2.26 – 2.02 (m, 5H), 1.84 – 1.69 (m, 3H), 1.47 – 1.44 (m, 1H), 1.32 (d, J_P = 7 Hz, 3H), 1.18 (d, J_P = 15 Hz, 9H), 1.01 (d, *J* = 7 Hz, 3H), 0.95 (d, *J* = 7 Hz, 3H), 0.93 (d, *J* = 7 Hz, 3H), 0.75 (d, *J* = 7 Hz, 3H) ppm. **^{13}C NMR (101 MHz, $CDCl_3$) δ;** 175.1 (C), 161.7 (q, J_B = 50 Hz, 4 x C), 134.8 (8 x CH), 129.5 – 128.3 (m, 8 x C), 124.5 (q, J_F = 273 Hz, 8 x CF_3), 117.40 (hept, J_F = 4 Hz, 4 x CH), 93.97 (d, J_P = 11 Hz, CH), 93.83 (d, J_P = 13 Hz, CH), 70.6 (CH_2), 68.7 (CH), 64.9 (CH), 57.8 (d, J_P = 2 Hz, CH), 57.5 (CH), 36.3 (d, J_P = 42 Hz, C), 33.9 (d, J_P = 3 Hz, CH_2), 31.57 (CH), 31.3 (d, J_P = 3 Hz, CH_2), 29.6 (d, J_P = 2 Hz, CH_2), 28.7 (d, J_P = 9 Hz, CH), 28.0 (d, J_P = 2 Hz, CH_2), 26.6 (d, J_P = 4. Hz, 3 x (CH_3)), 19.5 (CH_3), 19.4 (CH_3), 16.4 (CH_3), 14.6 (CH_3), 8.9 (d, J_P = 27 Hz, CH_3) ppm. **^{31}P NMR(202 MHz, $CDCl_3$) δ;** 62.1 (s) ppm. **HRMS (ESI):** calc. for $[C_{23}H_{42}IrN_2OP]^+$: 587.2737, found 587.2745.

Ir-MaxPHOX catalyst 1*t*-Bu

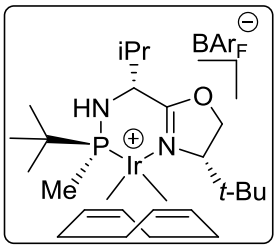

Compound **1*t*-Bu** was synthesized following **GM4**.

Orange solid. **Yield:** 58% (136 mg). **Mp**: 216 – 217 ºC. **[α]$_D$:** +79.0 (c 1.00, $CHCl_3$). **IR (KBr) υ_{max}:** 3404, 2970, 1608, 1353, 1276 cm^{-1}. **^{1}H NMR (400 MHz, $CDCl_3$) δ;** 7.70 (br s, 8H), 7.53 (s, 4H), 4.96 – 4.86 (m, 1H), 4.66 (dd, *J* = 10, 3 Hz, 1H), 4.59–4.52 (m, 1H), 4.35 – 4.24 (m, 2H), 4.11 – 3.99 (m, 1H), 3.95 – 3.87 (m, 1H), 3.81 (dd, *J* = 9, 3 Hz, 1H), 2.43 – 2.15 (m, 5H), 2.16 – 2.03 (m, 1H), 1.98 – 1.85 (m, 1H), 1.63 (d, J_P = 7 Hz, 3H), 1.52 – 1.41 (m, 2H), 1.37 (br d, *J* = 8 Hz, 1H), 1.11 (d, J_P = 15 Hz, 9H), 1.09 (d, *J* = 7 Hz, 3H),, 0.96 (s, 9H), 0.92 (d, *J* = 7 Hz, 3H) ppm. **^{13}C NMR (101 MHz, $CDCl_3$) δ;** 176.2 (C), 161.8 (q, J_B = 50 Hz, 4 x C), 134.9 (8 x CH), 129.0 (qq, J_F= 31, J_F= 3 Hz, 8 x C), 124.7 (q, J_F = 273 Hz, 8 x CF_3), 117.6 (sept, J_F = 4 Hz, 4 x CH), 94.3 (d, J_P = 11 Hz, CH), 90.5 (d, J_P = 14 Hz, CH), 72.4 (CH_2), 71.7 (CH), 61.1 (CH), 60.2 (d, J_P = 4 Hz, CH), 57.7 (CH), 37.5 (d, J_P = 35 Hz, C), 37.2 (d, J_P = 4 Hz, CH_2), 34.2 (C), 32.3 (d, J_P =

2 Hz, CH_2), 29.3 (CH_2), 28.6 (d, J_P = 8 Hz, CH), 25.5 (d, J_P = 3 Hz, 3 x CH_3), 25.4 (3 x CH_3), 24.7 (d, J_P = 2 Hz, CH_2), 20.7 (CH_3), 16.6 (CH_3), 13.8 (d, J_P = 32 Hz, CH_3) ppm. **^{31}P NMR (202 MHz, $CDCl_3$) δ;** 57.2 ppm. **HRMS (ESI):** calc. for $[C_{24}H_{45}IrN_2OP]^+$: 601.2893, found 601.2890.

Ir-MaxPHOX catalyst 2*t*-Bu

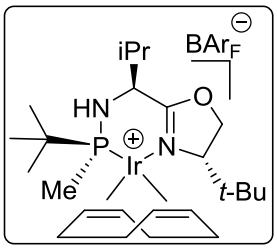

Compound **2*t*-Bu** was synthesized following **GM4**.

This compound is described in Albert Cabré's PhD thesis

Ir-MaxPHOX catalyst 3*t*-Bu

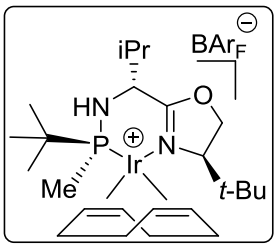

Compound **3*t*-Bu** was synthesized following **GM4**.

This compound is described in Albert Cabré's PhD thesis

Ir-MaxPHOX catalyst 4*t*-Bu

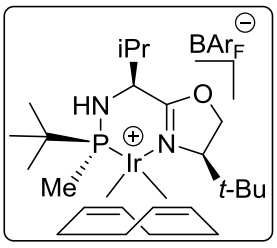

Compound **4*t*-Bu** was synthesized following **GM4**.

Orange solid. **Yield:** 75% (350 mg). **Mp**: 210 – 211 ºC. **[α]$_D$:** +39.7 (c 1.00, $CHCl_3$). **IR (KBr) υ_{max}:** 2971, 1597, 1354, 1277, 1135 cm^{-1}. **^{1}H NMR (400 MHz, $CDCl_3$) δ;** 7.70 (br m, 8H), 7.53 (br s, 4H), 4.88 – 4.71 (m, 2H), 4.67 (dd, J = 10, 3 Hz, 1H), 4.34 (t, J = 10 Hz, 1H), 3.98 (dt, J = 12, 3 Hz, 1H), 3.97 – 3.87 (m, 1H), 3.76 (dd, J = 9, 3 Hz, 1H), 3.48 – 3.33 (m, 1H), 2.56 – 2.44 (m, 1H), 2.43 – 2.35 (m, 2H), 2.31 – 2.18 (m, 1H), 2.18 – 2.08 (m, 1H), 2.08 – 1.91 (m, 2H), 1.66 – 1.47 (m, 2H), 1.38 (d, J_P = 8 Hz, 3H), 1.20 (d, J_P = 15 Hz, 9H), 1.01 (d, J = 7 Hz, 3H), 0.94 (s, 9H), 0.89 (d, J = 7 Hz, 3H) ppm. **^{13}C NMR (101 MHz, $CDCl_3$) δ;** 176.1 (C), 161.8 (q, J_B = 50 Hz, 4 x C), 134.9 (8 x CH), 129.0 (qq, ^2J_F= 31, ^4J_F= 3 Hz, 8 x C), 124.7 (q, J_F = 273 Hz, 8 x CF_3), 117.6 (sept, J_F = 4 Hz, 4 x CH), 95.3 (d, J_P = 12 Hz, CH), 93.0 (d, J_P = 13 Hz, CH), 72.6 (CH), 72.0 (CH_2), 62.4 (CH), 58.6 (CH), 57.5 (CH), 36.3 (d, J_P = 4 Hz, CH_2), 35.4 (d, J_P = 40 Hz, C), 33.9

(C), 31.5 (d, J_P = 2 Hz, CH_2), 29.7 (d, J_P = 2 Hz, CH_2), 28.8 (d, J_P = 9 Hz, CH), 27.1 (d, J_P = 4 Hz, 3 x CH_3), 25.6 (d, J_P = 2 Hz, CH_2), 24.7 (d, J_P = 2 Hz, CH_2), 25.4 (3 x CH_3), 19.8 (CH_3), 16.3 (CH_3), 10.0 (d, J_P = 26 Hz, CH_3) ppm. **^{31}P NMR (162 MHz, $CDCl_3$) δ;** 62.9 ppm. **HRMS (ESI):** calc. for $[C_{24}H_{45}IrN_2OP]^+$: 601.2893, found 601.2886.

REFERENCES

[1] P. Västilä, I. M. Pastor, H. Adolfsson, *J. Org. Chem.* **2005**, *70*, 2921–2929.

[2] I. M. Pastor, P. Västilä, H. Adolfsson, *Chem. - A Eur. J.* **2003**, *9*, 4031–4045.

[3] S. Orgué, A. Flores-Gaspar, M. Biosca, O. Pàmies, M. Diéguez, A. Riera, X. Verdaguer, *Chem. Commun.* **2015**, *51*, 17548–17551.

Experimental Section for Chapter 6

P-Stereogenic and Non P-Stereogenic Ir-MaxPHOX in the Asymmetric Hydrogenation of *N*-Aryl Imines

E. Salomó, P. Rojo, P. Hernández-Lladó, A. Riera, X. Verdaguer, *J. Org. Chem.* **2018**, *83*, 4618–4627.

SYNTHESIS OF NON P-STEREOGENIC Ir-MaxPHOX CATALYSTS

(*S*)-2-((diphenylphosphanyl)amino)-*N*-((*R*)-1-hydroxy-3-methylbutan-2-yl)-3-methylbutanamide borane, 6.3

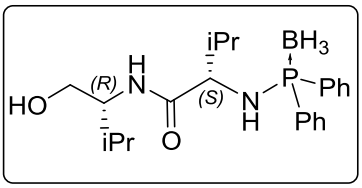

In a N_2 purged round bottom flask, 182 µL (0.989 mmol, 1 eq) of chlorodiphenylphosphine and 200 mg of amine (*R,S)*-**5.6-iPr** (0.989 mmol, 1 eq) were weighed. Then 15 mL of anhydrous CH_2Cl_2 were added. We observed the appearance of white solid. Then 152 µL of Et_3N (1.088 mmol, 1.1 eq) were added. The white solid dissolved. The reaction was left stirring for 1 h and then 141 µL of $BH_3.SMe_2$, (1.484 mmol, 1.5 eq), was dropwise added. The reaction was left stirring overnight at room temperature. The reaction mixture solvents were removed under reduced pressure and the crude was purified by column chromatography (SiO_2, hexanes:EtOAc), which yielded 313 mg (79%, 0.781 mmol) of product as a colorless oil.

Colorless oil. **Yield:** 79% (313 mg). **^{1}H NMR (400 MHz, $CDCl_3$) δ;** 7.74 – 7.55 (m, 4H), 7.54 – 7.37 (m, 6H), 5.88 (br d, *J* = 8 Hz, 1H), 3.65 – 3.50 (m, 2H), 3.39 (qd, *J* = 11, 4 Hz, 2H), 3.02 (d, *J* = 11 Hz, 1H), 2.03 – 1.95 (m, 1H), 1.80 (h, *J* = 7 Hz, 1H), 0.98 (d, *J* = 7 Hz, 3H), 0.93 (d, *J* = 7 Hz, 3H), 0.90 (d, *J* = 7 Hz, 3H), 0.86 (d, *J* = 7 Hz, 3H), 0.72 – 0.08 (m, BH_3) ppm. **^{13}C NMR (101 MHz, $CDCl_3$) δ;** 173.7 (d, *J* = 2 Hz, C), 133.0 (d, *J* = 26 Hz, C), 132.3 (d, *J* = 15 Hz, C), 131.6 (2 x CH) , 131.5 (2 x CH), 131.5 – 131.3 (m, 2 x CH), 128.7 (d, *J* = 6 Hz, 2 x CH), 128.6 (d, *J* = 7 Hz, 2 x CH), 63.4 (CH_2), 63.2 (CH), 57.5 (CH), 32.6 (d, *J* = 7 Hz, CH), 28.7 (CH), 19.5 (CH_3), 19.4 (CH_3), 18.8 (CH_3), 18.6 (CH_3) ppm. **HRMS (ESI):** calc. for $[C_{22}H_{34}O_2N_2BP + H]^+$: 401.2524, found 401.2519.

The compound could not be obtained pure enough to perform a proper IR spectra or a $[\alpha]_D$ analysis.

(*S*)-2-((di(*o*-tolyl)phosphanyl)amino)-*N*-((*R*)-1-hydroxy-3-methylbutan-2-yl)-3-methylbutanamide borane, 6.4

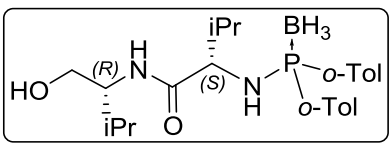

In a N_2 purged round bottom flask, 200 mg (0.804 mmol, 1 eq) of chlorodi(*o*-tolyl)phosphine and 179 mg of amine (*R,S)*-**5.6-iPr** (0.885 mmol, 1.1 eq) were weighed. Then 15 mL of anhydrous CH_2Cl_2 were added. We observed the appearance of white

solid. Then 135 µL of Et_3N (0.965 mmol, 1.2 eq) were added. The white solid dissolved. The reaction was left stirring for 1 h and then 114 µL of $BH_3.SMe_2$, (1.206 mmol, 1.5 eq), was dropwise added. The reaction was left stirring overnight at room temperature. The reaction mixture solvents were removed under reduced pressure and the crude was purified by column chromatography (SiO_2, hexanes:EtOAc), which yielded 213 mg (64%, 0.515 mmol) of product as a waxy solid.

Waxy solid. **Yield:** 64% (220 mg). **Mp**: 56 – 57 ºC. **^{1}H NMR (400 MHz, $CDCl_3$) δ;** 7.89 (ddt, *J* = 13, 8, 2 Hz, 2H), 7.43 – 7.36 (m, 2H), 7.35 – 7.27 (m, 2H), 7.20 – 7.12 (m, 2H), 5.82 (d, *J* = 8 Hz, 1H), 3.75 (td, *J* = 10, 7 Hz, 1H), 3.59 (dddd, *J* = 8, 7, 5, 4 Hz, 1H), 3.47 – 3.35 (m, 2H), 2.96 (dd, *J* = 10, 4 Hz, 1H), 2.24 (s, 1H), 2.10 (d, *J* = 14 Hz, 3H), 2.02 – 1.94 (m, 1H), 1.88 – 1.79 (m, 1H), 0.95 – 0.88 (m, 12H), 1.42 – 0.61 (m, 3H, BH_3) ppm. **^{13}C NMR (101 MHz, $CDCl_3$) δ;** 173.7 (d, J_P = 2 Hz, C), 140.8 (d, J_P = 9 Hz, CH), 140.7 (d, J_P = 8 Hz, CH), 132.4 (d, J_P = 10 Hz, CH), 132.3 (d, J_P = 10 Hz, CH), 131.9 (C), 131.9 – 131.7 (m, 2 x CH), 131.5 – 131.4 (m, 2 x CH), 130.7 (C), 126.2 (d, J_P = 6 Hz, CH), 126.1 (d, J_P = 6 Hz, CH), 63.6 (CH_2), 62.8 (d, J_P = 3 Hz, CH), 57.5 (CH), 32.8 (d, J_P = 6 Hz, CH), 28.7 (CH), 21.6 (d, J_P = 5 Hz, CH_3), 21.4 (d, J_P = 4 Hz, CH_3), 19.5 (CH_3), 19.3 (CH_3), 18.9 (CH_3), 18.8 (CH_3) ppm. **^{31}P NMR (202 MHz, $CDCl_3$) δ;** 55.9 (m, P-BH_3) ppm. . **HRMS (ESI):** calc. for $[C_{24}H_{38}O_2N_2BP + H]^+$: 429.2837, found 429.2835.

The compound could not be obtained pure enough to perform a proper IR spectra or a $[\alpha]_D$ analysis.

Dicyclohexyl phosphinous acid borane, 6.7[1]

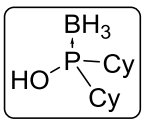

In a N_2 purged round bottom flask, 2 g (8.59 mmol, 1 eq) of chlorodicyclohexylphosphine were weighed. Then 8 mL of anhydrous THF were added and the reaction was cooled to 0 ºC. $BH_3.SMe_2$, 815 µL (8.59 mmol, 1 eq), was dropwise added. The reaction was left stirring 1 hour at room temperature. Then it was cooled again to 0 ºC and 2g (51.5 mmol, 6 eq) of NaOH dissolved in 32 mL of H_2O/THF (1/2) were slowly added. The solution was left stirring overnight at room temperature. Using a diluted solution of HCl the reaction was quenched and brought to neutral pH. It was then extracted thrice with Et_2O. The organic layers were dried over $MgSO_4$ and concentrated on a rotary evaporator under reduced pressure.

Purification by column chromatography (SiO_2, hexanes:EtOAc) yielded 1.67 g (85%, 7.3 mmol) of product as a white solid.

^{1}H NMR (400 MHz, $CDCl_3$) δ; 2.68 (br s, 1H), 1.92 – 1.68 (m, 12H), 1.56 – 1.40 (m, 2H), 1.40 – 1.20 (m, 8H), 0.97 – 0.01 (m, 3H, P–BH_3) ppm.

(*S*)-2-((dicyclohexylphosphanyl)amino)-*N*-((*S*)-1-hydroxy-3-methylbutan-2-yl)-3-methylbutanamide borane, (*S*,*S*)-6.8

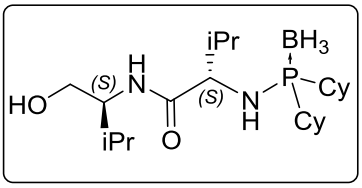

A solution of dicyclohexyl phosphinous acid borane (1 eq) and methansulfonic anhydride (1.2 eq) in CH_2Cl_2 (0.2M) was cooled to 0 ºC. To this solution, anhydrous NEt_3 (2.5 eq) was slowly added, and the mixture was stirred 1 h at 0 ºC. Amine (*S,S)*-**5.6-iPr** (1.5 eq) was then added and the solution was stirred overnight at room temperature. Water was added and the mixture was allowed to warm to room temperature. The organic layer was separated and the aqueous phase was extracted twice with CH_2Cl_2. The combined extracts were washed with brine and concentrated under reduced pressure. Purification by column chromatography (SiO_2, hexanes:EtOAc) yielded the corresponding products as a white solid.

White solid. **Yield:** 41% (150 mg). **Mp**: 200–201 ºC. **[α]$_D$:** –5.6 (c 0.53, $CHCl_3$). **IR (KBr) υ_{max}:** 3297, 2918, 2386, 2343 and 1648 cm^{-1}. **^{1}H NMR (400 MHz, $CDCl_3$) δ;** 5.9 (br d, *J* = 7 Hz, 1H), 3.75 – 3.60 (m, 3H), 3.52 (td, *J* = 10, 6 Hz, 1H), 2.77 (br s, 1H), 2.23 (dd, *J* = 10, 4 Hz, 1H), 1.95 – 1.60 (m, 14H), 1.43 – 1.15 (m, 10H), 0.99 (d, *J* = 4 Hz, 3H), 0.98 – 0.96 (m, 6H), 0.96 (d, *J* = 4 Hz, 3H), 0.78 – -0.07 (m, P–BH_3).ppm. **^{13}C NMR (101 MHz, $CDCl_3$) δ;** 174.3 (C), 63.9 (CH), 62.3 (CH), 57.7 (CH), 35.2 (d, J_P = 32 Hz, CH), 34.9 (d, J_P = 41 Hz, CH), 33.7 (d, J_P = 5 Hz, CH), 28.8 (CH), 26.8 – 25.2 (m, 10 x CH_2), 19.4 (CH_3), 19.0 (CH_3), 18.9 (CH_3), 18.7 (CH_3) ppm. **^{31}P NMR (202 MHz, $CDCl_3$) δ;** 73.3 – 71.1 (m, P–BH_3) ppm. **HRMS (ESI):** calc. for $[C_{22}H_{46}O_2N_2BP + H]^+$: 413.3463, found 413.3458.

(*S*)-2-((dicyclohexylphosphanyl)amino)-*N*-((*R*)-1-hydroxy-3-methylbutan-2-yl)-3-methylbutanamide borane, (*S,R*)-6.8

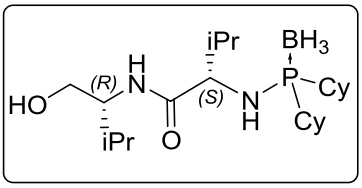

A solution of dicyclohexyl phosphinous acid borane (1 eq) and methansulfonic anhydride (1.2 eq) in CH_2Cl_2 (0.2M) was cooled to 0 ºC. To this solution, anhydrous NEt_3 (2.5 eq) was slowly added, and the mixture was stirred 1 h at 0 ºC. Amine (*R,S)*-**5.6-iPr** (1.5 eq) was then added and the solution was stirred overnight at room temperature. Water was added and the mixture was allowed to warm to room temperature. The organic layer was separated and the aqueous phase was extracted twice with CH_2Cl_2. The combined extracts were washed with brine and concentrated under reduced pressure. Purification by column chromatography (SiO_2, hexanes:EtOAc) yielded the corresponding products as a white solid.

White solid. **Yield:** 59% (214 mg). **Mp**: 122–123 ºC. **$[\alpha]_D$:** +25.0 (c 0.58, $CHCl_3$). **IR (KBr) υ_{max}:** 3318, 2935, 2854, 2368 and 1652 cm^{-1}. **^{1}H NMR (400 MHz, $CDCl_3$) δ;** 5.86 (br s, 1H), 3.72 – 3.65 (m, 3H), 3.41 (td, *J* = 10, 7 Hz, 1H), 2.78 (br s, 1H), 2.16 (br d, *J* = 8 Hz, 1H), 1.97 – 1.60 (m, 14H), 1.44 – 1.14 (m, 10H), 1.00 (d, *J* = 7 Hz, 3H), 0.99 – 0.93 (m, 9H), 0.72 – 0.08 (m, BH_3) ppm. **^{13}C NMR (101 MHz, $CDCl_3$) δ;** 174.5 (C), 63.7 (CH_2), 62.9 (d, *J* = 2 Hz, CH), 57.6 (CH), 35.1 (d, J_P = 43 Hz, CH), 34.9 (d, J_P = 36 Hz, CH), 33.4 (d, *J* = 6 Hz, CH), 28.8 (CH), 26.8 – 25.2 (m, 10 x CH_2), 19.6 (CH), 19.4 (CH), 19.0 (CH), 18.9 (CH) ppm. **^{31}P NMR (202 MHz, $CDCl_3$) δ;** 74.5 – 69.7 (m, P–BH_3) ppm. **HRMS (ESI):** calc. for $[C_{22}H_{46}O_2N_2BP + H]^+$: 413.3463, found 413.3461.

1,1-dicyclohexyl-*N*-((*S*)-1-((*S*)-4-isopropyl-4,5-dihydrooxazol-2-yl)-2-methylpropyl)phosphanamine borane, (*S,S*)-6.9

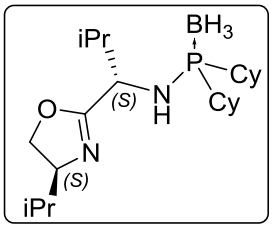

Aminophosphane (*S,S*)-**5.14** (1 eq) was dissolved in CH_2Cl_2 (0.08 M) and $SOCl_2$ (2.4 eq) was added drop wise at 0 ºC. The solution was stirred 4 h at room temperature. The solution was then cooled down to 0 ºC and $NaHCO_3$ saturated aqueous solution was added slowly until pH 8-9. The mixture was left stirring for 15 min at room temperature. The two phases were separated and the aqueous phase was extracted twice with CH_2Cl_2. The combined organic layers were washed with brine. The organic layer was dried over $MgSO_4$ and concentrated on a rotary evaporator under reduced

pressure. Purification by column chromatography (SiO_2, hexanes:EtOAc) yielded the product as a white solid.

White Solid. **Yield:** 96% (120 mg). **Mp**: 122–123 ºC. **$[\alpha]_D$:** –29.3 (c 0.53, $CHCl_3$). **IR (KBr) υ_{max}:** 3318, 2922, 2845, 2390, 2330 and 1666 cm^{-1}. **^{1}H NMR (400 MHz, $CDCl_3$) δ;** 4.27 (t, 1H), 4.01 (t, *J* = 8 Hz, 1H), 3.94 – 3.76 (m, 2H), 2.26 (br d, *J* = 10 Hz, 1H), 1.99 – 1.59 (m, 14H), 1.47 – 1.16 (m, 10H), 1.01 (d, *J* = 7 Hz, 3H), 0.94 – 0.88 (m, 9H), 0.70 – 0.10 (m, 3H, BH_3) ppm. **^{13}C NMR (101 MHz, $CDCl_3$) δ;** 168.1 (C), 71.9 (CH), 70.9 (CH_2), 56.1 (d, *J* = 2 Hz, CH), 35.8 (d, J_P = 34 Hz, CH), 34.3 (d, J_P = 44 Hz, CH), 34.0 (d, *J* = 4 Hz, CH), 33.0 (CH), 26.9 – 25.2 (m, 10 x CH), 19.2 (CH_3), 18.5 (CH_3), 18.2 (CH_3), 18.1 (CH_3) ppm. **^{31}P-NMR (202 MHz, $CDCl_3$) δ** 73.0 – 71.2 (m, P-BH_3) ppm. **HRMS (ESI):** calc. for $[C_{22}H_{44}ON_2BP + H]^+$: 395.3357, found 395.3350.

1,1-dicyclohexyl-*N*-((*S*)-1-((*R*)-4-isopropyl-4,5-dihydrooxazol-2-yl)-2-methylpropyl)phosphanamine borane, (*S*,*R*)-6.9

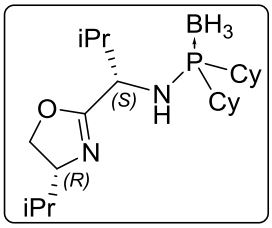

Aminophosphane (*S*,*R*)-**5.14** (1 eq) was dissolved in CH_2Cl_2 (0.08 M) and $SOCl_2$ (2.4 eq) was added drop wise at 0 ºC. The solution was stirred 4 h at room temperature. The solution was then cooled down to 0 ºC and $NaHCO_3$ saturated aqueous solution was added slowly until pH 8-9. The mixture was left stirring for 15 min at room temperature. The two phases were separated and the aqueous phase was extracted twice with CH_2Cl_2. The combined organic layers were washed with brine. The organic layer was dried over $MgSO_4$ and concentrated on a rotary evaporator under reduced pressure. Purification by column chromatography (SiO_2, hexanes:EtOAc) yielded the product as a white solid.

White Solid. **Yield:** 99% (66 mg). **Mp**: 123.5–124.5 ºC. **$[\alpha]_D$:** +16.0 (c 0.31, $CHCl_3$). **IR (KBr) υ_{max}:** 3328, 2916, 2398, 2362 and 1667 cm^{-1}. **^{1}H NMR (400 MHz, $CDCl_3$) δ;** 4.28 (dd, *J* = 9, 8 Hz, 1H), 3.97 – 3.73 (m, 3H), 2.14 (dd, *J* = 10, 3 Hz, 1H), 1.97 – 1.59 (m, 14H), 1.47 – 1.17 (m, 10H), 0.98 (d, *J* = 7 Hz, 3H), 0.96 – 0.91 (m, 6H), 0.89 (d, *J* = 7 Hz, 3H), 0.72 – 0.05 (m, 3H, BH_3) ppm. **^{13}C NMR (101 MHz, $CDCl_3$) δ;** 168.2 (C), 71.9 (CH), 70.4 (CH_2), 55.9 (CH), 35.7 (d, J_P = 33 Hz, CH), 34.3 (d, J_P = 44 Hz, CH), 33.8 (CH), 32.5 (CH), 27.0 – 25.1 (m, 10 x CH_2), 19.2 (CH_3), 18.4 (CH_3), 18.3 (CH_3), 18.1(CH_3).ppm. **^{31}P NMR (202 MHz, $CDCl_3$) δ;** δ 73.6 – 72.0 (m, P-BH_3) ppm. **HRMS (ESI):** calc. for $[C_{22}H_{44}ON_2BP + H]^+$: 395.3357, found 395.3349.

Complex (*S*,*S*)-6.10

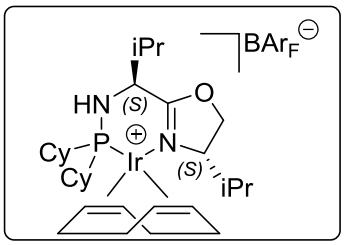

The borane protected ligand (*S*,*S*)-**6.9** (1 eq) was dissolved in freshly distilled pyrrolidine (0.06 M) and stirred for 16 h at 90 ºC. Afterwards, pyrrolidine was removed *in vacuo*. When no pyrrolidine remained, the crude was further dried under vacuum for 30 min at 50 ºC (the crude was under N_2 during all the procedure). A solution of $[Ir(COD)(Cl)]_2$ (0.5 eq) in CH_2Cl_2 (0.06 M) was added to the free ligand via cannula. The resulting mixture was stirred for 40 min at room temperature. $NaBAr_F$ (1 eq) was then added and the solution was stirred 1 h more at room temperature. The resulting crude was filtered through a small plug of silica gel, (first washed with Et_2O) under N_2, eluting with hexanes:CH_2Cl_2 (50-100%). An orange fraction was collected and concentrated to yield the Ir complex as a deep orange solid.

Orange solid. **Yield:** 74% (145 mg). **Mp**: 167–168 ºC. **$[\alpha]_D$:** +46.9 (c 0.60, $CHCl_3$). **IR (KBr) υ_{max}:** 2929, 2855, 1628, 1276 and 1129 cm^{-1}. **^{1}H NMR (400 MHz, $CDCl_3$) δ;** 7.75 – 7.68 (m, 8H), 7.53 (br s, 4H), 4.84 – 4.75 (m, 1H), 4.55 – 4.47 (m, 2H), 4.26 (t, *J* = 10 Hz, 1H), 4.12 – 4.04 (m, 1H), 3.95 – 3.86 (m, 1H), 3.54 – 3.47 (m, 1H), 3.47 – 3.36 (m, 2H), 2.42 – 2.34 (m, 2H), 2.26 – 2.18 (m, 2H), 2.16 – 1.52 (m, 17H), 1.42 – 1.15 (m, 12H), 1.09 (d, *J* = 7 Hz, 3H), 1.02 (d, *J* = 7 Hz, 3H), 0.88 (d, *J* = 7 Hz, 3H), 0.82 (d, *J* = 7 Hz, 3H) ppm. **^{13}C NMR (101 MHz, $CDCl_3$) δ;** 175.0 (C), 161.7 (q, J_B = 50 Hz, 4 x C), 134.8 (8 x CH), 129.5 – 128.3 (m, 8 x C), 124.5 (q, J_F = 273 Hz, 8 x CF_3), 117.40 (hept, J_F = 4 Hz, 4 x CH), 92.70 (d, J_P = 11 Hz, CH), 89.0 (d, J_P = 13 Hz, CH), 69.9 (CH), 69.2 (CH), 62.6 (CH), 59.9 (CH), 59.7 (CH), 41.1 (d, J_P = 32 Hz, CH), 38.2 (CH), 37.1 (d, J_P = 33 Hz, CH), 36.0 (CH_2), 31.9 (CH), 31.9 (CH_2), 29.6 – 25.6 (m, 12 x CH_2), 20.6 (CH_3), 19.9 (CH_3), 18.6 (CH_3), 15.1 (CH_3) ppm. **^{31}P NMR (202 MHz, $CDCl_3$) δ;** 60.7 (s) ppm. **HRMS (ESI-positive mode):** calc. for $[C_{30}H_{53}ON_2IrP]^+$: 681.3519, found 681.3502. **HRMS (ESI-negative mode):** calc. for $[C_{32}H_{12}BF_{24}]^-$: 863.0654, found 863.0634.

Complex (*S*,*R*)-6.10

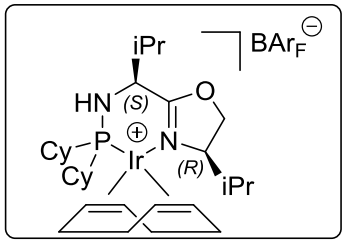

The borane protected ligand (*S*,*R*)-**6.9** (1 eq) was dissolved in freshly distilled pyrrolidine (0.06 M) and stirred for 16 h at 90 ºC. Afterwards, pyrrolidine was removed *in vacuo*. When no pyrrolidine remained, the crude was further dried under vacuum for 30 min at 50 ºC (the crude was under N_2 during all the procedure). A solution of $[Ir(COD)(Cl)]_2$ (0.5 eq) in CH_2Cl_2 (0.06 M) was added to the free ligand via cannula. The resulting mixture was stirred for 40 min at room temperature. $NaBAr_F$ (1 eq) was then added and the solution was stirred 1 h more at room temperature. The resulting crude was filtered through a small plug of silica gel, (first washed with Et_2O) under N_2, eluting with hexanes:CH_2Cl_2 (50-100%). An orange fraction was collected and concentrated to yield the Ir complex as a deep orange solid.

Orange solid. **Yield:** 52% (102 mg). **$[\alpha]_D$:** –41.2 (c 0.49, $CHCl_3$). **IR (KBr) υ_{max}:** 2940, 2856, 1622, 1351 and 1271 cm^{-1}. **^{1}H NMR (400 MHz, $CDCl_3$) δ;** 7.74 – 7.67 (m, 8H), 7.53 (br s, 4H), 4.80 – 4.73 (m, 1H), 4.61 (p, *J* = 7 Hz, 1H), 4.54 (dd, *J* = 10, 4 Hz, 1H), 4.28 (t, *J* = 10 Hz, 1H), 4.05 – 3.99 (m, 1H), 3.90 (dt, *J* = 10, 3 Hz, 1H), 3.82 – 3.76 (m, 1H), 3.39 – 3.31 (m, 1H), 2.52 – 1.16 (m, 33H), 1.11 (d, *J* = 7 Hz, 3H), 0.93 (d, *J* = 7 Hz, 3H), 0.92 (d, *J* = 7 Hz, 3H), 0.74 (d, *J* = 7 Hz, 3H) ppm. **^{13}C NMR (101 MHz, $CDCl_3$) δ;** 175.0 (C), 161.7 (q, J_B = 50 Hz, 4 x C), 134.8 (8 x CH), 129.5 – 128.3 (m, 8 x C), 124.5 (q, J_F = 273 Hz, 8 x CF_3), 117.40 (hept, J_F = 4 Hz, 4 x CH), 93.8 (d, J_P = 12 Hz, CH), 92.0 (CH), 70.3 (CH_2), 68.4 (CH), 61.7 (CH), 60.1 (CH), 58.7 (CH), 39.7 (d, J_P = 37 Hz, CH), 37.6 (d, J_P = 29 Hz, CH), 35.3 (CH_2), 31.8 (CH), 30.9 – 25.5 (m, 13 x CH_2 and 1 x CH), 20.1 (CH_3), 18.9 (CH_3), 16.2 (CH_3), 14.2 (CH_3) ppm. **^{31}P NMR (202 MHz, $CDCl_3$) δ;** 59.7 (s) ppm. **HRMS (ESI-positive mode):** calc. for $[C_{30}H_{53}ON_2IrP]^+$: 681.3519, found 681.3501. **HRMS (ESI-negative mode):** calc. for $[C_{32}H_{12}BF_{24}]^-$: 863.0654, found 863.0880.

SYNTHESIS OF Ir-MaxPHOX WITH DIFFERENT COUNTERANIONS

[Ir(Cl)(5.8a-iPr)(cod)], 6.11

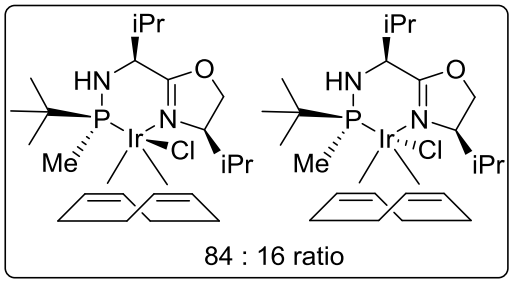

In a N_2 purged schlenk flask, 45 mg of **5.8a-iPr** borane protected ligand (0.148 mmol, 1 eq) were dissolved with freshly distilled pyrrolidine (0.06 M) and then stirred for 16 h at 90 ºC. Afterwards pyrrolidine was removed *in vacuo*. When no pyrrolidine remained, the crude was further dried under vacuum for 30 min at 50 ºC (the crude was under vacuum/N_2 during all the procedure). The crude was dissolved with 2 mL of anhydrous CH_2Cl_2 and 50 mg of $[Ir(COD)(Cl)]_2$ (0.074 mmol, 0.5 eq) were then added. The resulting mixture was stirred for 40 min at room temperature. The solvent was then removed under reduced pressure. Purification by column chromatography (SiO_2, CH_2Cl_2:MeOH) yielded a red oil as product. Crystallization attempts proved unsuccessful. We believe the red oil obtained is a mixture of two diastereoisomers. The two singlets detected on the ^{31}P NMR support this theory

Orange/Red oil. **^{31}P NMR (202 MHz, $CDCl_3$) δ;** 57.4 (s) and 51.0 (s) ppm. **HRMS (ESI-positive mode):** calc for $[C_{23}H_{43}ON_2IrP]^+$: 587.2737, found 587.2719.

(We have not determined which diastereoisomer is the major and which is the minor)

[Ir(5.8a-iPr)(cod)]BF_4, 6.12

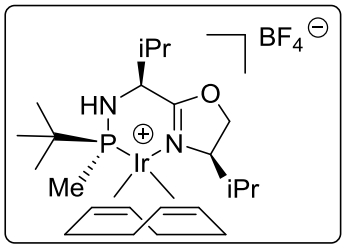

In a N_2 purged schlenk flask, 45 mg of **5.8a-iPr** borane protected ligand (0.148 mmol, 1 eq) were dissolved with freshly distilled pyrrolidine (0.06 M) and then stirred for 16 h at 90 ºC. Afterwards pyrrolidine was removed *in vacuo*. When no pyrrolidine remained, the crude was further dried under vacuum for 30 min at 50 ºC (the crude was under vacuum/N_2 during all the procedure). The crude was dissolved with 2 mL of anhydrous CH_2Cl_2 and 50 mg of $[Ir(COD)(Cl)]_2$ (0.074 mmol, 0.5 eq) were then added. The resulting mixture was stirred for 40 min at room temperature. Finally, 17 mg of $NaBF_4$ (0.148 mmol, 1 eq) were added and the solution was left stirring overnight at room temperature. Purification by column

chromatography (SiO_2, CH_2Cl_2:MeOH) yielded 63 mg (63%, 0.093 mmol) of product as an orange/red solid. The complex can be further purified if desired through crystallization. Orange solid. **Yield:** 49% (52 mg). **Mp**: 200–202 ºC. **$[\alpha]_D$:** –18.5 (c 0.40, $CHCl_3$). **IR (KBr) υ_{max}:** 3346, 2956, 2874, 1620 and 1213 cm^{-1}. **^{1}H NMR (400 MHz, $CDCl_3$) δ;** 5.11 – 5.02 (m, 1H), 4.91 – 4.84 (m, 1H), 4.69 (t, *J* = 10 Hz, 1H), 4.56 (dd, *J* = 10, 4 Hz, 1H), 4.19 – 4.13 (m, 1H), 4.02 (dt, *J* = 10, 4 Hz, 1H), 3.63 – 3.57 (m, 1H), 3.57 – 3.46 (m, 1H), 2.63 – 2.53 (m, 1H), 2.53 – 2.42 (m, 1H), 2.39 – 2.17 (m, 3H), 2.16 – 2.06 (m, 2H), 1.84 – 1.65 (m, 4H), 1.42 (d, J_P = 8 Hz, 3H), 1.22 (d, J_P = 15 Hz, 9H), 1.10 (d, *J* = 7 Hz, 3H), 1.01 (d, *J* = 7 Hz, 3H), 0.98 (d, *J* = 7 Hz, 3H), 0.79 (d, *J* = 7 Hz, 3H) ppm. **^{13}C NMR (101 MHz, $CDCl_3$) δ;** 175.7 (C), 95.1 (d, J_P = 13 Hz, CH), 92.8 (d, J_P = 11 Hz, CH), 70.8 (CH_2), 68.5 (CH), 64.0 (CH), 57.9 (CH), 56.1 (CH), 36.3 (d, J_P = 42 Hz, C), 34.3 (CH_2), 31.8 (CH), 31.3 (CH_2), 29.8 (CH_2), 28.9 (d, J_P = 9 Hz, CH), 28.0 (CH_2), 26.9 (d, *J* = 4 Hz, 3 x CH_3), 19.8 (CH_3), 19.3 (CH_3), 17.1 (CH_3), 15.1 (CH_3), 8.7 (d, J_P = 27 Hz, CH_3) ppm. **^{31}P NMR (202 MHz, $CDCl_3$) δ;** 61.9 (s) ppm. **HRMS (ESI-positive mode):** calc for $[C_{23}H_{43}ON_2IrP]^+$: 587.2737, found 587.2721. **HRMS (ESI-negative mode):** calc for $[BF_4]^-$: 87.0035, found 87.0034.

SYNTHESIS OF THE HYDROGENATION SUBSTRATES

General Method 1: Synthesis of *N*-aryl imines

The corresponding ketone (1 eq) was dissolved in a dry, N_2 purged round bottom flask in anhydrous Et_2O (0.5 M). Then the corresponding amine (3 eq) was added. The mixture was cooled to 0 ºC. Then neat TiCl4 (0.5 eq) was carefully added dropwise. The reaction was left stirring overnight at room temperature. The solution is filtered through celite with more Et_2O. The solvent is then removed under reduced pressure obtaining this way the crude as an oil. The crudes were purified by crystallization or by Kugelrohr distillation. High purity was required so the following catalytic reactions performed appropriately.

Acetophenone *N*-phenyl imine, 6.1[2]

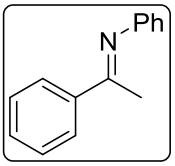

Compound **6.1** was synthesized applying **GM1**.

Yield: 73% (10.9 g). **^{1}H NMR (400 MHz, $CDCl_3$) δ;** 8.02 – 7.91 (m, 2H), 7.55 – 7.40 (m, 3H), 7.41 – 7.30 (m, 2H), 7.13 – 7.04 (m, 1H), 6.84 – 6.76 (m, 2H), 2.23 (s, 3H) ppm.

4-Methoxyacetophenone *N*-phenyl imine. I1.[2]

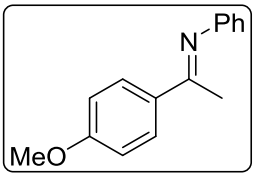

Compound **I1** was synthesized applying **GM1**.

Yield: 63% (9.5 g). **^{1}H NMR (400 MHz, $CDCl_3$) δ;** 8.04 – 7.92 (m, 2H), 7.39 – 7.31 (m, 2H), 7.10 – 7.04 (m, 1H), 6.98 – 6.93 (m, 2H), 6.82 – 6.76 (m, 3H), 3.87 (s, 3H), 2.20 (s, 3H) ppm.

3-Methoxyacetophenone *N*-phenyl imine, I2.[3]

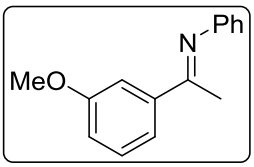

Compound **I2** was synthesized applying **GM1**.

Yield: 38% (5.7 g). **^{1}H NMR (400 MHz, $CDCl_3$) δ;** 7.61 – 7.54 (m, 1H), 7.53 – 7.48 (m, 1H), 7.39 – 7.31 (m, 3H), 7.11 – 7.06 (m, 1H), 7.04 – 7.00 (m, 1H), 6.81 – 6.77 (m, 2H), 3.88 (s, 3H), 2.22 (s, 3H) ppm.

2-Methoxyacetophenone *N*-phenyl imine, I3.

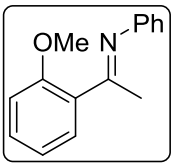

Compound **I3** was synthesized applying **GM1**.

Yield: 33% (5.4 g). **^{1}H NMR (400 MHz, $CDCl_3$) δ;** 7.61 – 7.57 (m, 1H), 7.41 – 7.32 (m, 3H), 7.04 – 7.00 (m, 1H), 6.97 – 6.93 (m, 1H), 6.87 – 6.84 (m, 2H), 6.78 – 6.73 (m, 1H), 6.68 – 6.64 (m, 1H), 3.88 (s, 3H), 2.19 (s, 3H) ppm.

4-Chloroacetophenone *N*-phenyl imine, I4.[2]

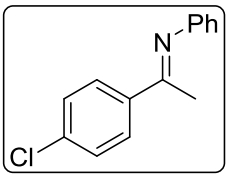

Compound **I4** was synthesized applying **GM1**.

Yield: 51% (9.0 g). **^{1}H NMR (400 MHz, $CDCl_3$) δ;** 7.94 – 7.88 (m, 2H), 7.43 – 7.38 (m, 2H), 7.38 – 7.32 (m, 2H), 7.12 – 7.06 (m, 1H), 6.81 – 6.76 (m, 2H), 3.08 (q, *J* = 7 Hz, 1H), 2.21 (s, 3H), 1.40 (t, *J* = 7 Hz, 1H) ppm.

1-(Naphthalen-2-yl)-*N*-phenylethan-1-imine, I5.[4]

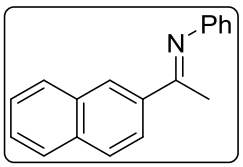

Compound **I5** was synthesized applying **GM1**.

Yield: 62% (5.4 g). **^{1}H NMR (400 MHz, $CDCl_3$) δ;** 8.37 – 8.33 (m, 1H), 8.24 – 8.21 (m, 1H), 7.95 – 7.85 (m, 3H), 7.57 – 7.49 (m, 2H), 7.40 – 7.34 (m, 2H), 7.13 – 7.08 (m, 1H), 6.87 – 6.82 (m, 2H), 2.36 (s, 3H) ppm.

***N*,1-Diphenylpropan-1-imine, I6.**[2]

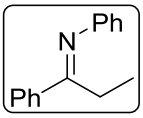

Compound **I6** was synthesized applying **GM1**.

Yield: 47% (3.7 g). **^{1}H NMR (400 MHz, $CDCl_3$) δ;** 7.95 – 7.90 (m, 2H), 7.48 – 7.42 (m, 3H), 7.37 – 7.31 (m, 2H), 7.07 (tt, *J* = 8, 1 Hz, 1H), 6.81 – 6.77 (m, 2H), 2.66 (q, *J* = 8 Hz, 2H), 1.08 (t, *J* = 8 Hz, 3H) ppm.

Acetophenone *N*-(4-methoxyphenyl) imine, I7.[2]

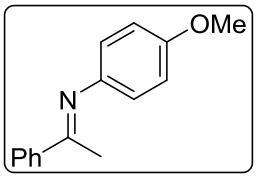

Compound **I7** was synthesized applying **GM1**.

Yield: 55% (5.3 g). **^{1}H NMR (400 MHz, $CDCl_3$) δ;** 8.03 – 7.89 (m, 2H), 7.50 – 7.39 (m, 3H), 6.93 – 6.87 (m, 2H), 6.80 – 6.72 (m, 2H), 3.82 (s, 3H), 2.25 (s, 3H) ppm.

Acetophenone *N*-(3,5-dimethylphenyl) imine, I8.[5]

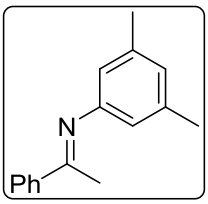

Compound **I8** was synthesized applying **GM1**.

Yield: 57% (7.1 g). **^{1}H NMR (400 MHz, $CDCl_3$) δ;** 7.98 – 7.94 (m, 2H), 7.48 – 7.40 (m, 3H), 6.72 (tp, *J* = 1, 1 Hz, 1H), 6.44 – 6.40 (m, 2H), 2.32 – 2.30 (m, 6H), 2.23 (s, 3H) ppm.

Acetophenone *N*-(*p*-tolyl) imine, I9.[6]

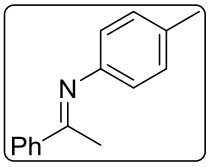

Compound **I9** was synthesized applying **GM1**.

Yield: 40% (7.2 g). **^{1}H NMR (400 MHz, $CDCl_3$) δ;** 8.01 – 7.92 (m, 2H), 7.48 – 7.41 (m, 3H), 7.18 – 7.14 (m, 2H), 6.73 – 6.67 (m, 2H), 2.35 (s, 3H), 2.24 (s, 3H) ppm.

The following compounds can be found in the literature and were synthesized as is therein reported: **I10**,[7] **I11**,[8] **I12**,[8] **I13**,[9] **I14**,[10] **I15**,[11] **I18**,[12] **I19**[13] and **I20**[14].

Compounds **I16** and **I17** are commercial compounds.

HYDROGENATION OF IMINES WITH Ir-MAXPHOX CATALYSTS

General Method 2: Hydrogenation of *N*-aryl imines at atmospheric H_2 pressure

The corresponding imine (1 eq) and the corresponding catalyst (0.01 eq) were placed in a round bottom flask. The flask was purged with N_2 and deoxygenated anhydrous solvent was added. The reaction was then set at the desired temperature. While stirring, a H_2 filled balloon was connected. Using another needle as a gas exit the round bottom flask was purged with H_2 until the solution went from orange to yellow (usually less than 3-4 minutes). The gas exit was removed and the reaction was left stirring overnight. The next day the reaction was concentrated under reduced pressure to afford the hydrogenated compounds as yellow oils and solids.

(–)-(*R*)-*N*-(1-phenylethyl)aniline, [2]

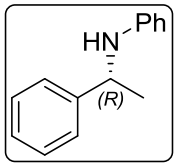

This compound was synthesized applying **GM2**.

^{1}H NMR (400 MHz, $CDCl_3$) δ; 7.41 – 7.25 (m, 4H), 7.28 – 7.18 (m, 1H), 7.18 – 7.03 (m, 2H), 6.68 – 6.59 (m, 1H), 6.55 – 6.46 (m, 2H), 4.48 (q, *J* = 7 Hz, 1H), 4.02 (br s, 1H), 1.51 (dd, *J* = 7, 1 Hz, 3H) ppm. **HPLC:** CHIRALCEL OD-H. Heptane/iPrOH 90:10, 1 mL/min, λ = 220 nm. t_R(+)= 15.4 min, t_R(–)= 17.0 min. (*ee* = 96% by HPLC)

(–)-(*R*)-*N*-(1-(4-methoxyphenyl)ethyl)aniline.[2]

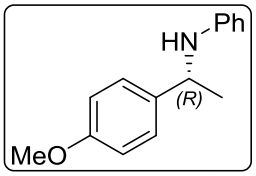

This compound was synthesized applying **GM2**.

^{1}H NMR (400 MHz, $CDCl_3$) δ; 7.30 – 7.26 (m, 2H), 7.11 – 7.06 (m, 2H), 6.87 – 6.84 (m, 2H), 6.53 – 6.47 (m, 2H), 4.44 (q, *J* = 6.7 Hz, 1H), 3.78 (s, 3H), 1.49 (d, *J* = 6.7 Hz, 3H) ppm. **HPLC:** CHIRALPAK IA. Heptane/iPrOH 96:4, 0.5 mL/min, λ = 210 nm. t_R(+)= 16.1 min, t_R(–)= 17.6 min. (*ee* = 95% by HPLC)

(–)-(*R*)-*N*-(1-(3-methoxyphenyl)ethyl)aniline.[3]

This compound was synthesized applying **GM2**.

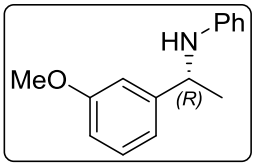

^{1}H NMR (400 MHz, $CDCl_3$) δ; 7.26 – 7.21 (m, 1H), 7.11 – 7.05 (m, 2H), 6.98 – 6.94 (m, 1H), 6.94 – 6.91 (m, 1H), 6.76 (ddd, *J* = 8, 3, 1 Hz, 1H), 6.64 (tt, *J* = 7, 1 Hz, 1H), 6.54 – 6.48 (m, 2H), 4.45 (q, *J* = 7 Hz, 1H), 4.01 (s, 1H), 3.78 (s, 3H), 1.51 (d, *J* = 7 Hz, 3H) ppm. **HPLC:** CHIRALCEL OJ. Heptane/EtOH 50:50-0.2% DEA, 0.5 mL/min, λ = 210 nm. t_R(+)= 18.1 min, t_R(–)= 20.8 min. (*ee* = 92% by HPLC)

(–)-(*R*)-*N*-(1-(2-methoxyphenyl)ethyl)aniline.[15]

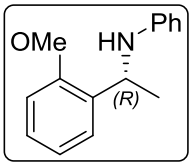

This compound was synthesized applying **GM2**.

^{1}H NMR (400 MHz, $CDCl_3$) δ; 7.27 – 7.20 (m, 1H), 7.15 – 7.08 (m, 1H), 7.03 – 6.96 (m, 2H), 6.83 – 6.77 (m, 2H), 6.54 (tt, *J* = 7, 1 Hz, 1H), 6.46 – 6.37 (m, 2H), 4.77 (q, *J* = 7 Hz, 1H), 3.82 (s, 3H), 1.40 (d, *J* = 7 Hz, 3H) ppm. **HPLC:** CHIRALCEL OJ. Heptane/EtOH 70:30-0.2% DEA, 0.5 mL/min, λ = 210nm. t_R(+)= 14.5 min, t_R(–)= 19.1 min. (*ee* = 28% by HPLC)

(–)-(*R*)-*N*-(1-(4-chlorophenyl)ethyl)aniline.[2]

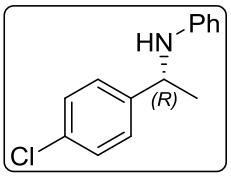

This compound was synthesized applying **GM2**.

^{1}H NMR (400 MHz, $CDCl_3$) δ; 7.25 – 7.18 (m, 4H), 7.05 – 6.97 (m, 2H), 6.62 – 6.54 (m, 1H), 6.43 – 6.35 (m, 2H), 4.38 (q, *J* = 7 Hz, 1H), 1.42 (d, *J* = 7 Hz, 3H) ppm. **HPLC:** CHIRALCEL OD-H. Heptane/iPrOH 95:5, 1 mL/min, λ = 210 nm. t_R(+)= 10.4 min, t_R(–)= 14.8 min. (*ee* = 94% by HPLC)

(–)-(*R*)-*N*-(1-(naphthalen-2-yl)ethyl)aniline.[16]

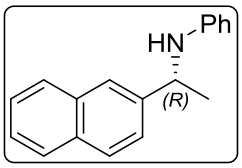

This compound was synthesized applying **GM2**.

^{1}H NMR (400 MHz, $CDCl_3$) δ; 7.84 – 7.77 (m, 4H), 7.50 (dd, *J* = 8, 2 Hz, 1H), 7.48 – 7.39 (m, 2H), 7.13 – 7.03 (m, 2H), 6.66 – 6.59 (m, 1H), 6.59 – 6.53 (m, 2H), 4.64 (q, *J* = 7 Hz, 1H), 4.18 – 4.04 (m, 1H), 1.59 (d, *J* = 7 Hz, 3H) ppm. **HPLC:** CHIRALCEL OJ. Heptane/EtOH 50:50, 0.8 mL/min, λ = 210 nm. t_R(+)= 14.4 min, t_R(–)= 17.2 min. (*ee* = 94% by HPLC)

(–)-(*R*)-*N*-(1-phenylpropyl)aniline.[2]

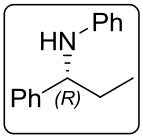

This compound was synthesized applying **GM2**.

^{1}H NMR (400 MHz, $CDCl_3$) δ; 7.39 – 7.27 (m, 4H), 7.27 – 7.18 (m, 1H), 7.11 – 7.04 (m, 2H), 6.62 (tt, *J* = 7, 1 Hz, 1H), 6.56 – 6.43 (m, 2H), 4.22 (t, *J* = 7 Hz, 1H), 4.04 (br s, 1H), 1.90 – 1.72 (m, 2H), 0.95 (t, *J* = 7 Hz, 3H) ppm. **HPLC:** CHIRALCEL OD-H. Heptane/iPrOH 95:5, 0.5 mL/min, λ = 210 nm. t_R(+)= 11.9 min, t_R(–)= 14.8 min. (*ee* = 74% by HPLC)

(–)-(*R*)-4-methoxy-*N*-(1-phenylethyl)aniline.[2]

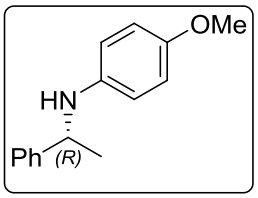

This compound was synthesized applying **GM2**.

^{1}H NMR (400 MHz, $CDCl_3$) δ; 7.39 – 7.28 (m, 4H), 7.24 – 7.19 (m, 1H), 6.74 – 6.61 (m, 2H), 6.47 (d, *J* = 9 Hz, 2H), 4.41 (q, *J* = 7 Hz, 1H), 3.69 (s, 3H), 1.50 (d, *J* = 7 Hz, 3H) ppm. **HPLC:** CHIRALPAK IC Heptane/iPrOH 96:4, 0.5 mL/min, λ = 210 nm. t_R(+)= 17.3 min, t_R(–)= 18.4 min. (*ee* = 93% by HPLC)

(–)-(*R*)-3,5-dimethyl-*N*-(1-phenylethyl)aniline.[17]

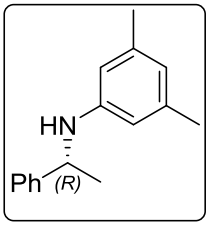

This compound was synthesized applying **GM2**.

^{1}H NMR (400 MHz, $CDCl_3$) δ; 7.38 – 7.28 (m, 3H), 7.24 – 7.19 (m, 1H), 6.32 – 6.27 (m, 1H), 6.18 – 6.10 (m, 2H), 4.47 (q, *J* = 7 Hz, 1H), 3.90 (br s, 1H), 2.16 (s, 6H), 1.49 (d, *J* = 7 Hz, 3H) ppm. **HPLC:** CHIRALCEL OD-H. Heptane/iPrOH 95:5, 0.5 mL/min, λ = 254 nm. t_R(+)= 10.7 min, t_R(–)= 12.4 min. (*ee* = 90% by HPLC)

(–)-(*R*)-4-methyl-*N*-(1-phenylethyl)aniline.[18]

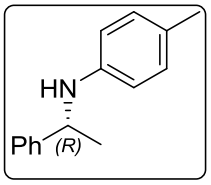

This compound was synthesized applying **GM2**.

^{1}H NMR (400 MHz, $CDCl_3$) δ; 7.38 – 7.28 (m, 4H), 7.24 – 7.19 (m, 1H), 6.94 – 6.84 (m, 2H), 6.47 – 6.39 (m, 2H), 4.45 (q, *J* = 7 Hz, 1H), 2.18 (s, 3H), 1.50 (d, *J* = 7 Hz, 3H) ppm. **HPLC:** CHIRALCEL OJ. Heptane/iPrOH 50:50, 1 mL/min, λ = 210 nm. t_R(+)= 12.2 min, t_R(–)= 15.4 min. (*ee* = 95% by HPLC)

Hydrogenation of substrates I10, I11, I13, I14 and I15

The corresponding substrate (1 eq) and the corresponding catalyst (0.01 eq) were placed in a pressure reactor. This was purged with N_2 and deoxygenated anhydrous solvent was added. The reactor was charged with H_2 to the desired pressure. The reaction was left stirring overnight. The next day the reaction was concentrated under reduced pressure to afford the hydrogenated compounds.

All the reduced substrates can be found in the literature; **I10**,[19] **I11**,[20] **I13**,[21] **I14**[10] and **I15**[22].

Ir-MaxPHOX IRIDACYCLES

General Method 3: Synthesis of chlorine iridacycles 6.13 and 6.14

The following compounds were synthesized using a methodology adapted from one previously reported by Pfaltz & coworkers.[9]

100 mg of catalysts ***ent*-1iPr** or ***ent*-3iPr** respectively (0.069 mmol, 1 eq) and 27 mg of *N*,1-diphenylethan-1-imine (0.138 mmol, 2 eq) were placed into a round bottom flask. It was then purged with N_2 and THF (2 mL) was added. The solution was purged with a H_2 balloon until the orange reaction color changed to yellow. The reaction mixture was stirred at r.t. during 4 hours. The solvent was removed with a N_2 flow and LiCl (100 mg) and SiO_2 (100 mg) were added. Finally EtOAc (2 mL) were added and the reaction was left stirring overnight. The solvent was again removed with a N_2 flow. The crude was suspended in Pentane/TBME (1:1) and eluted through SiO_2. Only the yellow colored band was collected affording the desired pure products as solids. The solids obtained were crystalized with Hexanes/CH_2Cl_2 until X-ray quality crystals were obtained.

Imine iridacycle 6.13

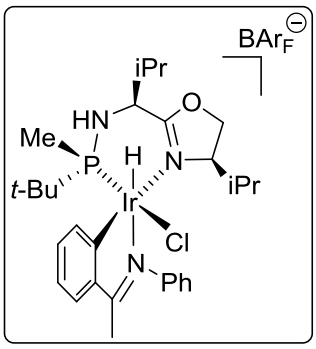

Compound **6.13** was synthesized employing **GM3**.

Yellow solid. **Yield:** 60% (29 mg). **^{1}H NMR (400 MHz, CD_2Cl_2) δ;** 7.80 – 7.68 (m, 2H), 7.57 – 7.50 (m, 1H), 7.40 – 7.30 (m, 2H), 7.17 (tt, *J* = 7, 1 Hz, 1H), 6.96 – 6.91 (m, 3H), 5.02 – 4.96 (m, 1H), 4.30 (dd, *J* = 9, 5 Hz, 1H), 3.98 (dd, *J* = 10, 9 Hz, 1H), 3.01 – 2.93 (m, 1H), 2.74 – 2.65 (m, 1H), 2.41 (s, 3H), 1.86 (dd, *J* = 9, 1 Hz, 3H), 1.84 – 1.78 (m, 1H), 1.12 (br d, *J* = 10 Hz, 1H), 0.86 (d, *J* = 7 Hz, 3H), 0.81 (d, *J* = 7 Hz, 3H), 0.78 (d, *J* = 7 Hz, 3H), 0.64 (d, *J* = 7 Hz, 3H), 0.57 (d, J_P = 14 Hz, 9H), -19.76 (d, $J_{P(cis)}$ = 26 Hz, 1H) ppm. **^{13}C NMR (101 MHz, CD_2Cl_2) δ;** 180.0 (C), 168.5 (C), 155.6 – 154.2 (m, C), 149.5 (C), 148.4 (C), 143.2 (d, *J* = 1 Hz, CH), 130.6 (CH), 129.2 (CH), 128.4 – 127.7 (m, 2 x CH), 125.5 (CH), 123.6 (CH), 121.9 (CH), 119.8 (CH), 68.8 (CH_2), 67.5 (CH), 57.5 (d, *J* = 2 Hz, CH), 37.4 (d, J_P = 37 Hz, C), 28.1 (d, *J* = 8 Hz, CH), 27.8 (CH), 25.8 (d, *J* = 4 Hz, 3 x CH_3), 22.3 – 21.3 (m, CH_3), 20.1 (CH_3), 18.2 (CH_3), 17.6 (CH_3), 16.8 (CH_3), 13.4 (CH_3) ppm. **^{31}P NMR (202 MHz, CD_2Cl_2) δ;** 36.3 (d, J_H = 20 Hz) ppm. **HRMS (ESI):** calc for $[C30H47IrN3OP - Cl]^+$: 674.2846, found 674.2834.

Imine iridacycle 6.14

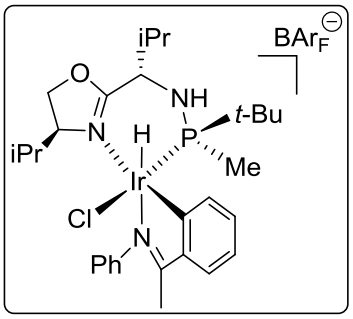

Compound **6.14** was synthesized employing **GM2**. Yellow solid. **Yield:** 56% (27 mg). **^{1}H NMR (400 MHz, CD_2Cl_2) δ;** 7.85 – 7.56 (m, 2H), 7.51 – 7.48 (m, 1H), 7.41 – 7.26 (m, 2H), 7.15 (tt, *J* = 8, 1 Hz, 1H), 7.01 – 6.74 (m, 3H), 4.93 (dtd, *J* = 9, 3, 1 Hz, 1H), 4.20 (dd, *J* = 9, 3 Hz, 1H), 3.73 – 3.68 (m, 1H), 3.65 (dd, *J* = 9, 9 Hz, 1H), 2.89 (hd, *J* = 7, 3 Hz, 1H), 2.35 (s, 3H), 2.07 – 1.95 (m, 1H), 1.55 – 1.49 (m, 1H), 1.07 (d, J_P = 15 Hz, 9H), 0.90 (d, J_P = 9 Hz, 3H), 0.86 (d, *J* = 7 Hz, 3H), 0.77 (d, *J* = 7 Hz, 3H), 0.63 (d, *J* = 7 Hz, 3H), 0.43 (d, *J* = 7 Hz, 3H), -19.62 (d, $J_{P(CIS)}$ = 23 Hz, 1H) ppm. **^{13}C NMR (101 MHz, CD_2Cl_2) δ;** 180.3 (C), 162.1 (C), 154.3 (C), 149.6 (C), 148.3 (C), 143.4 (2 x CH), 130.4 (CH), 128.7 (2 x CH), 128.6 (CH), 125.3 (CH), 119.6 (2 x CH), 70.3 (CH), 67.5 (CH_2), 57.8 (CH), 36.2 (d, J_P = 43 Hz, C), 30.6 (d, *J* = 6 Hz, CH), 28.6 (CH), 26.4 (3 x CH_3), 19.4 (CH_3), 18.3 (CH_3), 17.4 (CH_3), 16.2 (CH_3), 13.6 (CH_3), 9.1 (d, J_P = 42 Hz, CH_3) ppm. **^{31}P NMR (202 MHz, CD_2Cl_2) δ;** 43.93 (d, J_H = 19 Hz) ppm. **HRMS (ESI):** calc for $[C30H47IrN3OP - Cl]^+$: 674.2846, found 674.2835.

Procedure for the hydrogenation of imines using iridacycle 6.13

100 mg of imine *N*,1-diphenylethan-1-imine (0.51 mmol, 1 eq) and 4 mg of 9 imine iridacyle **6.13** (0.0051 mmol, 0.01 eq) were placed in a round bottom flask. The flask was purged with N_2 and 2 mL of deoxygenated anhydrous CH_2Cl_2 were added. 9 mg of $NaBAr_F$ (0.10 mmol, 0.02 eq) were added. While stirring, a H_2 filled balloon was connected. Using another needle as a gas exit the round bottom flask was purged with H_2 for 3-4 minutes. The gas exit was removed and the reaction was left stirring overnight. The next day the reaction was concentrated under reduced pressure to afford 101 mg of the amine *N*-(1-phenylethyl)aniline as a yellow oil (*ee* = 91% by HPLC)

REFERENCES

[1] M. Stankevic, G. Andrijewski, K. M. Pietrusiewicz, *Synlett* **2004**, 311–315.

[2] A. Baeza, A. Pfaltz, *Chem. - A Eur. J.* **2010**, *16*, 4003–4009.

[3] Y. Liu, H. Du, *J. Am. Chem. Soc.* **2013**, *135*, 6810–6813.

[4] M. Bonsignore, M. Benaglia, L. Raimondi, M. Orlandi, G. Celentano, *Beilstein J. Org. Chem.* **2013**, *9*, 633–640.

[5] K. Kutlescha, G. T. Venkanna, R. Kempe, *Chem. Commun.* **2011**, *47*, 4183.

[6] T. Schwob, R. Kempe, *Angew. Chem. Int. Ed.* **2016**, *55*, 15175–15179.

[7] J. Barluenga, M. A. Fernández, F. Aznar, C. Valdés, *Chem. - A Eur. J.* **2004**, *10*, 494–507.

[8] C. R. Venkat Reddy, S. Urgaonkar, J. G. Verkade, *Org. Lett.* **2005**, *7*, 4427–4430.

[9] Y. Schramm, F. Barrios-Landeros, A. Pfaltz, *Chem. Sci.* **2013**, *4*, 2760.

[10] P. Schnider, G. Koch, R. Pretot, G. Wang, F. M. Bohnen, C. Kriiger, A. Pfaltz, *Chem. Eur. J.* **1997**, *3*, 887–892.

[11] J. Capra, T. Le Gall, *Synlett* **2010**, *2010*, 441–444.

[12] S. Prateeptongkum, I. Jovel, R. Jackstell, N. Vogl, C. Weckbecker, M. Beller, *Chem. Commun.* **2009**, 1990.

[13] C. Pizzo, P. Faral-Tello, G. Yaluff, E. Serna, S. Torres, N. Vera, C. Saiz, C. Robello, G. Mahler, *Eur. J. Med. Chem.* **2016**, *109*, 107–113.

[14] G. A. Smirnov, E. P. Sizova, O. A. Luk"yanov, *Russ. Chem. Bull.* **2004**, *53*, 635–640.

[15] M. R. Radlauer, M. W. Day, T. Agapie, *Organometallics* **2012**, *31*, 1068.

[16] G. Wang, C. Chen, T. Du, W. Zhong, *Adv. Synth. Catal.* **2014**, *356*, 1747–1752.

[17] S. Wübbolt, M. S. Maji, E. Irran, M. Oestreich, *Chem. - A Eur. J.* **2017**, *23*, 6213–6219.

[18] Q. Sun, Y. Wang, D. Yuan, Y. Yao, Q. Shen, *Organometallics* **2014**, *33*, 994–1001.

[19] J. P. Brand, J. Waser, *Org. Lett.* **2012**, *14*, 744–747.

[20] J. Yu, G. Kehr, C. G. Daniliuc, C. Bannwarth, S. Grimme, G. Erker, *Org. Biomol. Chem.* **2015**, *13*, 5783–5792.

[21] A. Lefranc, Z.-W. Qu, S. Grimme, M. Oestreich, *Chem. - A Eur. J.* **2016**, *22*, 10009–10016.

[22] J. Ściebura, J. Gawroński, *Tetrahedron: Asymmetry* **2013**, *24*, 683–688.

Experimental Section for Chapter 7

MaxPHOX iridacycles on the asymmetric hydrogenation of *N*-alkyl imines

E. Salomó, A. Gallen, A.Grabulosa, A. Riera, X. Verdaguer *(submitted)*

NMR DETECTION OF Ir-MaxPHOX IRIDACYCLES

Complex 7.3

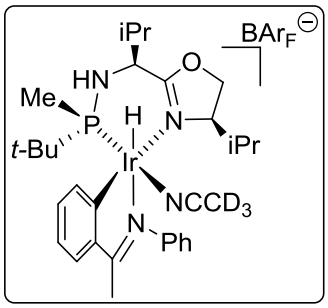

For this procedure all solvents were degassed with freeze-pump-thaw cycles.

A Schlenk flask was charged with 10 mg of complex ***ent*-1iPr** (0.007 mmol, 1 eq) and 3 mg (0.014 mmol, 2 eq) of acetophenone *N*-phenyl imine, **A0**. The flask was purged with three vacuum/N_2 cycles and the solids were dissolved in 1.5 mL of THF. The solution was stirred for 3 h. Then 0.5 mL of ACN-d^3 were added and the mixture was stirred for 30 min. The solvents are evaporated under reduced pressure. We dissolve the crude in ACN-d^3 and perform the NMR spectra.

^{1}H NMR (400 MHz, ACN-d^3) δ; –19.87 (d, *J* = 26 Hz, 1H) ppm. **^{31}P NMR (202 MHz, ACN-d^3) δ;** 34.17 – 33.92 (m, 1H) ppm.

Complex 7.4

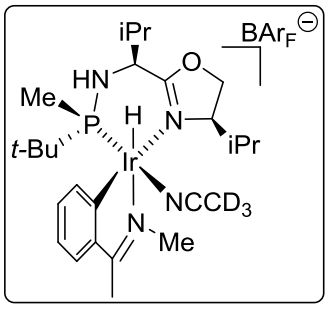

For this procedure all solvents were degassed with freeze-pump-thaw cycles.

A Schlenk flask was charged with 10 mg of complex ***ent*-1iPr** (0.007 mmol, 1 eq) and 3 mg (0.014 mmol, 2 eq) of acetophenone *N*-methyl imine, **I1**. The flask was purged with three vacuum/N_2 cycles and the solids were dissolved in 1.5 mL of THF. The solution was stirred for 3 h. Then 0.5 mL of ACN-d^3 were added and the mixture was stirred for 30 min. The solvents are evaporated under reduced pressure. We dissolve the crude in ACN-d^3 and perform the NMR spectra.

The spectra obtained presented many byproducts and iridacycle **7.4** could not be assigned.

PREPARATION OF THE ADDITIVES (A0-A14) FOR THE IN SITU CATALYSIS

General Method 1: Synthesis of *N*-aryl imines

The corresponding ketone (1 eq) was dissolved in a dry, N_2 purged round bottom flask in anhydrous Et_2O (0.5 M). Then the corresponding amine (3 eq) was added. The mixture was cooled to 0 ºC. Then neat TiCl4 (0.5 eq) was carefully added dropwise. The reaction was left stirring overnight at room temperature. The solution is filtered through celite with more Et_2O. The solvent is then removed under reduced pressure obtaining this way the crude as an oil. The crudes were purified by crystallization or by Kugelrohr distillation. High purity was required so the following catalytic reactions performed appropriately.

Acetophenone *N*-phenyl imine, A0[1]

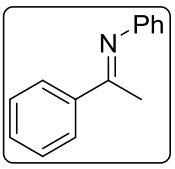

Compound **A0** was synthesized applying **GM1**.

Yield: 73% (10.9 g). **^{1}H NMR (400 MHz, $CDCl_3$) δ;** 8.02 – 7.91 (m, 2H), 7.55 – 7.40 (m, 3H), 7.41 – 7.30 (m, 2H), 7.13 – 7.04 (m, 1H), 6.84 – 6.76 (m, 2H), 2.23 (s, 3H) ppm.

Acetophenone *N*-(4-methoxyphenyl) imine, A1.[1]

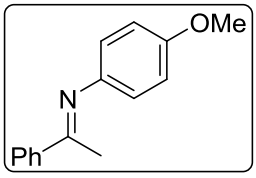

Compound **A1** was synthesized applying **GM1**.

Yield: 55% (5.3 g). **^{1}H NMR (400 MHz, $CDCl_3$) δ;** 8.03 – 7.89 (m, 2H), 7.50 – 7.39 (m, 3H), 6.93 – 6.87 (m, 2H), 6.80 – 6.72 (m, 2H), 3.82 (s, 3H), 2.25 (s, 3H) ppm.

4-Methoxyacetophenone *N*-phenyl imine, A2.[1]

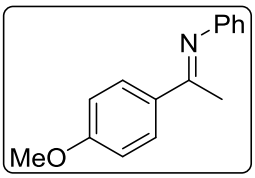

Compound **A2** was synthesized applying **GM1**.

Yield: 63% (9.5 g). **^{1}H NMR (400 MHz, $CDCl_3$) δ;** 8.04 – 7.92 (m, 2H), 7.39 – 7.31 (m, 2H), 7.10 – 7.04 (m, 1H), 6.98 – 6.93 (m, 2H), 6.82 – 6.76 (m, 3H), 3.87 (s, 3H), 2.20 (s, 3H) ppm.

3-Methoxyacetophenone *N*-phenyl imine, A3.[2]

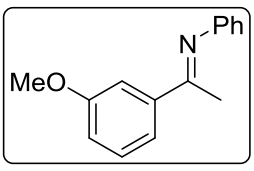

Compound **A3** was synthesized applying **GM1**.

Yield: 38% (5.7 g). **^{1}H NMR (400 MHz, $CDCl_3$) δ;** 7.61 – 7.54 (m, 1H), 7.53 – 7.48 (m, 1H), 7.39 – 7.31 (m, 3H), 7.11 – 7.06 (m, 1H), 7.04 – 7.00 (m, 1H), 6.81 – 6.77 (m, 2H), 3.88 (s, 3H), 2.22 (s, 3H) ppm.

4-Chloroacetophenone *N*-phenyl imine, A4.[1]

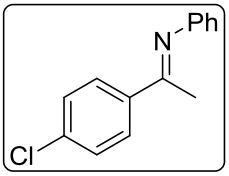

Compound **A4** was synthesized applying **GM1**.

Yield: 51% (9.0 g). **^{1}H NMR (400 MHz, $CDCl_3$) δ;** 7.94 – 7.88 (m, 2H), 7.43 – 7.38 (m, 2H), 7.38 – 7.32 (m, 2H), 7.12 – 7.06 (m, 1H), 6.81 – 6.76 (m, 2H), 3.08 (q, *J* = 7 Hz, 1H), 2.21 (s, 3H), 1.40 (t, *J* = 7 Hz, 1H) ppm.

Acetophenone *N*-(3,5-dimethylphenyl) imine, A7.[3]

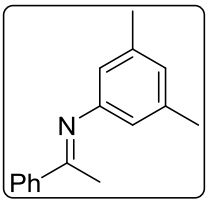

Compound **A7** was synthesized applying **GM1**.

Yield: 57% (7.1 g). **^{1}H NMR (400 MHz, $CDCl_3$) δ;** 7.98 – 7.94 (m, 2H), 7.48 – 7.40 (m, 3H), 6.72 (tp, *J* = 1, 1 Hz, 1H), 6.44 – 6.40 (m, 2H), 2.32 – 2.30 (m, 6H), 2.23 (s, 3H) ppm.

***N*,1-Diphenylpropan-1-imine, A10.**[1]

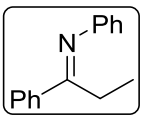

Compound **A10** was synthesized applying **GM1**.

Yield: 47% (3.7 g). **^{1}H NMR (400 MHz, $CDCl_3$) δ;** 7.95 – 7.90 (m, 2H), 7.48 – 7.42 (m, 3H), 7.37 – 7.31 (m, 2H), 7.07 (tt, *J* = 8, 1 Hz, 1H), 6.81 – 6.77 (m, 2H), 2.66 (q, *J* = 8 Hz, 2H), 1.08 (t, *J* = 8 Hz, 3H) ppm.

The following compounds can be found in the literature and were synthesized as is therein reported: **A5**,[4] **A6**,[4] **A8**[5], **A11**[6] and **A14**.[7]

Compounds **A9**, **A12** and **A13** are commercial compounds.

SYNTHESIS OF THE *N*-METHYL AND *N*-ALKYL IMINES (I1-I18)

General Method 2 (methyl imines): The corresponding ketone (1 eq) was placed in a dry, N_2-purged round bottom flask. Activated molecular sieves were added (4 Å, 1 g per mmol of ketone) and then a solution of methyl amine in EtOH (33 wt. %, 6 eq). The mixture was left stirring for 48 h at room temperature. The solution was then filtered through celite with CH_2Cl_2 and the solvent was removed under reduced pressure to give an oil. The crudes obtained were used straight away on the next reactions or were purified by Kugelrohr distillation when required.

(*E*)-*N*-methyl-1-phenylethan-1-imine, I1.[8]

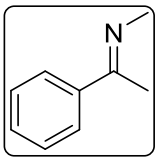

Compound **I1** was synthesized applying **GM2**.

^{1}H NMR (400 MHz, $CDCl_3$) δ; 7.84 – 7.60 (m, 2H), 7.48 – 7.30 (m, 3H), 3.35 (q, *J* = 1 Hz, 3H), 2.24 (q, *J* = 1 Hz, 3H) ppm.

(*E*)-1-(4-methoxyphenyl)-*N*-methylethan-1-imine, I2.[8]

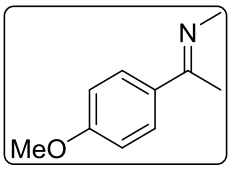

Compound **I2** was synthesized applying **GM2**.

^{1}H NMR (400 MHz, $CDCl_3$) δ; 7.76 – 7.64 (m, 2H), 6.90 – 6.82 (m, 2H), 3.81 (s, 3H), 3.30 (q, *J* = 1 Hz, 3H), 2.19 (q, *J* = 1 Hz, 3H) ppm.

(*E*)-1-(3-methoxyphenyl)-*N*-phenylethan-1-imine, I3.[8]

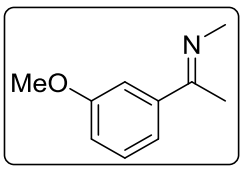

Compound **I3** was synthesized applying **GM2**.

^{1}H NMR (400 MHz, $CDCl_3$) δ; 7.36 – 7.33 (m, 1H), 7.33 – 7.26 (m, 2H), 6.93 (ddd, *J* = 7, 3, 2 Hz, 1H), 3.84 (s, 3H), 3.35 (q, *J* = 1 Hz, 3H), 2.23 (q, *J* = 1 Hz, 3H) ppm.

(*E*)-1-(4-chlorophenyl)-*N*-methylethan-1-imine, I4.[8]

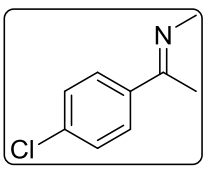

Compound **I4** was synthesized applying **GM2**.

^{1}H NMR (400 MHz, $CDCl_3$) δ 7.74 – 7.65 (m, 2H), 7.42 – 7.29 (m, 2H), 3.34 (q, *J* = 1 Hz, 3H), 2.21 (q, *J* = 1 Hz, 3H) ppm.

(*E*)-1-(4-fluorophenyl)-*N*-methylethan-1-imine, I5.[8]

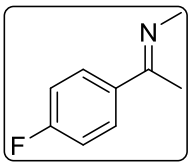

Compound **I5** was synthesized applying **GM2**.

^{1}H NMR (400 MHz, $CDCl_3$) δ; 7.78 – 7.71 (m, 2H), 7.07 – 7.00 (m, 2H), 3.34 – 3.32 (m, 3H), 2.22 (q, *J* = 1 Hz, 3H) ppm.

(*E*)-*N*-methyl-1-(4-(trifluoromethyl)phenyl)ethan-1-imine, I6.[8]

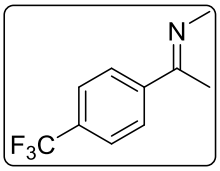

Compound **I6** was synthesized applying **GM2**.

^{1}H NMR (400 MHz, $CDCl_3$) δ; 7.88 – 7.83 (m, 2H), 7.65 – 7.60 (m, 2H), 3.41 – 3.31 (m, 3H), 2.26 (q, *J* = 1 Hz, 3H) ppm.

(*E*)-*N*-methyl-3,4-dihydronaphthalen-1(2H)-imine, I7.[8]

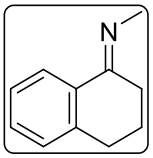

Compound **I7** was synthesized applying **GM2**.

^{1}H NMR (400 MHz, $CDCl_3$) δ; 8.03 (dd, *J* = 8, 2 Hz, 1H), 7.26 – 7.13 (m, 2H), 7.09 – 7.04 (m, 1H), 3.28 – 3.18 (m, 3H), 2.83 – 2.68 (m, 2H), 2.57 – 2.42 (m, 2H), 1.95 – 1.83 (m, 2H) ppm.

Substrates **I11**, **I12** and **I17** were synthesized applying **GM2** and can be found in the literature.[8]

General Method 3 (other alkyl imines): The corresponding ketone (1 eq) was dissolved in a dry, N_2-purged round bottom flask in anhydrous Et_2O (0.5 M) and then the corresponding amine (3 eq) was added. The mixture was cooled to 0 ºC and neat $TiCl_4$ (0.5 eq) was carefully added dropwise. The reaction was left stirring overnight at room temperature and the solution was filtered through celite with more Et_2O. The solvent was then removed under reduced pressure to give an oil. The crudes were purified by crystallization or by Kugelrohr distillation.

(*E*)-1-phenyl-*N*-propylethan-1-imine, I8.[8]

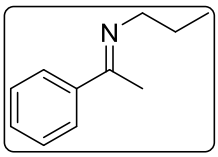

Compound **I8** was synthesized applying **GM3**.

^{1}H NMR (400 MHz, $CDCl_3$) δ; 7.81 – 7.71 (m, 2H), 7.44 – 7.31 (m, 3H), 3.49 – 3.40 (m, 2H), 1.77 (h, *J* = 7 Hz, 2H), 1.02 (t, *J* = 7 Hz, 3H) ppm.

(*E*)-*N*-isobutyl-1-phenylethan-1-imine, I9.[9]

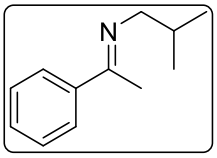

Compound **I9** was synthesized applying **GM3**.

^{1}H NMR (400 MHz, $CDCl_3$) δ; 7.82 – 7.70 (m, 2H), 7.41 – 7.31 (m, 3H), 3.27 (dt, *J* = 7, 1 Hz, 2H), 2.22 (t, *J* = 1 Hz, 3H), 2.07 (dp, *J* = 13, 7 Hz, 1H), 1.01 (d, *J* = 7 Hz, 6H) ppm.

(*E*)-1-(4-chlorophenyl)-*N*-phenylethan-1-imine, I10.[10]

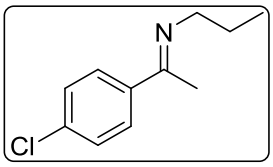

Compound **I10** was synthesized applying **GM3**.

^{1}H NMR (400 MHz, $CDCl_3$) δ; 7.74 – 7.68 (m, 2H), 7.35 – 7.30 (m, 2H), 3.50 – 3.35 (m, 2H), 2.21 (t, *J* = 1 Hz, 3H), 1.83 – 1.70 (m, 2H), 1.01 (t, *J* = 7 Hz, 3H) ppm.

Substrates **I15**[11] and **I18**[12] were synthesized applying **GM3** and can be found in the literature. Substrate **I14**[13] was also previously described in the literature. Substrates **I14** and **I16** are commercially available.

IN SITU HYDROGENATION OF IMINES (I1-I18) WITH Ir-MaxPHOX (1IPR-4IPR) + ADDITIVES (A0-A14)

General Method 4: 5 mg of Ir-MaxPHOX (**1iPr-4iPr**) ($3.45x10^{-3}$ mmol, 0.01 eq) and the corresponding additive (**A0**-**A14**) (0.345 mmol, 0.02 eq) were placed in glass pressure tube. The tube was purged with vacuum-nitrogen cycles and then 2 mL of CH_2Cl_2 were added. The tube was the purged with vacuum-hydrogen cycles and charged with 3 bars of H_2. The mixture was left to stir for 30 min at room temperature to form the iridacycle. The corresponding imine (**I1-I18**) was dissolved in 1 mL of CH_2Cl_2 and added using a pressure syringe. The mixture was left stirring overnight. The tube was depressurized and the solvent removed under vacuum to afford the hydrogenated compounds as a dark yellow oils or solids. The ee value was determined by HPLC analysis of the corresponding trifluoroacetamide derivative on a chiral stationary phase

Trifluoroacylation of amines for the ee determination with HPLC/GC

The corresponding amine (0.35 mmol, 1 eq) was placed in a round bottom flask and dissolved in 2 mL of CH_2Cl_2. At this point, 213 µL of pyridine (2.1 mmol, 6 eq) and 143 µL of trifluoroacetic anhydride (1.0 mmol, 3 eq) were added and the mixture was left stirring for 2 h. The reaction was concentrated under reduced pressure and the crude was purified with a short silica column to afford the products as colorless oils.

(–)-(*S*)-*N*-methyl-1-phenylethan-1-amine.[13]

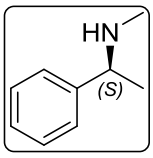

This compound was synthesized applying **GM4**.

^{1}H NMR (400 MHz, $CDCl_3$) δ; 7.36 – 7.26 (m, 4H), 3.65 (q, *J* = 7 Hz, 1H), 2.31 (s, 3H), 1.37 (d, *J* = 7 Hz, 3H) ppm. **HPLC:** CHIRALCEL OD-H. Heptane/iPrOH 98:02, 0.5 mL/min, λ = 210 nm. t_S(–)= 13.4 min, t_R(+)= 14.7 min. (*ee* = 92% by HPLC)

(–)-(*S*)-1-(4-chlorophenyl)-*N*-methylethan-1-amine.[13]

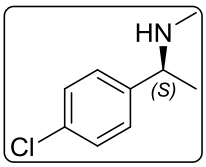

This compound was synthesized applying **GM4**.

^{1}H NMR (400 MHz, $CDCl_3$) δ; 7.40 – 7.19 (m, 4H), 3.62 (q, *J* = 7 Hz, 1H), 2.29 (s, 3H), 1.32 (d, *J* = 7 Hz, 3H) ppm. **GC**: *β*-DEX (30 m). 140 ºC (50 min). T_{det} = 300 ºC. T_{inj} = 220 ºC. Split 50:1, Flux: 1 mL/ min; He. t_S (–) = 38.7 min, t_R (+) = 39.1 min. (*ee* = 95% by HPLC)

(–)-(*S*)-1-(4-fluorophenyl)-*N*-methylethan-1-amine.[14]

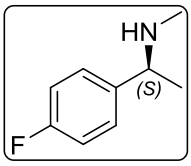

This compound was synthesized applying **GM4**.

^{1}H NMR (400 MHz, $CDCl_3$) δ; 7.29 – 7.22 (m, 2H), 7.04 – 6.95 (m, 2H), 3.63 (q, *J* = 7 Hz, 1H), 2.29 (s, 3H), 1.33 (d, *J* = 7 Hz, 3H) ppm. **GC**: *β*-DEX (30 m). 120 ºC ---5 ºC/min----130 ºC (40 min)----30 ºC/min---210 ºC (5 min). T_{det} = 300 ºC. T_{inj} = 220 ºC. Split 50:1, Flux: 1 mL/ min; He. t_S (–) = 22.4 min, t_R (+) = 22.7 min. (*ee* = 94% by HPLC)

(–)-(*S*)-1-(3-methoxyphenyl)-*N*-methylethan-1-amine.[15]

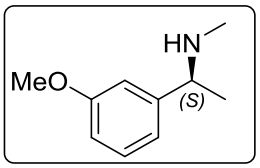

This compound was synthesized applying **GM4**.

^{1}H NMR (400 MHz, $CDCl_3$) δ; 7.27 – 7.22 (m, 1H), 6.90 – 6.86 (m, 2H), 6.78 (ddd, *J* = 8, 3, 1 Hz, 1H), 3.81 (s, 3H), 3.62 (q, *J* = 7 Hz, 1H), 2.31 (s, 3H), 1.35 (d, *J* = 7 Hz, 3H) ppm. **GC**: *β*-DEX (30 m). 120 ºC (10 min)---2 ºC/min----140 ºC (60 min)----20 ºC/min---210 ºC (5 min). T_{det} = 300 ºC. T_{inj} = 220 ºC. Split 50:1, Flux: 1 mL/ min; He. t_S (–) = 51.8 min, t_R (+) = 52.2 min. (*ee* = 89% by HPLC)

(–)-(*S*)-1-(4-methoxyphenyl)-*N*-methylethan-1-amine.[16]

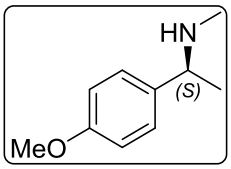

This compound was synthesized applying **GM4**.

^{1}H NMR (400 MHz, $CDCl_3$) δ; 7.24 – 7.17 (m, 2H), 6.92 – 6.81 (m, 2H), 3.80 (s, 3H), 3.60 (q, *J* = 7 Hz, 1H), 2.30 (s, 3H), 1.34 (d, *J* = 7 Hz, 3H) ppm. **HPLC:** CHIRALCEL OJ. Heptane/EtOH 95:05, 0.5 mL/min, λ = 210 nm. t_R(+)= 15.1 min, t_S(–)= 16.7 min. (*ee* = 91% by HPLC)

(–)-(*S*)-*N*-methyl-1-(4-(trifluoromethyl)phenyl)ethan-1-amine.[14]

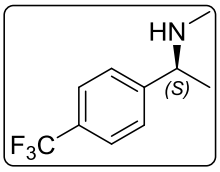

This compound was synthesized applying **GM4**.

^{1}H NMR (400 MHz, $CDCl_3$) δ; 7.58 (dtd, *J* = 9, 2, 1 Hz, 2H), 7.47 – 7.37 (m, 2H), 3.71 (q, *J* = 7 Hz, 1H), 2.30 (s, 3H), 1.35 (d, *J* = 7 Hz, 3H).ppm. **HPLC:** CHIRALPAK AS. Heptane/iPrOH 98:02, 0.5 mL/min, λ = 210 nm. t_R(+)= 10.2 min, t_S(–)= 11.9 min. (*ee* = 93% by HPLC)

(+)-(*S*)-*N*-methyl-1,2,3,4-tetrahydronaphthalen-1-amine.[13]

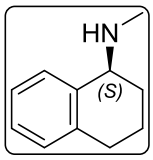

This compound was synthesized applying **GM4**.

^{1}H NMR (400 MHz, $CDCl_3$) δ; 7.37 – 7.29 (m, 1H), 7.19 – 7.11 (m, 2H), 7.11 – 6.99 (m, 1H), 3.66 (t, *J* = 5 Hz, 1H), 2.89 – 2.62 (m, 2H), 2.50 (s, 3H), 2.04 – 1.81 (m, 3H), 1.81 – 1.67 (m, 1H) ppm. **GC**: *β*-DEX (30 m). 160 ºC (30 min). T_{det} = 300 ºC. T_{inj} = 220 ºC. Split 50:1, Flux: 1 mL/ min; He. t_S (+) = 25.7 min, t_R (–) = 26.3 min. (*ee* = 90% by HPLC)

(–)-(*S*)-*N*-(1-phenylethyl)propan-1-amine.[17]

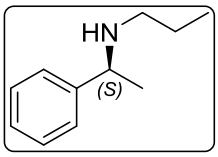

This compound was synthesized applying **GM4**.

^{1}H NMR (400 MHz, $CDCl_3$) δ; 7.28 – 7.21 (m, 4H), 7.19 – 7.14 (m, 1H), 3.68 (q, *J* = 7 Hz, 1H), 2.40 (ddd, *J* = 11, 8, 6 Hz, 1H), 2.31 (ddd, *J* = 11, 8, 7 Hz, 1H), 1.44 – 1.33 (m, 2H), 1.28 (d, *J* = 7 Hz, 3H), 0.80 (t, *J* = 7 Hz, 3H) ppm. **HPLC:** CHIRALPAK ADH. Heptane/iPrOH 98:02, 0.5 mL/min, λ = 210 nm. t_R(+)= 8.9 min, t_S(–)= 9.9 min. (*ee* = 93% by HPLC)

(–)-(*S*)-2-methyl-*N*-(1-phenylethyl)propan-1-amine.[9]

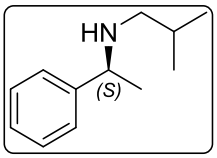

This compound was synthesized applying **GM4**.

^{1}H NMR (400 MHz, $CDCl_3$) δ; 7.34 – 7.29 (m, 4H), 7.25 – 7.21 (m, 1H), 3.74 (q, *J* = 7 Hz, 1H), 2.34 (dd, *J* = 11, 6 Hz, 1H), 2.21 (dd, *J* = 11, 7 Hz, 1H), 1.71 (dh, *J* = 13, 7 Hz, 1H), 1.35 (d, *J* = 7 Hz, 3H), 0.87 (dd, *J* = 7, 2 Hz, 6H) ppm. **HPLC:** CHIRALCEL OD-H. Heptane/iPrOH 98:02, 0.5 mL/min, λ = 210 nm. t_R(+)= 10.4 min, t_S(–)= 12.1 min. (*ee* = 93% by HPLC)

(–)-(*S*)-*N*-(1-(4-chlorophenyl)ethyl)propan-1-amine.[10]

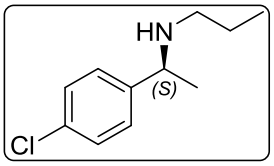

This compound was synthesized applying **GM4**.

^{1}H NMR (400 MHz, $CDCl_3$) δ; 7.32 – 7.23 (m, 4H), 3.74 (q, *J* = 6 Hz, 1H), 2.45 (ddd, *J* = 11, 8, 6 Hz, 1H), 2.35 (ddd, *J* = 11, 8., 7 Hz, 1H), 1.51 – 1.41 (m, 2H), 1.32 (d, *J* = 6 Hz, 3H), 0.87 (t, *J* = 7 Hz, 3H).ppm. **HPLC:** CHIRALCEL OJ. Heptane/iPrOH 98:02, 0.4 mL/min, λ = 210 nm. t_S(–)= 17.1 min, t_R(+)= 19.2 min. (*ee* = 94% by HPLC)

Amines **I11**,[8] **I12**,[8] **I13**,[13] **I15**,[8] **I17** and **I18**[12] can be found in the literature.

NEW MAXPHOX IRIDACYCLE CATALYSTS (7.7-7.10)

Synthesis of the catalysts 7.7-7.10

This complexes were synthesized by Albert Gallén and will be reported in his PhD thesis. A Schlenk flask was charged with 50 mg of complex ***ent*-1iPr** (0.035 mmol, 1 eq) and 13.5 mg (0.069 mmol, 2 eq) of acetophenone *N*-phenyl imine, **A0**. The flask was purged with three vacuum/N_2 cycles and the solids were dissolved in 3 mL of THF. The solution was transferred into a pressure tube and stirred for 2 h under 2 bar of H_2. During this period, the initially orange solution turned yellow. At the due time, the hydrogen was vented and a drop of ACN was added to afford **7.7**. PPh_3 (1 eq) or Me_3P (1 eq) were added to form **7.8** and **7.9**, respectively. To form **7.10** the pressure tube was vented and repressurized with 3 bar of ethylene. The solution was stirred at room temperature for 30 min. The solvent was evacuated and the crude was recrystallized in CH_2Cl_2/pentane to afford each catalyst (**7.7-7.10**).

Hydrogenation of *N*-alkyl imines with catalysts 7.7-7.10

The corresponding catalyst **7.7-7.10** ($3.13x10^{-3}$ mmol, 0.01 eq) was placed in a glass pressure tube, purged with vacuum-nitrogen cycles and 2 mL of CH_2Cl_2 were added. The tube was the purged with vacuum-hydrogen cycles and charged with 3 bar of H_2. When required, the tube was cooled down to the desired temperature. The corresponding *N*-alkyl imine **I1-I18** (0.313 mmol, 1.00 eq) was dissolved in 1 mL of CH_2Cl_2 and added using a pressure syringe. The mixture was left stirring overnight at the desired temperature. The tube was depressurized and the solvent removed under vacuum to afford the corresponding hydrogenated compound as a dark yellow oil or solid. The ee value was determined by HPLC/GC analysis of the corresponding trifluoroacetamide derivative on a chiral stationary phase.

REFERENCES

[1] A. Baeza, A. Pfaltz, *Chem. - A Eur. J.* **2010**, *16*, 4003–4009.

[2] Y. Liu, H. Du, *J. Am. Chem. Soc.* **2013**, *135*, 6810–6813.

[3] K. Kutlescha, G. T. Venkanna, R. Kempe, *Chem. Commun.* **2011**, *47*, 4183.

[4] C. R. Venkat Reddy, S. Urgaonkar, J. G. Verkade, *Org. Lett.* **2005**, *7*, 4427–4430.

[5] Y. Schramm, F. Barrios-Landeros, A. Pfaltz, *Chem. Sci.* **2013**, *4*, 2760.

[6] J. Capra, T. Le Gall, *Synlett* **2010**, *2010*, 441–444.

[7] Y. Sun, H. Jiang, W. Wu, W. Zeng, X. Wu, *Org. Lett.* **2013**, *15*, 1598–1601.

[8] V. N. Wakchaure, P. S. J. Kaib, M. Leutzsch, B. List, *Angew. Chem. Int. Ed. Engl.* **2015**, *54*, 11852–6.

[9] C. Wang, X. Wu, L. Zhou, J. Sun, *Chem. - A Eur. J.* **2008**, *14*, 8789–8792.

[10] X. Verdaguer, U. E. W. Lange, S. L. Buchwald, *Angew. Chem. Int. Ed.* **1998**, *37*, 1103–1107.

[11] M. R. Adams, C.-H. Tien, R. McDonald, A. W. H. Speed, *Angew. Chem. Int. Ed.* **2017**, *56*, 16660–16663.

[12] P. Schnider, G. Koch, R. Pretot, G. Wang, F. M. Bohnen, C. Kriiger, A. Pfaltz, *Chem. Eur. J.* **1997**, *3*, 887–892.

[13] X. Verdaguer, U. E. W. Lange, M. T. Reding, S. L. Buchwald, *J. Am. Chem. Soc.* **1996**, *118*, 6784–6785.

[14] I. Akihiro, K. Mastomi, K. Yokusu, Y. Manabu, I. Kenjin, O. Takashi, U. Koji, *Optically Active 1-(Fluoro-, Trifluoromethyl-or Trifluoromethoxy-Substituted Phenyl)alkylamine N-Monoalkyl Derivatives and Process for Producing Same*, **2004**, WO2004022521.

[15] M. Garrido, J. Vicente, A. M. Miquel, M. J. Jorge, *Method of Obtaining Phenyl Carbamates*, **2008**, EP1939172.

[16] K. Marcseková, B. Wegener, S. Doye, *European J. Org. Chem.* **2005**, 4843–4851.

[17] O. Saidi, A. J. Blacker, M. M. Farah, S. P. Marsden, J. M. J. Williams, *Chem. Commun.* **2010**, *46*, 1541.

Experimental Section for Chapter 8

Highly Enantioselective Iridium-Catalyzed Hydrogenation of Cyclic Enamides

E. Salomó, S. Orgué, A. Riera, X. Verdaguer, *Angew. Chem. Int. Ed.* **2016**, *55*, 7988–7992.

SYNTHESIS OF HYDROGENATION SUBSTRATES

General Method 1: Synthesis of cyclic β-enamides.[1]

In a round bottom flask equipped with a Dean-Stark, the ketone (1 eq), the amide (2.5 eq) and toluene sulfonic acid (0.1 eq) were dissolved in toluene (0.16 M). The mixture was refluxed during 20 h. After cooling down to room temperature, a saturated solution of hydrogen carbonate (0.07 M) was added and the mixture was warmed to 60 ºC and stirred for 30 min. After cooling down to room temperature, the layers were separated (if there was an insoluble solid, it was collected with the aqueous layer). The aqueous layer was then extracted thrice with CH_2Cl_2, the organic layers were collected and combined with the previous toluene layer, dried over $MgSO_4$ and concentrated. The crude obtained was purified via crystallization (plus a previous column when needed) in order to achieve high purity for the enantioselective hydrogenations.

N-(3,4-dihydronaphthalen-2-yl)acetamide, 8.6.[2]

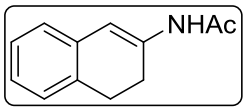

Compound **8.6** was synthesized applying **GM1**.

^{1}H NMR (400 MHz, $CDCl_3$) δ; 7.20 – 6.93 (m, 4H), 6.60 (br s, 1H), 2.96 – 2.81 (m, 2H), 2.55 – 2.35 (m, 2H), 2.12 (s, 3H) ppm.

N-(5-methoxy-3,4-dihydronaphthalen-2-yl)acetamide, E1.[3]

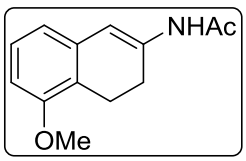

Compound **E1** was synthesized applying **GM1**.

^{1}H NMR (400 MHz, $CDCl_3$) δ; 7.04 – 6.92 (m, 2H), 6.72 – 6.62 (m, 2H), 6.55 (br s, 1H), 3.78 (s, 3H), 2.86 (t, *J* = 8 Hz, 2H), 2.42 (t, *J* = 8Hz, 2H), 2.10 (s, 3H) ppm.

N-(6-bromo-3,4-dihydronaphthalen-2-yl)acetamide, E2.[4]

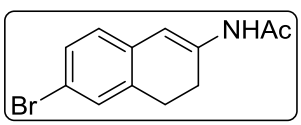

Compound **E2** was synthesized applying **GM1**.

IR (KBr) υ_{max}: 3270, 3176, 2987, 1663, 1647 cm^{-1}. **^{1}H NMR (400 MHz, $CDCl_3$) δ;** 7.24 (dd, *J* = 8, 2 Hz, 1H), 7.21 – 7.18

(m, 1H), 7.07 (br s, 1H), 6.89 (d, *J* = 8 Hz, 1H), 6.56 (br s, 1H), 2.86 (t, *J* = 8 Hz, 2H), 2.41 (td, *J* = 8 Hz, 2H), 2.12 (s, 3H) ppm.

***N*-(8-methoxy-3,4-dihydronaphthalen-2-yl)acetamide, E3.**[4]

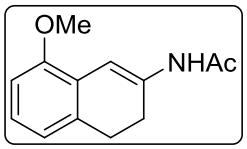

Compound **E3** was synthesized applying **GM1**.

IR (KBr) υ_{max}: 3404, 2928, 1610, 1354, 1277 cm^{-1}. **^{1}H NMR (400 MHz, $CDCl_3$) δ** 7.17 (br s, 1H), 7.03 (t, *J* = 8 Hz, 1H), 6.70 (d, *J* = 8 Hz, 3H), 3.81 (s, 3H), 2.89 – 2.81 (m, 2H), 2.52 (t, *J* = 8 Hz, 2H), 2.10 (s, 3H) ppm.

***N*-(7-methoxy-3,4-dihydronaphthalen-2-yl)acetamide, E4.**[5]

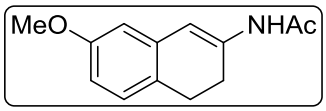

Compound **E4** was synthesized applying **GM1**.

IR (KBr) υ_{max}: 3265, 3163, 2935, 1666, 1577 cm^{-1}. **^{1}H NMR (400 MHz, $CDCl_3$) δ;** δ 7.08 (s, 1H), 7.00 – 6.95 (m, 1H), 6.66 – 6.54 (m, 2H), 3.77 (s, 3H), 2.85 – 2.78 (m, 2H), 2.45 – 2.39 (m, 2H), 2.12 (s, 3H) ppm.

***N*-(3,4-dihydronaphthalen-2-yl)benzamide, E5.**[1]

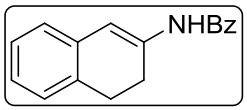

Compound **E5** was synthesized applying **GM1**.

Mp: 129–130 ºC. **IR (KBr) υ_{max}:** 3342, 3015, 2944, 1651, 1600 cm^{-1}. **^{1}H NMR (400 MHz, $CDCl_3$) δ;** 7.81 (m, 2H, CH), 7.54 (m, 1H, CH), 7.47 (m, 1H, CH), 7.26 (s, 1H, CH), 7.24 (br s, 1H, NH), 7.15 (m, 1H, CH), 7.07 (m, 3H, CH), 2.95 (m, 2H, CH_2), 2.59 (m, 2H, CH_2) ppm.

***N*-(3,4-dihydronaphthalen-2-yl)propionamide, E6.**[1]

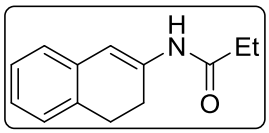

Compound **E6** was synthesized applying **GM1**.

White solid. **Mp**: 104.5–105.5 ºC. **IR (KBr) υ_{max}:** 3302, 3020, 2933, 1662, 1576 cm^{-1}. **^{1}H NMR (400 MHz, $CDCl_3$) δ;** 7.17 – 6.95 (m, 4H), 6.50 (br s, 1H), 2.96 – 2.78 (m, 2H), 2.49 – 2.40 (m, 2H), 2.33 (q, *J* = 8 Hz, 2H), 1.22 (t, *J* = 8 Hz, 3H) ppm. **HRMS (ESI):** calc for $[C_{13}H_{15}ON + H]^+$: 202.1226, found 202.1227.

***N*-(1-methyl-3,4-dihydronaphthalen-2-yl)acetamide, E7.**

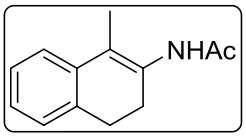

Compound **E7** was synthesized applying **GM1**.

White solid**. Yield:** 68% (2.14 g). **Mp**: 129–130 ºC. **IR (KBr) υ_{max}:** 3211, 3018, 2933, 1638, 1526 cm^{-1}. **^{1}H NMR (400 MHz, DMSO-d_6) δ;** 9.10 (br s, 1H), 7.22 – 7.13 (m, 2H), 7.12 – 7.05 (m, 2H), 2.77 – 2.65 (m, 2H), 2.43 – 2.35 (m, 2H), 1.95 (s, 3H), 1.88 (s, 3H) ppm. **^{13}C NMR (101 MHz, $CDCl_3$) δ;** 168.4 (C), 135.9 (C), 135.0 (C), 131.8 (C), 127.0 (CH), 126.3 (2 x CH), 123.3 (CH), 121.7 (C), 28.5 (CH_2), 26.8 (CH_2), 23.9 (CH_3), 13.2 (CH_3) ppm. **HRMS (ESI):** calc for $[C_{13}H_{15}ON+H]^+$: 202.1226, found 202.1227.

***N*-(3,4-dihydronaphthalen-1-yl)acetamide, 8.8.**[1,6]

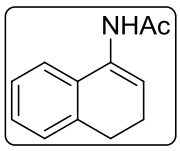

Sodium acetate (1.10 eq) was added to a colourless suspension of hydroxylamine hydrochloride (1.10 eq) in MeOH (1 M) at room temperature and stirred for 30 min. **3,4-dihydronaphthalen-1(2H)-one** (1.00 eq) was added in 90 min and the suspension was stirred overnight (16 h) at room temperature. Water (2 M) was added within 60 min and the reaction mixture was stirred vigorously for further 60 min at room temperature. The resulting precipitated 3,4-dihydronaphthalen-1(2H)-one oxime was filtered off, washed with water and dried.

Acetic anhydride (3.00 eq), acetic acid (3.00 eq), iron powder (325 mesh, 2.10 eq) and TMSCl (2–5 drops) were consecutively added to a mixture of 3,4-dihydronaphthalen-1(2H)-one oxime (1.00 eq) in toluene (0.66 M). This suspension was stirred for 5 hours at 70 °C, cooled to room temperature, filtered through celite and washed twice with toluene. The filtrate was washed twice with aqueous NaOH (2 M), dried over MgSO4, filtered and the filtrate was evaporated under reduced pressure. The crude enamide was purified by recrystallization to allow a white solid (48%).

^{1}H NMR (400 MHz, $CDCl_3$) δ; 7.25 – 7.12 (m, 3H), 6.74 (br s, 0.75H), 6.61 (br s, 0.25H), 6.46 (t, *J* = 5 Hz, 0.75H), 6.00 – 5.92 (m, 0.25H), 2.88 – 2.80 (m, 0.50H), 2.80 – 2.77 (t, *J* = 8 Hz, 1.50H), 2.48 – 2.32 (m, 2H), 2.18 (s, 2H), 1.96 (s, 1H) ppm.

***N*-(5-methoxy-3,4-dihydronaphthalen-1-yl)acetamide, E8.**[6,7]

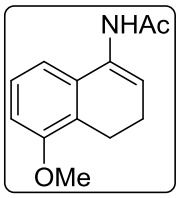

5-methoxy-3,4-dihydronaphthalen-1(2*H*)-one (1 eq) was dissolved in toluene (1.7 M). The mixture was stirred and cooled in an ice bath. NH_3 (7 N) in MeOH (1.5 eq) was added, followed by a dropwise addition of $Ti(Oi\text{-}Pr)_4$ (2 eq). After 10 min, the solution was allowed to warm to room temperature and stirred for 24 h. The reaction mixture was then cooled in an ice bath and treated with Et_3N (4.0 eq) followed by Ac_2O (2.0 eq). The solution was then stirred at room temperature for 3 h. The reaction mixture was treated with EDTE (2.1 eq), heated up to 55 °C and stirred for 15 min. The mixture was then allowed to cool to room temperature and was poured into a separatory funnel containing a solution (1 : 1) EtOAc and water / NH_4OH (3 : 1). The aqueous phase was separated and then extracted with MTBE. The combined organic extracts were dried over $MgSO_4$, filtered and concentrated to give the crude enamide. Recrystallization provided the pure enamide as a white solid. **Yield:** 47% (2.84 g). **IR (KBr) υ_{max}:** 3240, 3035, 2929, 1660, 1597 cm^{-1}. **^{1}H NMR (400 MHz, $CDCl_3$) δ;** 9.05 (s, 1H), 7.16 (t, *J* = 8 Hz, 1H), 6.91 (d, *J* = 8 Hz, 1H), 6.86 (d, *J* = 8 Hz, 1H), 6.14 (t, *J* = 5 Hz, 1H), 3.78 (s, 3H), 2.64 (t, *J* = 8 Hz, 2H), 2.23 (dt, *J* = 8, 4 Hz, 2H), 2.00 (s, 3H) ppm.

***N*-(6-methoxy-3,4-dihydronaphthalen-1-yl)acetamide, E9.**[6,7]

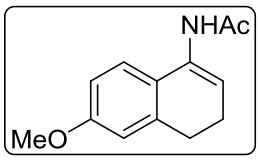

6-methoxy-3,4-dihydronaphthalen-1(2*H*)-one (1 eq) was dissolved in toluene (1.7 M). The mixture was stirred and cooled in an ice bath. NH_3 (7 N) in MeOH (4.5 eq) was added, followed by a dropwise addition of $Ti(Oi\text{-}Pr)_4$ (2 eq). After 10 min, the solution was allowed to warm to room temperature and stirred for 48 h. The reaction mixture was then cooled in an ice bath and treated with Et_3N (4.0 eq) followed by Ac_2O (2.0 eq). The solution was then stirred at room temperature for 3 h. The reaction mixture was treated with EDTE (2.1 eq), heated up to 55 °C and stirred for 15 min. The mixture was then allowed to cool to room temperature and was poured into a separatory funnel containing a solution (1 : 1) EtOAc and water / NH_4OH (3 : 1). The aqueous phase was separated and then extracted with MTBE. The combined organic extracts were dried over $MgSO_4$, filtered and concentrated to give the crude enamide. Recrystallization provided the pure enamide as a white solid. **Yield:** 46% (2.82 g). **IR (KBr) υ_{max}:** 3235, 3035, 2928, 1658, 1604 cm^{-1}. **^{1}H NMR (400**

MHz, DMSO-*d*$_6$) δ; 9.01 (s, 1H), 7.11 (d, *J* = 8 Hz, 1H), 6.86 – 6.64 (m, 2H), 6.01 (t, *J* = 5 Hz, 1H), 3.72 (s, 3H), 2.64 (t, *J* = 8 Hz, 2H), 2.27 – 2.16 (m, 2H), 1.98 (s, 3H) ppm.

***N*-(1*H*-inden-3-yl)acetamide, E11.**[8]

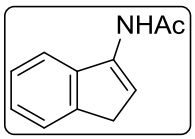

2,3-dihydro-1*H*-inden-1-one was dissolved in toluene (1.7 M). The mixture was stirred and cooled in an ice bath. NH_3 (7 N) in MeOH (4.5 eq) was added, followed by a dropwise addition of Ti(Oi-Pr)$_4$ (2 eq). After 10 min, the solution was allowed to warm to room temperature and stirred for 48 h. The reaction mixture was then cooled in an ice bath and treated with Et_3N (4.0 eq) followed by Ac_2O (2.0 eq). The solution was then stirred at room temperature for 3 h. The reaction mixture was treated with EDTE (2.1 eq), heated up to 55 °C and stirred for 15 min. The mixture was then allowed to cool to room temperature and was poured into a separatory funnel containing a solution (1 : 1) EtOAc and water / NH_4OH (3 : 1). The aqueous phase was separated and then extracted with MTBE. The combined organic extracts were dried over $MgSO_4$, filtered and concentrated to give the crude enamide. Purification by chromatographic column followed by recrystallization provided the pure enamide as a brown solid.

Yield: 27% (1.79 g).**^{1}H NMR (400 MHz, $CDCl_3$) δ;** 7.54 – 7.45 (m, 1H), 7.39 – 7.23 (m, 4H), 6.87 (t, *J* = 2 Hz, 1H), 3.44 (d, *J* = 2 Hz, 2H), 2.24 (s, 3H) ppm.

***N*-(2*H*-chromen-4-yl)acetamide, E12.**[8]

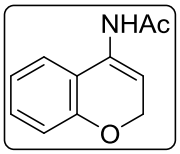

Chroman-4-one (1 eq) was dissolved in toluene (1.7 M). The mixture was stirred and cooled in an ice bath. NH_3 (7 N) in MeOH (4.5 eq) was added, followed by a dropwise addition of Ti(OiPr)$_4$ (2 eq). After 10 min, the solution was allowed to warm to room temperature and stirred for 48 h. The reaction mixture was then cooled in an ice bath and treated with Et_3N (4.0 eq) followed by Ac_2O (2.0 eq). The solution was then stirred at room temperature for 3 h. The reaction mixture was treated with EDTE (2.1 eq), heated up to 55 °C and stirred for 15 min. The mixture was then allowed to cool to room temperature and was poured into a separatory funnel containing a solution (1 : 1) EtOAc and water / NH_4OH (3 : 1). The aqueous phase was separated and then extracted with MTBE. The combined organic extracts were dried over $MgSO_4$, filtered and concentrated to give the crude enamide. Purification by

chromatographic column followed by recrystallization provided the pure enamide as a white solid.

Yield: 41% (2.54 g).**^{1}H NMR (400 MHz, $CDCl_3$) δ;** 7.21 – 7.16 (m, 1H), 7.07 (d, *J* =8 Hz, 0H), 6.94 (td, *J* = 8, 1 Hz, 1H), 6.87 (dd, *J* = 8, 1 Hz, 1H), 6.80 (s, 1H), 6.44 (t, *J* = 4 Hz, 1H), 4.81 (d, *J* = 4 Hz, 1H), 2.19 (s, 1H) ppm.

Substrates **E10,**[9] **E13**,[10] , **E15**,[11] **E16**[12] were previously reported in the literature and were synthesized accordingly. Substrate **E14** is commercially available.

ASYMMETRIC HYDROGENATIONS

General Method 2: Hydrogenation of enamides

The corresponding enamide (1 eq) and the corresponding catalyst (0.01 eq) were placed in a stainless steel high pressure reactor. The reactor was entered into a glove box and deoxygenated anhydrous solvent was added. The reactor was closed, removed from the glove box and connected to a hydrogen manifold. While stirring, the reactor was purged with vacuum-hydrogen cycles and then it was charged at the corresponding hydrogen gas pressure. The hydrogen manifold was unplugged and the mixture was left to stirr overnight at room temperature. The reactor was depressurized and the reaction mixture was filtered through a short silica pad and subsequently eluted with CH_2Cl_2 or EtOAc. The resulting solution was concentrated under vacuum to afford the hydrogenated compounds as white to brown solids.

(–)-(*S*)-*N*-(1,2,3,4-tetrahydronaphthalen-2-yl)acetamide.[2,5]

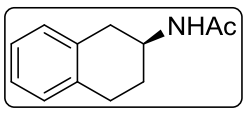

Following **GM2**, *N*-(3,4-dihydronaphthalen-2-yl)acetamide **8.6** (65 mg, 345 µmol) and catalyst **4iPr** (5 mg, 3.45 µmol) were mixed and dissolved in MeOH (2 mL). The reactor was charged with 3 bars of H_2 and the reaction was stopped after 12 h. The crude was then filtered through a short silica pad and concentrated under vacumm to afford the corresponding acetamide with complete conversion.

^{1}H NMR (400 MHz, $CDCl_3$) δ; 7.19 – 7.03 (m, 4H), 5.51 (s, 1H), 4.36 – 4.23 (m, 1H), 3.12 (dd, *J* = 16, 5 Hz, 1H), 2.96 – 2.81 (m, 2H), 2.68 – 2.60 (m, 1H), 2.09 – 2.01 (m, 1H), 1.98 (s, 3H), 1.84 – 1.74 (m, 1H) ppm. **HPLC:** CHIRALCEL OJ. Heptane/iPrOH 70:30-0.2% NEt_3, 0.5 mL/min, λ = 254 nm. $t_{(S)}$ (–) = 8.1 min, $t_{(R)}$ (+) = 9.5 min. (*ee* = 99% by HPLC)

(–)-(*S*)-*N*-(5-methoxy-1,2,3,4-tetrahydronaphthalen-2-yl)acetamide.[13][14]

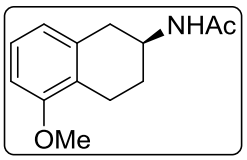

Following **GM2**, *N*-(5-methoxy-3,4-dihydronaphthalen-2-yl)acetamide **E1** (75 mg, 345 µmol) and catalyst **4iPr** (5 mg, 3.45 µmol) were mixed and dissolved in EtOAc (2 mL). The reactor was charged with 3 bars of H_2 and the reaction was stopped after 12 h. The crude was then filtered through a short silica pad and concentrated under vacumm to afford the corresponding acetamide with complete conversion.

^{1}H NMR (400 MHz, $CDCl_3$) δ; 7.10 (t, 1H, *J* = 8 Hz), 6.68 (d, 2H, *J* = 8 Hz), 5.63 (s, 1H), 4.28 (m, 1H), 3.81 (s, 3H), 3.08 (dd, 1H, *J* = 16, 5 Hz,), 2.80 – 2.71 (m, 2H), 2.64 (dd, 1H, *J* = 16, 8 Hz), 2.01 (m, 1H), 1.96 (s, 3H), 1.78 (td, 1H, *J* = 15, 8Hz) ppm. **HPLC:** CHIRALPAK AD-H. Heptane/iPrOH 90:10, 1.0 mL/min, λ = 210 nm. $t_{(S)}$ (–) = 9.0 min, $t_{(R)}$ (+) = 11.0 min. (*ee* = 99% by HPLC)

(–)-(*S*)-*N*-(6-bromo-1,2,3,4-tetrahydronaphthalen-2-yl)acetamide.[4]

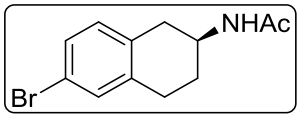

Following **GM2**, *N*-(6-bromo-3,4-dihydronaphthalen-2-yl)acetamide **E2** (92 mg, 345 µmol) and catalyst **4iPr** (5 mg, 3.45 µmol) were mixed and dissolved in EtOAc (2 mL). The reactor was charged with 3 bars of H_2 and the reaction was stopped after 12 h. The crude was then filtered through a short silica pad and concentrated under vacumm to afford the corresponding acetamide with complete conversion.

^{1}H NMR (400 MHz, $CDCl_3$) δ; 7.30 – 7.21 (m, 2H), 6.93 (d, *J* = 8 Hz, 1H), 5.46 (br s, 1H), 4.33 – 4.20 (m, 1H), 3.06 (dd, *J* = 16, 5 Hz, 1H), 2.95 – 2.75 (m, 2H), 2.57 (dd, *J* = 16, 8 Hz, 1H), 2.08 – 2.00 (m, 1H), 1.98 (s, 3H), 1.83 – 1.70 (m, 1H) ppm. **HPLC:** CHIRALCEL OJ. Heptane/EtOH-0.2% DEA 90:10, 0.5 mL/min, λ = 210 nm. $t_{(S)}$ (–) = 16.6 min, $t_{(R)}$ (+) = 18.9 min. (*ee* = 99% by HPLC)

(–)-(*S*)-N-(8-methoxy-1,2,3,4-tetrahydronaphthalen-2-yl)acetamide.[4]

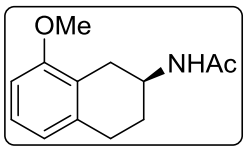

Following **GM2**, *N*-(8-methoxy-3,4-dihydronaphthalen-2-yl)acetamide **E3** (75 mg, 345 µmol) and catalyst **4iPr** (5 mg, 3.45 µmol) were mixed and dissolved in EtOAc (2 mL). The reactor was charged with 3 bars of H_2 and the reaction was stopped after 12 h. The crude was then filtered through a short silica pad and concentrated under vacumm to afford the corresponding acetamide with complete conversion.

^{1}H NMR (400 MHz, $CDCl_3$) δ; 7.14 – 7.08 (m, 1H), 6.72 (d, *J* = 7 Hz, 1H), 6.67 (d, *J* = 8 Hz, 1H), 5.49 (br s, 1H), 4.33 – 4.22 (m, 1H), 3.80 (s, 3H) 3.06 (dd, *J* = 17, 6 Hz, 1H), 2.95 – 2.78 (m, 2H), 2.45 (dd, *J* = 17, 8 Hz, 1H), 2.07 – 1.98 (m, 1H), 1.98 (s, 3H), 1.80 – 1.70 (m, 1H) ppm. **HPLC:** CHIRALCEL OJ. Heptane/iPrOH 90:10, 0.5 mL/min, λ = 210 nm. $t_{(S)}$ (–) = 29.8 min, $t_{(R)}$ (+) = 35.7 min. (*ee* = 99% by HPLC)

(–)-(*S*)-*N*-(7-methoxy-1,2,3,4-tetrahydronaphthalen-2-yl)acetamide.[5]

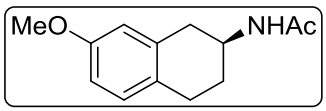

Following **GM2**, *N*-(7-methoxy-3,4-dihydronaphthalen-2-yl)acetamide **E4** (75 mg, 345 µmol) and catalyst **4iPr** (5 mg, 3.45 µmol) were mixed and dissolved in EtOAc (2 mL). The reactor was charged with 3 bars of H_2 and the reaction was stopped after 12 h. The crude was then filtered through a short silica pad and concentrated under vacumm to afford the corresponding acetamide with complete conversion.

^{1}H NMR (400 MHz, $CDCl_3$) δ; 7.01 (d, *J* = 8 Hz, 1H), 6.72 (dd, *J* = 8, 3 Hz, 1H), 6.59 (d, *J* = 3 Hz, 1H), 4.34 – 4.24 (m, 1H), 3.77 (s, 3H), 3.09 (dd, *J* = 16, 5 Hz, 1H), 2.88 – 2.72 (m, 2H), 2.62 (dd, *J* = 16, 8 Hz, 1H), 2.05 – 1.99 (m, 1H), 1.97 (s, 3H), 1.82 – 1.73 (m, 1H) ppm. **HPLC:** CHIRALCEL OD-H. Heptane/iPrOH 80:20, 1.0 mL/min, λ = 210 nm. $t_{(S)}$ (–)= 6.1 min, $t_{(R)}$ (+)= 8.0 min. (*ee* = 99% by HPLC)

(–)-(*S*)-*N*-(1,2,3,4-tetrahydronaphthalen-2-yl)benzamide.[1]

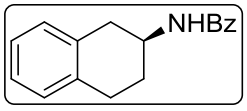

Following **GM2**, *N*-(3,4-dihydronaphthalen-2-yl)benzamide **E5** (68 mg, 345 µmol) and catalyst **4iPr** (5 mg, 3.45 µmol) were mixed and dissolved in CH_2Cl_2 (2 mL). The reactor was charged with 3 bars of H_2 and the reaction

was stopped after 12 h. The crude was then filtered through a short silica pad and concentrated under vacumm to afford the corresponding acetamide with complete conversion.

^{1}H NMR (400 MHz, $CDCl_3$) δ; 7.78 – 7.72 (m, 2H), 7.54 – 7.37 (m, 3H), 7.19 – 7.06 (m, 4H), 6.16 – 6.09 (br s, 1H), 4.58 – 4.45 (m, 1H), 3.25 (dd, *J* = 16, 5 Hz, 1H), 3.05 – 2.85 (m, 2H), 2.77 (dd, *J* = 16, 8 Hz, 1H), 2.24 – 2.12 (m, 1H), 1.98 – 1.84 (m, 1H) ppm. **HPLC:** CHIRALPAK IA. Heptane/EtOH-0.2% DEA 70:30, 0.5 mL/min, λ = 254 nm. $t_{(S)}$ (–) =10.2 min, $t_{(R)}$ (+) = 11.5 min. (*ee* = 99% by HPLC)

(–)-(*S*)-*N*-(1,2,3,4-tetrahydronaphthalen-2-yl)propionamide.[1]

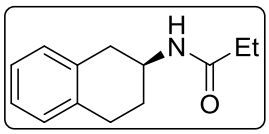

Following **GM2**, *N*-(3,4-dihydronaphthalen-2-yl)propionamide **E6** (69 mg, 345 µmol) and catalyst **4tBu** (5 mg, 3.45 µmol) were mixed and dissolved in CH_2Cl_2 (2 mL). The reactor was charged with 3 bars of H_2 and the reaction was stopped after 12 h. The crude was then filtered through a short silica pad and concentrated under vacumm to afford the corresponding acetamide with complete conversion.

^{1}H NMR (400 MHz, $CDCl_3$) δ; 7.16 – 7.02 (m, 4H), 5.44 (s, 1H), 4.37 – 4.22 (m, 1H), 3.13 (dd, *J* = 16, 5 Hz, 1H), 2.98 – 2.79 (m, 2H), 2.64 (dd, *J* = 16, 8 Hz, 1H), 2.19 (q, *J* = 8 Hz, 2H), 2.09 – 2.00 (m, 1H), 1.84 – 1.72 (m, 1H), 1.16 (t, *J* = 8 Hz, 3H) ppm. **HPLC:** CHIRALCEL OJ. Heptane/EtOH-0.2% DEA 90:10, 0.5 mL/min, λ = 210 nm. $t_{(S)}$ (–) = 15.3 min, $t_{(R)}$ (+) = 19.4 min. (*ee* = 99% by HPLC)

(–)-*N*-((1*R*,2*S*)-1-methyl-1,2,3,4-tetrahydronaphthalen-2-yl)acetamide.

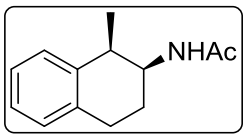

Following **GM2**, *N*-(1-methyl-3,4-dihydronaphthalen-2-yl)acetamide **E7** (69 mg, 345 µmol) and catalyst **4tBu** (5 mg, 3.45 µmol) were mixed and dissolved in CH_2Cl_2 (2 mL). The reactor was charged with 3 bars of H_2 and the reaction was stopped after 12 h. The crude was then filtered through a short silica pad and concentrated under vacumm to afford the corresponding acetamide with complete conversion.

^{1}H NMR (400 MHz, $CDCl_3$) δ; 7.22 – 7.03 (m, 4H), 5.41 (br s, 1H), 4.43 – 4.28 (m, 1H), 3.22 – 3.12 (m, 1H), 2.96 – 2.82 (m, 2H), 1.98 (s, 3H), 1.97 – 1.82 (m, 2H), 1.23 (d,

J = 7 Hz, 3H) ppm. **HPLC:** CHIRALPAK IC. Heptane/EtOH-0.2% DEA 95:5, 0.5 mL/min, λ = 210 nm. $t_{(S)}$ (–) = 33.7 min, $t_{(R)}$ (+) = 36.7 min. (*ee* = 99% by HPLC)

(+)-(*R*)-*N*-(1,2,3,4-tetrahydronaphthalen-1-yl)acetamide.[2,15]

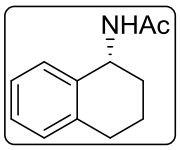

Following **GM2**, *N*-(3,4-dihydronaphthalen-1-yl)acetamide **8.8** (65 mg, 345 µmol) and catalyst **4iPr** (5 mg, 3.45 µmol) were mixed and dissolved in MeOH (2 mL). The reactor was charged with 3 bars of H_2 and the reaction was stopped after 12 h. The crude was then filtered through a short silica pad and concentrated under vacumm to afford the corresponding acetamide with complete conversion.

^{1}H NMR (400 MHz, $CDCl_3$) δ; δ 7.22 – 7.05 (m, 4H), 5.69 (br s, 1H), 5.23 – 5.08 (m, 1H), 2.89 – 2.68 (m, 2H), 2.09 – 1.95 (m, 4H), 1.89 – 1.73 (m, 3H) ppm. **GC**: β-DEX (30 m), 130 ºC, 1 mL/min, He. $t_{(S)}$ (–) = 17.9 min, $t_{(R)}$ (+) = 18.7 min. (*ee* = 99% by GC)

(+)-(*R*)-*N*-(5-methoxy-1,2,3,4-tetrahydronaphthalen-1-yl)acetamide.

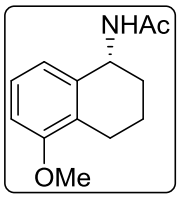

Following **GM2**, *N*-(5-methoxy-3,4-dihydronaphthalen-1-yl)acetamide **E8** (75 mg, 345 µmol) and catalyst **4tBu** (5 mg, 3.45 µmol) were mixed and dissolved in CH_2Cl_2 (2 mL). The reactor was charged with 3 bars of H_2 and the reaction was stopped after 12 h. The crude was then filtered through a short silica pad and concentrated under vacumm to afford the corresponding acetamide with complete conversion.

^{1}H NMR (400 MHz, $CDCl_3$) δ; 7.15 (t, *J* = 8 Hz, 1H), 6.90 (d, *J* = 8 Hz, 1H), 6.74 (d, *J* = 8 Hz, 1H), 5.67 (br d, *J* = 9 Hz, 1H), 5.24 – 5.06 (m, 1H), 3.82 (s, 3H), 2.78 – 2.65 (m, 1H), 2.65 – 2.52 (m, 1H), 2.01 (s, 4H), 1.86 – 1.73 (m, 3H) ppm. **HPLC:** CHIRALPAK IA. Heptane/EtOH-0.2% DEA 90:10, 0.5 mL/min, λ = 210 nm. $t_{(R)}$ (+) = 15.0 min, $t_{(S)}$ (–) = 17.2 min. (*ee* = 99% by HPLC)

(+)-(*R*)-*N*-(6-methoxy-1,2,3,4-tetrahydronaphthalen-1-yl)acetamide.[15]

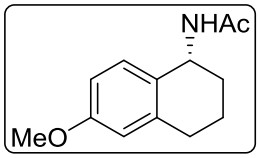

Following **GM2**, *N*-(6-methoxy-3,4-dihydronaphthalen-1-yl)acetamide **E9** (75 mg, 345 µmol) and catalyst **4tBu** (5 mg, 3.45 µmol) were mixed and dissolved in CH_2Cl_2 (2 mL). The reactor

was charged with 3 bars of H_2 and the reaction was stopped after 12 h. The crude was then filtered through a short silica pad and concentrated under vacumm to afford the corresponding acetamide with complete conversion.

^{1}H NMR (400 MHz, $CDCl_3$) δ; 7.19 (d, *J* = 9 Hz, 1H), 6.80 – 6.68 (m, 1H), 6.61 (d, *J* = 3 Hz, 1H), 5.64 (d, *J* = 8 Hz, 1H), 5.19 – 5.06 (m, 1H), 3.78 (s, 3H), 2.89 – 2.64 (m, 2H), 2.07 – 1.92 (m, 4H), 1.89 – 1.74 (m, 3H) ppm. **HPLC:** CHIRALPAK IA. Heptane/EtOH-0.2% DEA 90:10, 0.5 mL/min, λ = 210 nm. $t_{(R)}$ (+) = 17.3 min, $t_{(S)}$ (–) = 20.1 min. (*ee* = 99% by HPLC)

The corresponding amides of substrates **E10**,[13] **E13**,[16] **E14**,[16] **E15**[16] and **E16**[16] were obtained by applying **GM2**. These amides are reported in the literature.

REFERENCES

[1] J. L. Renaud, P. Dupau, A.-E. Hay, M. Guingouain, P. H. Dixneuf, C. Bruneau, *Adv. Synth. Catal.* **2003**, *345*, 230–238.

[2] D. J. Frank, A. Franzke, A. Pfaltz, *Chem. - A Eur. J.* **2013**, *19*, 2405–2415.

[3] G. Q. Li, H. Gao, C. Keene, M. Devonas, D. H. Ess, L. Kürti, *J. Am. Chem. Soc.* **2013**, *135*, 7414–7417.

[4] I. Arribas, M. Rubio, P. Kleman, A. Pizzano, *J. Org. Chem.* **2013**, *78*, 3997–4005.

[5] C. Pautigny, C. Debouit, P. Vayron, T. Ayad, V. Ratovelomanana-Vidal, *Tetrahedron: Asymmetry* **2010**, *21*, 1382–1388.

[6] Z. Hang, C. P. Vandenbossche, S. G. Koenig, S. P. Singh, R. P. Bakale, *Org. Lett.* **2008**, *10*, 505–507.

[7] J. T. Reeves, Z. Tan, Z. S. Han, G. Li, Y. Zhang, Y. Xu, D. C. Reeves, N. C. Gonnella, S. Ma, H. Lee, et al., *Angew. Chem. Int. Ed.* **2012**, *51*, 1400–1404.

[8] H. Bernsmann, M. Van Den Berg, R. Hoen, A. J. Minnaard, G. Mehler, M. T. Reetz, J. G. De Vries, B. L. Feringa, *J. Org. Chem.* **2005**, *70*, 943–951.

[9] Z. Cai, G. Liu, G. Jiao, C. Senanayake, W. Tang, *Synthesis (Stuttg).* **2013**, *45*, 3355–3360.

[10] M. J. Burk, G. Casy, N. B. Johnson, *J. Org. Chem.* **1998**, *63*, 6084–6085.

[11] J. Lee, S. Bernard, X.-C. Liu, *React. Funct. Polym.* **2009**, *69*, 650–654.

[12] K. Wakasugi, A. Iida, T. Misaki, Y. Nishii, Y. Tanabe, *Adv. Synth. Catal.* **2003**, *345*, 1209–1214.

[13] G. Liu, X. Liu, Z. Cai, G. Jiao, G. Xu, W. Tang, *Angew. Chem. Int. Ed.* **2013**, *52*, 4235–4238.

[14] G. G. L., Y. Qizhuang, *J. Med. Chem.* **1989**, *32*, 478–486.

[15] Q. Z. Jiang, D. M. Xiao, Z. G. Zhang, P. Cao, X. M. Zhang, *J. Org. Chem.* **1999**,

38, 516–518.

[16] E. Cristóbal-Lecina, P. Etayo, S. Doran, M. Revés, P. Martín-Gago, A. Grabulosa, A. R. Costantino, A. Vidal-Ferran, A. Riera, X. Verdaguer, *Adv. Synth. Catal.* **2014**, *356*, 795–804.

Appendix 1

Spectra Selection

^{1}H NMR (400 MHz, $CDCl_3$)

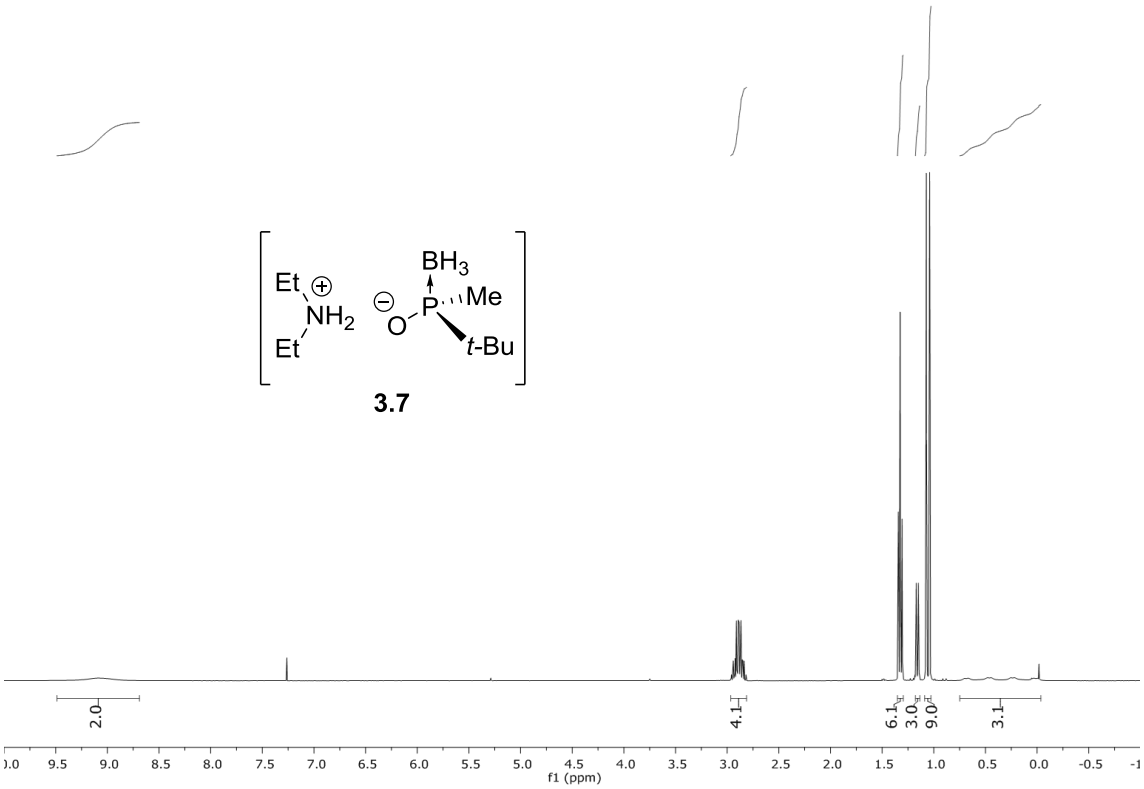

3.7

^{13}C NMR (202 MHz, $CDCl_3$)

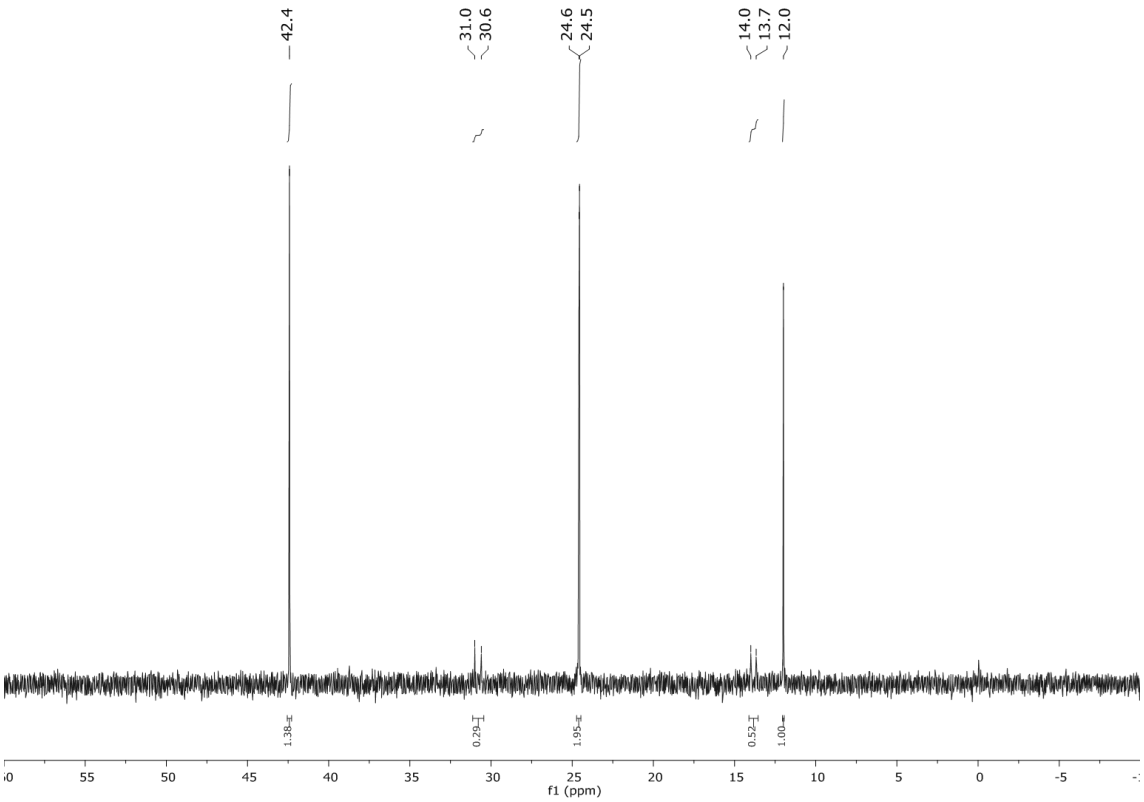

^{1}H NMR (400 MHz, $CDCl_3$)

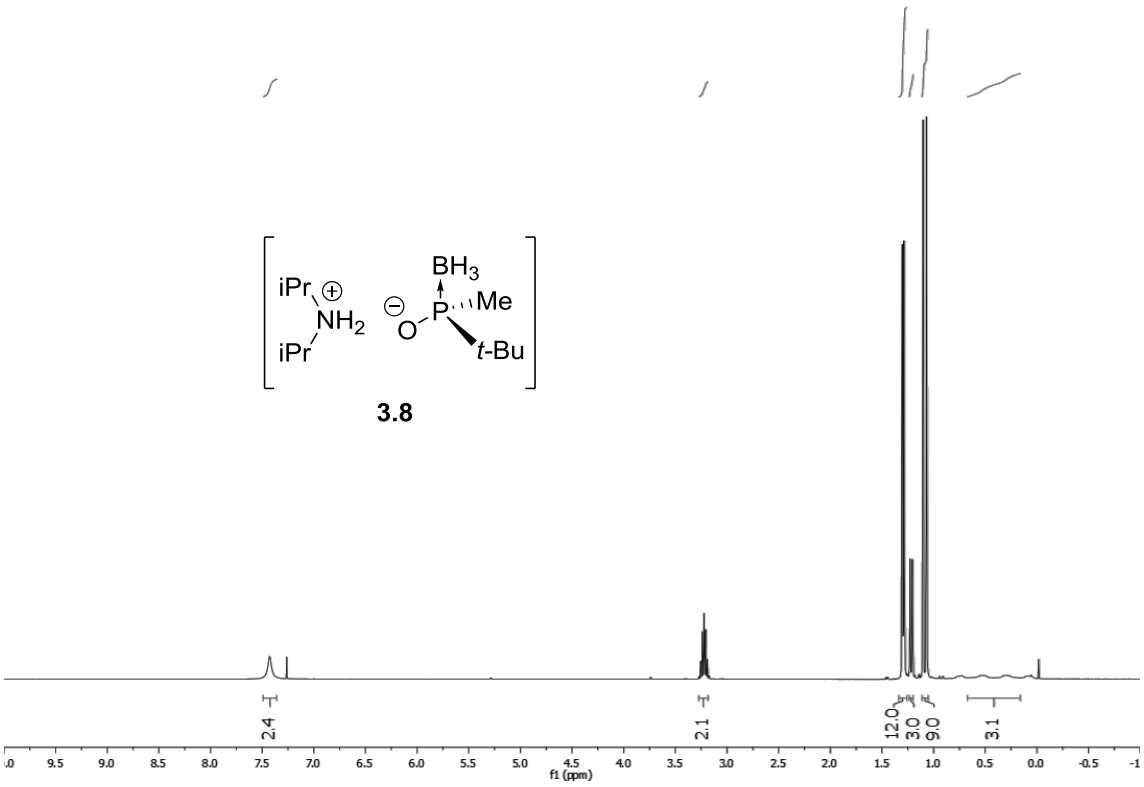

3.8

^{13}C NMR (202 MHz, $CDCl_3$)

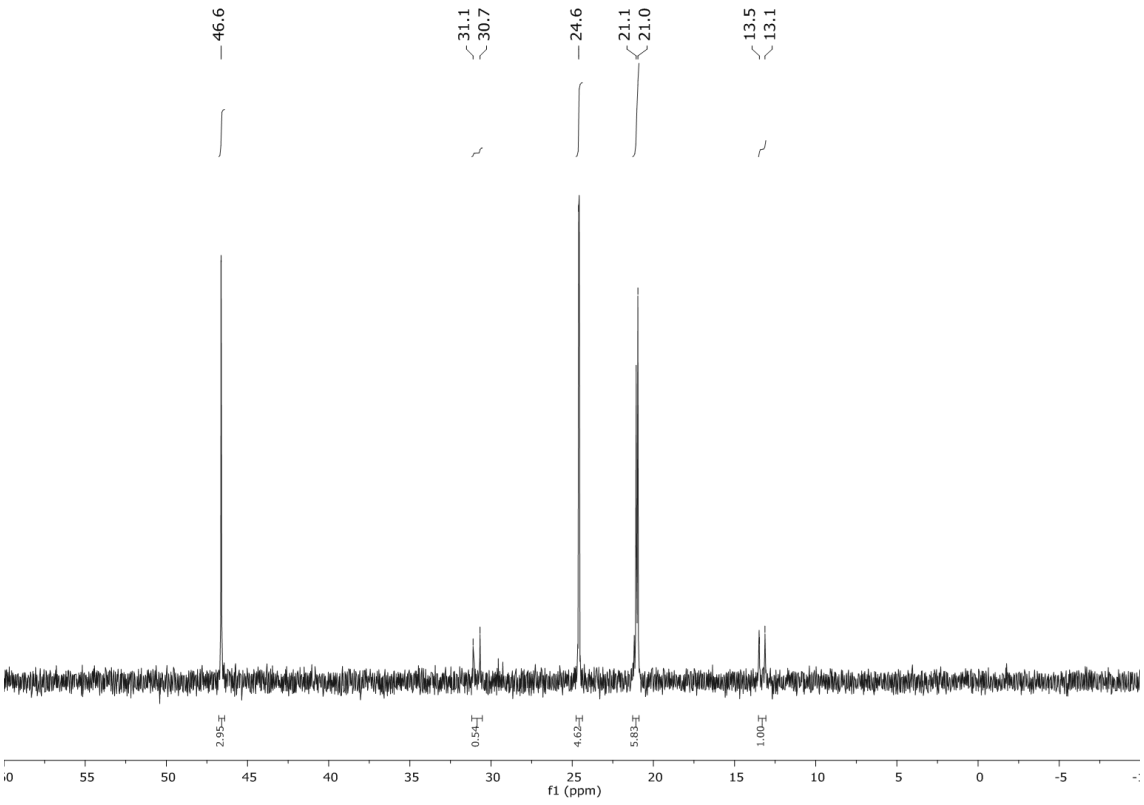

^{1}H NMR (400 MHz, $CDCl_3$)

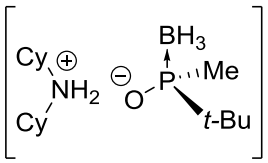

3.9

^{13}C NMR (202 MHz, $CDCl_3$)

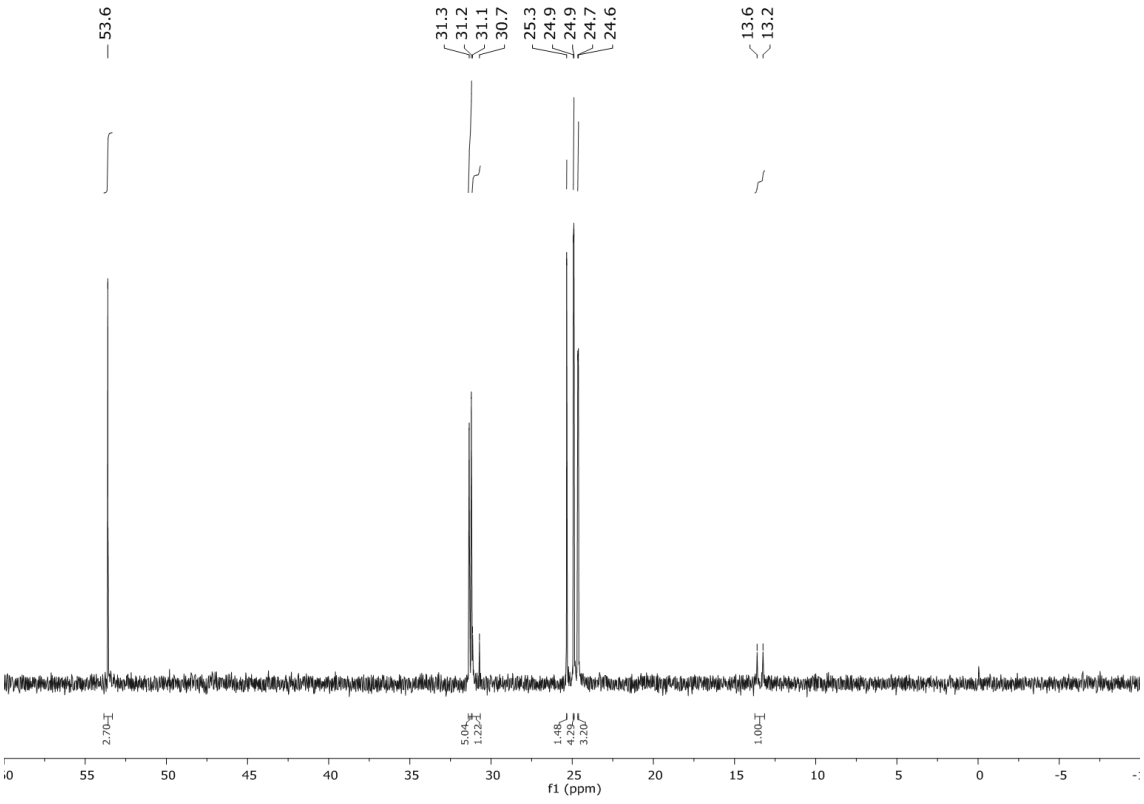

^{1}H NMR (400 MHz, $CDCl_3$)

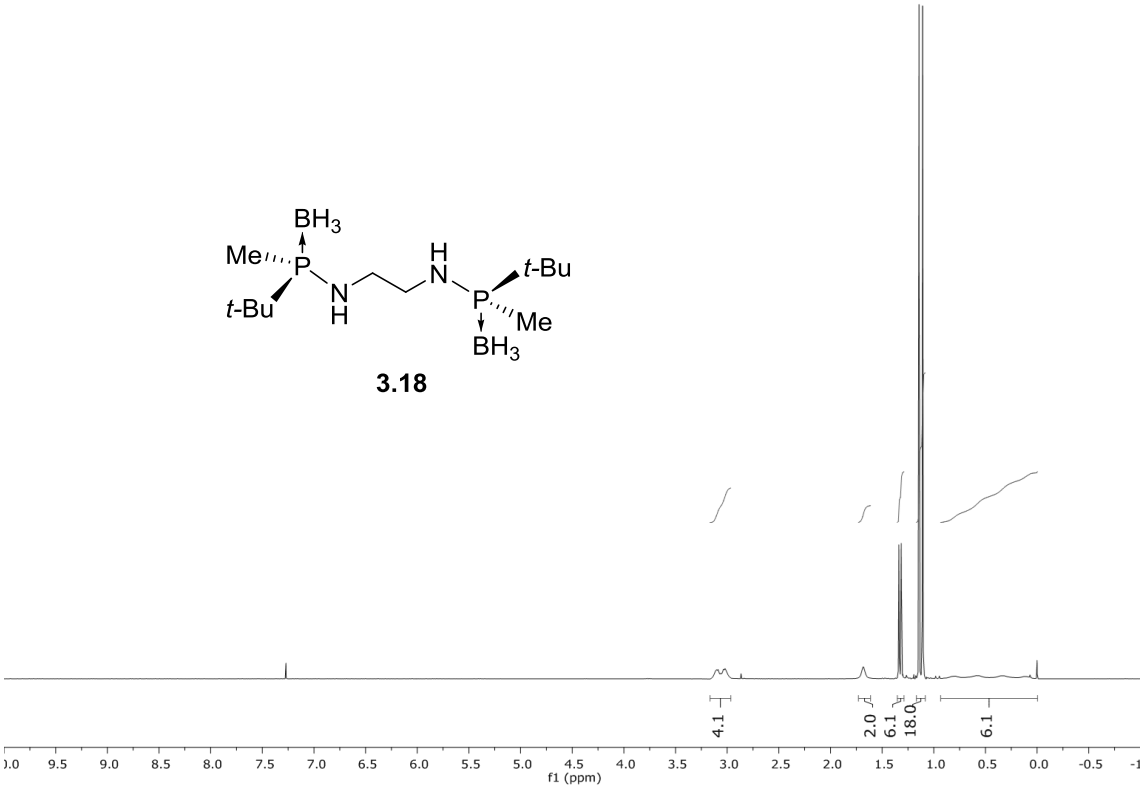

3.18

^{13}C NMR (202 MHz, $CDCl_3$)

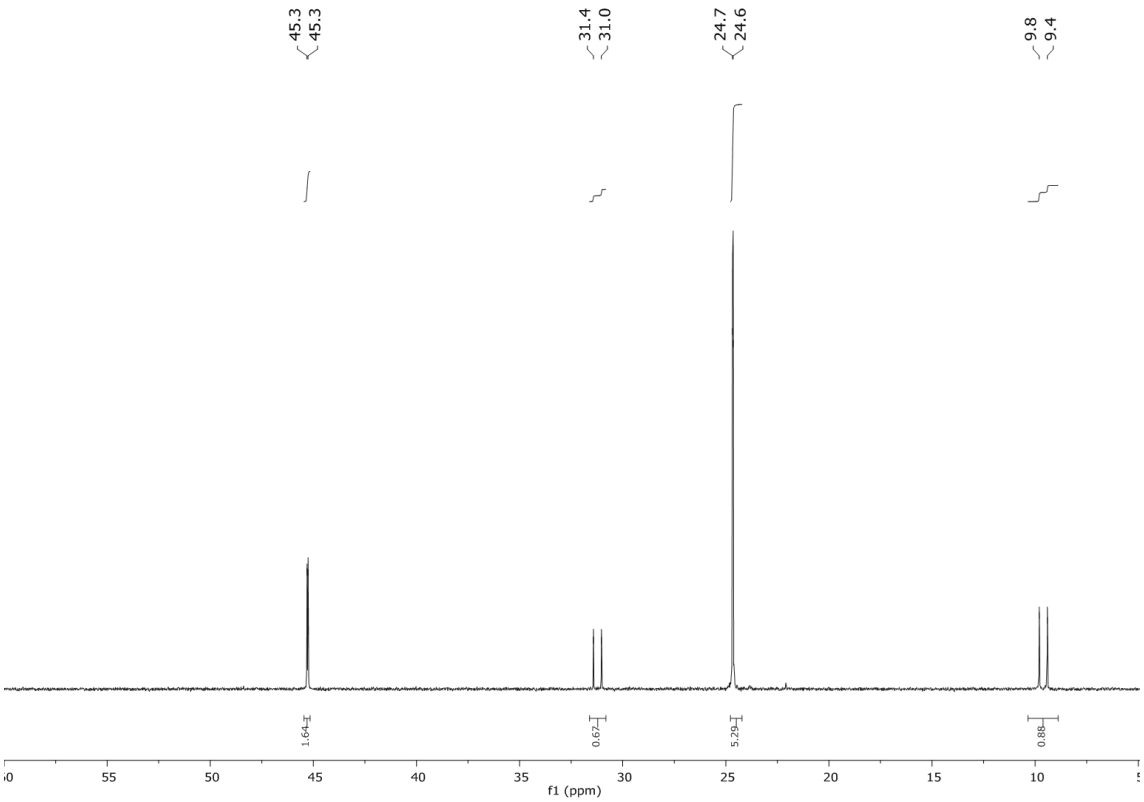

^{1}H NMR (400 MHz, $CDCl_3$)

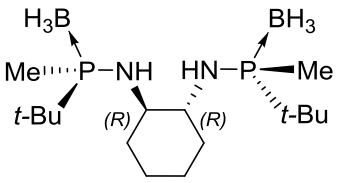

3.19

^{13}C NMR (202 MHz, $CDCl_3$)

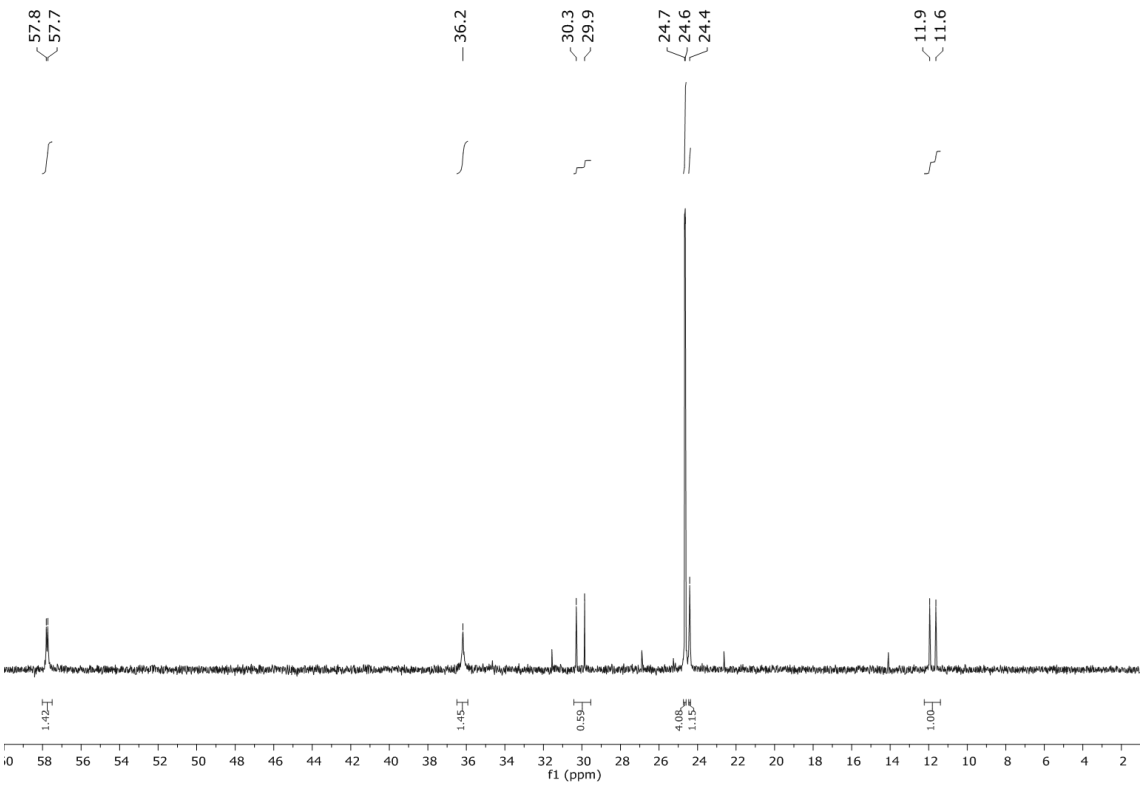

^{1}H NMR (400 MHz, $CDCl_3$)

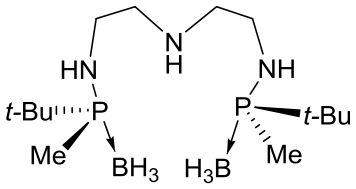

3.20

^{13}C NMR (202 MHz, $CDCl_3$)

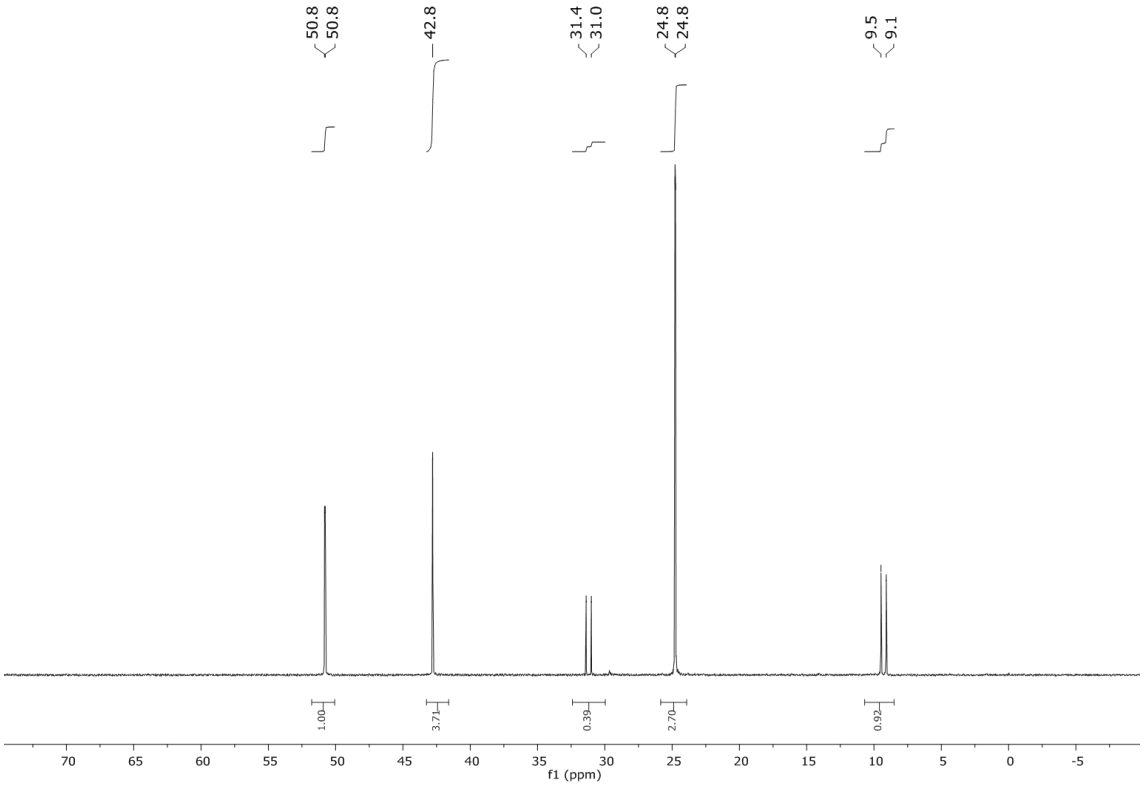

^{1}H NMR (400 MHz, $CDCl_3$)

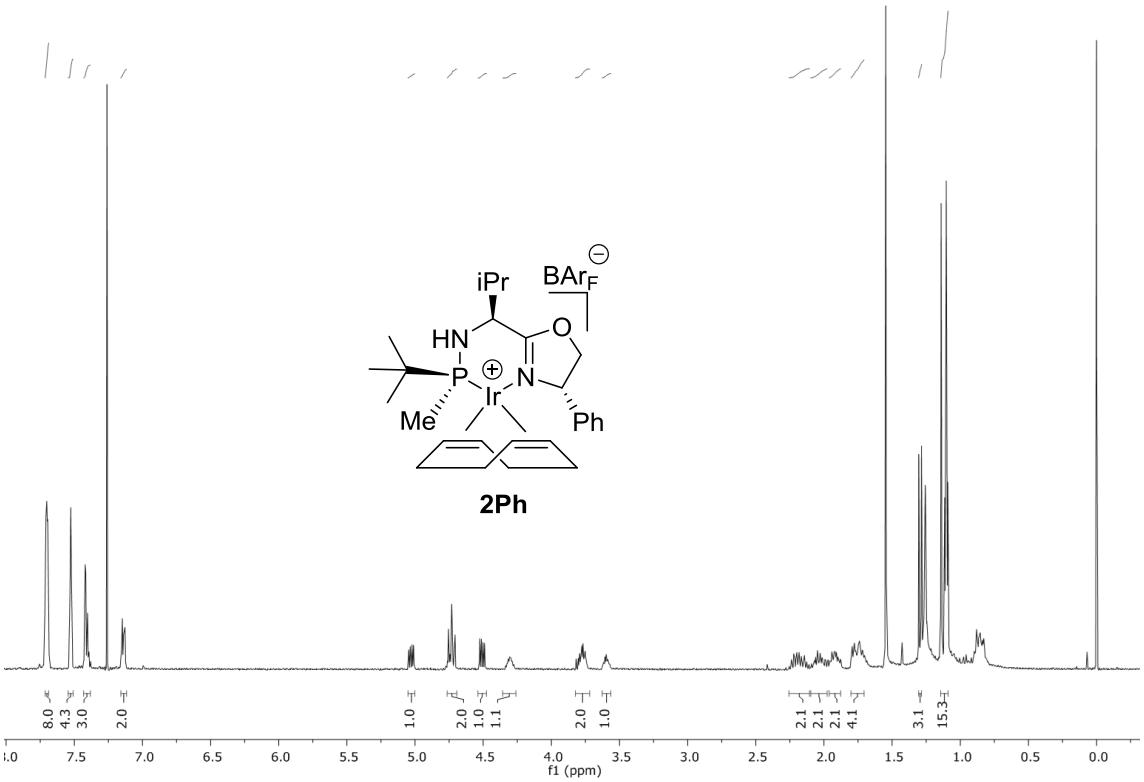

^{1}H NMR (400 MHz, $CDCl_3$)

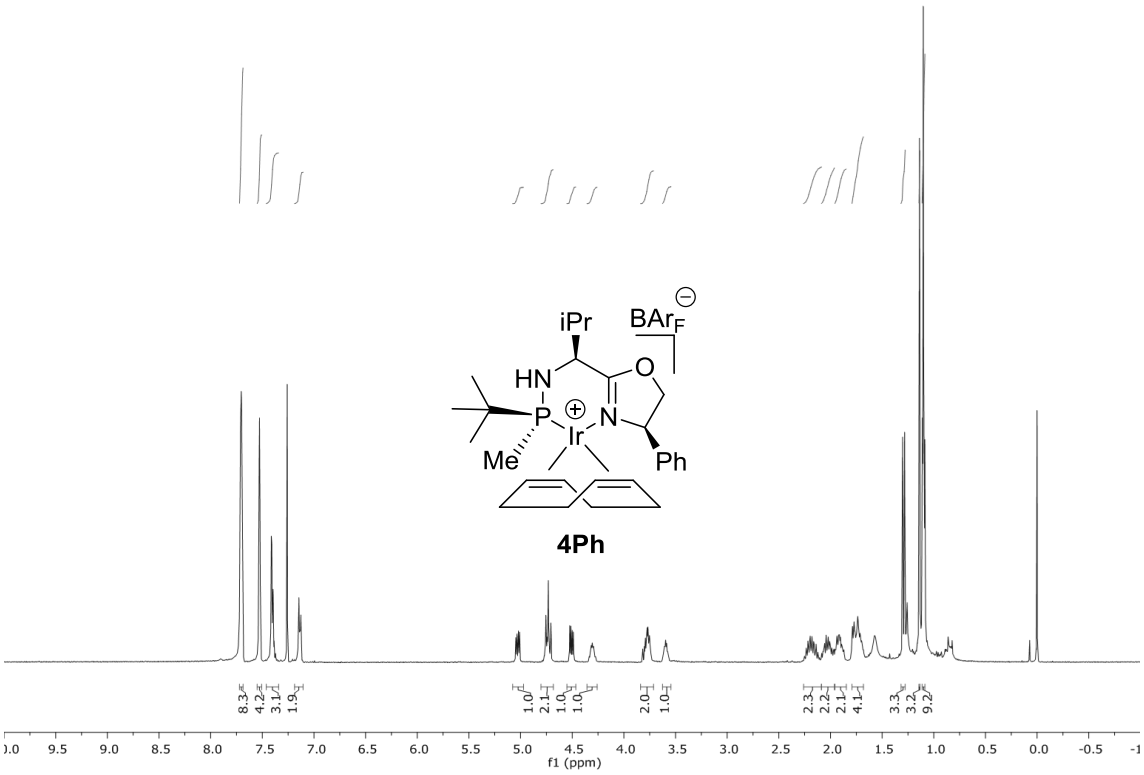

^{31}P NMR (202 MHz, $CDCl_3$)

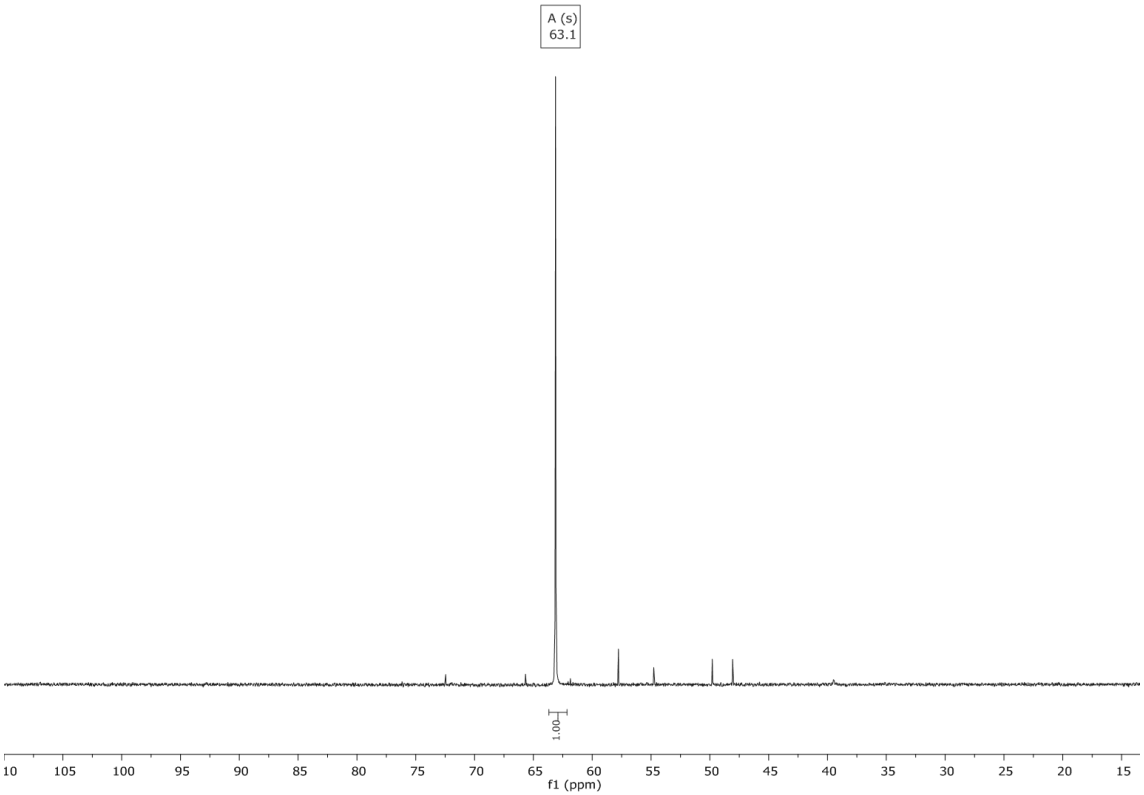

^{1}H NMR (400 MHz, $CDCl_3$)

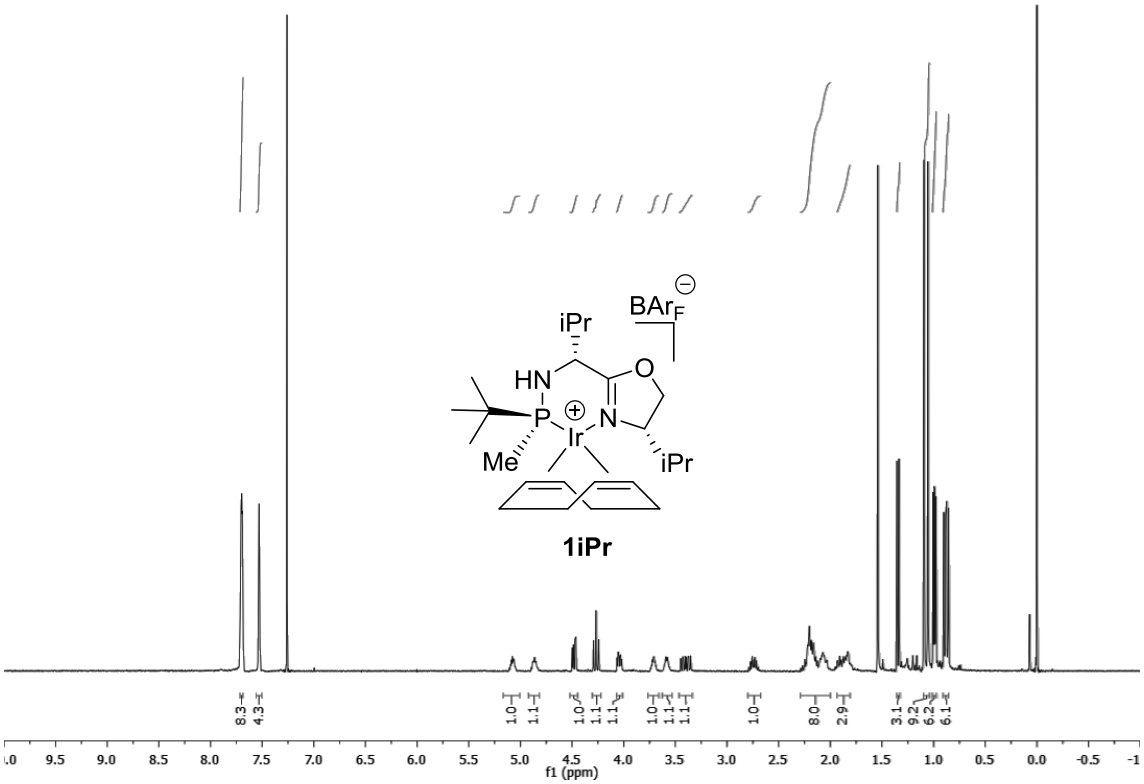

^{31}P NMR (202 MHz, $CDCl_3$)

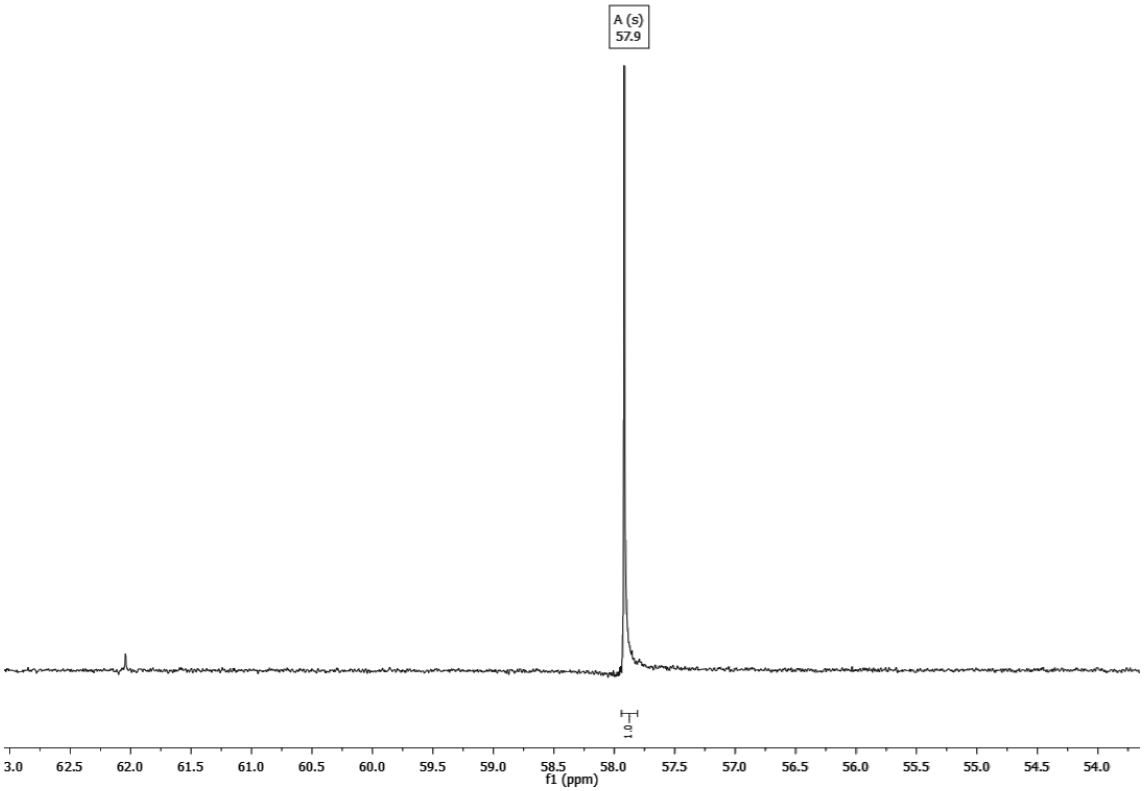

^{1}H NMR (400 MHz, $CDCl_3$)

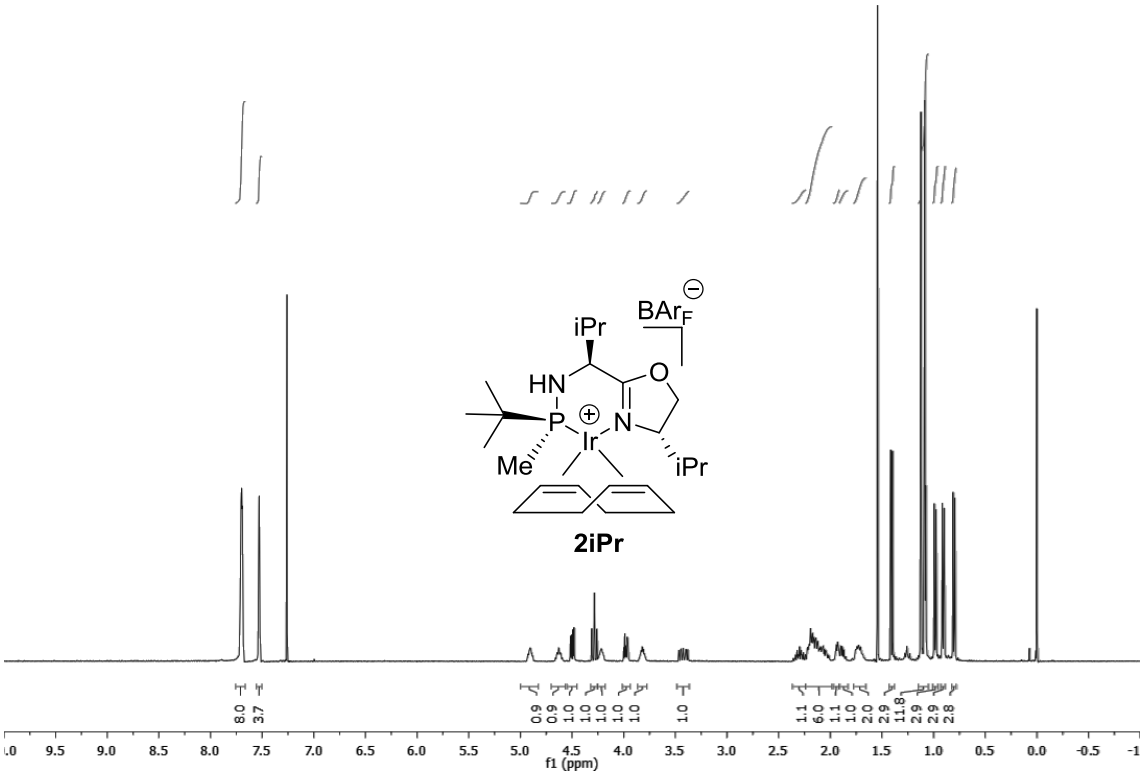

^{31}P NMR (202 MHz, $CDCl_3$)

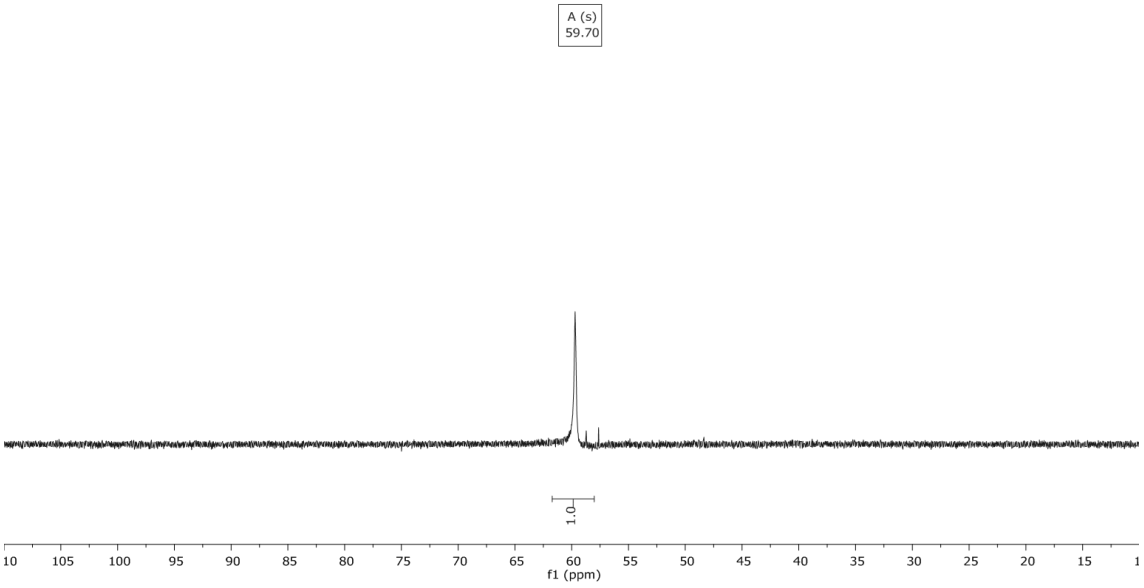

^{1}H NMR (400 MHz, $CDCl_3$)

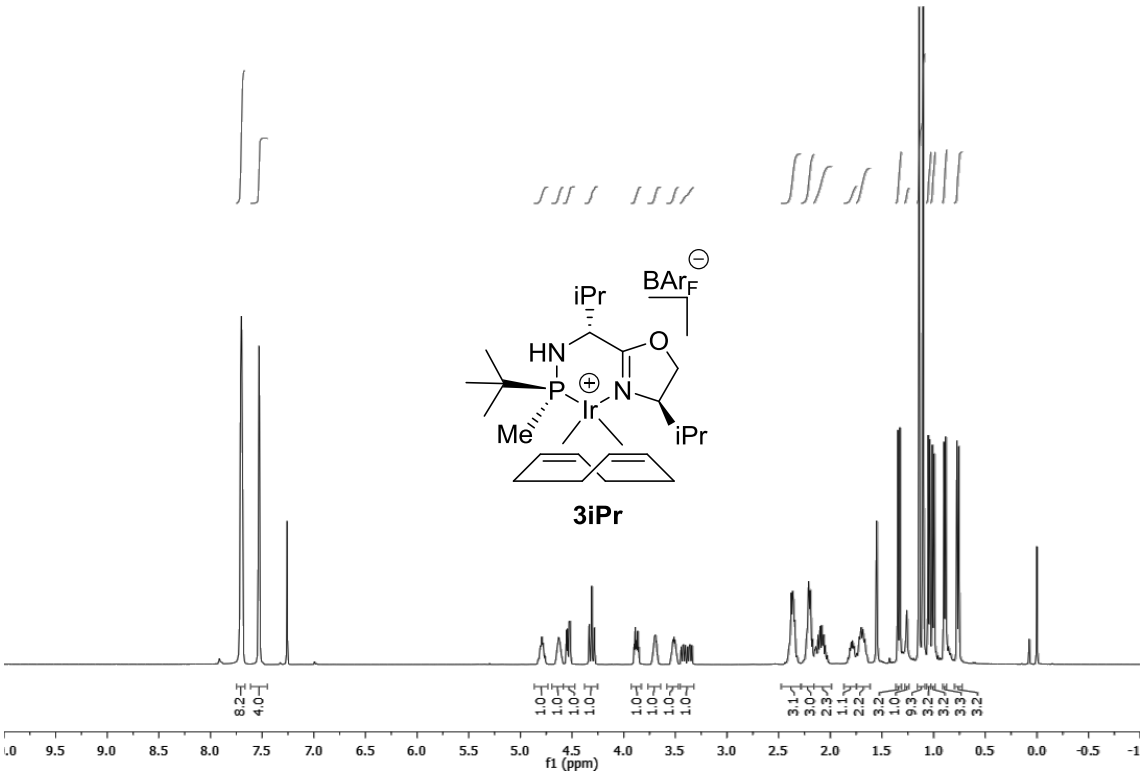

^{31}P NMR (202 MHz, $CDCl_3$)

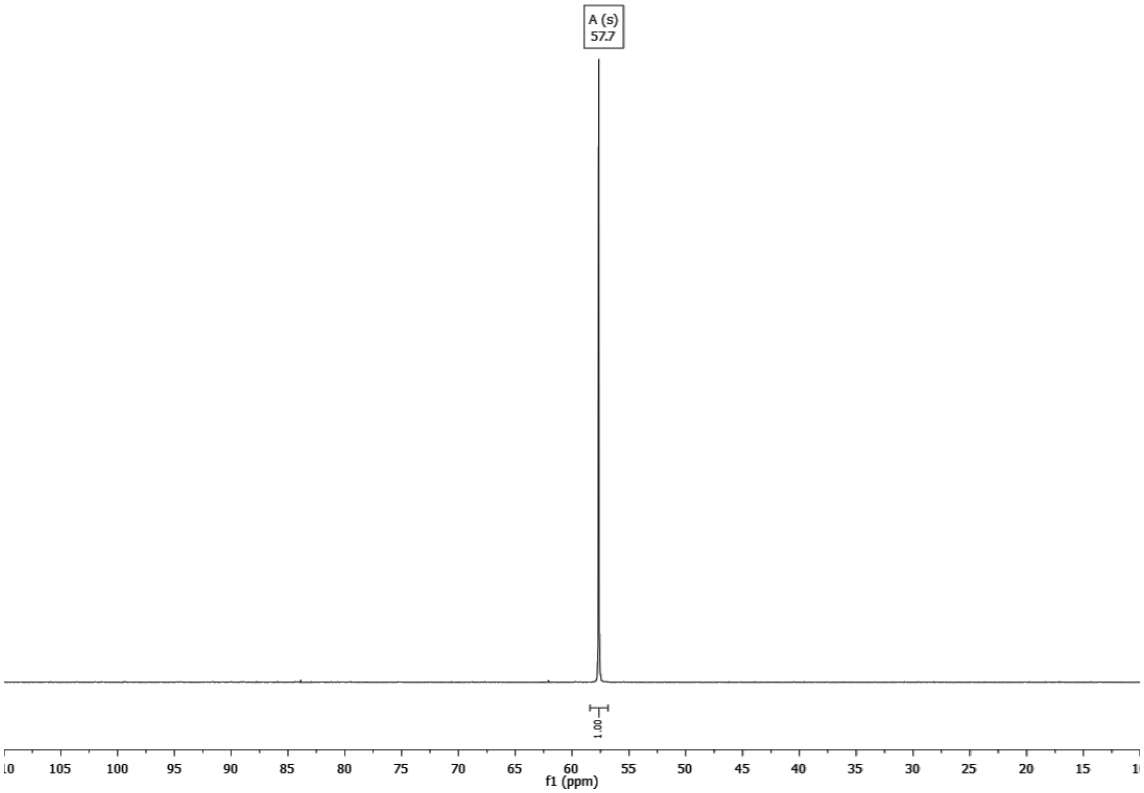

^{1}H NMR (400 MHz, $CDCl_3$)

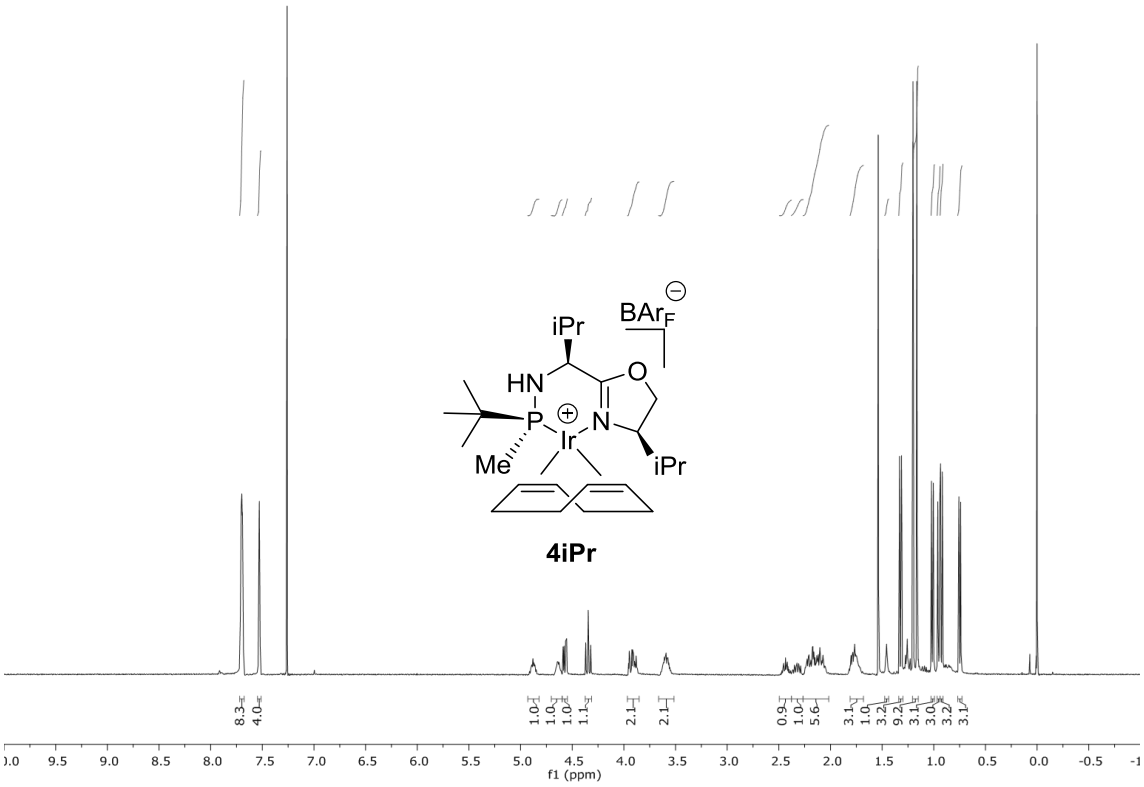

^{31}P NMR (202 MHz, $CDCl_3$)

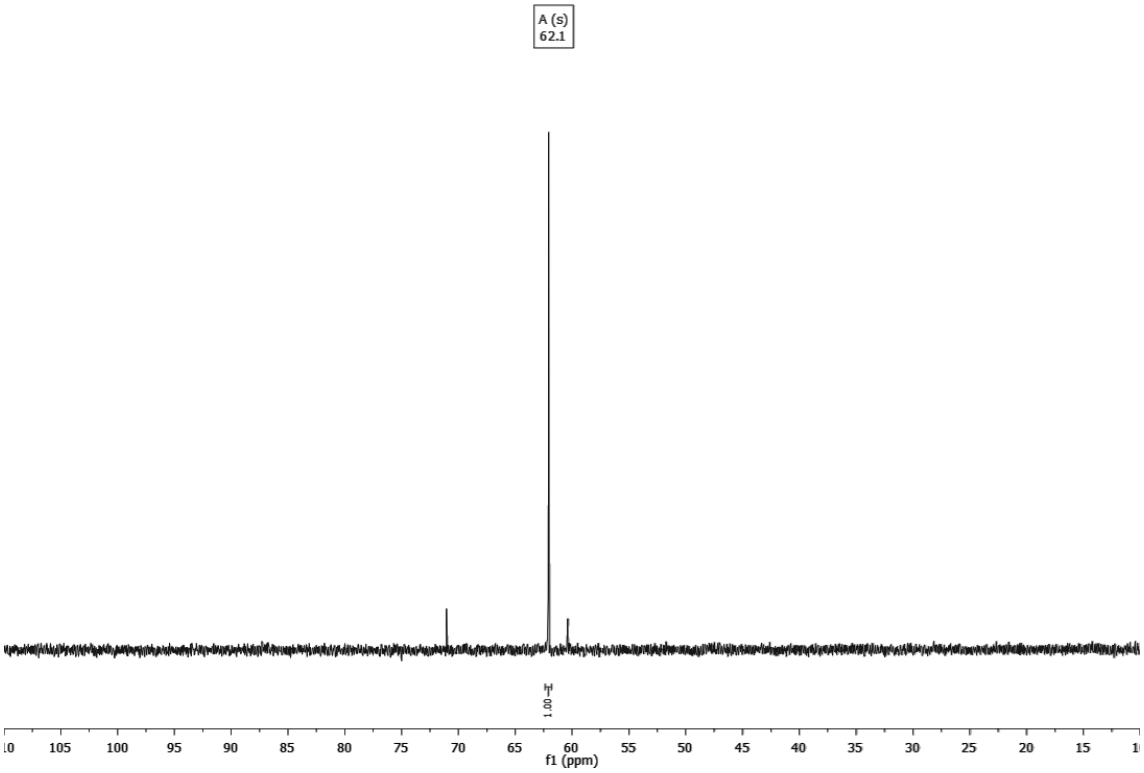

^{1}H NMR (400 MHz, $CDCl_3$)

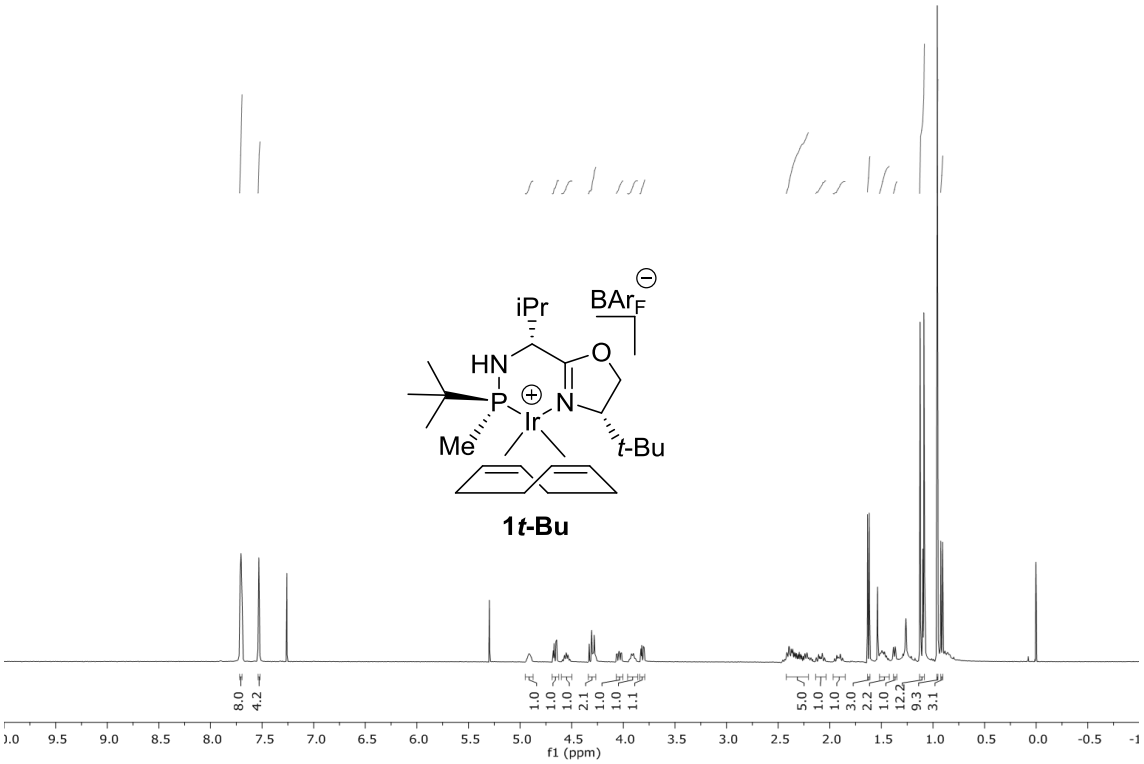

^{31}P NMR (202 MHz, $CDCl_3$)

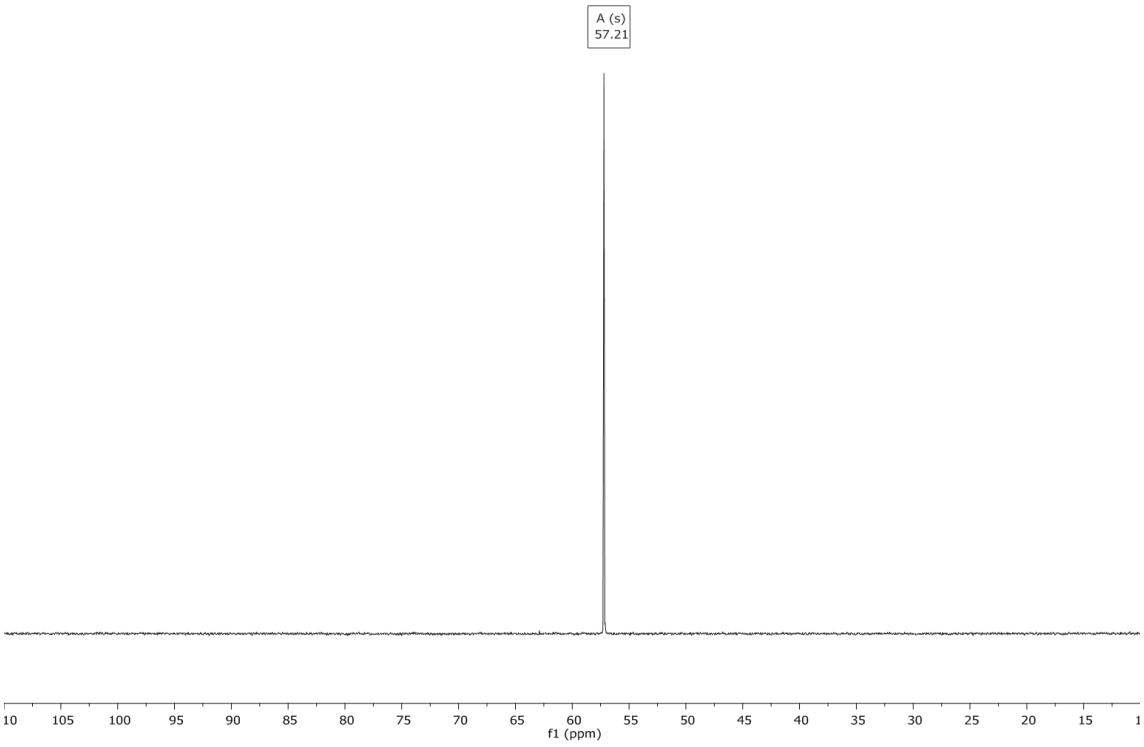

^{1}H NMR (400 MHz, $CDCl_3$)

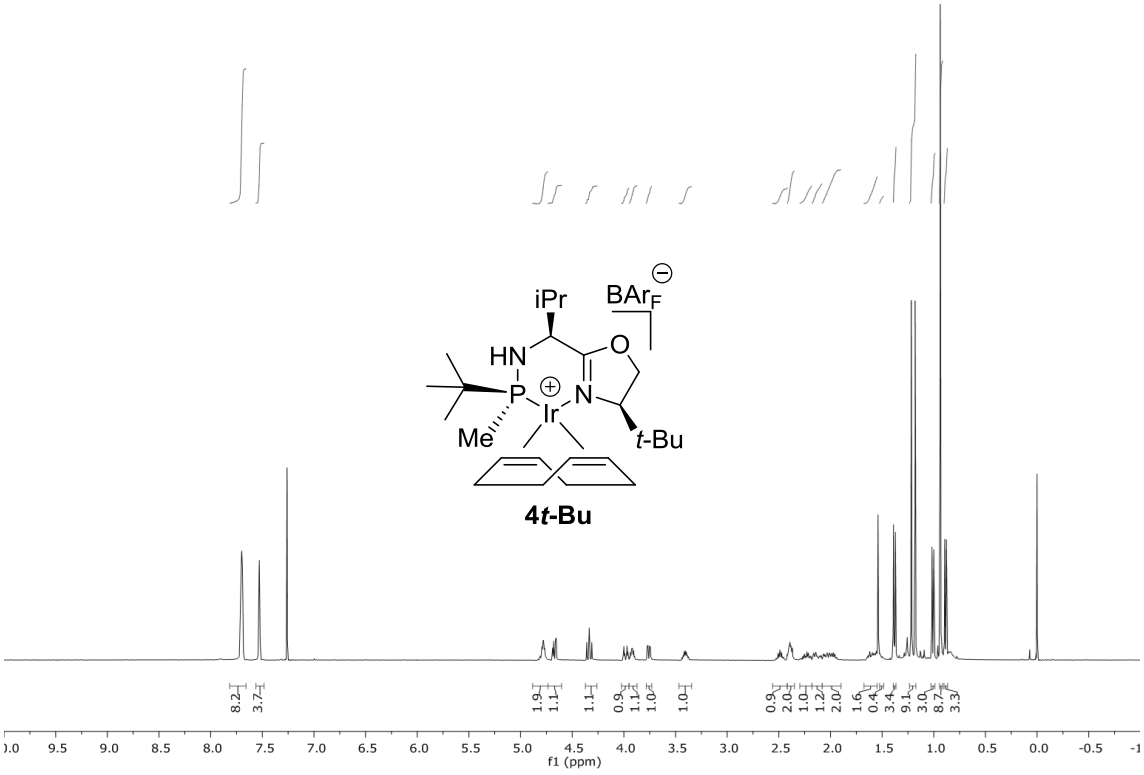

^{31}P NMR (202 MHz, $CDCl_3$)

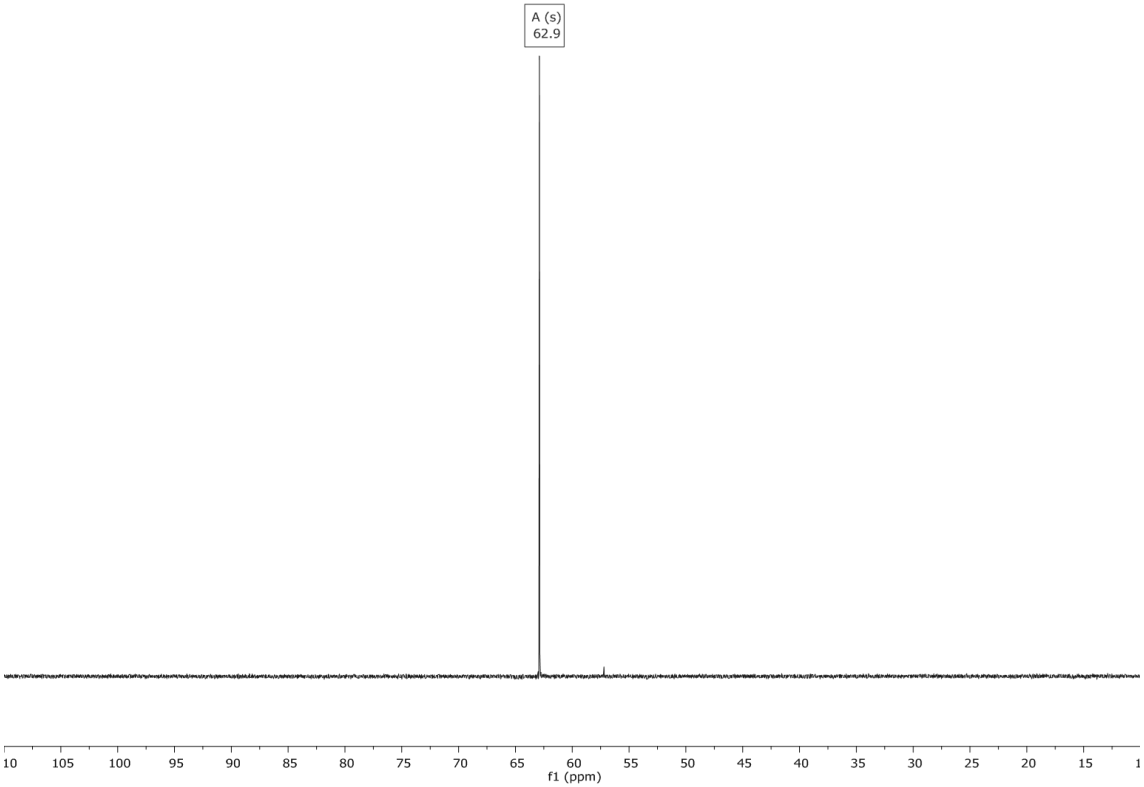

^{1}H NMR (400 MHz, $CDCl_3$)

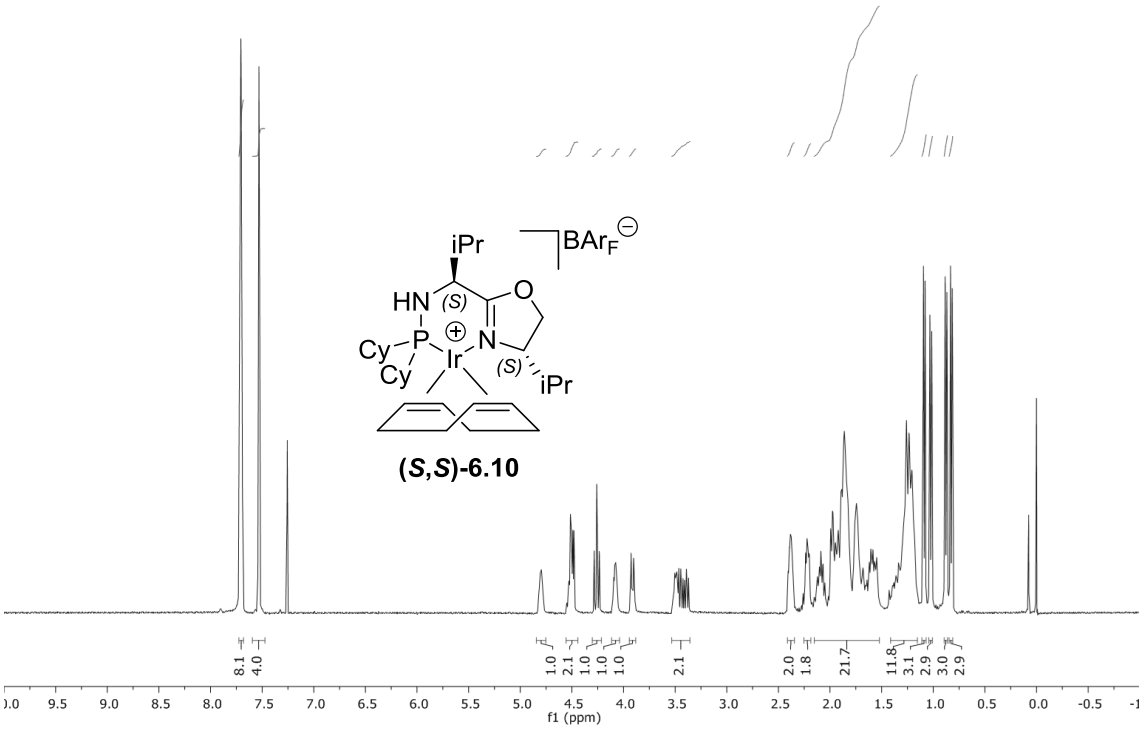

^{31}P NMR (202 MHz, $CDCl_3$)

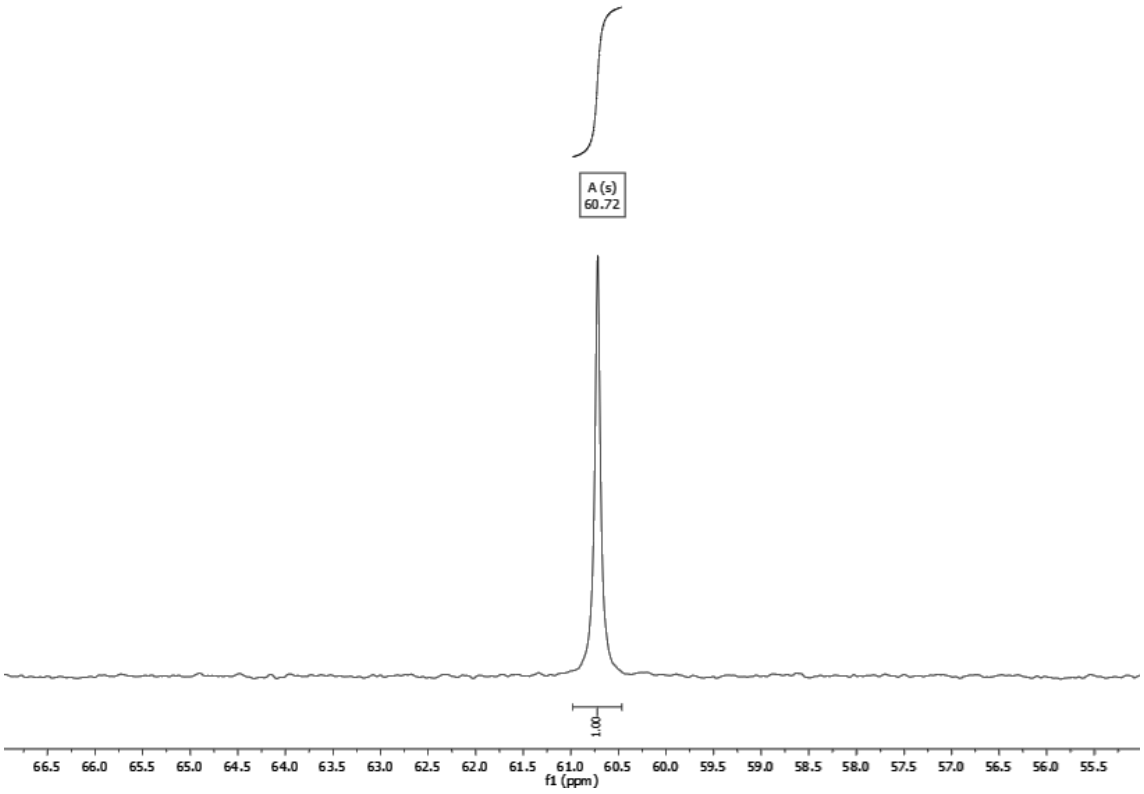

^{1}H NMR (400 MHz, $CDCl_3$)

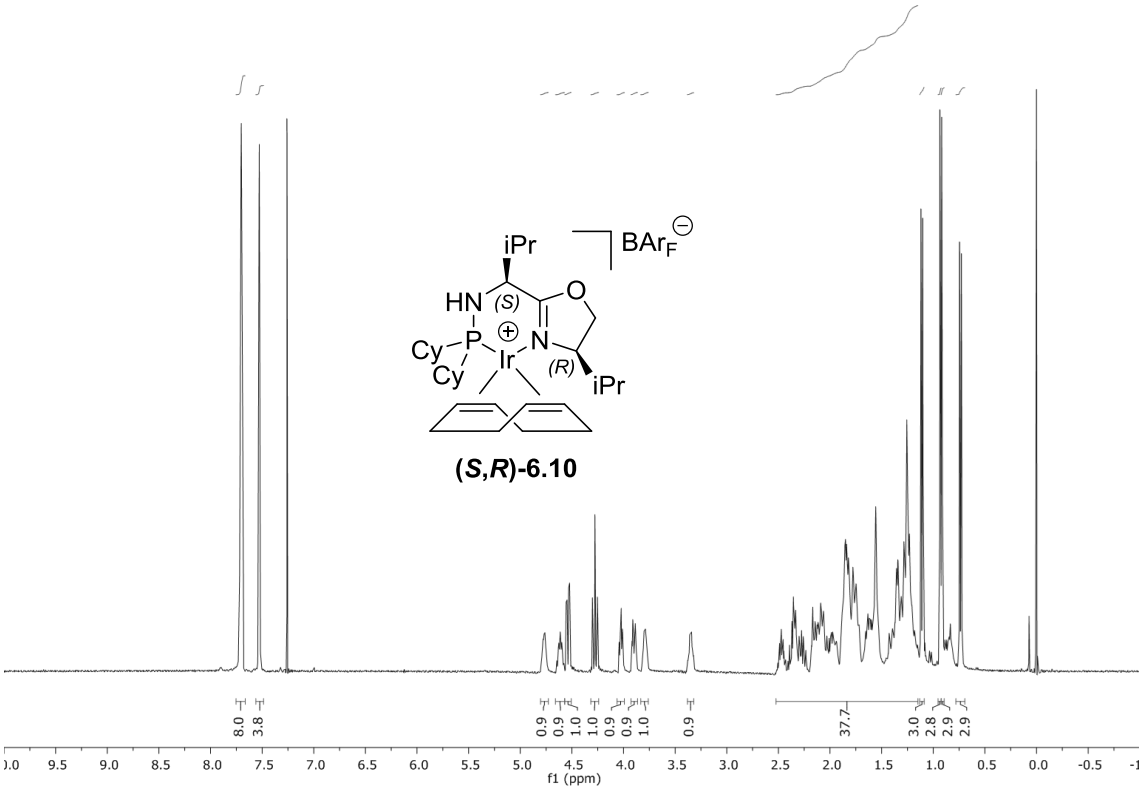

^{31}P NMR (202 MHz, $CDCl_3$)

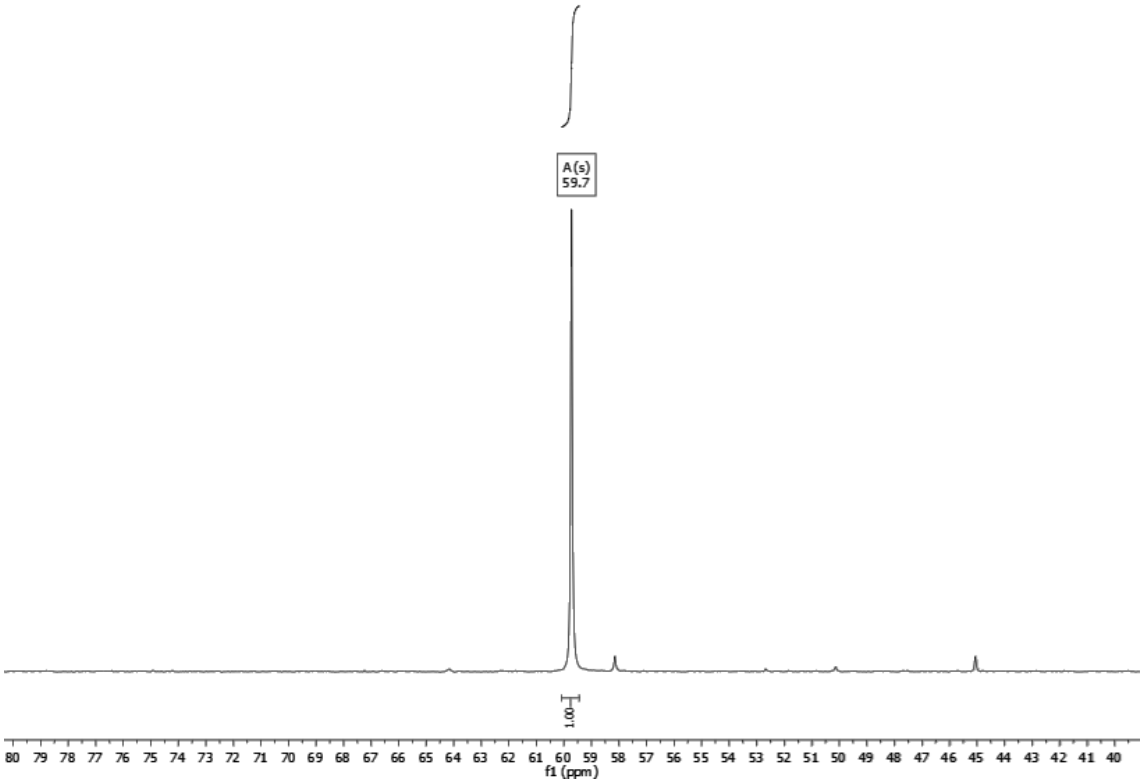

^{31}P NMR (202 MHz, $CDCl_3$)

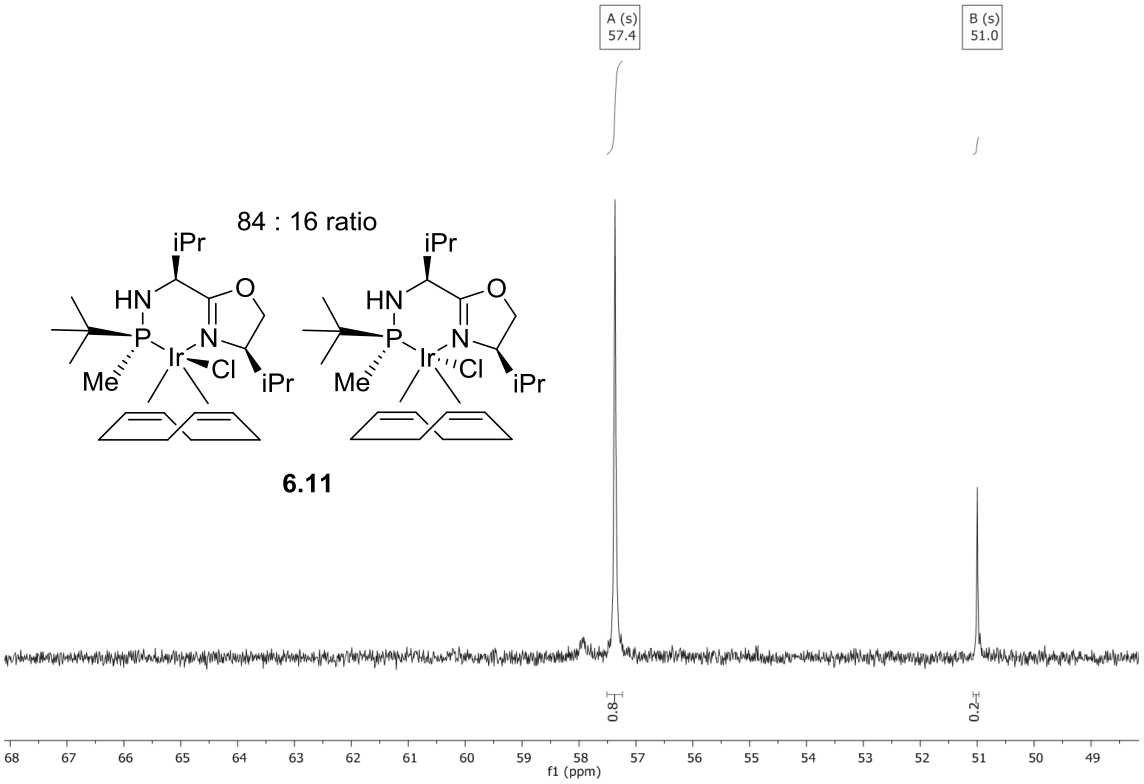

^{1}H NMR (400 MHz, $CDCl_3$)

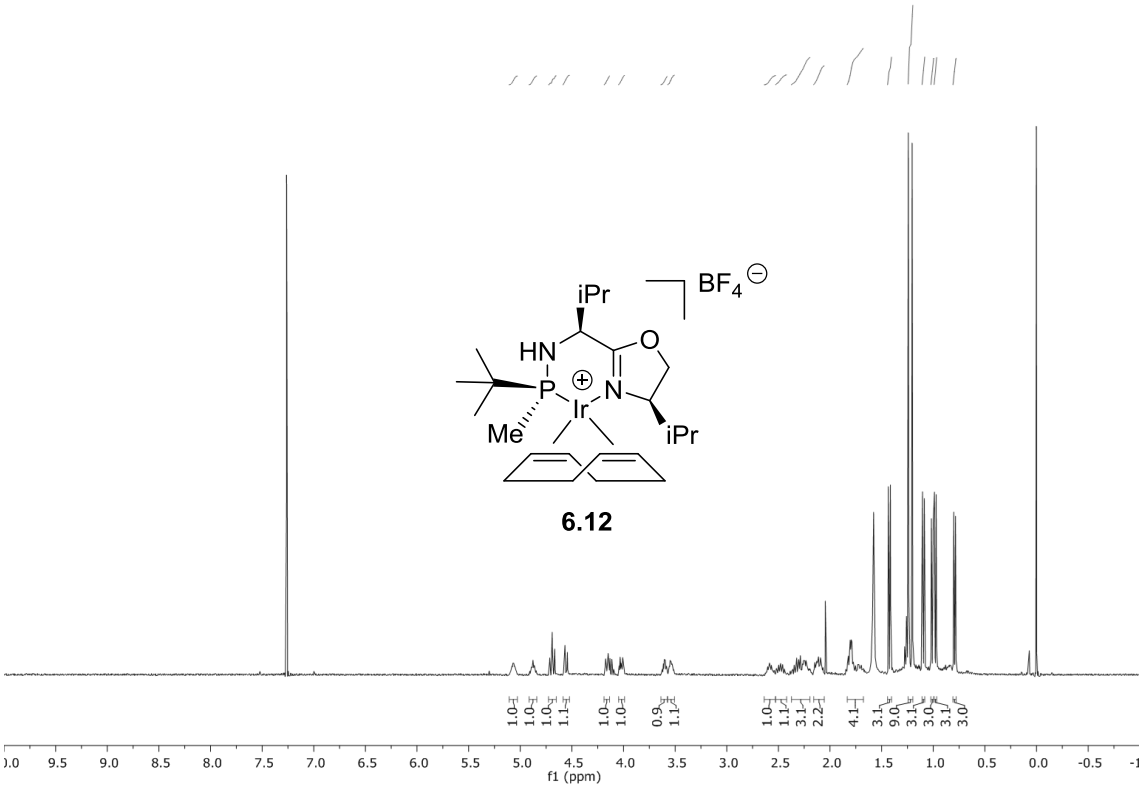

^{31}P NMR (202 MHz, $CDCl_3$)

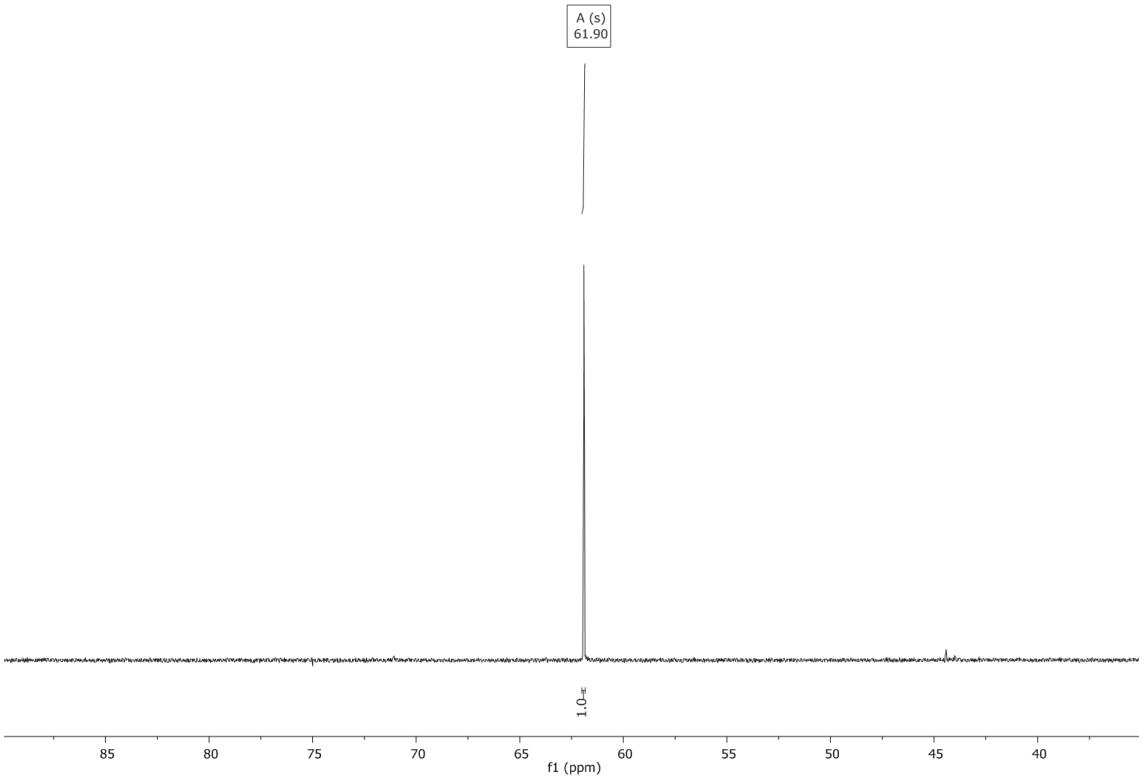

^{1}H NMR (400 MHz, $CDCl_3$)

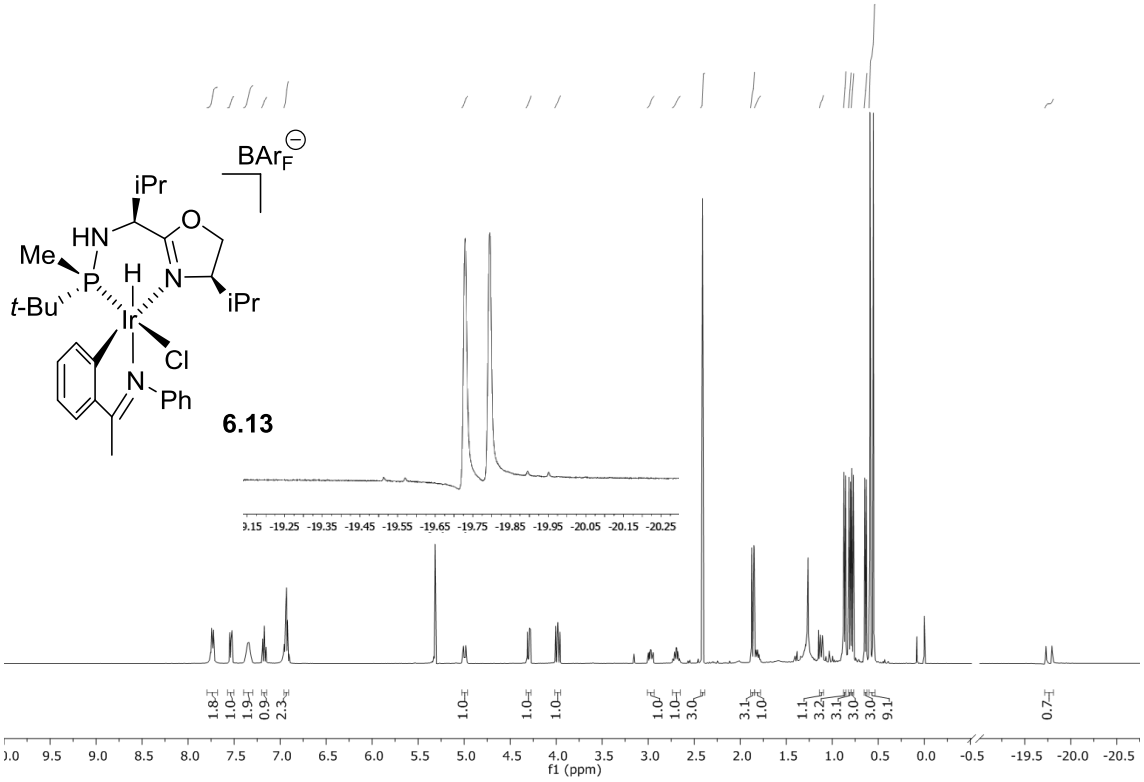

^{31}P NMR (202 MHz, $CDCl_3$)

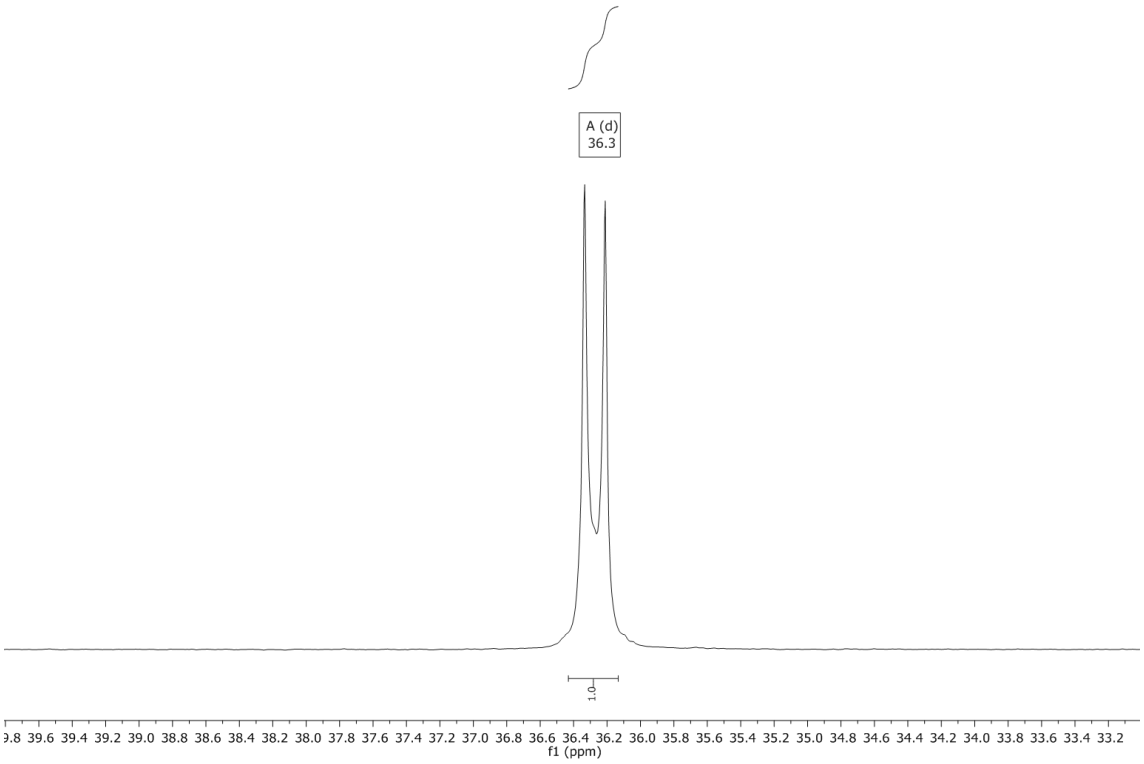

^{1}H NMR (400 MHz, $CDCl_3$)

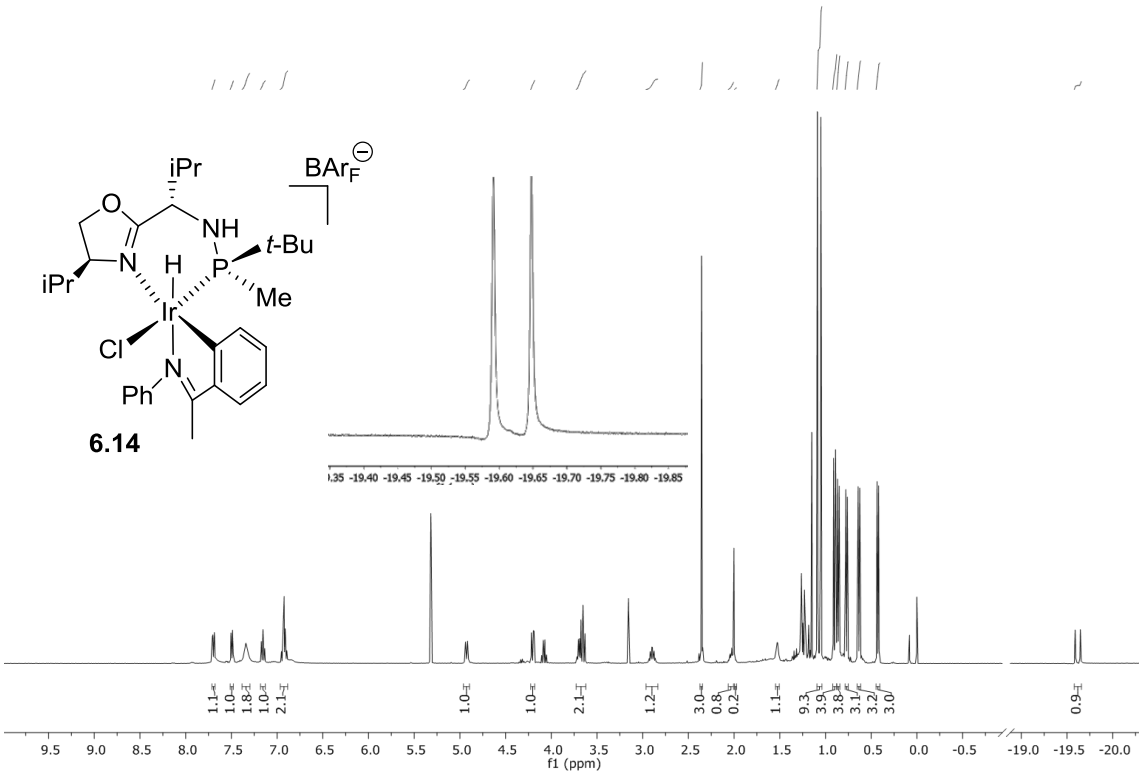

^{31}P NMR (202 MHz, $CDCl_3$)

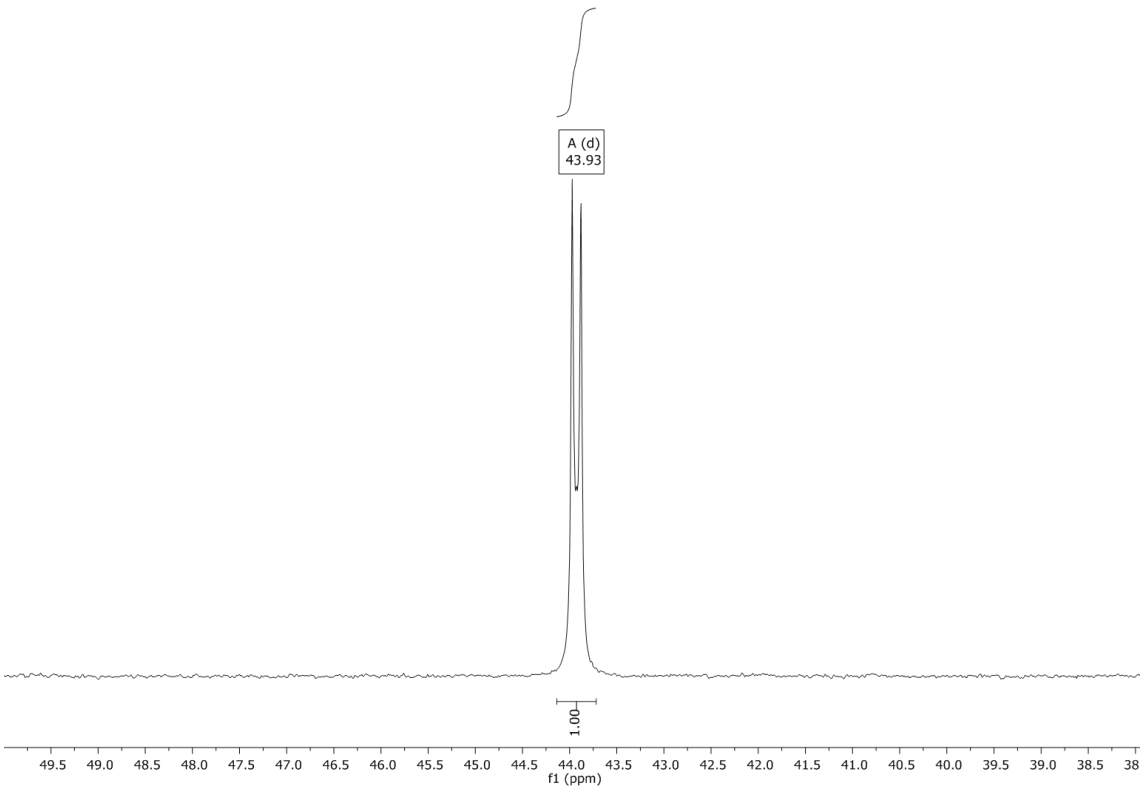

Appendix 2

Index of Structrures

Chapter 2;

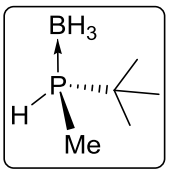

(*R*)-**2.1**

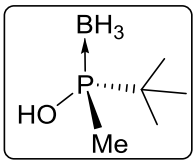

(*S*)-**2.8**

Chapter 3;

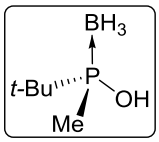

3.1

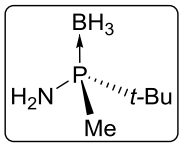

(*S*)-**3.3**

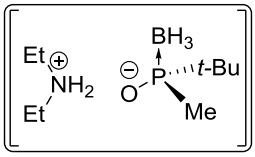

3.7

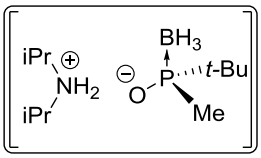

3.8

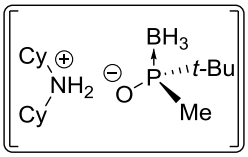

3.9

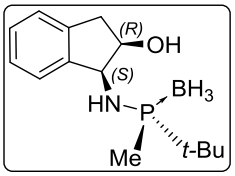

3.10

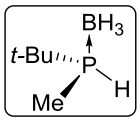

3.12

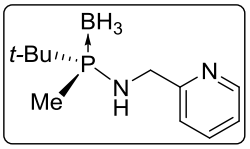

3.13

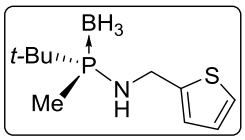

3.14

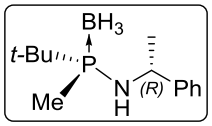

3.15

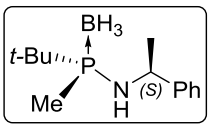

3.16

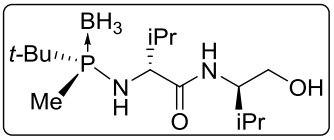

3.17

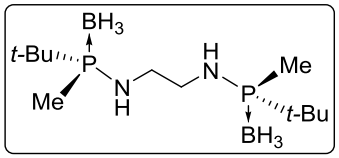

3.18

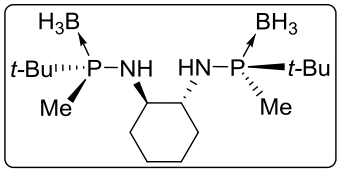

3.19

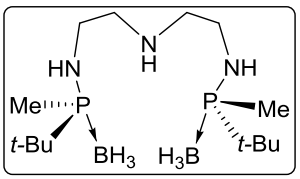

3.20

Chapter 5;

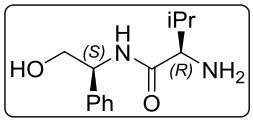

(*S*,*R*)-**5.6Ph**

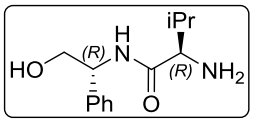

(*R*,*R*)-**5.6-Ph**

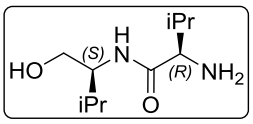

(*S*,*R*)-**5.6-iPr**

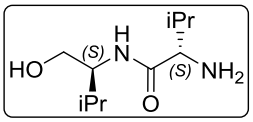

(*S*,*S*)-**5.6-iPr**

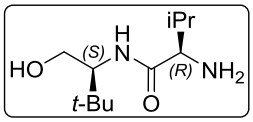

(*S*,*R*)-**5.6-*t*-Bu**

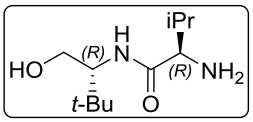

(*R*,*R*)-**5.6-*t*-Bu**

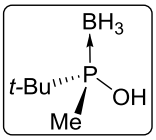

5.4

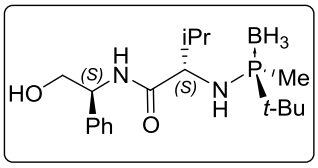

5.7b-Ph

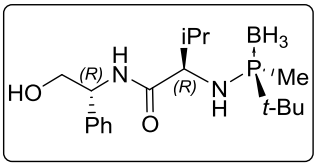

5.7c-Ph

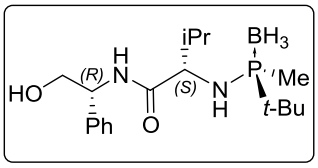

5.7d-Ph

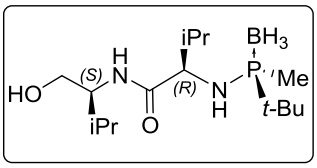

5.7a-iPr

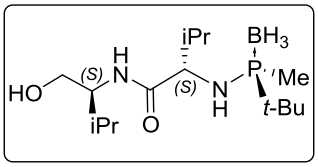

5.7b-iPr

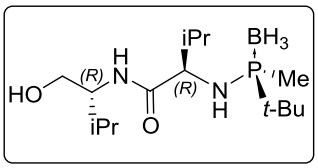

5.7c-iPr

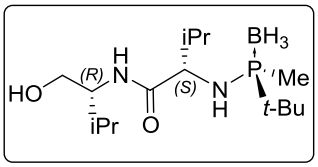

5.7d-iPr

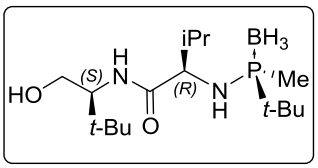

5.7a-*t*-Bu

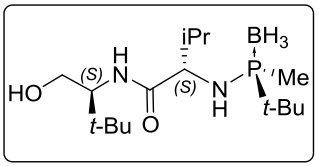

5.7b-*t*-Bu

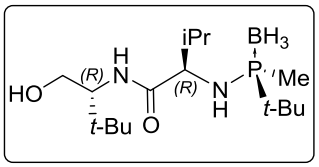

5.7c-*t*-Bu

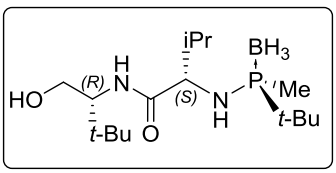

5.7d-*t*-Bu

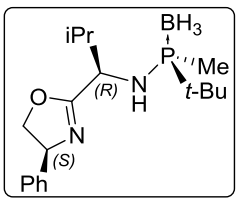

5.8a-Ph

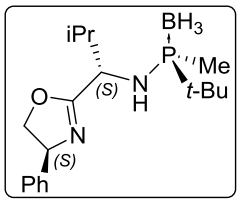

5.8b-Ph

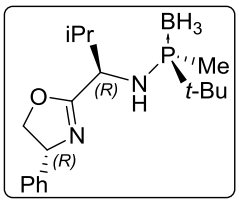

5.8c-Ph

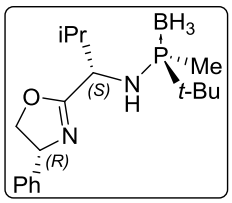

5.8d-Ph

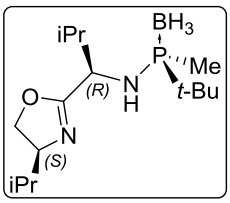

5.8a-iPr

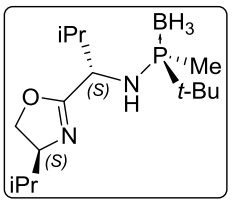

5.8b-iPr

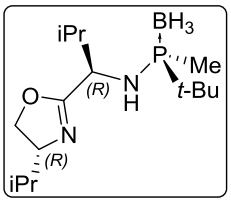

5.8c-iPr

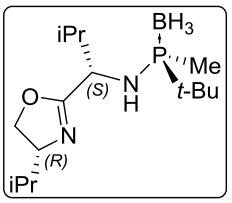

5.8d-iPr

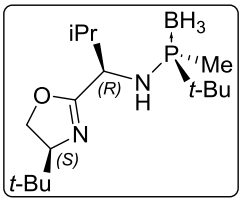

5.8a-*t*-Bu

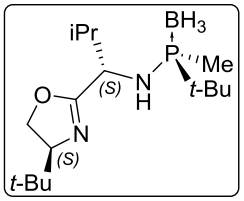

5.8b-*t*-Bu

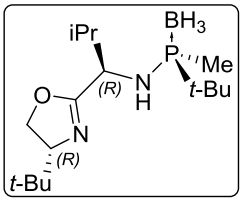

5.8c-*t*-Bu

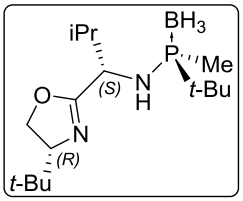

5.8d-*t*-Bu

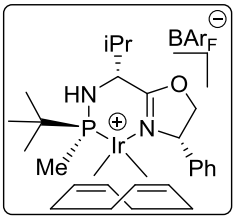

1Ph

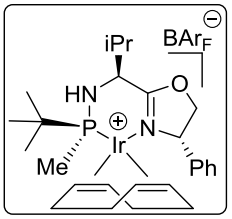

2Ph

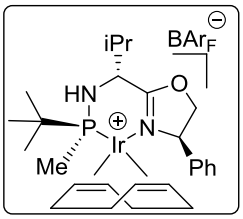

3Ph

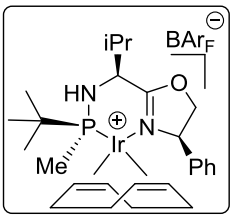

4Ph

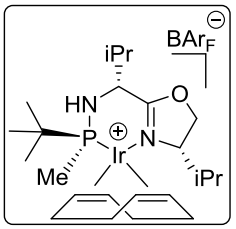

1iPr

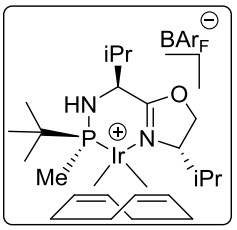

2iPr

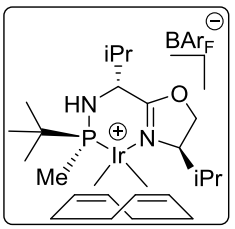

3iPr

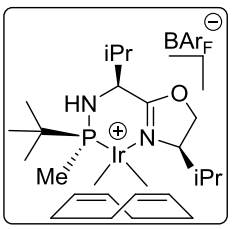

4iPr

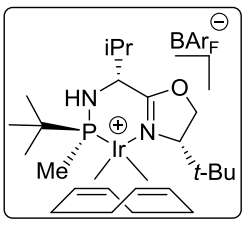

1*t*-Bu

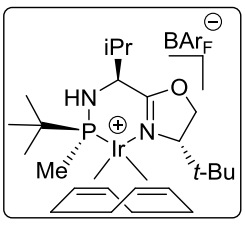

2*t*-Bu

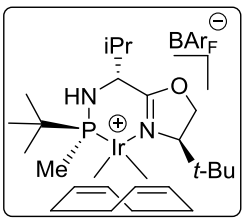

3*t*-Bu

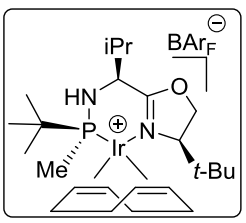

4*t*-Bu

Chapter 6;

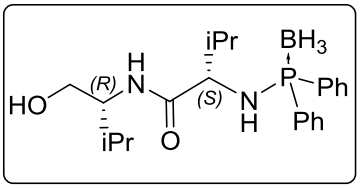

6.3

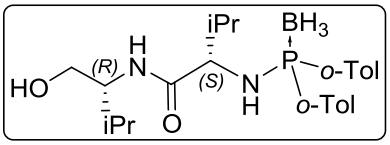

6.4

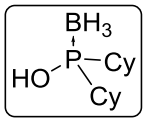

6.5

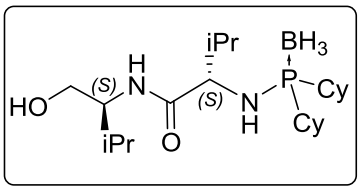

(*S*,*S*)-**6.8**

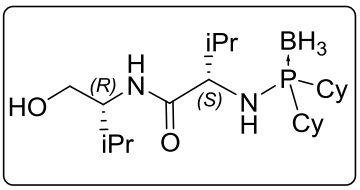

(*S*,*R*)-**6.8**

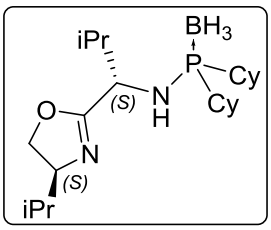

(*S*,*S*)-**6.9**

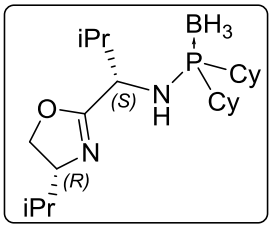

(*S*,*R*)-**6.9**

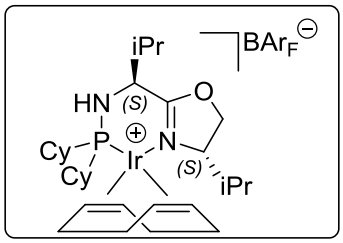

(*S*,*S*)-**6.10**

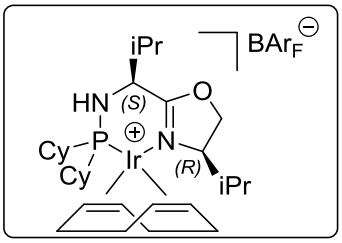

(*S*,*R*)-**6.10**

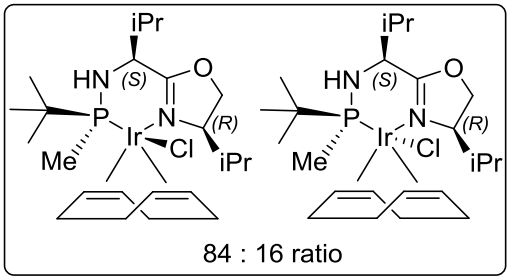

6.11

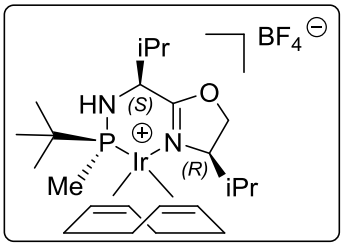

6.12

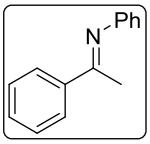

6.1

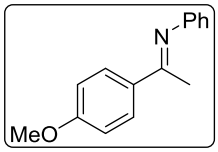

I1

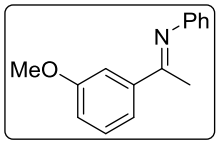

I2

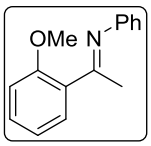

I3

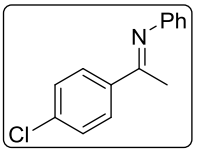

I4

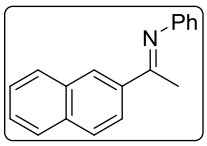

I5

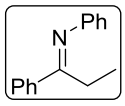

I6

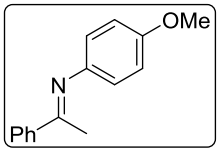

I7

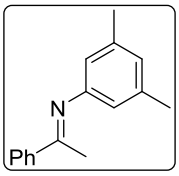

I8

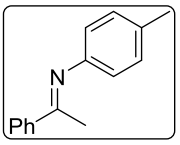

I9

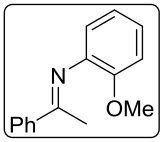

I10

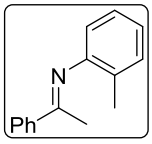

I11

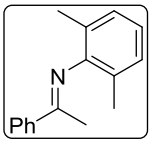

I12

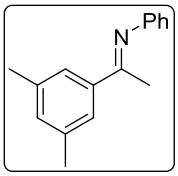

I13

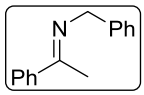

I14

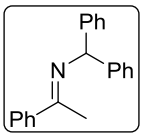

I15

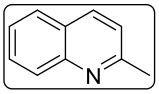

I16

I17

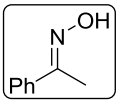

I18

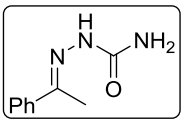

I19

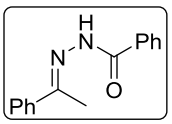

I20

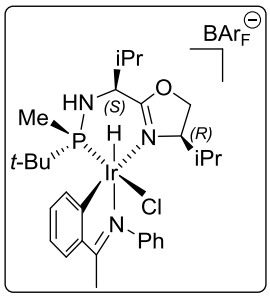

6.13

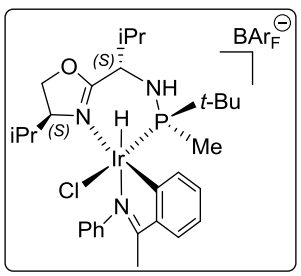

6.14

Chapter 7;

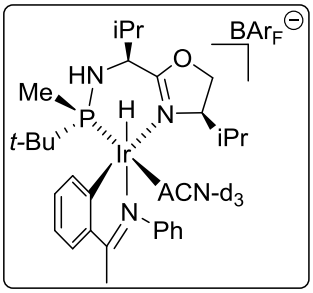

7.3

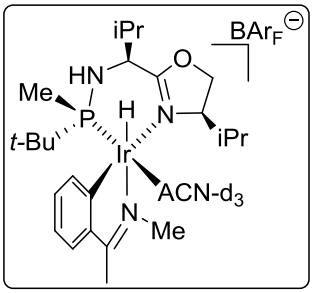

7.4

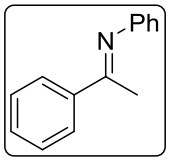

A0

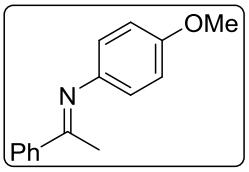

A1

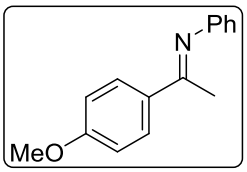

A2

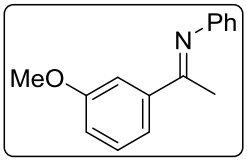

A3

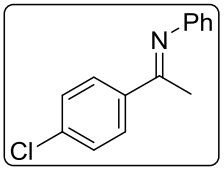

A4

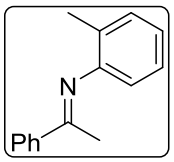

A5

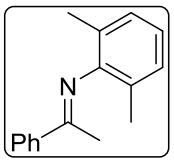

A6

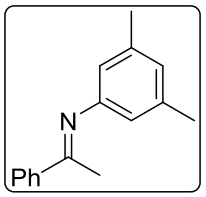

A7

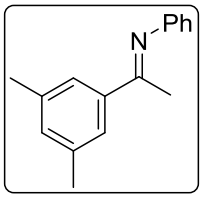

A8

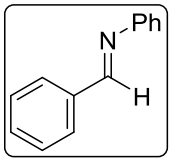

A9

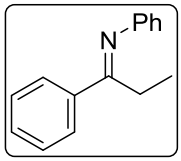

A10

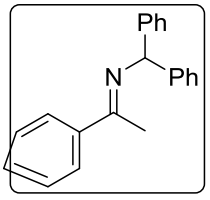

A11

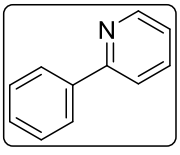

A12

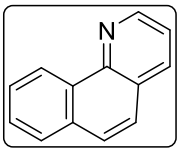

A13

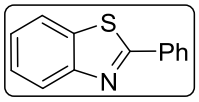

A14

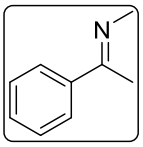

I1

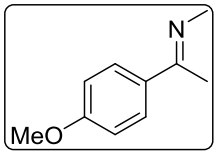

I2

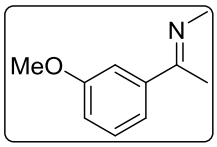

I3

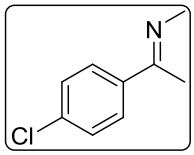

I4

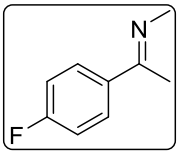

I5

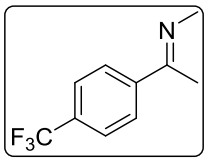

I6

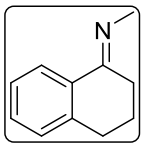

I7

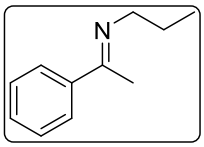

I8

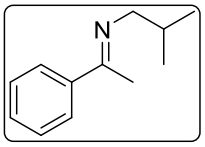

I9

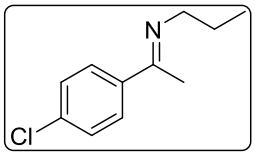

I10

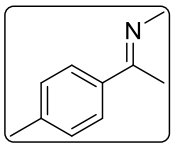

I11

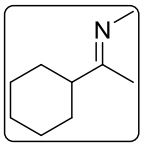

I12

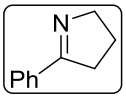

I13

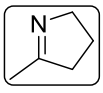

I14

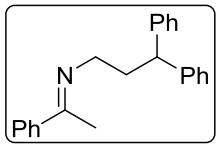

I15

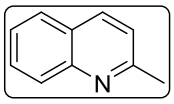

I16

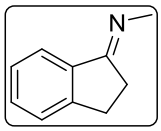

I17

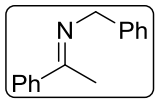

I18

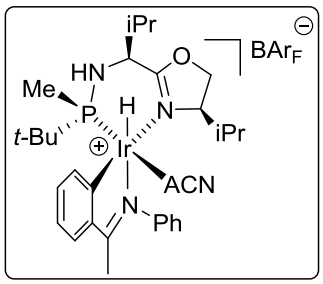

7.7

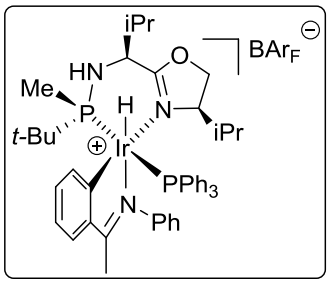

7.8

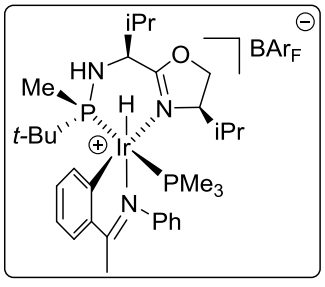

7.9

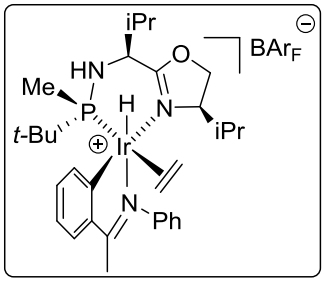

7.10

Chapter 8;

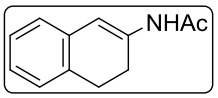

8.6

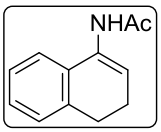

8.8

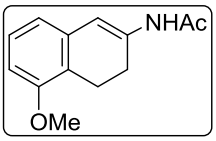

E1

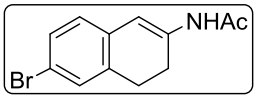

E2

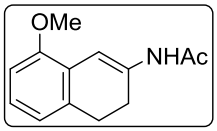

E3

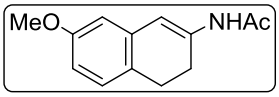

E4

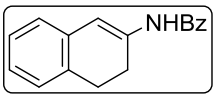

E5

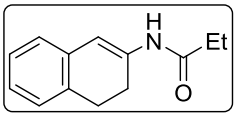

E6

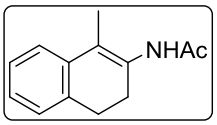

E7

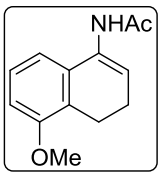

E8

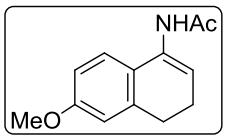

E9

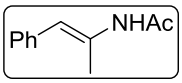

E10

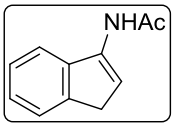

E11

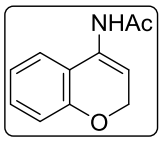

E12

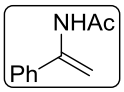

E13

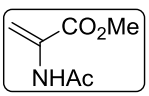

E14

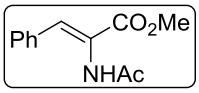

E15

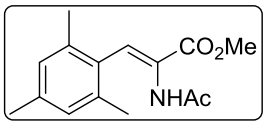

E16

Appendix 3

X-Ray Diffraction Data

Chapter 3;

Figure 1. X-ray structure of **3.8**. Ortep diagram displays ellipsoids at 50% probability. Only hydrogen atoms involved in the H-bond network are depicted.

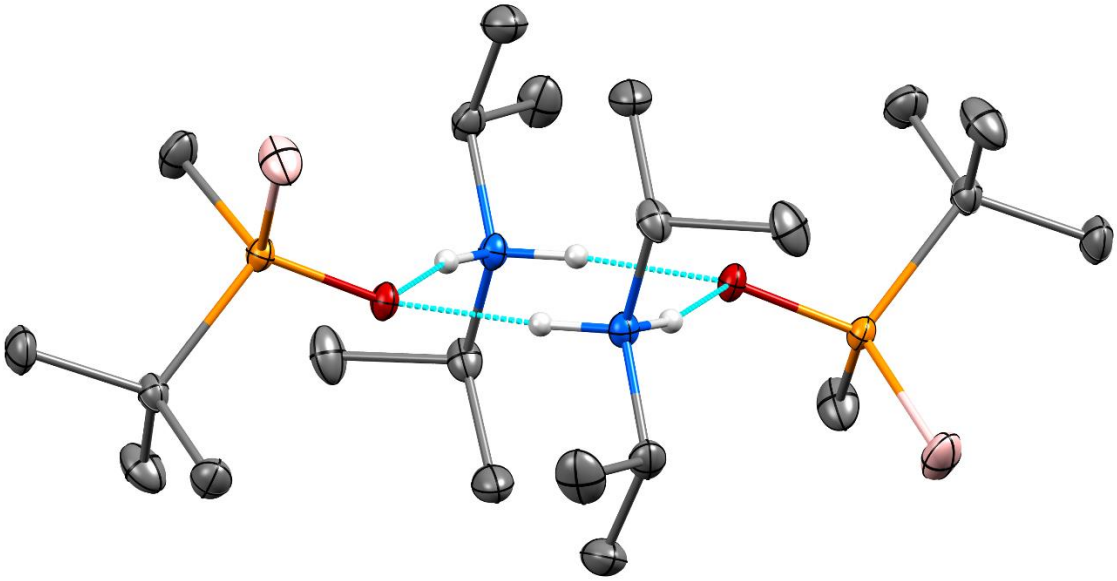

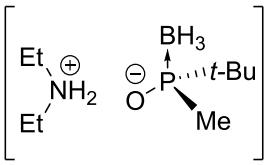

3.8

Table 1. Crystal data and structure refinement for **3.8**

Identification code	**3.8**	
Empirical formula	$C_{22}H_{62}B_2N_2O_2P_2$	
Formula weight	470.29	
Temperature	100(2) K	
Wavelength	0.71073 Å	
Crystal system	Monoclinic	
Space group	P2(1)	
Unit cell dimensions	a = 8.08480(10)Å	α= 90°.
	b = 13.48510(10)Å	β = 103.6300(10)°.
	c = 14.8690(2)Å	γ = 90°.
Volume	1575.43(3) $Å^3$	
Z	2	
Density (calculated)	0.991 mg/m^3	
Absorption coefficient	0.156 mm^{-1}	
F(000)	528	
Crystal size	? x ? x ? mm^3	
Theta range for data collection	2.066 to 53.950°.	
Index ranges	-17<=h<=18,-30<=k<=30,-33<=l<=33	
Reflections collected	121989	
Independent reflections	35990[R(int) = 0.0262]	
Completeness to theta =53.950°	98.5%	
Absorption correction	Multi-scan	
Max. and min. transmission	0.977 and 0.752	
Refinement method	Full-matrix least-squares on F^2	
Data / restraints / parameters	35990/ 1/ 311	
Goodness-of-fit on F^2	1.023	
Final R indices [I>2sigma(I)]	R1 = 0.0298, wR2 = 0.0880	
R indices (all data)	R1 = 0.0381, wR2 = 0.0927	
Flack parameter	x =0.001(11)	
Largest diff. peak and hole	0.488 and -0.384 $e.Å^{-3}$	

Chapter 6;

Figure 2. X-ray structures of iridacycle **6.13**. The Ortep diagram shows ellipsoids at 50% probability. Only the hydrogen atom attached to iridium has been drawn.

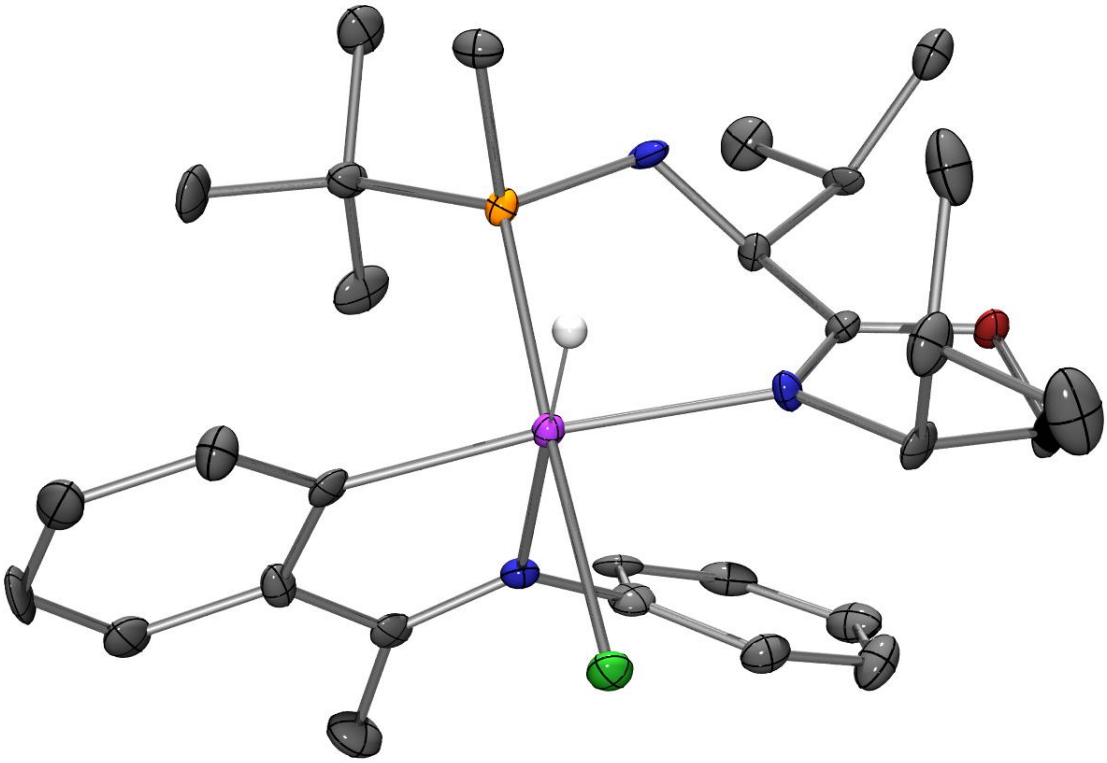

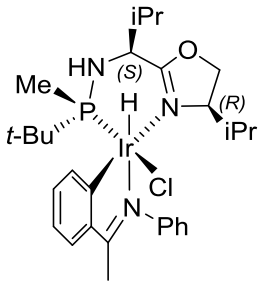

6.13

Table 2. Crystal data and structure refinement for **6.13.**

Identification code	**6.13**	
Empirical formula	$C_{29}H_{44}ClIrN_3OP$	
Formula weight	709.29	
Temperature	100(2) K	
Wavelength	0.71073 Å	
Crystal system	Monoclinic	
Space group	P2	
Unit cell dimensions	a = 8.8193(7)Å	α= 90°.
	b = 14.8781(10)Å	β = 108.396(2)°.
	c = 12.2570(8)Å	γ = 90°.
Volume	1526.11(19) $Å^3$	
Z	2	
Density (calculated)	1.544 mg/m^3	
Absorption coefficient	4.540 mm^{-1}	
F(000)	712	
Crystal size	0.15 x 0.08 x 0.03 mm^3	
Theta range for data collection	1.751 to 30.137°.	
Index ranges	-11<=h<=12,-20<=k<=19,-16<=l<=12	
Reflections collected	17554	
Independent reflections	17554[R(int) =?]	
Completeness to theta =30.137°	89.3%	
Absorption correction	Multi-scan	
Max. and min. transmission	0.876 and 0.674	
Refinement method	Full-matrix least-squares on F^2	
Data / restraints / parameters	17554/ 2/ 338	
Goodness-of-fit on F^2	1.034	
Final R indices [I>2sigma(I)]	R1 = 0.0323, wR2 = 0.0841	
R indices (all data)	R1 = 0.0349, wR2 = 0.0906	
Flack parameter	x =-0.018(9)	
Largest diff. peak and hole	1.064 and -1.370 e.$Å^{-3}$	

Figure 3. X-ray structures of iridacycle **6.14**. The Ortep diagram shows ellipsoids at 50% probability. Only the hydrogen atom attached to iridium has been drawn.

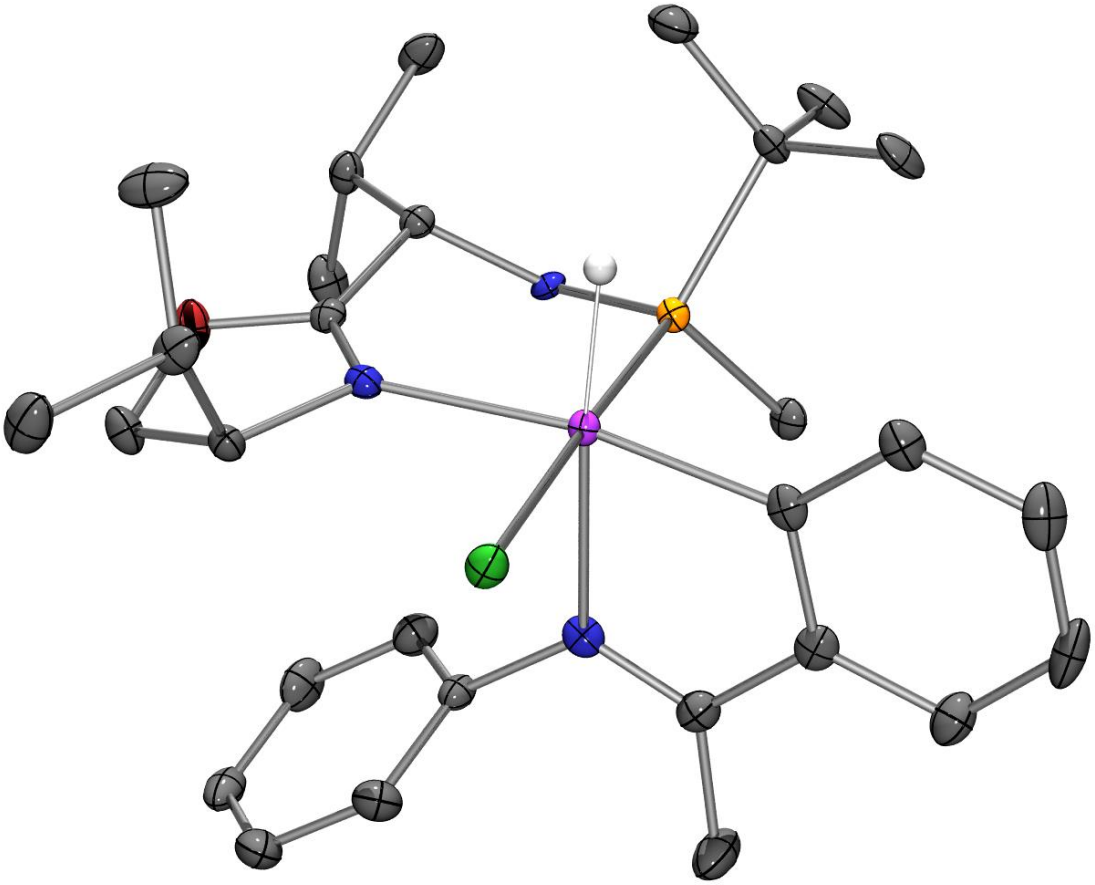

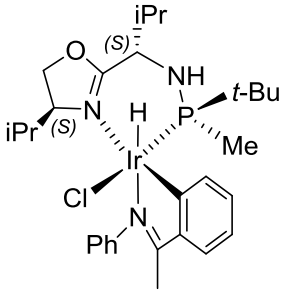

6.14

Table 3. Crystal data and structure refinement for **6.14**

Identification code	**6.14**	
Empirical formula	$C_{30}H_{45}Cl_3IrN_3OP$	
Formula weight	793.21	
Temperature	100(2) K	
Wavelength	0.71073 Å	
Crystal system	Orthorhombic	
Space group	P2(1)2(1)2(1)	
Unit cell dimensions	a = 10.0790(4)Å	α= 90°.
	b = 17.3965(7)Å	β = 90°.
	c = 19.0940(7)Å	γ = 90°.
Volume	3347.9(2) $Å^3$	
Z	4	
Density (calculated)	1.574 mg/m^3	
Absorption coefficient	4.302 mm^{-1}	
F(000)	1588	
Crystal size	0.15 x 0.04 x 0.02 mm^3	
Theta range for data collection	2.133 to 32.575°.	
Index ranges	-15<=h<=9,-26<=k<=21,-28<=l<=19	
Reflections collected	23923	
Independent reflections	10830[R(int) = 0.0387]	
Completeness to theta =32.575°	92.0%	
Absorption correction	Multi-scan	
Max. and min. transmission	0.919 and 0.703	
Refinement method	Full-matrix least-squares on F^2	
Data / restraints / parameters	10830/ 39/ 370	
Goodness-of-fit on F^2	1.024	
Final R indices [I>2sigma(I)]	R1 = 0.0335, wR2 = 0.0587	
R indices (all data)	R1 = 0.0422, wR2 = 0.0614	
Flack parameter	x =-0.007(4)	
Largest diff. peak and hole	1.100 and -0.944 e.$Å^{-3}$	

Fins una altra Cowboy especial!